Understanding Huntington's Disease Pathogenesis using Next Generation Sequencing Analyses

by

Theresa Anne Wasylenko

B.S., University of Michigan (2009)

Submitted to the Department of Biology
in partial fulfillment of the requirements for the degree of

Doctor of Philosophy in Biology

at the

MASSACHUSETTS INSTITUTE OF TECHNOLOGY

February 2015 [February 2016]

Signature redacted

Author .....
Department of Biology
October 31, 2015

Signature redacted

Certified by .....
David Housman
Virginia and D. K. Ludwig Professor for Cancer Research
Thesis Supervisor

Signature redacted

Accepted by .....
Michael Hemann
Associate Professor of Biology, Co-chair, Biology Graduate Committee

Understanding Huntington's Disease Pathogenesis using Next Generation Sequencing Analyses

by

Theresa Anne Wasylenko

Submitted to the Department of Biology
on October 31, 2015, in partial fulfillment of the
requirements for the degree of
Doctor of Philosophy in Biology

Abstract

Huntington's disease is one of nine expanded (CAG) repeat disorders. The expansion in Huntington's disease lies in the first exon of the huntingtin (*HTT*) gene and is pathogenic when $(CAG)_{\geq 40}$. Individuals with Huntington's disease develop motor, cognitive, and psychiatric symptoms in adulthood. These symptoms progress for approximately 15 years at which time they become fatal. The clinical manifestation of HD largely results from the extreme degeneration of neurons in the striatum and cortex. The *HTT* gene encodes the huntingtin (HTT) protein. Over the years, researchers have developed a rich understanding of the consequences of loss of wildtype HTT function, gain of toxic mutant HTT function, and mutant *HTT* RNA toxicity. However, the mechanisms through which pathology develops are still largely ambiguous. Given the widespread involvement of HTT in cellular processes, next generation DNA sequencing technologies offer a rich opportunity to explore genome-wide effects of the HD mutation and may help answer mechanistic questions.

The application of many next generation DNA sequencing methods is a new luxury for researchers. DNA sequencing methods have undergone a rapid technical evolution which has accelerated the financial feasibility of applying DNA sequencing involved methods on a routine basis. In this thesis, two high throughput analysis techniques, RNA-Seq and ChIP-Seq, were applied to Huntington's disease models to better understand disease mechanisms, and a third high throughput analysis technique, Ribo-Seq, was optimized for future HD studies.

RNA-Seq on Huntington's disease model mice and their wildtype littermates demonstrated extensive and progressive dysregulation of the transcriptome in HD striatum and cortex, with most of the affected genes having a lower steady state expression in mutant tissues. ChIP-Seq with an antibody against trimethylated-Histone3-Lysine4 (H3K4Me3) demonstrated both a general reduction of H3K4me3 levels and a unique histone profile at the promoters of HD downregulated genes. Analysis of RNA-Seq results for splicing changes showed that mutant *HTT* itself is mis-spliced. This mis-splicing product is translated into a small, pathogenic HTT fragment which may have considerable implications for HD therapeutic design.

In addition to CNS degeneration, severe muscle dysfunction is an early clinical observation in HD and many CAG repeat expansion disorders. Proper muscle form and function is dependent on an extensive alternative splicing program. Thus RNA-Seq data on muscle tissue from mouse models of several CAG expansion disorders was examined for genome-wide splicing alterations. Widespread mis-splicing was detected in the muscle of both Spinocerebellar ataxia 7 and Huntington's disease mouse models and minor splicing dysregulation was detected in Spinal-bulbar muscular atrophy.

Lastly, methods were developed to examine translational control and mRNA localization in the brain of Huntington's disease mice. Concurrent Ribo-Seq and RNA-Seq in diseased and wildtype animals would answer if there was altered translational control. The Ribo-Seq protocol designed in cell culture was optimized for use on brain tissue and is ready for application in HD mouse models. Analysis of the localization of mRNA transcripts to neuronal projections can be studied by combining fractionation experiments with RNA-Seq. A method to prepare high quality RNA from isolated neuronal projections was developed and is now applicable to RNA-Seq studies.

Thesis Supervisor: David Housman
Title: Virginia and D. K. Ludwig Professor for Cancer Research

Acknowledgments

I must gratefully acknowledge many for making my six years at MIT a wonderful experience. My advisor David Housman has afforded me the freedom to pursue my thesis studies with independence but has always been available with encouragement and direction when these projects took unexpected turns. Most importantly though, David has cared deeply about how I develop as a person. David, you have been an inspiring example of how to live with passion, and I appreciate the time you have taken to understand me and help me grow in many areas of life.

Zachary Crook was my bay-mate for three years and main mentor in the lab. He taught me most of what I know about benchwork, designing experiments, troubleshooting, and stand-up comedy. Zach, I greatly appreciated your wisdom and patience as I grew as a graduate researcher and your loyalty as a friend. Eric Wang was my computational mentor. Given I could barely type on a command line when I entered the lab, Eric's direction and patience were integral for me completing a thesis on deep sequencing analyses. In addition, I found it very inspiring to watch Eric optimistically tackle new ideas that most would find too daunting.

I worked closely with Ferah Yildirim for nearly my entire PhD. Ferah has been a wonderful role model in the lab as well as a close friend. Julia Alberta and Shanie Coven Easter made my life considerably easier as they were the organizing forces in lab. Whether it was reagents, mice, forms, or big picture advice, they were always ready and willing to help. Jill Crittenden shared an endless knowledge about brain form and function and was always excited to mull over scientific results with me. Hilary Bowden and Thomas Wang let me 'borrow' reagents regularly and made our lab environment comfortable and fun. Hilary, whether fixing lab equipment, exercising, lab parties, or retreats, you turned everything into an adventure! My talented UROPs Alissa Borschenko, Alina Li, and Charlotte Albright were a joy to have in lab and watch grow as scientists.

I have enjoyed close collaborations with Chris Ng, Ernest Fraenkel, Andreas Neueder, Kirupa Sathasivam, Gillian Bates, Malini Vashishtha, Leslie Thompson,

and Ryan Lim. I was very fortunate to work with such talented scientists across the world. I also worked closely with the BioMicroCenter here at MIT while generating high-throughput data. Thank you Stuart Levine and Shmulik Motola for being so responsive, diligent, and flexible. I thank my classmates, especially Renin Hazan and Bena Chan, for the time we have shared over the long journey of graduate school. I am also grateful to Jonathan King and Wendy Gilbert who have served on my thesis committee. Your support, questions, and suggestions have been invaluable resources in shaping both my thesis and career. I thank Diana Rosas, the final member of my defense committee, for her time in reviewing this thesis and her insight into my projects.

Membership in MIT's Tech Catholic Community (TCC) has been an integral part of my time at MIT. It is through TCC's activities and fellowship that I have grown spiritually and matured as a young adult. I specially thank Allison Chang, Michelle Lustrino, and Camille Carlisle. Your friendship has, and will continue to, greatly enrich my life. I have been blessed to have Fr. Richard Clancy and Deacon Augustine Hwang as spiritual mentors. Your support, especially as Tom and I prepared for marriage, has been a tremendous blessing.

To my brothers - Matt, Pat, Nick, Mark, and Paul - and their wives - Krista, Krystal, Allegra, Elisha, and Megan - your love and laughter and beautiful families have been a wonderful reminder of the gift of life. And to my little sister Mary - you are an All-Star and you bring more joy to my life than you could ever imagine. Whether it is basketball, shopping, cards, babysitting, or even homework, I have loved every minute shared with you.

To my best friend and husband Tom - you have been my rock throughout grad school. You have listened patiently through many practice talks, amended even more algorithms, gave structure to my sometimes scattered ideas, shared my successes, helped me grow from my failures, and never let me lose sight of true priorities. I cannot sufficiently express my gratitude for you and for our life together, but know that I love you. To my Mom and Dad - your unconditional love, support, and guidance prepared me for and sustained me through MIT. This thesis is dedicated to you.

As I reflect on my time at MIT, I am humbled by the number of wonderful people who have enriched my life these last six years, and so I finally thank God for the beautiful opportunity I have had in attending MIT.

Contents

List of Figures

List of Tables

Chapter 1

Introduction to Huntington's Disease and Sequencing Technologies

1.1 Background of Huntington's Disease

In 1872, George Huntington succinctly characterized a distinct choreic disorder as being (1) accompanied by insanity, (2) hereditary, and (3) adult onset (republished in (Huntington, 2003)). This choreic disorder soon came to bear his name as Huntington's disease (HD). Over time, a comprehensive understanding of symptoms was established. In addition to the impaired motor control characteristic of the disease, individuals often suffer from both cognitive decline (loss of executive function skills) and psychiatric disturbances (anger and depression most common), as broadly noted by Dr. Huntington. These cognitive and psychiatric symptoms frequently precede the involuntary choreic movements (Bates et al., 2002). In 1993, the The Huntington's Disease Collaborative Research Group confirmed the hereditary nature of the disease, discovering the underlying genetic cause was an expansion of a CAG repeat in exon 1 of the Huntingtin (*HTT*) gene (THDCR, 1993). This mutation is autosomal dominant. Unaffected individuals have two *HTT* alleles with a repeat length around 20 (ranging from 11-35). Individuals with one allele in which the CAG repeat has expanded past 39, annotated as $(CAG)_{\geq 40}$, will develop HD during adulthood, whilst those with a rare allele of $(CAG)_{>70}$ will have childhood onset (Bates et al., 2002).

Once onset occurs, symptoms progressively worsen over a ~15-20 year period until they are eventually fatal (Bates et al., 2002).

These symptoms result from severe and selective degeneration of neurons, specifically those of the striatum and motor cortex. Although it has been over 20 years since the discovery of the causative mutation, a therapy to prevent or slow this degeneration in patients has not been successful. The only FDA approved drug for HD is tetrabenazine (TBZ). TBZ provides symptomatic relief for chorea through a reduction of dopamine signaling (reviewed in (de Tommaso, 2011)). However, the balance between improved symptoms and adverse side-effects (most alarmingly a frequent aggravation of psychiatric symptoms) leaves HD patients with little therapeutic relief.

1.2 An Overview of the *HTT* Gene and Encoded HTT Protein

HTT is essential for mammalian development (Zeitlin et al., 1995). However, an individual with only one functional copy of *HTT* (a null mutation in the second allele) had no abnormal phenotype, demonstrating a depletion of normal *HTT* is well tolerated (Ambrose et al., 1994). The *HTT* gene encodes Huntingtin (HTT), a ~350 KDa protein that is expressed ubiquitously with elevated levels found in the brain and testes (Strong et al., 1993; Li et al., 1993). The CAG trinucleotide codes for the amino acid glutamine. The stretch of glutamines encoded by the CAG repeat is commonly referred to as 'polyQ'.

1.2.1 The Structure of HTT

HTT homologues have been characterized across vertebrates and are highly conserved (Schmitt et al., 1995; Lin et al., 1994; Matsuyama et al., 2000; Baxendale et al., 1995). All vertebrate huntingtin proteins contain a polyQ$_{\geq 4}$ but the polyQ is only subject to large expansions and contractions in humans. Increased polyQ length correlates with organismal complexity (Tartari et al., 2008) and seems especially important in neu-

rons, as deletion of the polyQ in mice results in a neurological phenotype (Clabough & Zeitlin, 2006). Non-pathogenic polyQ tracts have a disputed structure; a prevailing theory is that this region is disordered in an unbound state yet adopts a more defined structure upon interaction with binding partners (Schaefer et al., 2012; Caron et al., 2013). In higher vertebrates, a polyproline (polyP) tract immediately follows the polyQ. The polyP enhances protein solubility and influences post-translational modifications of the first 17 residues of HTT (Steffan et al., 2004). Another well conserved feature of HTT is a group of three functional clusters of HEAT repeats. HEAT repeats form bi-helical structures that assemble into rod-like super domains. The super domains act as scaffolds for many cellular interactions (Andrade & Bork, 1995). The polyQ, polyP, and the HEAT repeat regions all play a role in meditating a diverse set of binding interactions (Qin et al., 2004; Schaefer et al., 2012; Harjes & Wanker, 2003; Li & Li, 2004; Andrade & Bork, 1995; Neuwald & Hirano, 2000).

The 'N17' region comprises the first 17 residues of HTT; these residues immediately precede the polyglutamine region and are also strongly conserved in vertebrates (Tartari et al., 2008). N17 has many characterized functions. It forms an amphipathic α-helical structure that is important for localizing HTT to membranes (Atwal et al., 2007), interacts with the nuclear pore to facilitate export into the cytoplasm (Cornett et al., 2005), and at least partially regulates HTT turnover when covalently modified (Kalchman et al., 1996; Jana et al., 2005; Steffan et al., 2004).

Even though HTT is composed of >3,000 amino acids, the N17, polyQ, polyP, (which are all located in exon 1) and HEAT repeats are the only well characterized domains. It is important to note that there are many sites for post-translational modification and cleavage throughout the length of HTT (reviewed in (Cattaneo et al., 2005)), an active C-terminal nuclear export signal, and a more ambiguous nuclear localization signal in the N-terminus (but downstream of exon 1) (Atwal et al., 2007; Xia et al., 2003).

1.2.2 The Function of HTT

Two cellular roles of HTT have been well established: transcriptional regulation and vesicle/organelle transport. HTT exerts most of its transcriptional regulation indirectly. For example, HTT sequesters Repressor Element-1 Silencing Transcription Factor/Neuron-Restrictive Silencer Factor (REST/NRSF) outside of the nucleus (Zuccato et al., 2003; Zuccato & Cattaneo, 2007). In the absence of HTT, REST translocates into the nucleus and represses transcription of important neuronal genes, including Brain Derived Neurotrophic Factor (*BDNF*). BDNF, as its name implies, is an important support protein for the brain in general (Binder & Scharfman, 2004; Huang & Reichardt, 2001). Medium spiny neurons (MSNs), which largely compose the striatum, are particularly dependent on BDNF for proper development (Ivkovic et al., 1997), survival (Baquet et al., 2004; Duan et al., 2003; Widmer & Hefti, 1994; Nakao et al., 1995; Ventimiglia et al., 1995), and differentiation (Mizuno et al., 1994; Widmer & Hefti, 1994; Ventimiglia et al., 1995). An appreciable amount of BDNF is not synthesized within striatal cells; cortical afferents reaching the striatum are the main source of the precious neurotrophin (Altar et al., 1997). Loss of wildtype HTT leads to REST-mediated repression of BDNF transcription in the cortex, and subsequently a reduction of BDNF protein in the striatum.

HTT, especially N-terminal fragments, can translocate into the nucleus and directly interact with chromatin as well. ChIP experiments on mouse models and postmortem human tissue showed HTT physically present at gene promoters, as well as intronic and intergenic regions (Benn et al., 2008b). *In vitro* experiments demonstrated HTT directly binds DNA, altering its conformation and likely influencing transcription factor binding (Benn et al., 2008b).

The other well studied role of HTT is in the transport of vesicles and organelles. HTT interacts with the HAP1-p150^{Glued} motor complex (Engelender et al., 1997; Li et al., 1998), facilitating dynein/dynactin-mediated vesicle and organelle transport along microtubules (Gunawardena et al., 2003; Caviston et al., 2007). This process is especially critical for transport of the vesicles containing BDNF from the cortex to

the striatum (Gauthier et al., 2004).

In addition to localization in the nucleus and along microtubules, HTT is present at both the ER and plasma membrane (Kegel et al., 2005; Atwal et al., 2007), but its membrane-associated functions are not well understood. Given HTT's multitude of binding partners, diverse cellular localization, and ubiquitous expression, many cast HTT as a general scaffolding protein for many cellular processes that has adapted important neuronal functions in higher eukaryotes.

1.3 Roots of Pathology

How the trinucelotide expansion in the coding sequence of *HTT* induces pathology has been a central question since 1993. The only difference in the resulting protein would be additional glutamines at the N-terminus. This could reduce the ability of the mutant protein to perform critical functions, especially functions in the brain. Or the additional glutamines could confer new properties to the mutant HTT protein, which given its diverse localization and binding, could affect many cellular processes. There is the distinct possibility that the mutation could cause pathology before the protein level, with the DNA/RNA CAG expansion influencing toxicity directly. Current evidence suggests that all such possibilities contribute to HD pathology, with the strongest influence coming from toxic new properties of the expanded repeat protein; while the consequences of these toxic new properties are well documented, the mechanisms remain elusive.

1.3.1 Loss-of-Function of Normal HTT

The strongest evidence against loss-of-function driven pathology is the phenotype of people with only one *HTT* allele. Individuals with Wolf-Hirschhorn syndrome have a chromosome 4 deletion that includes *HTT*, yet do not develop HD (Gottfried et al., 1981). And, as mentioned before, an individual with only one functional *HTT* allele due to a balanced translocation is also free from this fully penetrant disease (Ambrose et al., 1994). Individuals who are homozygous for the expanded HD allele

have a normal age of onset with only mild, if any, acceleration of disease progression (Myers et al., 1989; Squitieri, 2003; Wexler et al., 1987), which considered with the fact that *HTT* null is embryonic lethal, suggests that mutant HTT retains enough normal function that cellular distress does not manifest until early adulthood.

Even though a 50% reduction in *HTT* does not lead to HD, it is possible that loss of wildtype *HTT* still contributes to HD pathogenesis. In both human and HD mouse models, some of wildtype HTT is sequestered into aggregates formed by mutant HTT (Busch, 2003; Dyer & McMurray, 2001). Indeed, there have been many observations that normal function is disrupted. This includes increased REST localization in the nucleus, decreased transcription of the *BDNF* gene, and decreased transport of BDNF protein (Zuccato et al., 2003). A mouse model of selective *BDNF* depletion in the cortex strikingly recapitulates many phenotypic aspects of HD mouse models and of HD patients (Strand et al., 2007; Baquet et al., 2004). Therapeutic targeting of *BDNF* levels has shown promise in an HD mouse model as well (Duan et al., 2008). Later studies though, showed that REST was upregulated by mutant HTT through the transcription factor Sp1 (Ravache et al., 2010), suggesting REST mediated repression is a combination of loss-of-function and gain-of-function effects. Studies in mice demonstrate that the pattern of transcriptional dysregulation is conserved across models with varying wildtype Htt dosage, further supporting the notion that wildtype Htt may play a smaller role in transcriptional dysregulation than first believed (Seredenina & Luthi-Carter, 2012).

To summarize, loss of wildtype HTT function is not a driver of the HD phenotype, but likely reduces a cell's ability to endure the stress of mutant HTT.

1.3.2 Gain-of-Function of Mutant HTT

It widely believed that much of pathology is driven by a toxic gain of function by mutant HTT. Clearance of mutant protein, through increased autophagy (Ravikumar et al., 2002, 2004), largely relieves the HD phenotype. Hence the bulk of research has focused on how mutant HTT disrupts cellular processes. While this research is extensive, I will highlight three main areas that are most relevant to this thesis:

aggregation of mutant HTT, transcriptional dysregulation, and mitochondrial defects.

One of the hallmarks of HD pathology is the formation of intranuclear and cytoplasmic aggregates (Difiglia, 1997). The expanded polyglutamines of HTT seem to transition from a disordered structure to a β-strand organization (Poirier, 2005) with a propensity to aggregate; this is true of the eight other polyglutamine containing proteins that underlie the other CAG expansion disorders as well. Initially it was hypothesized that HTT aggregates drive pathology by sequestering important proteins and / or burdening the cell's system for handling misfolded proteins. Indeed, aggregates sequester many proteins (Suhr et al., 2001) and efforts were taken to develop therapeutics to clear aggregates (Muchowski et al., 2000; Sittler et al., 2001). But aggregates were viewed with a new perspective starting in 2004 when Arraste et al. published the first evidence of inclusions being protective and HTT oligomers driving pathology (Arrasate et al., 2004). In addition to oligomers, soluble HTT has many aberrant interactions with other proteins (Li & Li, 2004; Culver et al., 2012). Now many in the field perceive aggregates as the cell's way of preventing soluble mutant HTT from wreaking havoc. While aggregates may cause a degree of cellular stress, they seem to prevent oligomers from causing considerably more.

Experts agree that transcriptional dysregulation is a severe and central pathological program in HD brain, with the vast majority of affected genes downregulated. However, the cause of dysregulation remains an unfinished puzzle with many disparate pieces. There is likely some contribution to transcriptional dysregulation, as mentioned above, by loss of wildtype HTT. Models comparing mutant huntingtin with nearly complete nuclear or nearly complete cytoplasmic localization suggest the brunt of toxicity results from nuclear accumulation of mutant HTT and as an extension, the effect of mutant HTT on transcription (Schilling, 2004; Peters et al., 1999; Gu et al., 2015). There have been 15 transcription factors identified in mutant HTT aggregates and over 10 more whose activities are altered in disease models, although some altered activities seem to be context dependent (reviewed in (Seredenina & Luthi-Carter, 2012)). These transcription factors have both repressor and activator functions. Also, mutant HTT can directly bind DNA, recognizing more sequences

than wildtype HTT and is found associated with distinct promoters both in mouse models and patient tissue (Benn et al., 2008b). Given these many leads for how the presence of a mutant *HTT* allele affect transcription, it is striking that the result is an overwhelming repressive program. This program largely targets genes that are selectively expressed in neurons or have functions especially critical in neurons (Cha, 2007; Zuccato & Cattaneo, 2007). Chapter two of this thesis describes our efforts to explore chromatin structure as a possible unifying feature of downregulated genes.

Mitochondrial dysfunction is another critical feature of HD. Early evidence showed a decrease in the activity of several respiratory chain enzymes in human HD postmortem striatum (Gu et al., 1996). Since then, many mitochondrial defects have been noted. Cell lines established from the peripheral tissue (peripheral blood mononuclear cells, skin, and muscle) of HD patients exhibit structural disorganization of the matrix and cristae, a drastic enlargement of mitochondria, a reduced mitochondrial membrane potential (Squitieri et al., 2006, 2010), and an inverse relationship between polyQ length and ATP levels (Seong et al., 2005). A mouse model of HD shows increased mitochondrial glutathione levels, a compensatory mechanism to reduce reactive oxygen species in defective mitochondria (Choo et al., 2005). In murine primary striatal neurons, mutant Htt impairs transport of mitochondria along neuronal projections (Orr et al., 2008). More recently, reduced mitochondria number was observed in human HD postmortem striatum as well as downregulation of the energy metabolism regulator *PGC-1α* (Kim et al., 2010). The sum of the aforementioned effects leave the mitochondria in HD severely compromised and is considered a driver of pathology.

1.3.3 Mutant *HTT* RNA Toxicity

The role of pathogenic RNA in neurodegenerative disease has been more appreciated in the last decade and is reviewed in (Ranum & Day, 2004; Li & Bonini, 2010). The possibility of an RNA contribution to HD pathogenesis has gained more traction in recent years despite being first noted in 1996 by McLaughlin et al., who identified abnormal interactions between CAG RNA repeats and proteins from brain

lysate (McLaughlin et al., 1996). This alternative mechanism was more thoroughly interrogated in 2011, when DeMezer et al. reported that mutant *HTT* CAG RNA adopts a hairpin structure and forms intranuclear foci which potentially sequester RNA-binding proteins (de Mezer et al., 2011), similar to the pathogenic mechanism in myotonic dystrophy (Mankodi, 2001). However, there has not been a rigorous examination of proteins that bind the expanded CAG RNA nor the consequence of said binding.

In 2012, Banez-Coronel et al. investigated another mechanism of RNA toxicity. Prompted by studies showing triplet-repeat derived small RNAs (Krol et al., 2007; Yu et al., 2011), Banez-Coronel et al. investigated the presence and toxicity of small RNAs derived from the *HTT* CAG repeat (Bañez-Coronel et al., 2012). They did identify small CAG-repeated RNAs (sCAGs) in human HD postmortem brain and demonstrated a repeat-length correlation with cell death in a human neuronal cell line. However, further research is needed to demonstrate their results cannot be attributed to RAN translation of their constructs (these were mutated to not be **canonically** translated) (Zu et al., 2011) and address the mechanism of toxicity mediated by the sCAGs.

1.4 Experimental Models of HD

The completely genetic basis of HD has afforded the research community the ability to generate many relevant models. The bulk of this thesis will focus on mouse HD models, which can be grouped according to the nature of their HD mutation: N-terminal transgenic, full-length transgenic, and knock-in.

N-terminal transgenics express a human *HTT* fragment that was inserted at random into the genome. In general, these models exhibit the most aggressive HD-like phenotype amongst mouse models, with striking motor abnormalities and a shortened lifespan (Crook & Housman, 2011). The R6/2 mice studied in chapters 2 and 4 express a *HTT* exon 1-intron 1 fragment at a level similar to the two endogenous mouse *Htt* genes (Mangiarini et al., 1996). While the rapid disease onset of these

animals is not reminiscent of an adult onset disorder, they do offer a transcriptional profile most similar to that of human HD postmortem tissue (Scappini et al., 2007).

Full-length transgenics, such as the YAC128 we study in chapter 3, express the entire human *HTT* gene. They display an HD-like phenotype similar to the N-terminal transgenics but with delayed onset and slower manifestation (Slow et al., 2003).

A series of knock-in lines were created that carry an expansion of the CAG repeat in the endogenous mouse *Htt* gene. Some lines have only the repeat expanded while some are chimeric for mouse/human sequence around the CAG locus. HD knock-ins have more mild motor symptoms, exhibit pathology much later than transgenics, and have a normal lifespan (Crook & Housman, 2011). We examine many of these knock-in models in chapter 3 in order to understand the effect of repeat length on a mis-splicing event.

We also utilize a *Drosophila* model of HD in chapter 2. The *Drosophila* huntingtin homologue is poorly conserved and lacks a polyQ domain (Li et al., 1999). However, expression of pathogenic CAG repeats in *Drosophila* causes progressive, 'adult onset' neuropathology, loss of motor function, and reduced life-span (Marsh et al., 2003). The *Drosophila* model is particularly useful as a rapid system to evaluate phenotype enhancers and suppressors.

1.5 A Review of Applied Sequencing Technologies

While we have a rich understanding of the consequences of loss of wildtype HTT function, gain of toxic mutant HTT function, and mutant *HTT* RNA toxicity, the mechanisms through which pathology develops are still largely ambiguous. Given the widespread involvement of HTT in cellular processes, next generation DNA sequencing technologies offer a rich opportunity to explore genome-wide effects of the HD mutation and may help us answer mechanistic questions.

The application of many next generation DNA sequencing methods is a new luxury for researchers. The sequencing of the late 90s and early 2000s relied on a Sanger-

based method, also know as 'first generation' sequencing. The resulting data was exciting and we owe the first human genome sequence to Sanger sequencing. During the years that Sanger sequencing dominated biology, the related sequencing costs followed a Moore's Law prediction in which they decreased exponentially, as seen from Figure 1-1, from years 2001 to 2008. In 2008, sequencing centers transitioned from Sanger-based methods to several 'next generation' technologies. The shift in technology largely involved the ability to sequence in a massively parallel fashion, as DNA molecules were assessed through imaging and optics rather than electrophoresis. The rapid evolution of next-generation methods accelerated the financial feasibility of sequencing; to illustrate, the cost of sequencing a human genome has fallen from ~$3,000,000 ($102/Mb) in January 2008 to ~$4,200 ($0.05/Mb) in 2015 (KA, 2015).

As the use of routine sequencing became more realistic, many techniques that examine cells on a genome-wide level evolved. Three of them that are relevant for this thesis are RNA isolation and cDNA sequencing (RNA-Seq), Chromatin immunoprecipitation and sequencing (ChIP-Seq), and Ribosome profiling and cDNA sequencing (Ribo-Seq).

1.5.1 RNA-Seq

RNA-Seq is a method to assay the transcriptome. Prior to the advancements in DNA sequencing, much of transcriptomics data was generated by microarrays. In this process, DNA sequences from known transcripts are bound to a slide. Labelled cDNAs of interest are hybridized to immobilized DNA sequences and then unbound cDNA is washed away. Signal from bound molecules can be quantitated to estimate the amount of cDNAs. The microarray technology was important across the field of biology for understanding mRNA expression on a global level. In HD, microarray studies identified key repressed genes and established the severity of transcriptional dysregulation (Hodges et al., 2006; Scappini et al., 2007; Luthi-Carter et al., 2002; Cha, 2000). While yielding many critical insights, the utility of microarrays was limited by cross-hybridization of probes, poor dynamic range, and the necessity of a prior knowledge of transcripts for which to probe.

Soon after the transition to next-generation sequencing, RNA-Seq was developed as the method of choice to study transcriptomes. RNA is isolated from cells of interest. mRNA is selected for and transcribed into cDNA. cDNA libraries are prepared and sequenced. The resulting reads are mapped to the genome and illustrate the relative amount of starting material for most transcripts in the cells studied. RNA-Seq offers lower background noise, a larger dynamic range (10^5 vs 10^2), and higher technical reproducibility than microarrays (Marioni et al., 2008; Wang et al., 2009). In addition to expression levels, reads from RNA-Seq provide information on splicing events. RNA-Seq methods can also be adapted to study small RNA populations instead of mRNA and findings from these studies have been interesting in the context of HD (Hoss et al., 2014).

Bioinformatic options for analyzing the abundance of data generated from deep sequencing studies have expanded in parallel with improved sequencing capabilities. For all of our experiments we utilize the Bowtie small read aligner to map sequencing reads to the proper genome. Bowtie is a highly efficient alignment tool, both in time and memory, without compromised accuracy for short reads (Shang et al., 2014). Initially we also mapped to a custom made database for splice junctions, created from UCSC genome browser to correspond to read lengths being analyzed. We have since transitioned to using Tophat in conjunction with Bowtie to include splice junction mapping. When calling differential expression, we only consider reads mapping to constitutive exons in order to separate changes in splicing from changes in expression levels. We use the R package DESeq to call differential expression. DESeq assumes read count distribution follows a negative binomial model. It scales libraries by the highly recommended Trimmed Mean of M values normalization method (Dillies et al., 2013) and uses the Benjamini-Hochberg procedure to control the False Discovery Rate. In comparison between eight different software packages, DESeq was recommended as among the two safest choices in regards to consistency and false discovery (Seyednasrollah et al., 2015). While DESeq uses raw counts in analysis, we display our results as Reads Per Kilobase of exon per Million Mapped reads. This is an alternative normalization method that is more intuitive for understanding the

abundance of a transcript, regardless of length. The relationship between RPKMs and transcript level varies by the RNA content of the cells analyzed, but an estimate is ~5 RPKMs for one transcript per cell (Mortazavi et al., 2008). We analyze splicing separately from expression using the MISO software package. MISO analyzes alternative splicing events as a Bayesian inference problem. We developed our own pipeline for determining differential splicing from MISO output as there was not a well-established method incorporating biological replicates.

1.5.2 ChIP-Seq

The increase in sequencing capabilities has not only helped us better understand the transcriptome, but also the proteins that interact with the transcriptome. Many proteins, such as transcription factors and histones, associate with DNA to regulate expression of nearby genes. In order to understand how a particular factor influences the transcriptome, one can cross-link DNA to associated proteins (this preserves their interaction during downstream manipulation) and immunoprecipitate the protein of interest with the proper antibody. Any DNA associated with the protein of interest will also be isolated, and these DNAs can then be prepared for sequencing and mapped to the genome; the result is a genome-wide map of where the protein of interest may be influencing gene expression (Johnson et al., 2007).

The ChIP-Seq method has been particularly informative for understanding how histone modifications affect transcriptional regulation. We now appreciate that histone modifications are integral for organizing chromatin structure to be more or less favorable to transcriptional activation or elongation (Strahl & Allis, 2000). The extensive influence of histone modifications, and particularly the consequence when this influence is disrupted, has been the focus of many disease related studies (Bernstein et al., 2007). We explore Huntington's disease relevance in chapter 2, utilizing ChIP-Seq to explore how a specific modification, trimethylation of Histone3-Lysine4, may affect the dysregulation of the HD transcriptome.

1.5.3 Ribo-Seq

In 1988, Wolin and Walter demonstrated ~30 base fragments of mRNA are protected from RNase digestion by active eukaryotic ribosomes (S L Wolin, 1988). Twenty years later Ignolia et al. combined this concept with the emerging RNA-Seq technology to show that one could identify all of the transcripts in a population of yeast cells that were being actively translated at the time of harvest (Ingolia et al., 2009). Since then, this aptly named protocol of Ribo-Seq has yielded insights into general eukaryotic translational regulation (Spriggs & Bushell, 2010; Guo et al., 2010a; Gerashchenko et al., 2012) as well as how translational regulation may be disrupted in disease (Katz et al., 2014). In chapter 5, we discuss our efforts to optimize this protocol for use in studying translational regulation in our HD mouse models.

1.6 Thesis Overview

Chapter two describes the use of concurrent RNA-Seq and ChIP-Seq to better understand the initiation, progression, and extent of transcriptional dysregulation occurring in the R6/2 transgenic mouse model of HD.

Chapter three demonstrates that the smallest mutant HTT protein fragments found in postmortem human brain and HD knock-in mouse brain are the result of mis-splicing of mutant *HTT* mRNA. Using an adapted RNA-Seq protocol, we were able to visualize and quantify this mis-splicing event. We present a model describing how *HTT* mRNA with an expanded repeat in exon 1 disrupts U1 protection of a cryptic polyA signal in *HTT* intron 1; as a result, about 15% of *HTT* transcripts are not spliced at the 5' splice site of intron 1. These transcripts are cleaved, polyadenylated, and translated. The resulting protein fragment is highly pathogenic.

Chapter four examines a common pathological feature of several CAG repeat disorders: extreme muscle atrophy. Muscle from mouse models of Huntington's disease (HD), Spinocerebellar ataxia 7 (SCA7), and Spinal-bulbar muscular atrophy (SBMA) were analyzed through RNA-Seq, with an analytical emphasis on global splicing changes. The alternative splicing program in the HD and SCA7 muscle sam-

ples was largely perturbed, with many common splicing events affected. Mis-splicing in SBMA was markedly less severe, but was rescued with peripheral knockdown of the causative mutation.

Chapter five summarizes insights we have learned from our deep sequencing analyses. We highlight several experiments that would continue our work in applying these new sequencing technologies to better characterize the mechanisms of HD pathology. Of note, we propose to use fractionation and RNA-Seq to assess if RNA localization is altered in HD and concurrent RNA- and Ribo-Seq to determine if translational efficiency is altered in HD.

1.7 Figures

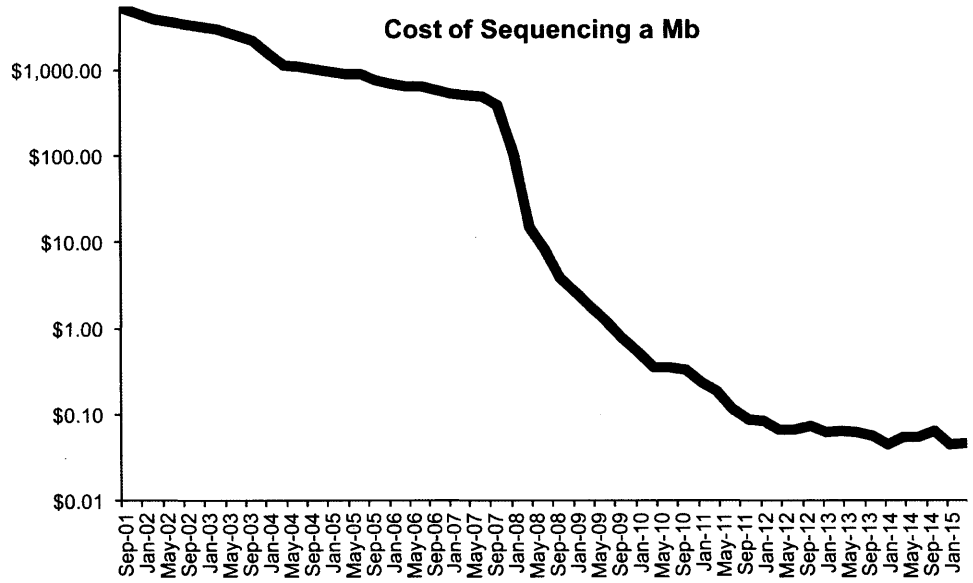

Figure 1-1: Cost of sequencing a Mb of DNA over the years. Graph was plotted with data from (KA, 2015).

Chapter 2

Transcriptional and Epigenetic Dysregulation in the R6/2 Transgenic HD Mouse Model

This chapter was adapted from (Vashishtha et al., 2013). I contributed to mouse handling, experimental design, isolation of RNA, preparation and analysis of libraries, analysis of RNA-Seq data, figure preparation, and manuscript text.

This work was supported by the National Institute of Health, the Cure Huntington's Disease Initiative, the Huntington's Disease Society of America, the Hereditary Disease Foundation, the National Cancer Institute, the National Science Foundation, and the Johns Hopkins Center Without Walls for Huntington's Disease.

2.1 Introduction

As mentioned in chapter 1, microarray studies demonstrated progressive transcriptional dysregulation in both cortex and striatum as a characteristic feature of HD (Cha, 2007). Transcriptional repression of key neuronal transcripts, including neurotransmitters, growth factors, and their cognate receptors, is consistently observed and implicated in disease pathogenesis. Among the critical genes whose expression is repressed in HD mouse models and human brain tissue are the dopamine receptor

2 (*Drd2*), preproenkephalin (*Penk1*), the cannabinoid receptor (*Cb2*), and brain-derived neurotrophic factor (*Bdnf*) (Cha, 2007; Zuccato & Cattaneo, 2007). To more deeply understand transcriptional dysregulation, we performed RNA-Seq on affected brain regions in a mouse model of HD.

We chose the R6/2 mouse model for our study because these mice show patterns of transcriptional dysregulation similar to postmortem HD brain (Hodges et al., 2006; Scappini et al., 2007). The R6/2 animals show a rapidly progressing HD-like phenotype of balance, coordination, and spatial memory deficits, with symptoms developing around ∽5-6 weeks (Mangiarini et al., 1996). This phenotype becomes extreme at 14 weeks at which time we must euthanize the animals.

2.2 Dysregulation in Striatum and Cortex

We performed RNA-Seq experiments on the striatum and cortex of R6/2 mice and their wildtype littermates. RNA-Seq data was gathered at two time points, early (8 weeks) and late (12 weeks) in disease progression. We used the R package 'DESeq' to identify genes that were significantly differentially expressed between wildtype and mutant animals for each of the four datasets (Appendix A Tables 1-4). These genes had $\log_2$(fold difference) > 0.5, residual variance < 10, and FDR < 0.1. We first checked 'canonically' HD dysregulated genes as identified by microarrays in late stage of disease progression (Seredenina & Luthi-Carter, 2012) and found these dysregulated in our 12wk datasets (Figure 2-1). Our results also confirmed early and progressive transcriptional dysregulation, as demonstrated in Figure 2-2 where gene expression is plotted for all dysregulated genes.

2.2.1 Novel Insights from RNA-Seq Data

Our RNA-Seq data revealed new HD transcriptional insights. Most intriguingly, upregulated genes in mutant animals were found to be significantly enriched for viral (interferon 1) induced genes (striatum p=1.3e-2, cortex p=2.9e-9, Figure 2-3). Many of these genes are lowly expressed and would be difficult to detect with microarrays.

This signature is found in SCA7 mouse models as well (Chort et al., 2013), suggesting a possibility that the RNA hairpins formed from the CAG repeat may trigger the viral dsRNA response. In the future, it would be interesting to explore publicly available datasets from other neurodegenerative disorders to see if interferon 1 upregulation is unique to CAG disorders.

Another new insight our data yielded was additional dysreguation to the RGS family. Genes *Rgs2*, *Rgs4*, and *Rgs9* have been implicated in HD (Seredenina et al., 2011; Seredenina & Luthi-Carter, 2012), which we confirm in our datasets. We find *Rgs-2*, *-4*, *-9*, *-13*, *-14*, and *-19* dysregulated in 12wk HD striatum and *Rgs-4*, *-8*, *-9*, *-11*, *-13*, *-14*, *-16*, and *-20* dysregulated in 12wk HD cortex. These genes have been implicated in schizophrenia, depression, and anxiety (Rivero et al., 2013; Lifschytz et al., 2012), as well as motor deficits in parkinson's disease (Lerner & Kreitzer, 2012), and have been shown to be important for synaptic plasticity (Vellano et al., 2011) and neuronal differentiation (Sharma et al., 2011). Given the more extensive dysregulation we detected with this family of genes, a closer look at their potential role in HD and transcriptional regulators of this specific family is warranted.

2.2.2 Gene Signature for Therapeutic Studies

One metric to see therapeutic improvement would be reversal of an HD gene signature. We selected genes from our dysregulated gene signature set that would be ideal for this metric. We focused on downregulated genes because upregulated genes tend to be lower abundance and largely associated with an inflammation signature which may be confounded by many therapies. In order to find 'robust' genes, we required the average RPKM across all animals to be $\geq$10, have a fold change $>$ 2, and have a coefficient of variation $<$ 0.3 (selected genes are listed in Appendix Tables A5&6). Plotted in Figure 2-4 are the cumulative density distributions of the gene signatures for wildtype and R6/2 animals. A Kolmogorov-Smirnov test demonstrates that the distribution of the signature genes is significantly different between the genotypes. The same significance test can be performed for data from therapeutically treated animals to determine transcriptional rescue.

2.3 Epigenetic Influence on Transcriptional Dysregulation

We hypothesized that a central event in the pathological program underlying transcriptional dysregulation includes alterations in chromatin structure in the regulatory regions of genes downregulated in HD. To evaluate this hypothesis, we focused on H3K4 trimethylation (H3K4me3), a mark of transcription start sites (TSSs) and active chromatin (Bernstein et al., 2002; Santos-Rosa et al., 2002; Kim et al., 2005). Growing evidence suggests that this mark is plastic and modulated in conditions of chronic stress, developmental disorders, and psychiatric disorders (Hunter et al., 2009; Tsankova et al., 2006; Jiang et al., 2008) as well as during long-term memory consolidation from contextual fear conditioning (Gupta et al., 2010), suggesting a critical function in brain.

2.3.1 H3K4 Trimethylation Changes at Dysregulated Promoters in HD Model Mice and Human HD

Using chromatin immunoprecipitation (ChIP), we examined H3K4me3 levels for *Bdnf*, which, as mentioned in chapter 1, is expressed in the **cortex**, provides trophic support for GABAergic medium spiny neurons, and is expressed at lower levels in HD (Zuccato & Cattaneo, 2007; Zuccato et al., 2001). Initial experiments focused on H3K4 trimethylation levels at the *Bdnf* locus in the R6/2 mouse. The mouse *Bdnf* gene has eight 5' exons that each contain a separate promoter and one 3' exon coding for the mature protein (Figure 2-5A) (Aid et al., 2007). Transcription from both exon II and IV is reduced in cortex from R6/2 mice as well as in human HD brain (Zuccato et al., 2008).

To examine if *Bdnf* expression correlated with H3K4me3 occupancy, ChIP was used to quantify H3K4me3 at *Bdnf* promoters II-IV and the coding region (IX) in cortices from 12wk old R6/2 mice and littermate controls. H3K4me3 was reduced by nearly one-half at *Bdnf* promoter II (Figure 2-5B). H3k4me3 was nearly absent

upstream of the REST binding site in promoter II and within the coding exon of the *Bdnf* gene (Figure 2-5C), consistent with other reports (Bernstein et al., 2002; Santos-Rosa et al., 2002). These results suggest that reduced transcription could be a consequence of changes in chromatin structure at the *Bdnf* locus, specifically a reduction in H3K4me3.

Reduction in H3K4me3 occupancy at exon II was observed during symptomatic stages of disease at 8 and 12wks but not in presymptomatic 4wk old mice (Figure 2-5D). Similar results were obtained for cortical and striatal *Penk1* and striatal *Drd2* loci (Figure 2-5E&F). In contrast, genes with expression levels that are unchanged, such as *Atp5b*, *Rpl13a*, and *Lin7c*, are not altered in H3K4me3 levels (Figure 2-5E). Western blots confirmed that the changes in H3K4me3 were gene-specific and not the result of a change in bulk H3K4me3 levels in cortices or striata (Appendix Figure A-1). The **H3K4me3** mark is **specifically** decreased at the downregulated genes that we tested. For example, we saw no disease-specific differences in the levels of **H3K36me3** occupancy, which also marks actively transcribed genes, within the coding regions of *Bdnf* and *Penk1* in the cortex or *Penk1* and *Drd2* in the striatum (Appendix Figure A-2).

We next extended our studies of H3K4me3 occupancy to human HD brain. Human HD postmortem brain can be classified based on neuropathological abnormalities. The brains are graded 0-4, with 0 being no discernible abnormalities and 4 extreme neuropathological changes. This grading scale closely correlates with clinical assessments at the time of death (Vonsattel et al., 1985). Levels of *BDNF* and synaptophysin (*SYP*) RNA in the superior frontal gyrus (SFG - a region of the cortex) and *DRD2* and *PENK1* RNA in the caudate (a region of the striatum) were significantly lower in the grade 3 samples and trended toward decreased expression in grade 2 samples (Figure 2-6A&B). Expression of a control gene, *ATP5B*, was not significantly altered as expected. H3K4me3 occupancy was significantly lower at *BDNF* exon II and *PENK1* and *SYP* promoters but unaltered at *BDNF* exon IV and the *ATP5B* promoters in the SFG grade 3 samples (Figure 2-6C). For caudate, H3K4me3 levels were lower at *DRD2*, *PENK1*, and *SYP* promoters in grade 2 samples and re-

duced even further at *DRD2* and *PENK1* promoters in grade 3 samples, potentially preceding corresponding gene expression alterations (Figure 2-6D). Taken together, these results show that the reduction of H3K4me3 occupancy occurs at downregulated genes in human HD brain.

2.3.2 H3K4me3 at the *Bdnf* TSS Is Reduced in R6/2 Mouse Cortex by ChIP-Seq

The findings described above prompted us to examine H3K4me3 occupancy across the genome in R6/2 and wildtype mice at 8 weeks and 12 weeks of age for both the cortex and striatum using ChIP-sequencing (ChIP-Seq). As expected, H3K4me3 was particularly enriched at TSSs (P value $<$ 1e-200 for each dataset).

To relate the genome-wide studies to our PCR-based results, we analyzed H3K4me3 occupancy around the *Bdnf* gene, including its TSSs. The H3K4me3 mark was present at the TSSs of *Bdnf* exons I-VII and absent at the coding exon. The ChIP-Seq data confirmed that the 12wk old R6/2 cortex showed reduced H3K4me3 levels at the REST-regulated *Bdnf* exon II and within this exon, H3K4me3 occupancy was decreased more extensively at the RE-1 site for REST binding (Figure 2-7).

2.3.3 Decreased H3K4me3 Occupancy Corresponds to Decreased Gene Expression Patterns

To identify genes with significantly different levels of H3K4 trimethylation, we focused our analysis on a -3/+2-kb window around each TSS. We counted the number of reads in each of these windows and used loess normalization to account for technical differences that might cause a systematic bias in the data between the R6/2 and wildtype mice, such as read complexity and genomic coverage. Integration of ChIP-Seq and RNA-Seq results revealed a high degree of overlap between genes with decreased H3K4me3 and decreased expression in R6/2 mice compared with wildtype mice at 8 and 12 weeks in both cortex and striatum [hypergeometric P values: 8wk cortex P = 0.01; 12wk cortex P = 7.1e-68; 8wk striatum P = 1.4e-5; 12wk striatum

P = 4.3e-77] (Figure 2-8). Overlap of genes with differential H3K4me3 levels (a more stringent cutoff used) and differential expression can be found here: `http://www.pnas.org/content/suppl/2013/07/19/1311323110.DCSupplemental/sd02.pdf`.

2.3.4 Downregulated Genes in R6/2 Mice Are Associated with A Specific H3K4me3 TSS Profile

Previous studies have shown that differences in the distribution of histone methylation around the TSS often distinguish classes of genes, even when these genes cannot be separated by their expression levels (Young et al., 2011; Heintzman et al., 2007; Pekowska et al., 2010; van Dijk et al., 2010). To investigate the H3K4me3 mark more rigorously, we used k-means clustering to identify five predominant patterns of H3K4me3 that occur in both wildtype and R6/2 mice (Figure 2-9A&B). Strikingly, there is a specific H3K4me3 profile in **wildtype** mice marking a very large fraction of genes that will be downregulated in the presence of mutant HTT. In particular, genes downregulated in R6/2 are very likely to be members of a particular cluster that we label as class 1, which has a broad peak of H3K4me3 downstream of the TSS in wildtype mice [P values: 12wk cortex P = 2.00e-59; 8wk cortex P = 1.12e-16; 12wk striatum P = 8.05e-38; 8wk striatum P = 1.82e- 9] (Figure 2-9C&D). This association strengthens from 8 to 12 weeks of age as R6/2 mice progress through the HD pathological program. Interestingly, genes in class 1 are enriched in GO biological processes critical for neuronal functions, such as signal transduction, G protein-coupled receptor signaling, neurogenesis, axon guidance, learning or memory, and regulation of transcription. It is important to note that class 1 genes show similar expression levels to other classes (Appendix Figure A-3). Therefore, we conclude that this pattern cannot be explained as a simple consequence of differences in transcription.

Although the class 1 H3K4me3 profile in wildtype mice is strongly associated with downregulation of expression of the corresponding genes in R6/2 animals, it is also important to note that, as the disease progresses, genes in the class 1 H3K4me3 group remain in that class. They do show a decrease in the levels of H3K4me3, but this

mark remains spread across the coding region in a profile that is distinct from other classes. Unlike genes that were downregulated, genes that were upregulated in R6/2 mice did not show any significant association to a particular H3K4me3 TSS profile, except for an association between upregulated genes in the 12wk R6/2 cortex and class 4 profile (P = 1.49e-4).

2.3.5 Potential Regulators of Differential Trimethylation

We used sequence analysis to identify potential transcriptional regulators that could be recruiting methyltransferases and demethylases to differentially expressed genes in R6/2 mice. Previous studies (Heintzman et al., 2007; Shu et al., 2011) have shown that the sites of such regulators should not be expected directly underneath the peaks of methylation. Therefore, we determined the location of chromatin accessible binding sites for regulatory proteins near the enriched H3K4me3 regions in wildtype and R6/2 mice based on an empirical spatial distribution derived from DNase-Seq and H3K4me3 ChIP-Seq data. Applying this method to our H3K4me3 data from wildtype mice yielded a set of sequences that we searched for known DNA binding motifs.

This analysis revealed several potential regulators that have been previously associated with HD. Genes downregulated for both expression and H3K4me3 are associated with motifs for REST/NRSF (12wk cortex P = 2.52e-11; 12wk striatum P = 2.67e-8) and Sp1 binding motif (12wk cortex P = 1.55e-10; 12wk striatum P = 9.85e-11). Both REST (Zuccato et al., 2003) and Sp1 (Dunah, 2002; Li et al., 2002) have been previously linked to HD. In addition, our motif analysis suggests other possible regulators linked to downregulation of expression and H3K4me3, including PPAR (reviewed in (Jin & Johnson, 2010)) and p53 (Bae et al., 2005; Steffan & Kazantsev, 2000).

2.3.6 Knockdown of H3K4me3 Demethylase Activity Reduces Toxicity and Modulates Mutant Htt Mediated Transcriptional Dysregulation

The identification of a specific signature of histone methylation associated with mutant HTT induced pathology suggested the possibility that intervention designed to impact this methylation pattern could have significant therapeutic benefit in HD. To explore this approach for HD, we sought a strategy to manipulate histone methylation in a targeted manner. In mice, there are several H3K4me3 demethylases, complicating interpretable knockdown of H3K4me3 demethylase activity. However we found we could assess whether an H3K4me3 demethylase might influence mutant HTT pathogenesis *in vivo* in *Drosophila.* Specifically, we analyzed the effects of partial loss of little imaginal disks (*lid*; CG9088), the only H3K4me3-specific demethylase (Lloret-Llinares et al., 2008) in *Drosophila.* In the *Drosophila* model used, the first exon of human *HTT* with an expanded polyglutamine domain (*HTTex1p-Q93*) is expressed in all neurons, resulting in reduced viability and progressive degeneration of neurons (Steffan et al., 2001). Numbers of HD flies surviving to adulthood (eclosing) when they had reduced *lid* (heterozygous for the lid^{10424} loss of function allele) were compared with HD flies homozygous for wildtype *lid.* We found that the number of eclosed *HTTex1p-Q93* flies wildtype for *lid* was 5.3 ± 1.5% of controls. The eclosion ratio of *HTTex1p-Q93* flies heterozygous for lid^{10424} increased to 12.4 ± 2.8% ($P = 0.013$, t test), suggesting neuroprotection (Figure 2-10A).

Neurodegeneration was analyzed by scoring the number of intact photoreceptor neurons in 7-d-old flies using the pseudopupil technique. When flies were reared at 22.5°C and shifted to 25°C on eclosion, the average number of rhabdomeres (light-gathering structures of photoreceptor neurons) per ommatidium was 4.10 ± 0.07 in *HTTex1p-Q93*-expressing flies with wildtype *lid*, whereas in *HTTex1p-Q93*-expressing flies with heterozygous lid^{10424}, the average number of rhabdomeres increased to 4.96 ± 0.16 ($P = 0.0038$, t test) (Figure 2-10B). Levels of the *HTT* transgene expression were not affected by heterozygosity for *lid* (Figure 2-10C). Thus, our results indicate

that reduced *lid* activity ameliorates mutant HTT-induced phenotypes in *Drosophila.*

2.4 Summary and Future Directions

We find that expression of CAG-expanded *HTT* is strongly associated with a specific pattern of histone methylation. Manipulation of histone methylation levels is neuroprotective in flies, suggesting that chromatin-modulating enzymes, including the JARID1 class of demethylases, are rational targets for HD therapeutics.

Genes that decrease in expression in R6/2 mice because of the presence of a pathological *HTT* exon 1 transgene have an unusual pattern of H3K4me3, even in wildtype animals, which spreads broadly downstream of the TSS. These data suggest that the profile may be associated with recruitment of proteins with presence or absence in R6/2 animals that causes transcriptional dysregulation. We propose that this observation – genes that will be downregulated in R6/2 animals have a specific distribution of H3K4me3, even in striatal and cortical cells of normal animals – is an important clue to understanding the mechanistic basis of transcriptional dysregulation in HD.

The view that the distinctive architecture of H3K4 methylation at TSSs is a defining functional characteristic of classes of promoters is supported by observations in a wide range of eukaryotic systems. For example, in *Arabidopsis*, genes with expression patterns that are altered in response to dehydration show a pattern of H3K4me3 at TSSs similar to the one that we observe for downregulated HD genes, and this pattern persists in both the dehydrated and watered state (van Dijk et al., 2010). The H3K4me3 classes that we observe also closely resemble the clusters previously reported for H3K4me2 in human CD4+ T cells (Shu et al., 2011). In this case, genes with tissue-specific expression showed a broader distribution of the mark extending into the expressed portion of the gene, suggesting that a unique chromatin signature at specific promoters may regulate their tissue-specific expression. Finally, there is precedence for specific classes of H3K4me3 profiles in brain that may be involved in tissue-specific expression, because five different classes of genes were identified in

neurons isolated from prefrontal cortex, with genes encoding proteins with neuronal function having a similar broad distribution of H3K4me3 (Shulha, 2012).

Considering these findings in diverse species, we suggest that the observed H3K4me3 architecture reveals a fundamental property controlling expression levels, and in HD, it determines a response to *HTT* exon 1 expression. One important open question is how the pattern of H3K4me3 relates to other epigenetic features. Expression of mutant *HTT* has recently been shown to be associated with changes in DNA methylation (Ng et al., 2013), and there are precedents for a connection between changes in DNA methylation and trimethylation of H3K4 (Deaton et al., 2011; Landan et al., 2012; Balasubramanian et al., 2012). We, therefore, propose that uncovering the regulatory mechanisms that establish, maintain, and respond to the characteristic epigenetic patterns at sensitive promoters, including the specific complexes formed and cross-talk between histone modifications and DNA modifications, should give insight into why these genes are particularly sensitive to the presence of mutant HTT and may provide insights into how to restore their transcription.

A key question that our studies raise is whether mutant HTT exerts its effects on downregulated promoters through a direct and preferential action with chromatin at the site of each promoter or alternatively, mutant HTT activates a cell signaling pathway that impacts H3K4me3 at target sites. Understanding which of these alternative mechanisms underlies the phenomena that we reported here will have impact on the strategy for additional development of therapeutic intervention for HD.

2.5 Methods

Note: All primer sequences used in the following methods can be downloaded with the following link: `http://www.pnas.org/lookup/suppl/doi:10.1073/pnas.1311323110/-/DCSupplemental/sd07.xlsx`.

2.5.1 Mouse Brain Tissue Preparation for ChIP-Seq and RNA-Seq Experiments

At King's College London, hemizygous R6/2 mice were bred by backcrossing R6/2 males to (CBA x C57BL/6) F1 females (B6CBAF1/OlaHsd; Harlan Olac) and maintained as previously described (Labbadia et al., 2011). Their CAG repeat was ~204. These mice were used for ChIP-PCR experiments. All experimental mice (Jackson Laboratory) for ChIP-Seq and RNA-Seq (~120 CAG repeats) were housed five per cage in a colony maintained on a 12h light/12h dark cycle (lights on from 0700 to 1900h) at constant temperature (23°C). Animals were provided with ad libitum access to food and water. All animal protocols were approved by the Institutional Animal Care and Use Committee at Massachusetts Institute of Technology and University of California at Irvine. R6/2 and wildtype mice were killed using CO_2 asphyxiation, which was followed immediately by postmortem dissection of the cortex and striatum. Bilateral cortical or striatal tissues were pooled from one mouse and then divided into two for RNA-Seq and ChIP-Seq experiments. Flash frozen tissues for RNA-Seq and cross-linked tissues for ChIP-Seq were stored at -80°C for later use.

2.5.2 RNA-Seq Library Preparation and Analysis

Flash-frozen tissues were homogenized, and RNA was extracted with TRIzol Reagent and purified with RNeasy columns (Qiagen); all samples had RNA integrity numbers greater than seven. The RNA-Seq protocol was adapted from a previously published protocol (Levin et al., 2010) using Invitrogen reagents unless noted otherwise.Two rounds of Oligo d(T)25 Magnetic Beads (New England BioLabs) were used to isolate mRNA from 1 to 3µg total RNA. Purified mRNA was fragmented with Ambion's RNA Fragmentation Kit for 5min at 70°C. mRNA was then ethanol precipitated, concentrated in 5µL water, and premixed with 3µg random hexamers for 5min at 65°C before chilling on ice. First-strand cDNA was synthesized as described but incubated as follows: 10min at 25°C, 50min at 42°C, and 15min at 70°C. First-strand cDNA was purified by phenol:chloroform:isoamyl alcohol extraction, ethanol precipitated with

0.1 volume 3M ammonium acetate to remove dNTPs, and resuspended in 104µL H2O. Second-strand cDNA was synthesized as described but incubated for 2.5h. Paired-end libraries for Illumina sequencing were then prepared from the cDNA as in a previously published protocol (Levin et al., 2010), except that adaptor-ligated cDNA was size-selected to 200-400 bp, and we performed PCR using Phusion High-Fidelity (HF) DNA Polymerase with HF buffer (New England BioLabs) and 10µL Q Solution (Qiagen). These paired-end, strand-specific cDNA libraries were then sequenced on the Illumina Genome Analyzer (36-bp reads) or HiSEq (40-bp reads).

Reads were mapped to the mm9 genome and a database of splice junctions using the Bowtie alignment program (Langmead et al., 2009) with setting –best -m1 -v2. Gene expression was calculated by counting reads mapping to constitutive exons for each gene. These raw counts were evaluated for differential expression using the R package DESeq (Anders & Huber, 2010) with a 10% false discovery rate cutoff and log2 difference of > 0.5 between wildtype and mutant conditions. Outliers were further excluded by restricting the residual variance quotients to less than 10. Gene expression is represented in tables and heatmaps as Reads Per Kilobase of exon per Million uniquely mapped reads (RPKMs). Heatmaps were produced using GENE-E (Broad Institute: `http://www.broadinstitute.org/cancer/software/GENE-E/`). RNA-Seq library statistics are displayed in Appendix Table A-7.

2.5.3 Analysis of Viral Response

Interferon induced genes were found using the Interferome database (Rusinova, 2013). Significance was determined using the R function 'phyper'. For the striatum, *phyper(18,814,10199,148,lower.tail=FALSE)* and cortex *phyper(32,814,10244,144,lower.tail=FALSE).*

2.5.4 RNA Extraction and qPCR for Human Samples

Cell were lysed in TRIzol, and RNA was run through the Qiagen RNeasy column with on-column DNase I digestion. cDNA was prepared from up to 1µg of RNA using RT supermix from BioRad. The resulting cDNA was diluted 1:5 in water and used for

qPCR by the SYBR green method (BioRad). Human brain samples had RINs > 4.

2.5.5 ChIP-PCR

Finely chopped pieces of one hemisphere of cortex or both halves of striatum were fixed with 1% formaldehyde at 37°C for 15min and then washed with ice-cold PBS two times. For human samples, $\backsim$100mg tissue was finely chopped and fixed with 1% (vol/vol) formaldehyde. The fixed brain sections were prepared as described previously (Sadri-Vakili & Cha, 2006). Before addition of the H3K4me3 antibody for immunoprecipitation, 0.5% (vol/vol) of each sample was taken as input. The cross-links were reversed in the input samples, and after precipitation, DNA was resuspended in 20µL deionized water. In the remaining sample, antibody was added and incubated overnight. After immunoprecipitation, washes, reversal of cross-links, and precipitation of DNA, the pellet was resuspended in 20µL deionized water, and this sample was denoted as the IP sample. Gene-specific primers were used for qPCR, and 1µL input and IP samples were used in each PCR. The Δcrossing threshold (Ct) values between IP and input were compared among different samples.

2.5.6 ChIP-Sequencing Preparation and Computational Analysis

Cortical and striatal tissues were cross-linked with 1% (vol/vol) formaldehyde for 10min, and the cross-linking was quenched by 0.125M final concentration glycine. The cross-linked tissue was then homogenized, rinsed with PBS, pelleted, and frozen in liquid nitrogen for later use.

ChIP-Seq assays were performed as previously described (Macisaac & Fraenkel, 2010). Cross-linked tissues were fragmented to the size range of 100-500 bp using a Bioruptor (Bioruptor Next Gen; Diagenode). An antibody that specifically recognizes H3K4 trimethylation (H3K4me3; catalog #17-614; Millipore) along with nonspecific rabbit IgG (catalog #17-614; Millipore) were incubated with beads for 6h before incubating with sonicated chromatin overnight. Resulting immunoprecipitated DNA

and nonspecific IgG-bound DNA were prepared for high-throughput sequencing using a library preparation kit from Beckman Coulter (catalog #A88267). Libraries were sequenced on an Illumina platform following the manufacturer's standard protocol.

Raw ChIP-Seq data were processed using the Illumina software pipeline. ChIP-Seq reads were aligned to the reference mouse genome (mm9; UCSC) using Bowtie (Langmead et al., 2009). Binding events were identified using the genome positioning system algorithm (Guo et al., 2010b). For 12wk samples, we used IgG-bound DNA as the control, and for 8wk samples, we used a uniform background. We used a calculated alignable genome size of 2.107 Gbp, a standard expected ChIP-Seq read distribution, a multiple hypothesis corrected enrichment q-value cutoff of 1e-2, and a minimum α-value of 30. Genes associated with binding events inferred from ChIP-Seq were identified using annotations from the refFlat (RefSeq database) file from the UCSC mm9 tables on May 30, 2011. For visualization of read density at specific loci, ChIP-Seq aligned reads were shifted according to a peak shift model built by MACS (Zhang et al., 2008a) and uploaded to the UCSC genome browser. ChIP-Seq library statistics are displayed in Appendix Table A-8.

2.5.7 Loess Regression

We used loess regression to minimize false positives when predicting differentially methylated genes. This method has been used routinely in expression analysis to account for sources of noise that may differ between high and low signals. Each regression point represents the raw number of reads in H3K4me3 peaks within a -2/+3kb window of a transcription start site (TSS). The regression was performed using robust weighted linear regression as the underlying piecewise regression model. The data were then normalized by subtracting the value for R6/2 predicted by the regression from each corresponding sample. Genes were considered differentially methylated if the R6/2 value fell outside of ± 1 SD of the normalized R6/2 dataset.

2.5.8 Clustering of Histone Methylation Patterns

To search for different patterns of histone methylation, we computed a binary vector representing whether one or more reads from the H3K4me3 ChIP-Seq experiment was detected at each base in a window -2/+3 kb around TSSs. These vectors were binned, normalized, and then clustered by the k-means algorithm for k = 5 using Euclidean distance and complete linkage.

2.5.9 Gene Ontology Analysis

Functional enrichments in gene ontology biological processes were calculated using the two unranked list approach in GOrilla (Eden et al., 2009). For enrichment within differentially expressed genes, all expressed genes [above fragments per kilobase of exon per million fragments mapped (FPKM) > 0.1] were used as a background. For enrichment within differentially H3K4 trimethylated genes and classes of H3K4 trimethylated genes based on TSS profile, all H3K4 trimethylated genes (above 50 tags in the -2/+3 kb TSS window) were used as a background.

2.5.10 Defining Potential Protein-DNA Binding Sites Directly Adjacent to H3K4me3-Enriched Regions

We used the GPS program to identify the sites near methylation peaks where transcription factors were most likely to bind. GPS is designed for the analysis of ChIP-Seq data for DNA binding proteins, where the binding event is likely to fall near the center of the distribution of sequenced reads. To apply GPS to our problem, we needed to determine where transcription factors that regulate histone modifications would bind with respect to the reads obtained from immunoprecipitation of H3K4me3. To compute this empirical spatial distribution of H3K4me3 reads for a typical protein-DNA binding event, we used DNase hypersensitive sites and H3K4me3 data obtained from a striatal cell line. Around each DNase hypersensitive site, we calculated the spatial distribution of H3K4me3 ChIP-Seq mapped reads in a $\pm$1,500bp window. This distribution has the shape of a valley, with a local minimum of trimethylation near

the center and enriched for a peak of H3K4me3 on either side of the center. Providing this distribution to GPS allows it to use the histone immunoprecipitation data to find the most probable site of the transcription factor that recruited the histone modifier. We then used ±100bp windows around each site predicted by GPS as input for analysis of sequence motifs. We focused on sites proximal (±2,000 bp) to the TSS.

2.5.11 Motif Analysis

We used a hypothesis-based approach to identify known protein-DNA recognition elements enriched in each dataset. The set of hypotheses is derived from all vertebrate position-specific scoring matrices (PSSMs) from TRANSFAC Release 2011.3 (Wingender et al., 1996) filtered for sufficient information content (>8 total bits). Because many of these motifs are very similar to each other, they were clustered based on pairwise distance by KL divergence of the PSSMs using Affinity Propagation. When presenting the results of the motif analysis, we show the motif within each cluster that had the most significant P value. The TAMO programming environment (Gordon et al., 2005) was used to store the PSSMs and calculate the max motif score for each sequence (across all k-mers in the sequence for a motif of width k).

Overrepresentation of motifs in a foreground set of sequences was assessed against a background set of sequences using the Mann-Whitney Wilcoxon ranked sum test. For each independent motif test, sequences were ranked by the maximum motif score in each sequence (across all k-mers in the sequence for a motif of width k). This ranked list was used to compute the U statistic from which we computed a P value. The background sequences were selected to match the GC content, CpG content, and distance to the TSS of each foreground set. To find motifs enriched in H3K4me3 sites adjacent to sets of differentially expressed genes, the background was a randomly generated set of sequences with the same TSS distance distribution as the foreground. For enrichment of motifs in particular classes of genes based on H3K4me3 TSS profile, the background set of genes in all other classes was used.

A comprehensive list of motifs can be found at: `http://www.pnas.org/content/suppl/2013/07/19/1311323110.DCSupplemental/sd06.pdf`. The tables at this link

show overrepresented TRANSFAC motifs in H3K4me3 valleys adjacent to the following groups of gene: (A) genes down-regulated for both expression and H3K4me3 levels in 12-wk striatum down-regulated, (B) genes down-regulated for both expression and H3K4me3 levels in 12-wk cortex, (C) class 1 genes by H3K4me3 TSS profiles in 12-wk striatum, and (D) class 1 genes by H3K4me3 TSS profiles in 12-wk cortex.

2.5.12 Western Immunoblotting

R6/2 and wildtype mice were killed using CO2 asphyxiation. Immediately, cortex and striatum were dissected, and tissues were snap-frozen in liquid nitrogen for later use. For total cellular protein extraction, brain tissues were lysed in ristocetin-induced platelet agglutination buffer (50mM Tris, pH 7.4, 150mM NaCl, 0.1% wt/vol SDS, 1% wt/vol Triton X-100, 1% wt/vol sodium deoxycholate, protease inhibitor mixture; Roche), incubated on ice for 15min, and lysed by sonication at a power of 2.5 for three 10s pulses. Protein was quantitated by the Lowry method, and 25µg protein were resolved on 4-12% precast SDS/ PAGE gel with Mes buffer system (Invitrogen). The resolved bands were transferred onto nitrocellulose membranes, blocked with Superblock, and incubated with primary antibodies against H3K4me3 and total H3 (#10799; Abcam). Membranes were subsequently probed with secondary fluorophore-coupled antibodies (Li-COR Biosciences) in Superblock for 1h at room temperature in the dark on a rotary platform with gentle agitation. The membranes were then scanned using Odyssey IR scanner using Odyssey imaging software. Protein expression was measured by integrated intensity readings in regions defined around protein bands and normalized to corresponding control bands of H3K4me3.

2.5.13 *Drosophila* Experiments

Flies were reared on standard cornmeal molasses medium at various temperatures. To compare phenotypes of mutant *HTT*-expressing animals in a normal vs. *lid*-reduced background, *wt/wt*; $^{+/+}$; *UAS > HTTex1p-Q93/UAS > HTTex1p-Q93* females were crossed to *elav-GAL4/Y; lid [10424]/CyO* males. Eclosion data from ≧1,000 segre-

gants were calculated as percent of *elav-GAL4/+; lid/+ HTT/+* or *elav-GAL4/+; +/CyO; HTT/+* flies versus *HTT* nonexpressing male siblings. Pseudopupil analysis was carried out on 7-d old flies as described (Marsh et al., 2003). Flies were reared at 22.5°C and shifted to 25°C on eclosion. To quantify expression of the *HTT* transgene, heads of female flies were homogenized in TRIzol reagent (Invitrogen), and RNA was prepared according to the manufacturers recommendations. First-strand cDNA was prepared from 1µg total RNA with the Maxima Universal First-Strand cDNA Synthesis Kit (Thermo Scientific) using random hexamer primers. The resulting cDNA was diluted 1:10 and quantitated in quantitative PCR (qPCR) reactions in an MJ Research Opticon thermal cycler using SYBR Green PCR Master Mix (Applied Biosystems). Transgene expression levels were determined compared with a template calibration curve and normalized to the levels of the *rp49* housekeeping gene.

2.6 Figures

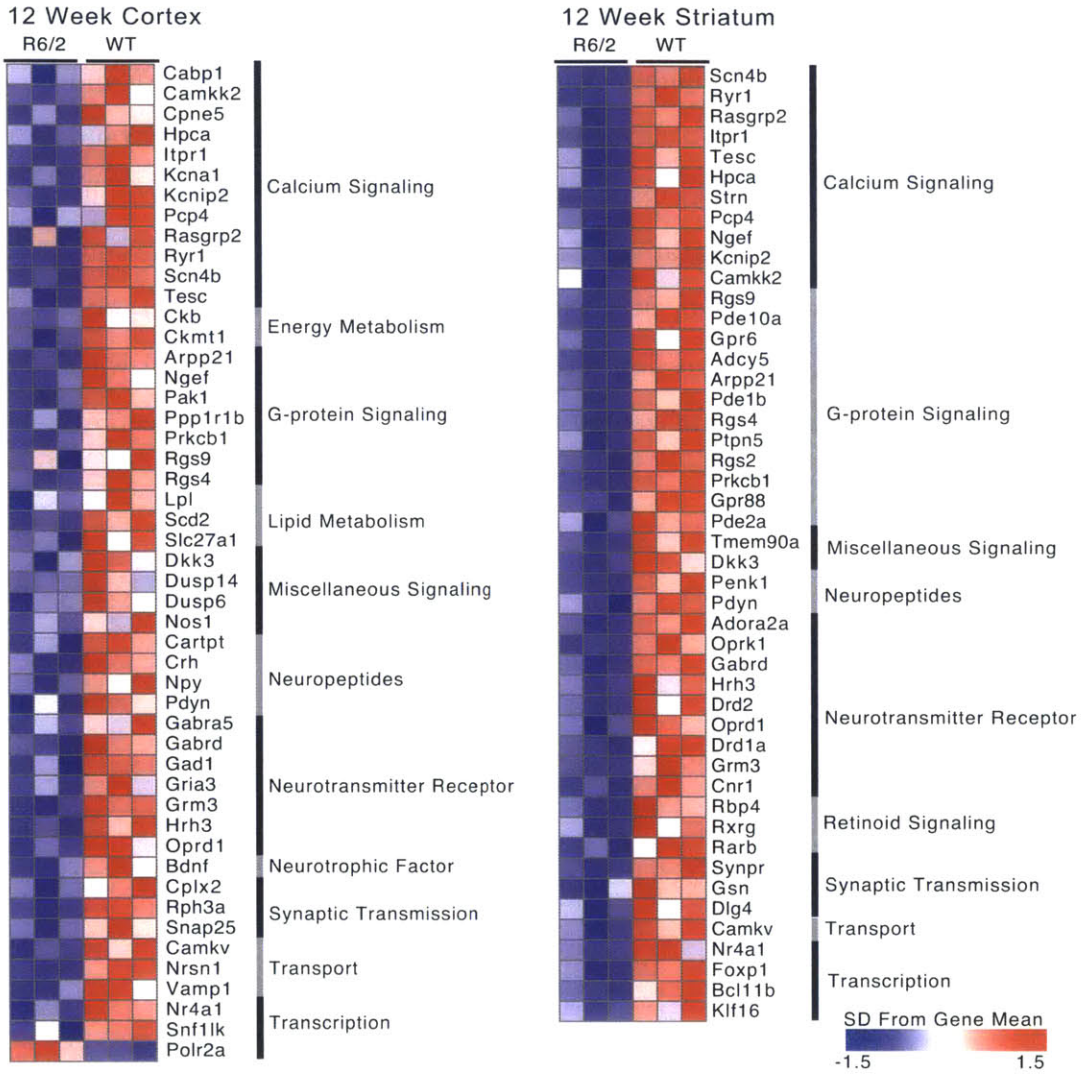

Figure 2-1: Heatmap of gene expression for key HD dysregulated genes in RNA-Seq data from 12wk cortex and striatum. Values indicate standard deviation from the gene mean.

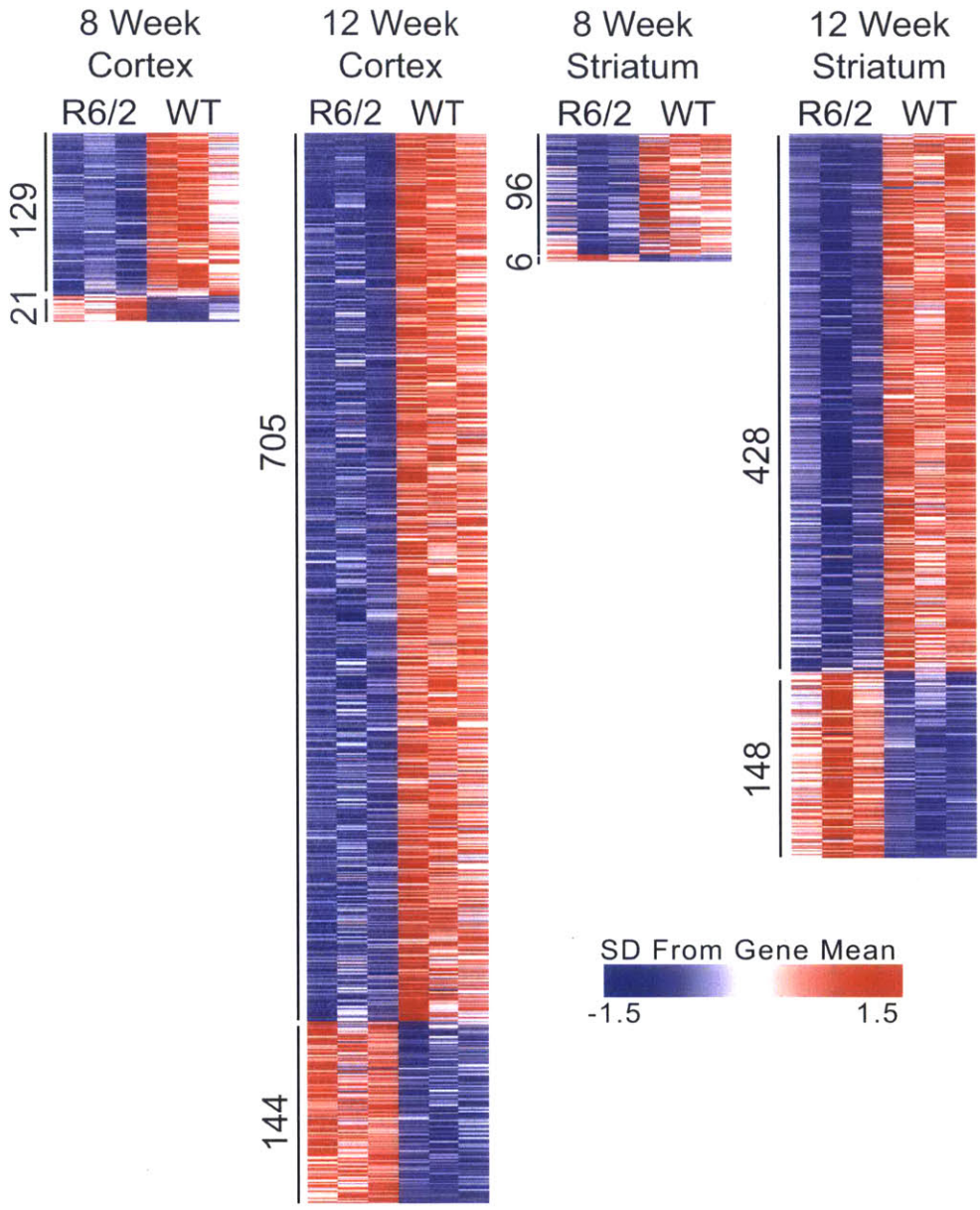

Figure 2-2: Heatmap of gene expression for all dysregulated genes. Values indicate standard deviation from the gene mean.

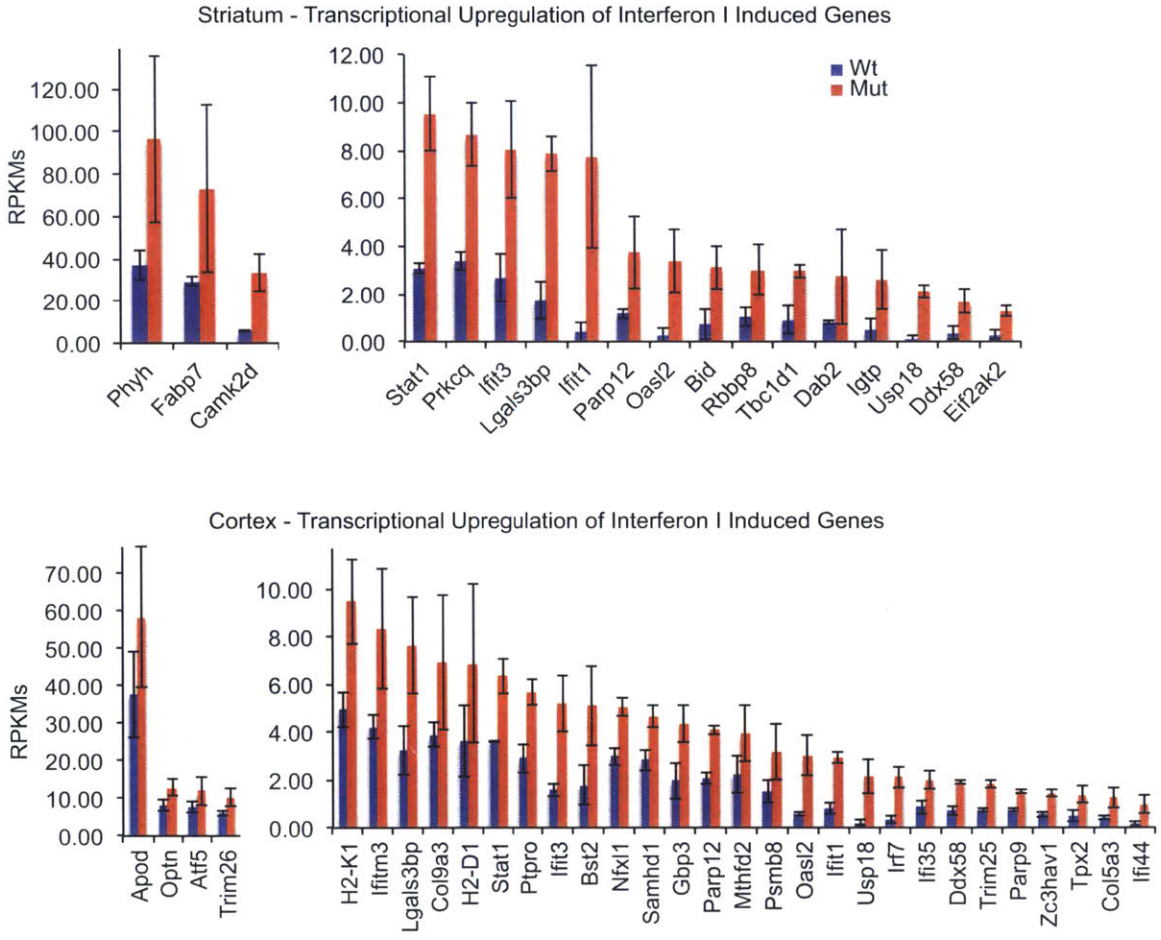

Figure 2-3: RPKM values are shown for interferon I induced genes that are upregulated in HD striatum (top) and cortex (bottom).

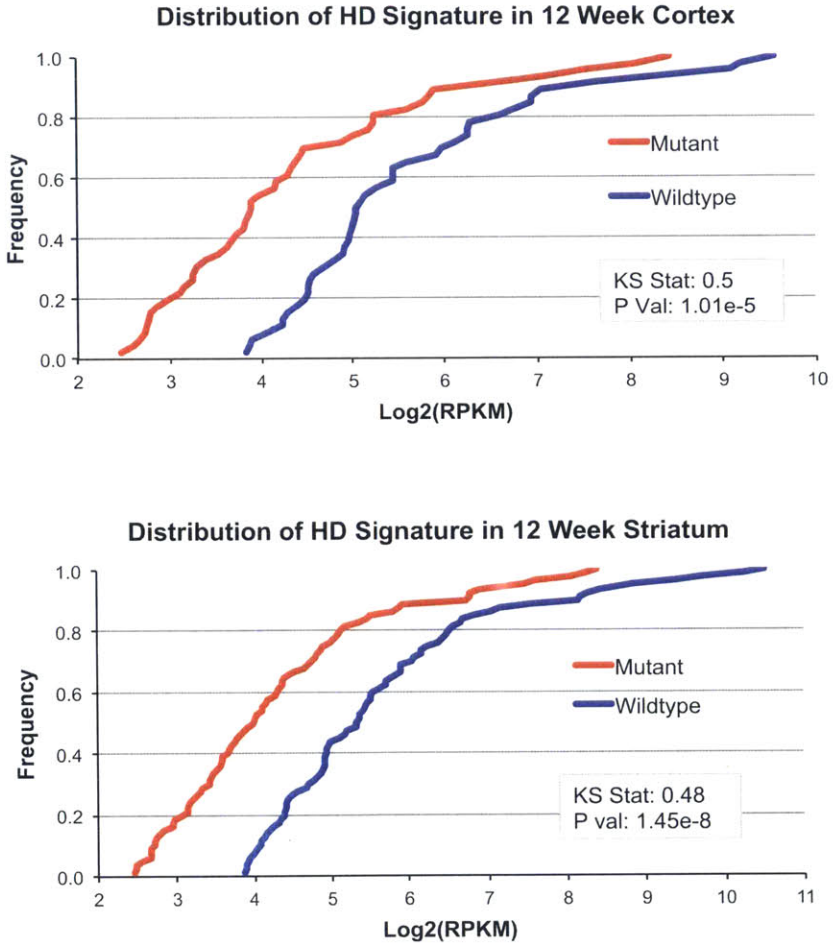

Figure 2-4: Cumulative density distribution for the cortex (top; 46 genes) and striatum (bottom; 80 genes) gene signatures. Distributions of gene signatures are significantly different for wildtype and mutant animals.

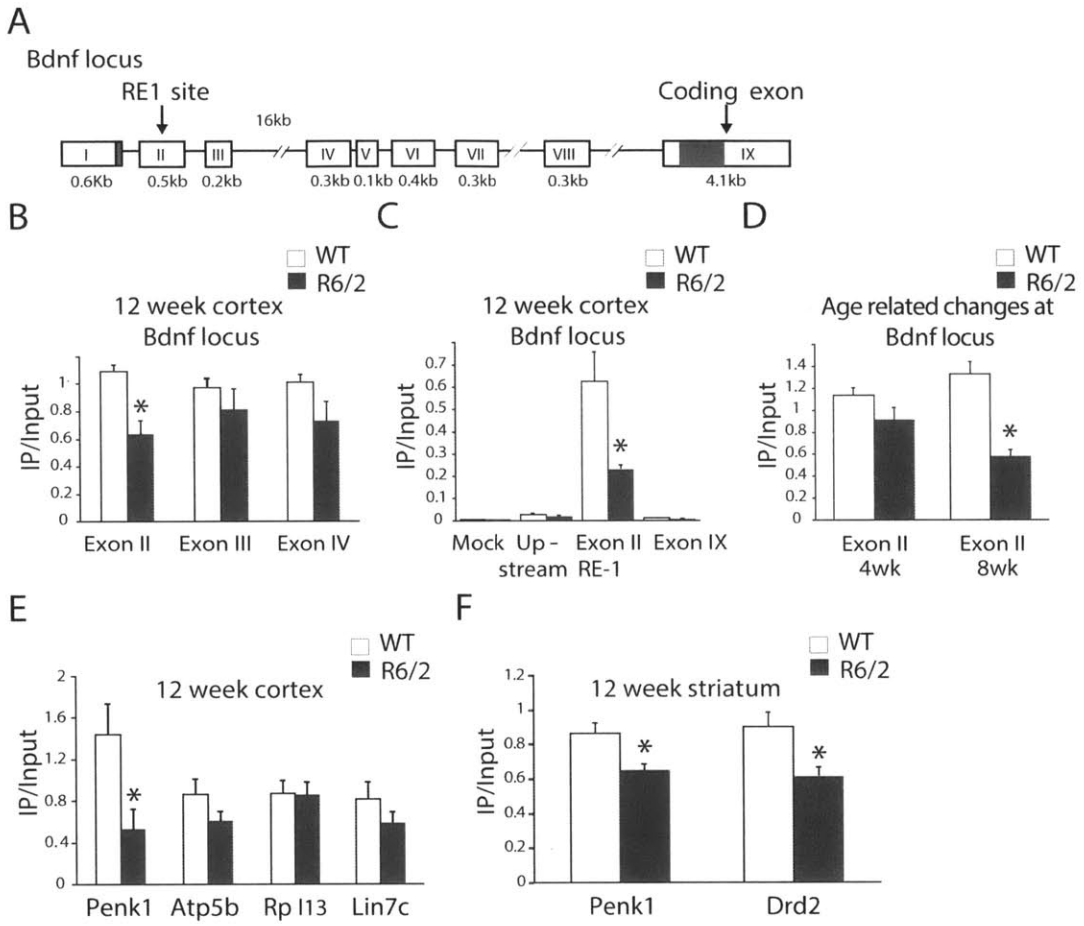

Figure 2-5: Levels of H3K4me3 are lower at downregulated genes in 12wk old R6/2 mouse cortex and striatum. (A) Schematic view of the mouse *Bdnf* locus. Transcription is alternately initiated at one of several upstream exons. Exon IX contains the coding region of the *Bdnf* gene. Exon II of *Bdnf* has a REST binding site, RE1. (B) ChIP shows that level of H3K4me3 measured at the exon II locus is nearly one-half of the wildtype levels in 12wk old mouse cortex ($P < 0.006$ by one-way ANOVA; n = 5). H3K4me3 levels are lower at exons III and IV as well; albeit, not significant. (C) H3K4me3 levels are specific to TSSs and nearly absent at a region upstream of the TSS and at the coding region. No antibody was added in the mock samples. (D) Changes in H3K4me3 levels at the exon II start site are progressive. (E) H3K4me3 levels were significantly lower at the TSS of *Penk1* in 12wk old R6/2 mouse cortex compared with wildtype mouse ($P < 0.05$ by one-way ANOVA; n = 4). At the TSSs of genes *Atp5b* and *Rpl13a*, the levels of H3K4me3 were similar or insignificantly lower. Similar results were found at the *Lin7c* locus, which is downstream of the *Bdnf* locus. (F) In 12wk old striatum, the levels of H3K4me3 were lower at the TSS of *Drd2* and *Penk1* loci ($P < 0.05$) by one-way ANOVA (n = 8). *$P < 0.05$.

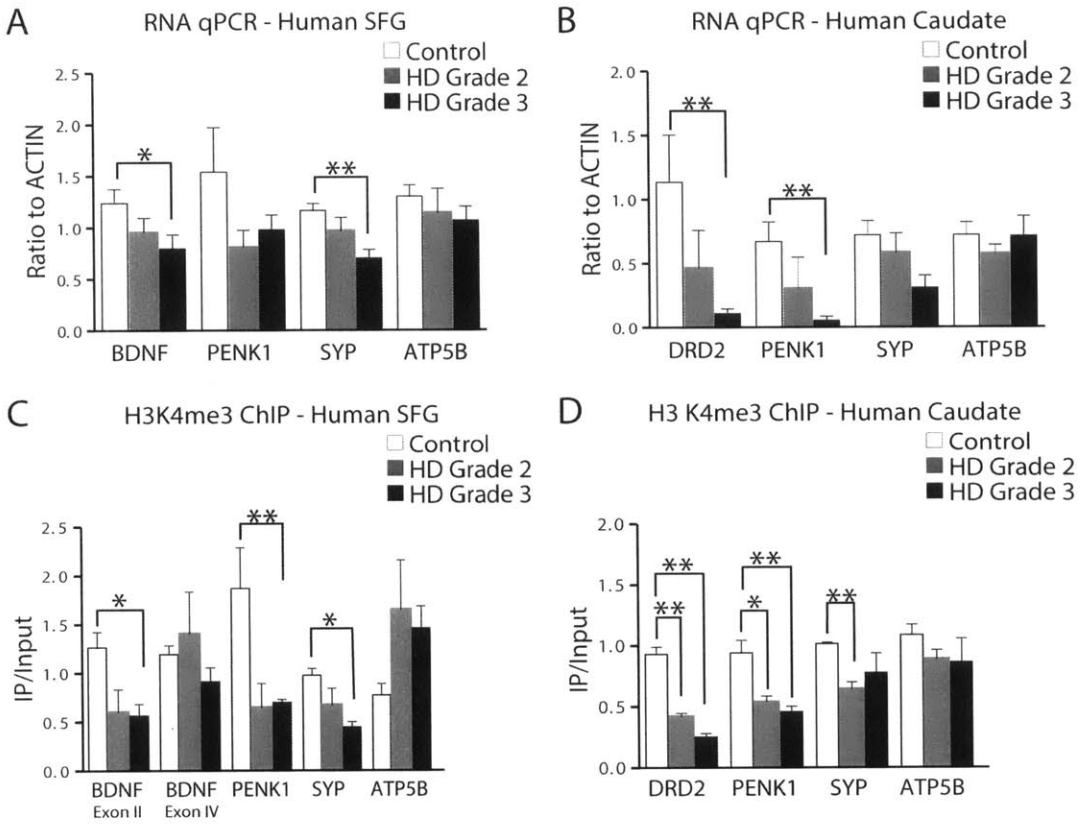

Figure 2-6: Genes with decreased expression in human HD tissue also have decreased H3K4me3 levels. (A) In the **SFG** (cortex), *BDNF* and *SYP* gene **expression** was lower in HD patient samples compared to control (*BDNF* $P < 0.05$; *SYP* $P < 0.01$). *ATP5B* expression did not change, and *PENK1* expression was lower in HD tissues, although the difference did not achieve significance. (B) In the **caudate** (striatum), *DRD2* and *PENK1* **expression** was significantly lower in grade 3 patient samples ($P < 0.01$) than in control levels. *ATP5B* expression did not change, and *SYP* expression trended to decreased expression. (C) In the **SFG**, levels of **H3K4me3** at *BDNF* exon II ($P<0.05$), *PENK* ($P<0.01$), and *SYP* ($P<0.05$) are significantly lower in grade 3 patient samples compared with control ($P < 0.05$), and they are not changed at *BDNF* exon IV promoter. H3K4me3 levels at *ATP5B* promoter are not significantly different between control and grades 2 and 3 patient samples although a trend toward increased occupancy was observed. (D) In the **caudate**, **H3K4me3** levels are significantly reduced at *DRD2* (grades 2 and 3; $P < 0.01$), *PENK1* (grades 2 and 3; $P < 0.05$ and $P < 0.01$, respectively), and *SYP* (grade 2; $P < 0.05$) promoters compared with control caudate samples. The *ATP5B* promoter showed no significant differences in H3K4me3 levels between control and HD samples. For both caudate and SFG, four control samples were compared with three grade 2 and five to six grade 3 samples, and t-tests were performed to calculate statistical significance. *$P < 0.05$; **$P < 0.01$.

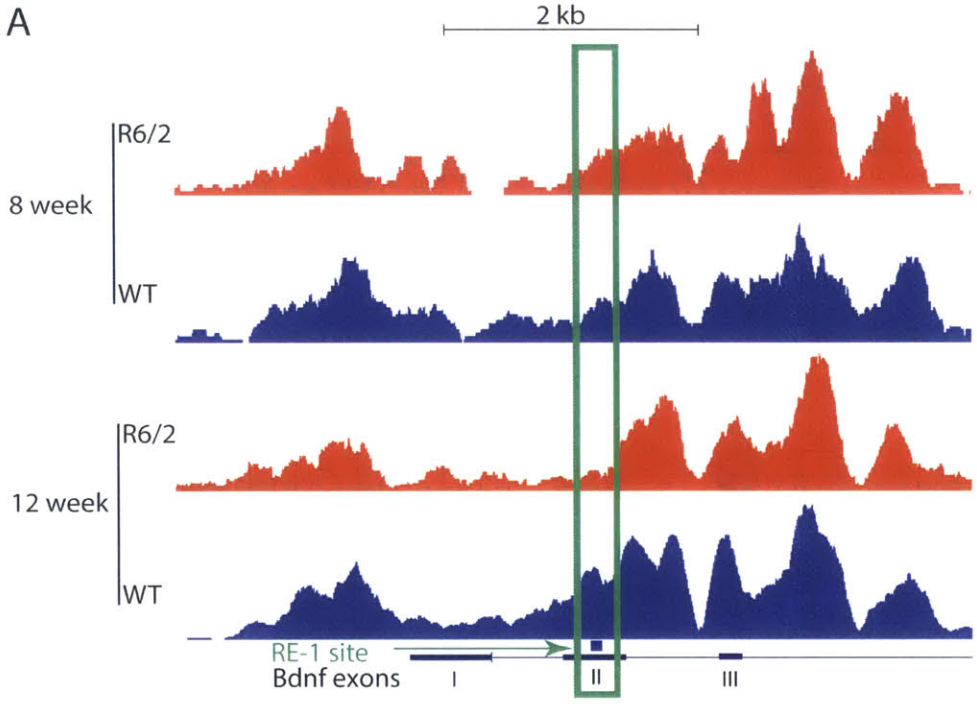

Figure 2-7: H3K4me3 levels are lower at the REST-regulated *Bdnf* promoter in 12wk old R6/2 mouse cortex. This is an expanded view of a 6kb region centered on the REST binding site RE-1 in exon II. The top two tracks are from cortices of 8wk old mice, and the bottom two tracks are from cortices of 12wk old mice. The REST-regulated promoter of *Bdnf*, indicated by the green box, shows a significant difference between the animals at 12wk, whereas this difference is not observed at 8wk. Other regions of the gene are largely unchanged at either 8 or 12wk of age.

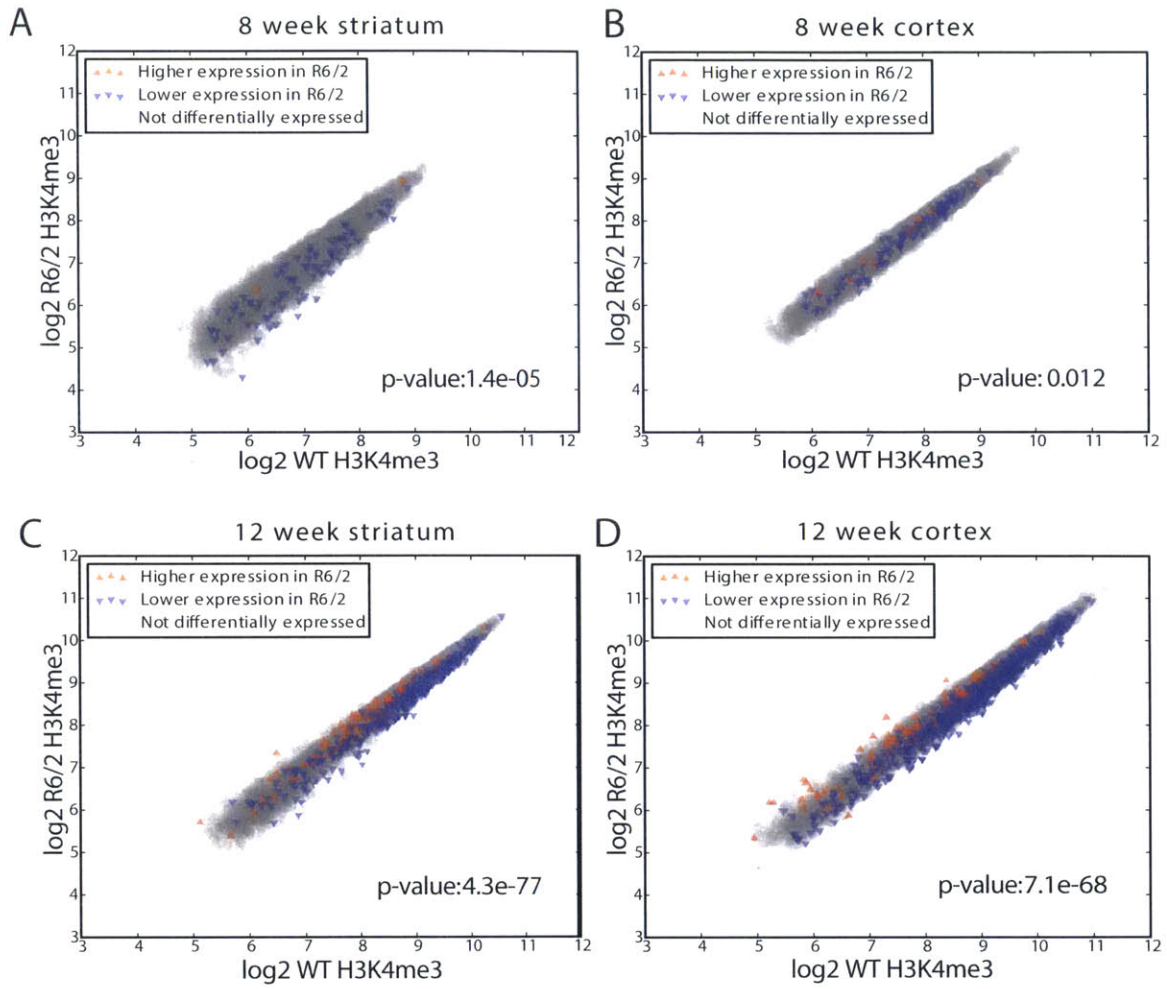

Figure 2-8: Scatter plots for (A) 8wk striatum, (B) 8wk cortex, (C) 12wk striatum, and (D) 12wk cortex show the extent of H3K4me3 signal detected in wildtype animals (x axis) vs. R6/2 animals (y axis) in a 2,000bp window around the primary TSS of each gene with sufficient H3K4me3 coverage. The number of reads in each sample was transformed to log2 and normalized by loess regression. Genes that show higher expression in R6/2 mice (red) and genes with lower expression in R6/2 mice (blue) are indicated. Note that a large group of genes had both lower H3K4me3 (below the diagonal) and expression levels (blue) in R6/2 mouse. P values represent the statistical significance of the overlap between genes downregulated in R6/2 and genes with lower H3K4me3 levels as computed using the hypergeometric distribution.

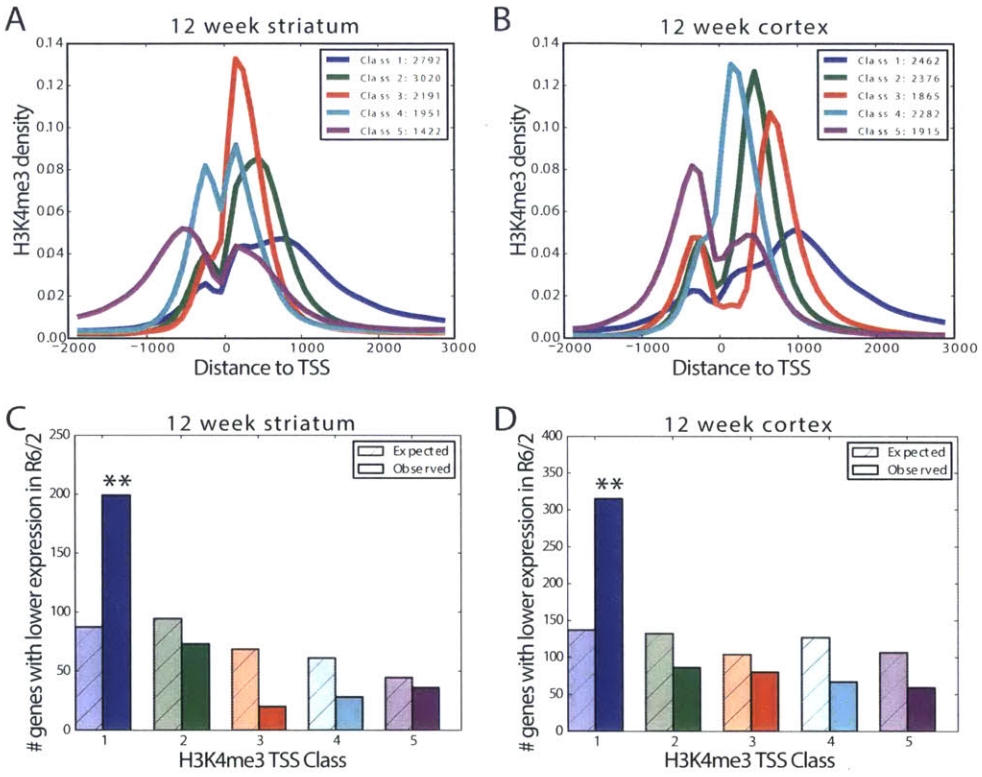

Figure 2-9: Genes downregulated in R6/2 mice have a distinct H3K4me3 profile in **wildtype** animals. Genes were clustered into five groups based on their H3K4me3 profiles in (A) striatum and (B) cortex of 12wk old wildtype animals. Plots show the density of sequence reads in a window from -2 to +3 kb of the TSS. The numbers of genes in each class are listed in A & B insets. Genes in class 1 (blue) show a broad peak of trimethylation starting at the TSS and extending into the coding region. In all datasets, this class is enriched in genes that are expressed at lower levels in R6/2. The numbers of genes with reduced expression expected and observed in each class are shown for (C) 12wk striatum and (D) 12wk cortex. **P<0.01.

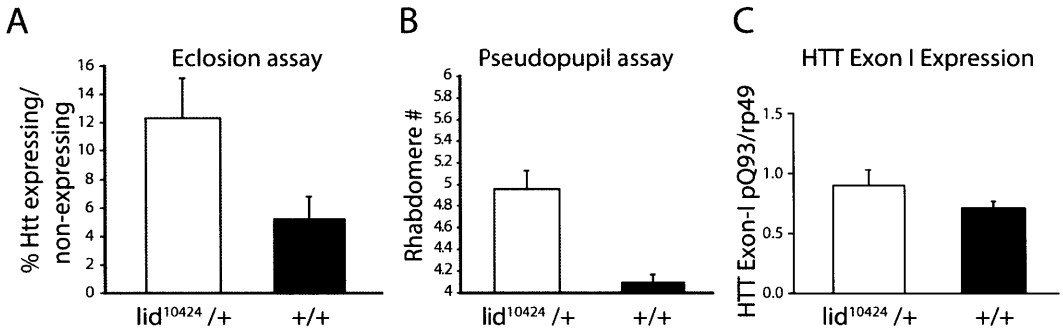

Figure 2-10: Reducing the dose of the demethylase *lid* leads to a significantly higher survival for flies with expanded polyglutamines. (A) The eclosion rate of Htt-challenged flies that were also heterozygous for a null *lid* allele($lid^{10424}/+$) compared with $+/+$ flies was improved (P = 0.013). Significance was measured by Student t test. (B) The effect of reduced levels of the demethylase *lid* on survival of photoreceptor neurons was evaluated by comparing the number of surviving photoreceptors in Htt-challenged animals. In this pseudopupil assay, reducing the dose of functional *lid* genes from two copies to one leads to a substantial improvement in photoreceptor neuron survival (P = 0.0038 comparing $lid^{10424}/+$ with $+/+$ flies). (C) Expression of the *HTT* exon 1 transgene was not altered in the crosses above as determined by qPCR.

Chapter 3

Aberrant Splicing of the Mutant *HTT* Gene Generates A Pathogenic Exon 1 Protein in Huntington's Disease

This chapter was adapted from (Sathasivam et al., 2013; Gipson et al., 2013). I contributed analysis of the *HTT/Htt* exon 1-intron 1 splice site and surrounding sequence, isolation of RNA for RNA-Seq experiments, design of adapted Tru-Seq library preparation, computational analyses of sequencing reads, construction of experimental design, and assisted with figure preparation and manuscript text. This work was supported by the UK Medical Research Council and the Cure Huntington's Disease Initiative (CHDI).

3.1 Introduction

The HTT protein, as mentioned before, is an extremely long ~350Kda protein. Many fragments of HTT have been found in both patient and mouse model tissue. It has been well-established that N-terminal fragments of mutant HTT represent the 'toxic' species (Ross & Tabrizi, 2011) and the search for the proteases that generate HTT

fragments has identified caspase-3 (Wellington et al., 2002), caspase-6 (Wellington et al., 2002), calpains (Kim et al., 2001; Gafni et al., 2004) and matrix metalloproteinase 10 (Miller et al., 2010). However, the potential importance of smaller N-terminal fragments is highlighted by their presence in HD postmortem brains (Difiglia, 1997), their release by formic acid solubilization from brain tissue (Lunkes et al., 2002), and the fact that nuclear inclusions are only detected by antibodies to N-terminal HTT epitopes (Difiglia, 1997; Schilling et al., 2007). In cell models, HTT can be cleaved into small fragments namely cp-A and cp-B (Lunkes et al., 2002) or cp-1 and cp-2 (Ratovitski et al., 2009, 2007) but the proteases responsible for this have not been identified. It has been recently shown that the smallest fragment present in the brains of *Hdh*Q150 knock-in mice is an exon 1 HTT protein (Landles et al., 2010). Analysis of the R6 transgenic mouse lines has previously shown an exon 1 HTT protein is produced by translation of an exon 1 *HTT* transcript (Mangiarini et al., 1996). This led us to investigate whether the exon 1 HTT protein in the *Hdh*Q150 knock-in mice is generated by aberrant splicing rather than proteolytic cleavage.

3.2 Structure of the Mouse and Human Huntingtin Exon 1-Intron 1 Junction

The major eukaryotic 5'-splice site consensus sequence is MAG|GURAGU (M is A or C and R is A or G; -3 to position +6 relative to the exon-intron junction) (Zhang, 1998). The huntingtin 5'-splice site of intron 1, identical in mouse and human, follows the consensus sequence except at positions -2 and -1 where cytosines are present (Figure 3-1A), which is rare (Zhang, 1998). Despite this unusual sequence composition, this splice site is predicted to have high splice site strength based on maximum entropy modeling (Yeo & Burge, 2004). Clustering of G and C repeats in the adjacent downstream intronic sequence likely helps to increase splice site strength, as has been demonstrated for other introns (Xiao et al., 2009). The sequence at the exon 1-intron 1 boundary completes the codon for a proline residue and then terminates in a stop

codon (Figure 3-1B).

3.3 Aberrant Splicing of Mouse *Htt* Exon 1 to Exon 2 Results in A Small Polyadenylated mRNA

3.3.1 Identification of A Small Polyadenylated Huntingtin RNA

The *Hdh*Q150 knock-in mouse model was generated by the insertion of approximately 150 CAGs into exon 1 of the mouse *Htt* gene (Figure 3-2A) (Lin et al., 2001). To determine whether exon 1 of *Htt* mRNA had spliced to exon 2, we used a series of RT-PCR assays on cDNA prepared from the brains of homozygous ($Hdh^{Q150/Q150}$), heterozygous ($Hdh^{+/Q150}$) and wildtype animals at 2 months of age (Figure 3-2B). Nonquantitative end-point RT-PCR products were comparable between all three genotypes for assays that amplified exon 2 and spanned the exon 1-exon 2 junction. In contrast, the levels of the RT-PCR products obtained for the exon 1- intron 1 boundary and for intron 1 sequences upstream of 1.2 kb were more intense in cDNA prepared from the brains of $Hdh^{Q150/Q150}$ as compared to $Hdh^{+/Q150}$ animals, which were in turn more intense than those obtained from their wildtype littermates.

Examination of the genomic sequence for *Htt* intron 1 identified a cryptic polyadenylation signal at positions 677bp and 1233bp. 3'rapid amplification of cDNA ends (RACE) for the first polyA signal showed the presence of a polyadenylated short mRNA in $Hdh^{Q150/Q150}$ and $Hdh^{+/Q150}$ but not wildtype brains (Figure 3-3). Using 3'RACE, we demonstrated this unspliced exon 1-intron 1 transcript was present throughout all brain regions tested (Appendix Figure B-1) as well as in a range of peripheral tissues (Appendix Figure B-2).

3.3.2 Examination of Exon 1-Intron 1 in RNA-Seq Data

To independently verify the presence of the exon 1-intron 1 transcript we employed RNA-Seq on RNA prepared from the cortex of $Hdh^{Q150/Q150}$ and wildtype mice. However, this region of mouse *Htt* proves to be a "dead zone" in RNA-Seq data. Our

very early RNA-Seq data from 2011 showed very little coverage for the entire exon 1 region (Figure 3-4). Mouse and human huntingtin have $> 75\%$ GC content in the first 55 bases downstream of the intron 1 5'-splice site. Similarly upstream, between the CAG repeat and 5'-splice site, there is a tract of $> 80\%$ GC bases in both mouse *Htt* and human *HTT*.

The combination of secondary structure adopted by the CAG repeat (Duzdevich et al., 2011) and the almost 200 bases of extremely high GC content present significant challenges for sequence analysis of the *Htt* exon 1-intron 1 boundary region due to the necessary PCR amplification steps. It is important to note that the low representation of the *Htt* 5' end is partly attributed to 3' bias. We isolate mRNA from the total RNA pool by using magnetic beads with oligo(dT) to bind to the polyA tail. Diminished representation of the 5' end of a gene results when RNA is inappropriately fragmented before this step. If RNA is isolated with a very high RNA integrity score (ratio of 28S to 18S can indicate degradation), the 3' bias is not an issue genome-wide. However, with genes as long as *Htt*, there will always be some loss of the 5' end. An alternative method for amplifying the mRNA signal, rRNA subtraction, is very effective but as that does not remove pre-mRNAs, introns show more signal due to the presence of unspliced transcripts. Given our question dealt with aberrant splicing, we decided to continue with the oligo(dT) pulldown and focus on improving amplification of the exon 1 region.

Two RNA-Sequencing steps involve the amplification of reads: the final PCR amplification of the library and the cluster amplification on the flow cell of the sequencer. Cluster amplification on the flow cell uses formamide to denature DNA fragments, which should adequately denature regions of high structure. However, a study by Aird et al. demonstrated that regions of DNA with $>65\%$ GC content were represented $\sim 1/100$ of mid-GC content reference DNA after library amplification (Aird et al., 2011). Thus we focused on optimizing PCR amplification of our libraries. Our first step was to switch to the Kappa polymerase system, which demonstrated more robust coverage of GC-rich regions than the traditional Phusion polymerase (Quail et al., 2012). Our results were much improved and encouraging of the mis-splicing event

(Figure 3-5A). We systematically evaluated the possible ways in which the sequence coverage could be further improved for this region of the huntingtin gene. Spiking in a GTP analogue (7-deaza-dGTP - reduces stacking interactions) or including DMSO did not significantly enhance the PCR reaction, but addition of betaine at 1M did result in substantially more reliable coverage of the *Htt* exon 1 region (Figure 3-5B).

While library preparation reagents have improved with overall coverage since 2011, without addition of betaine and the use of Kappa polymerase, the exon 1-intron 1 boundary of mutant *Htt* remains elusive as seen in other published HD RNA-Seq data (Appendix Figure B-3). With our adapted RNA-Sequencing protocol, we observed considerable read densities mapping to the first 1.2 kb of intron 1 in $Hdh^{Q150/Q150}$ but not wildtype littermate samples (Figure 3-5B&C). To approximate the percentage of non-spliced transcripts, we compared the 3'UTR read density of full-length *HTT* and the small *HTT* transcript using Mixture-of-Isoforms (MISO) software and found a 12-20% reduction in the full-length mRNA produced in the $Hdh^{Q150/Q150}$ samples (Figure 3-5D).

3.3.3 Aberrant Splicing Occurs in All HD Knock-In Mouse Models and Is Dependent on CAG Repeat Length

We utilized a series of knock-in mouse lines to determine whether aberrant splicing occurred in the context of a wide range of CAG repeats. Some knock-in lines, such as the Q150 (diagramed in Figure 3-2A), have only mouse *Htt* sequence around the CAG locus. Other lines are chimeric for human-mouse *Htt* around the CAG repeat, as diagramed in Figure 3-6A. The repeat sizes and construction of these lines are summarized in Table 3-1. We analyzed RNA at 2 months of age for each of the *Hdh*Q20, Q50, Q80, Q100, Q150 and zQ175 lines and were able to detect the same 3'RACE product in all samples except for *Hdh*Q20 (Figure 3-6B). Quantitative RT-PCR (qPCR) indicated that the spliced full-length *Htt* mRNA levels, as determined by amplifying the exon 1-exon 2 junction (Figure 3-7A) and exon 2 (Figure 3-7B) sequences, were largely comparable between genotypes for Q20, Q50, Q80 and Q100.

However, the full-length *Htt* transcripts were under-represented in the Q150 and zQ175 mice, consistent with a previous report (Giles et al., 2012). qPCR also showed that transcripts containing early intron 1 sequences were highly increased in a gene-dose dependent manner for all lines except *Hdh*Q20 (Figure 3-7C). The level of these transcripts also increased in a polyQ-length dependent manner when comparing the Q50, Q100 and Q150 lines (mouse *Htt* sequences only) or the Q80 and zQ175 lines (human-mouse chimeric *Htt*).

3.3.4 Aberrantly Spliced *Htt* Transcript is Translated and Produces an Exon 1 Htt Protein

Next we sought to determine whether the aberrantly spliced mRNA was translated. We performed RT-PCR on RNA isolated from polysome gradients prepared from homozygous zQ175 and wildtype brains at 2months of age. RT-PCR with primers to *Atp5b* demonstrated that the polysomes isolated from both genotypes were intact (Figure 3-8A). *Htt* early intron 1 sequences were associated with polysomes (fractions 12-18) from zQ175 mice but not wildtype littermates (Figure 3-8B), suggesting the aberrantly spliced transcript is being translated.

As mentioned before, an unspliced exon 1 is followed by a conserved stop codon, resulting in the production of an exon 1 protein that, in all vertebrates, terminates in a proline residue. It has been previously shown that the smallest N-terminal fragment generated in the *Hdh*Q150 lines corresponds to exon 1 Htt (Landles et al., 2010). To determine whether this is also present in other HD models, we performed immunoprecipitation with 3B5H10 (binds polyQ) and western blots were immunoprobed with S830 (binds N-terminus of Htt), MW8 (exon 1 encoded Htt C-terminal neo-epitope (Landles et al., 2010)), and 1H6 (binds Htt region encoded by exon 2/3). A summary diagram of the different antibodies is shown in Figure 3-9A. Comparison of the S830 and MW8 blots reveals that an exon 1 Htt protein (dotted lines) is present in the zQ175, *Hdh*Q100, and *Hdh*Q80 brains but not in those from their wildtype littermates or in the IgG controls (Figure 3-9B,C,&D).

3.4 Aberrant Splicing of Human *HTT* Exon 1 to Exon 2

To extrapolate these findings to human *HTT*, we performed *in silico* analysis and identified nine predicted polyadenylation signals in intron 1 (Appendix Figure B-4). 3'RACE was first performed on brain RNA from 2 month old YAC128 (Slow et al., 2003) mice, which are transgenic for full-length human *HTT*. The polyA signal with the highest predictive score (~7.3 kb) resulted in a polyadenylated transcript. To determine whether the aberrant splicing also occurs in human tissue, we performed 3'RACE for the same cryptic polyadenylation signal as used in the YAC128 mice. The polyadenylated transcript was clearly apparent in two fibroblast lines as well as in the sensory motor cortex of an HD patient with $(CAG)_{42}$ and the cortex of a juvenile HD individual with $(CAG)_{72}$. 3'RACE results for the YAC128 mice and human tissues are shown together in Figure 3-10. Two HD brain samples did not yield 3'RACE product (Figure 3-10, HC76 & HD2), probably reflecting differences in the extent to which the RNA had degraded in these tissues.

3.5 Summary of The Aberrant Splicing of Huntingtin

A summary of the results thus far for mouse *Htt* and human *HTT* is presented in Figure 3-11. Both mouse and human huntingtin have an immediate stop codon at the start of intron 1. Both genes have a cryptic intron 1 polyA site although at different positions within the intron. During transcription, these cryptic polyA sites are prematurely recognized and the resulting transcript is cleaved and translated into an exon 1 protein.

3.6 Splicing Factor SRSF6 May Mediate Mis-Splicing of Mutant Huntingtin

To investigate the underlying mechanism we used bioinformatics to predict regulatory motifs in exon 1 of *Htt* (Figure 3-12A) and mapped the binding site of SRSF6 to a CAG or CAGCAA repeat (Figure 3-12B). RNA co-immunoprecipitation with an antibody to SRSF6 captured *Htt* early intron 1 sequence from homozygous zQ175 mice with a much higher efficiency than those from wildtype brain lysates (Figure 3-12C). Exon 2 transcripts were not immunoprecipitated from either zQ175 or wildtype lysates consistent with SRSF6 binding to the expanded CAG repeat in the zQ175 mice and inhibiting the splicing of exon 1 to exon 2.

3.7 Architecture of the Huntingtin Gene and Its Influence on Splicing

We examined the huntingtin gene architecture more rigorously in an effort to think more broadly about the splicing of huntingtin exon 1-exon 2. The huntingtin gene structure is a good example of some general features that higher eukaryotic genes have acquired during the course of evolution. A number of bioinformatic surveys established that the first intron of a eukaryotic gene tends to be longer than subsequent introns (Bradnam & Korf, 2008; Gaffney & Keightley, 2006; Gazave et al., 2007; Kalari et al., 2006; Kriventseva & Gelfand, 1999; Marais, 2005; Smith, 1988; Zhang & Edwards, 2012) and in humans and mice the first intron tends to be a little less than three times longer than the remaining introns (Bradnam & Korf, 2008). The huntingtin gene is a dramatic example of this feature. Human *HTT* consists of 66 introns with an average intron length of ~2360 bases, while intron 1 alone is comprised of 11,850 bases. This discrepancy is even more pronounced in mice: average intron length is ~2080 bases, whereas intron 1 is 20,632 bases. In many species intron 1 length seems to be positively regulated with the expression level of the respective gene

(Marais, 2005; Jonsson et al., 1992; Palmiter et al., 1991; Rose & Last, 1997; Ho et al., 2001; Jeon et al., 2000; Morello et al., 2002). Furthermore, neuronal genes and genes that are involved in development seem to have a higher content of non-coding DNA, which might assist in the tight regulation of their expression (Gaffney & Keightley, 2006). In plants, the propensity of these elements to influence gene expression was termed intron-mediated enhancement (Mascarenhas et al., 1990; Rose, 2002). However, not much is known about the exact nature of these cis-acting regulatory elements in the first introns of higher animals. To date, there are no annotated non-coding RNAs in either human *HTT* or mouse *Htt* intron 1 (http://www.ensembl.org). There is also no evidence for a cryptic exon, which tends to appear in longer introns (Roy et al., 2008). So the question remains, does intron 1 of huntingtin have any particular cis-regulatory effects on the expression level of the transcript?

An extremely long intron 1 increases the potential for splice factor binding sites. Indeed, splice factor binding sites are scattered all along *HTT* intron 1, but cluster toward the 5'-end (SFmap(Akerman et al., 2009) and ESEfinder(Cartegni, 2003)). Additionally, transcription of longer intronic sequences not only allows for increased spatial, but also increased temporal regulation of splicing. While splicing is thought to usually occur co-transcriptionally (Han et al., 2011), the extreme length of *HTT* intron 1 could open up a kinetic window for additional factors to act on transcription, splicing, and/or cryptic polyadenylation site activation. In addition, the rare splice site sequence discussed earlier might result in a reduction in the kinetics of U1 small nuclear ribonucleoprotein complex recruitment or the higher instability of spliceosomes. This could lead to a delay in splicing and could contribute to the generation of the small, non-spliced polyadenylated transcript.

Another interesting layer of potential regulation is the local chromatin structure of *HTT* intron 1. Polyglutamine repeat expansion could affect a change in chromatin marks or the association of chromatin remodeling machinery, both of which have been shown to influence splicing (Batsché et al., 2005; Luco et al., 2010). Investigation of local chromatin structure might bring further valuable insights into the molecular mechanism by which the *HTT* exon 1 transcript is produced.

3.8 Summary and Implications of Mis-Spliced Product

We have identified a small exon 1-intron 1 polyadenylated mRNA transcript in the brains of all HD mouse models expressing mutant *Htt* (mouse) or *HTT* (human). Furthermore we have shown that the same transcript is also present in fibroblast lines derived from HD patients and in postmortem HD brains. We have shown that the SRSF6 splicing factor binds to the 5' end of the *Htt* gene with an expanded CAG repeat, consistent with its known recognition motif (Akerman et al., 2009). SRSF6 regulates splicing and facilitates translation of partially-spliced transcripts (Tranell et al., 2010; Swanson et al., 2010). SR proteins have also been associated with the displacement of the U1 snRNP (Labourier et al., 1999), a phenomenon that promotes polyadenylation from cryptic polyA signals within introns (Berg et al., 2012). Therefore, an increased association of SRSF6 with expanded CAG repeats could account for the CAG repeat length dependent production of the exon 1-intron 1 transcript. Translation of this transcript produces an exon 1 Htt/HTT protein. A diagram of this model is presented in Figure 3-13.

The pathological consequences of the expression of this aberrantly spliced product in mice have been demonstrated in multiple experiments. The R6 mouse lines are transgenic for a genomic fragment that spans the 5' end of the *HTT* gene, exon 1 and a portion of intron 1 (Mangiarini et al., 1996). Therefore the R6 lines can be considered to be models of aberrant splicing in HD and demonstrate that an exon 1 HTT protein is highly pathogenic, a result that was recapitulated in a set of independent experiments (Benn, 2005). Surprisingly, the late-stage phenotypes of R6/2 mice closely resemble those present in the *Hdh*Q150 knock-in mice (Woodman et al., 2007; Moffitt et al., 2009; Scappini et al., 2007; Labbadia et al., 2011); the main difference between these two models being the age of phenotype onset and rate of disease progression. This suggests that the pathogenic process in *Hdh*Q150 mice could be driven by the same exon 1 HTT fragment differing only in its abundance and accumulation over time.

Our discovery that exon 1 HTT is generated by aberrant splicing will provide the opportunity to test the extent to which an exon 1 protein contributes to disease pathogenesis in the knock-in lines, and the extent to which full-length HTT and/or other N-terminal HTT fragments, generated by proteolytic cleavage, are also pathogenic. RNA-targeted therapeutic approaches designed to lower the levels of *HTT* through the use of antisense oligonucleotides, RNAi or small hairpin RNAs are under development (Sah & Aronin, 2011). Many of these approaches would not prevent the production of exon 1 HTT and should be reviewed in the light of our findings.

3.9 Methods

3.9.1 Mouse Maintenance and Breeding

Hdh$^{Q150/Q150}$ homozygous, *Hdh*$^{+/Q150}$ heterozygous mice and wildtype littermates on a (CBA x C57BL/6) F1 background were obtained by intercrossing *Hdh*$^{+/Q150}$ heterozygous CBA/Ca and C57BL/6J congenic lines as described previously (Woodman et al., 2007). The *Hdh*Q50 and *Hdh*Q100 lines were generated by selective breeding for alterations in germ-line repeat size starting with a C57BL/6 congenic of the *Hdh*Q150 lines (Lin et al., 2001). The *Hdh*+/Q20, *Hdh*+/Q80 (Wheeler et al., 1999; White et al., 1997) and zQ175 (Menalled et al., 2003) knock-in mice were supplied from CHDI colonies maintained at The Jackson Laboratory (Bar Harbor, ME, USA). The *Hdh*Q20, *Hdh*Q50, *Hdh*Q80, *Hdh*Q100 and zQ175 lines were maintained by backcrossing to C57BL/6J (Charles River). All experimental procedures were performed in accordance with UK Home Office regulations. All animals had unlimited access to food and water, were subject to a 12-h light/dark cycle and housing conditions; environmental enrichment was as previously described (Hockly et al., 2003). Genomic DNA was isolated from an ear-punch. *Hdh*Q50, *Hdh*Q100, and *Hdh*Q150 mice were genotyped by PCR; CAG repeat length was measured as previously described (Sathasivam et al., 2010). The *Hdh*Q20 and *Hdh*Q80 mice were genotyped as described (White et al., 1997) using the Hotstart polymerase (Thermo Scientific). The

genotyping primers for zQ175 were as (Menalled et al., 2003) using the R6/2 genotyping protocol (Sathasivam et al., 2010). Dissected tissues were snap frozen in liquid nitrogen and stored at -80°C until further analysis.

3.9.2 RNA-Sequencing

Frozen tissues were homogenized with VWR PowerMax AHS 200 in TRIzol Reagent (Invitrogen). RNA was extracted according to the TRIzol protocol and purified with RNeasy columns (Qiagen). Samples were prepared using a modified strand-specific version of the Illumina Tru-Seq protocol. Illumina's protocol was followed except for strand-specific cDNA synthesis steps that were adapted from (Levin et al., 2010), with one exception for 6month samples, which did not include actinomycin in first-strand cDNA synthesis. The Agencourt Ampure XP system was used to remove dNTPs between first- and second-strand synthesis. Following second-strand cDNA synthesis, samples were run on Beckman Coulter Nucleic Acid Extractor SPRIte and digested with USER mix (New England Biolabs). Final PCR amplification was performed with either Fusion or KAPA HiFi polymerase and GC buffer (Kapa Biosystems). For two of the 22month samples, PCR enrichment included the additive betaine to improve read coverage in the GC-rich regions of the genome. The paired-end, strand-specific cDNA libraries were multiplexed onto the Illumina HiSeq (40 bp reads). Read data was mapped to the mm9 build with the Bowtie alignment program using setting –Best. Splicing was analyzed using the Python/C version of MISO (Katz et al., 2010). A custom General Feature Format (GFF) file was created for the two *Htt* isoforms. Coordinates for the short and long isoforms, respectively: chr5(35,104,760-35,105,959) and chr5(35,251,495-35,255,170). RPKM (Reads Per Kilobase of exon per Million mapped reads) tracks and PSI plots were created with Sashimi-plot, part of the MISO framework. MISO is available at: `http://genes.mit.edu/burgelab/miso/`; Sashimi-plot is available at: `http://genes.mit.edu/burgelab/miso/docs/sashimi.html`. RNA-Seq library statistics are displayed in Appendix Table B-1.

3.9.3 Mouse RT-PCR, Quantitative RT-PCR, and 3'RACE

RNA, RT-PCR, and quantitative RT-PCR were as described (Benn et al., 2008a), except that RNA was reverse transcribed from an oligo-dT primer and quantitative RT-PCR was performed using the SsoFast Probes Supermix (Bio-Rad) with a corresponding cycler program. 3'RACE was performed as described (Scotto Lavino et al., 2007). Bands were excised from gels, cloned (TA cloning kit, Invitrogen), and sequenced (Big Dye Terminator 3.1, ABI) using ABI3730xl DNA analyzer. Primer and probe sequences are detailed in Appendix Table B-2.

3.9.4 Human 3'RACE

Human sample information is included in Appendix Table B-3. RNA from human samples was extracted as previously described (Benn et al., 2008a). A total of 2µg total RNA was reverse transcribed (Invitrogen, Moloney murine leukemia virus) using the UAPdt18 primer. After the RT reaction, the mix was digested with 1U of RNase H (Invitrogen) for 1h at 37°C. The cDNA was subsequently diluted 1:10 in water and 2µL were used as template for the 3'RACE. All PCRs were carried out using the Promega GoTaq system. Each PCR contained 5µL of 5xGreen Flexi Buffer, 2µL 25mM MgCl2, 0.5µL 10mM dNTPs, each 0.5µL of 10mM primers, 2µL cDNA template, 0.125µL GoTaq polymerase, and water to 25µL. PCR protocols for human 3'RACE were as follows: first 3'RACE PCR: 1 cycle 94°C for 2 min; 10 cycles 94°C for 15s, 60°C for 25s, 72°C for 2min; 30 cycles 94°C for 15s, 61°C for 20s, 72°C for 1min 45s; 1 cycle 72°C for 6min followed by cooling to 10°C. Primers were UAPnest and 6568f. Second 3'RACE PCR: 1 cycle 94°C for 2min; 35 cycles 94°C for 15s, 62°C for 20s, 72°C for 1min; 1 cycle 72°C for 6 min followed by cooling to 15°C. Primers were UAPnest and 6621f. Third 3'RACE PCR: 1 cycle 94°C for 2min; 35 cycles 94°C for 15s, 62°C for 20s, 72°C for 20s; 1 cycle 72°C for 6min followed by cooling to 15°C. Primers were UAPnest and 7128f. Bands were excised from gels, cloned (TOPO-TA cloning kit, Invitrogen) and sequenced (Big Dye Terminator 3.1, ABI) using ABI3730xl DNA Analyzer. Primer sequences are listed in Appendix Table B-4.

3.9.5 Polysome Gradients

The 10-40% (wt/vol) sucrose stock solutions were prepared in 50mM Tris-Cl (pH 6.6), 140mM NaCl, and 12mM magnesium chloride. Immediately before use, cycloheximide (200µg/mL) and 1 mM DTT were added. Sucrose gradients were prepared as discontinuous gradients of 2mL layers of 40%, 32.5%, 25%, 17.5%, and 10%. Starting with 40% sucrose, each layer was frozen on dry ice before the next layer was put on top. The gradient was allowed to thaw overnight at 4°C whereby a continuous gradient was created by diffusion. Mouse brain tissue was lysed in freshly prepared polysome buffer [10mM TrisCl(pH 7.4), 140mM NaCl, 12mM magnesium chloride, 1% (wt/vol) Triton X-100, 1 mM DTT, 200µg/ml cycloheximide, 0.5U/µL RNAsin, and 10mM ribonucleoside vanadyl complex]. Lysates were used immediately and never frozen. Samples were centrifuged twice at 13,000xg at 4°C for 5min, and each time the supernatant was transferred to a new tube. A volume corresponding to 250µg absorbance at 260nm was layered on the 10-40% sucrose gradients. The gradients were centrifuged at 115,000-260,000xg at 4°C for 1h 40 min in a SW41-Ti swing out rotor. Fractions (18, 570µL) were collected and 300µL of each fraction were extracted twice with 800µL of a 1:1 mixture of phenol (equilibrated in 0.15M sodium acetate pH 5.3) and chloroform/iso-amyl alcohol (49:1). For each extraction, samples were rigorously mixed, centrifuged at 13,000xg at room temperature for 2min and the supernatant was transferred to a new tube. RNA was precipitated overnight at -20°C with a 1:1 mixture of ethanol and isopropanol (two times the volume of the sample) and 3M sodium acetate pH 5.3 (one-sixth the volume of the sample). Samples were centrifuged at 13,000xg at 4°C for 1h, washed with 0.5mL 70% (vol/vol) ethanol, dried, and resuspended in an equal volume of water. An equal volume of each sample was reverse transcribed using random hexamers. The cDNA was diluted 1:5 with water before quantitative RT-PCR analysis. For gel visualization, RNA was mixed with 2 times the volume of loading buffer [85% (vol/vol) formamide, 10% (vol/vol) glycerol, 8.5mM Tris-Cl pH 7.4, 0.004% (wt/vol) bromophenol blue], denatured for 5min at 65°C and analyzed on a 1.3% (wt/vol) agarose in 1xTAE gel (40mM Tris-acetate,

1mM EDTA, pH ~8.3) with 5V/cm.

3.9.6 Antibodies, Immunoprecipitation, and Western Blotting

3B5H10 (Sigma) is a monoclonal antibody that was raised against an N-terminal 171 amino acid fragment of HTT with 65Q and detects a polyQ tract (Peters-Libeu et al., 2005). S830 is a sheep polyclonal antibody raised against exon 1 HTT with 53Q (Sathasivam, 2001). MW8 is a monoclonal raised against the peptide AEEPLHRP at the C terminus of exon 1 HTT (Ko et al., 2001). 1H6 is a monoclonal antibody that recognizes SLRNSPEFQKLLGI (Lunkes et al., 2002). Six mg of epoxy-activated magnetic beads (Dynabeads M-270 Epoxy; Invitrogen) were washed four times with 0.5mL PBS. The beads were finally resuspended in 100µL PBS and mixed with 100µL of 3B5H10 antibody (1mg/mL). Slowly and under constant mixing, 100µL of 3M ammonium sulfate (in 0.1M sodium phosphate pH 7.4) were added. The tube was sealed and incubated at 30°C overnight with constant motion. Beads were washed twice for 1h with 0.5mL of Tris-Cl pH 8.8. Following this, beads were washed two times with 0.5mL PBS, two times with 0.5mL PBS/0.5% Triton X-100, and finally resuspended in 400µL PBS (supplemented with 0.2millig/mL BSA and 0.02% sodium azide). Immunoprecipitation, Western blotting, and immunoprobing were performed as previously described (Landles et al., 2010).

3.9.7 *SRSF6* RNA Coimmunoprecipitation

Mouse brain tissue was lysed in freshly prepared Triton buffer (50 mMHEPES/NaOH pH 7.6, 160mM NaCl, 7mM magnesium chloride, 3mM calcium chloride, 5mM potassium chloride, 1% (v/v) Triton X-100, 1mM phenylmethylsulfonyl fluoride, 0.5 U/µL RNAsin and complete protease and phosphatase inhibitor mixture). Lysates were used immediately and never frozen. Samples were centrifuged twice at 13,000xg at 4°C for 5min, and each time the supernatant was transferred to a new tube. Supernatant corresponding to 2mg total protein was immunoprecipitated for 5h on a rotating wheel at 4°C. Each reaction contained 9µL of protein G Dynabeads (prewashed

for 1h at 4°C in Triton buffer with 1mg/mL BSA), 3µg of anti-SRSF6 antibody (LS-B5712; LifeSpan BioSciences), and Triton buffer to a final volume of 400µL. Following immunoprecipitation, the magnetic beads were washed four times with 0.5mL Triton buffer, and finally resuspended in 300µL of AE buffer (50mM sodium acetate pH 5.3, 10mM EDTA pH 8.0). RNA was extracted by adding 300µL of phenol (equilibrated in 0.15M sodium acetate pH 5.3) and 100µL of chloroform/iso-amyl alcohol (49:1). Samples were rigorously mixed, centrifuged at 13,000xg at room temperature for 2min and the supernatant was transferred to a new tube. RNA was precipitated overnight at -20°C with a 1:1 mixture of ethanol and isopropanol (2 times the volume of the sample), 3M sodium acetate pH 5.3 (one-sixth the volume of the sample), and 40µg of glycogen. Samples were centrifuged at 13,000xg at 4°C for 1h, washed with 0.5mL 70% (vol/vol) ethanol, dried, and resuspended in water. An equal volume of each sample was reverse transcribed using random hexamers. The cDNA was diluted 1:5 with water before quantitative RT-PCR analysis.

3.9.8 Bioinformatics and Statistics

To predict splice factor binding sites, the following websites were used: RegRNA (`http://regrna.mbc.nctu.edu.tw/index.php`) (Huang et al., 2006; Smith et al., 2006) and ESEfinder 3.0 (`http://rulai.cshl.edu/cgi-bin/tools/ESE3/esefinder.cgi`) (Cartegni et al., 2003). To predict human polyadenylation sites, the intron 1 sequence of the human *HTT* gene was analyzed with the Softberry POLYAH algorithm (`http://linux1.softberry.com/all.htm`).

3.10 Figures and Tables

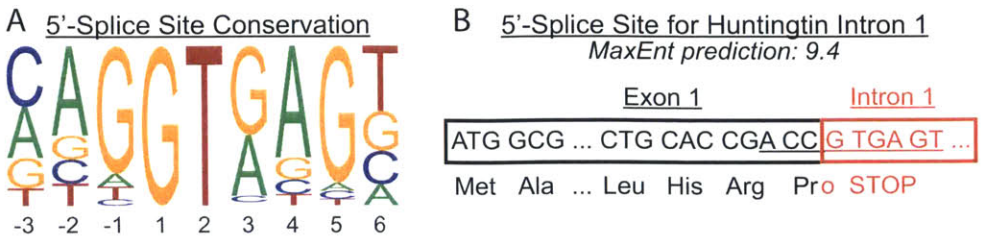

Figure 3-1: (A) 5'-splice site consensus sequences for high GC isotopes showing nucleotide conservation at the respective positions (plotted with data from (Zhang, 1998)). (B) The exon 1-intron 1 junction is conserved between human and mouse and predicted to be a strong splice site. There is an in-frame stop codon within the first four bases of intron 1.

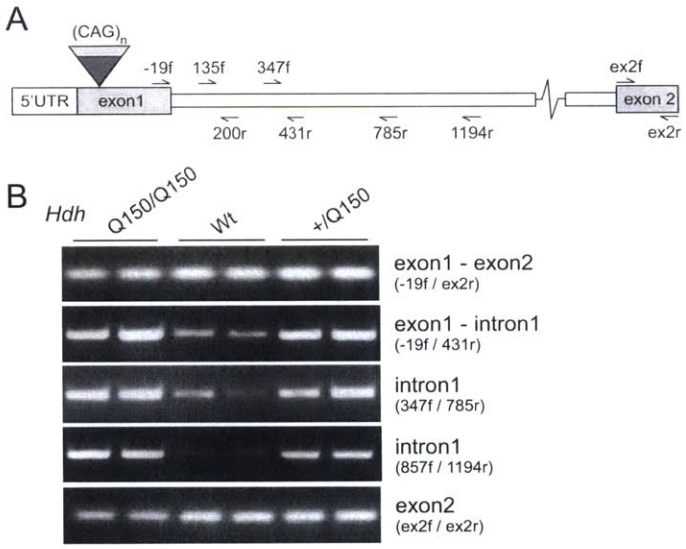

Figure 3-2: (A) Diagram of Hdh^{Q150} *Htt* allele with placement of primer pairs. (B) RT-PCR of *Htt* exon 1, intron 1, and exon 2 regions.

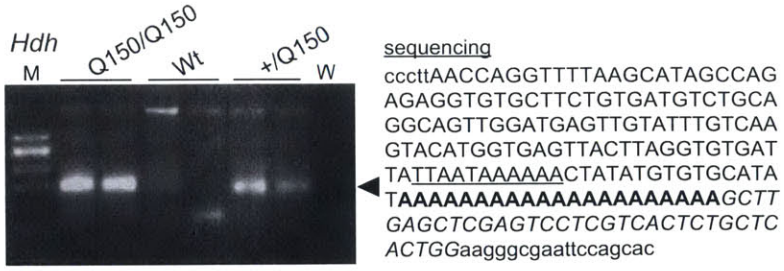

Figure 3-3: 3' RACE product was generated from mutant brain RNA but not from wildtype controls. The cryptic polyadenylation signal is underlined, the polyA tail is in bold, the primer sequence in italics, and the vector sequence in lowercase.

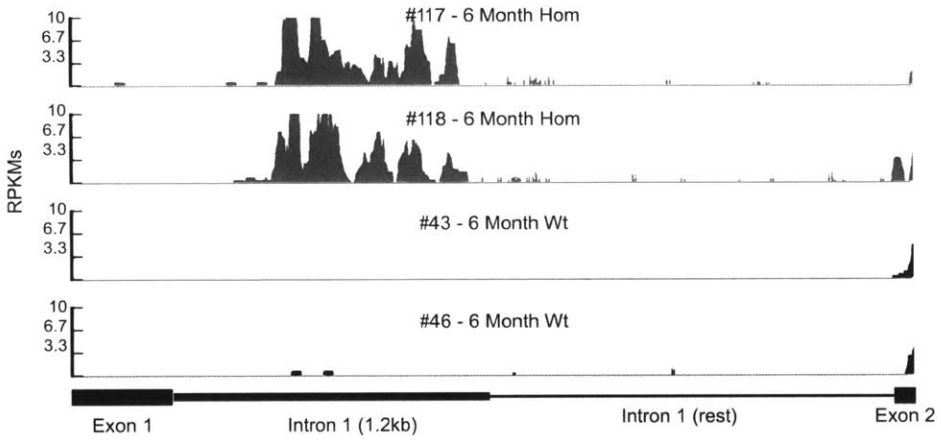

Figure 3-4: RNA-Seq of RNA from cortex of 6 month old homozygous (gray) and wildtype (black) mice. Reads were mapped to *Htt* exon 1-exon2. There are few reads mapping to exon 1, but a large read density mapping to the intron in mutant animals.

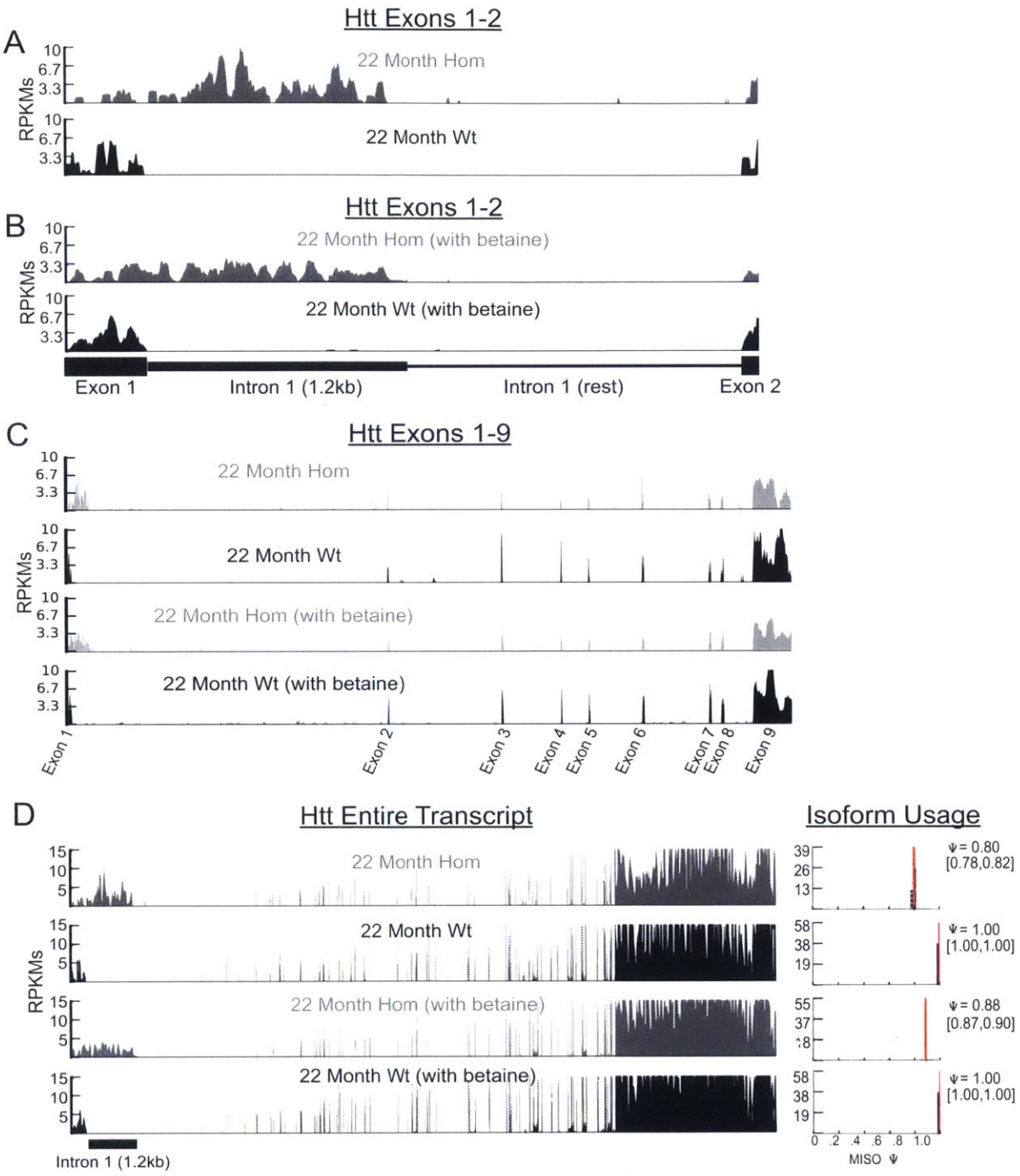

Figure 3-5: (A) RNA-Seq reads from cortex of 22month $Hdh^{Q150/Q150}$ and wildtype mice mapping to the *Htt* exon 1-exon 2 region. Final library amplification was performed with Kappa polymerase. (B) Same as in (A) but these libraries were amplified using the additive betaine. (C) A zoomed out view of the first 9 exons of *Htt* for comparison to exon 1. Note in this plot, the intron 1 region to which reads map is scaled as an intron in this representation whereas it is scaled as an exon in A, B, and D for clearer view. Introns are scaled by 50 and exons by 4. (D) RNA-Seq reads mapping to the entire *Htt* gene. Psi plots predict that normal splicing occurs in 88% and 80% of $Hdh^{Q150/Q150}$ transcripts.

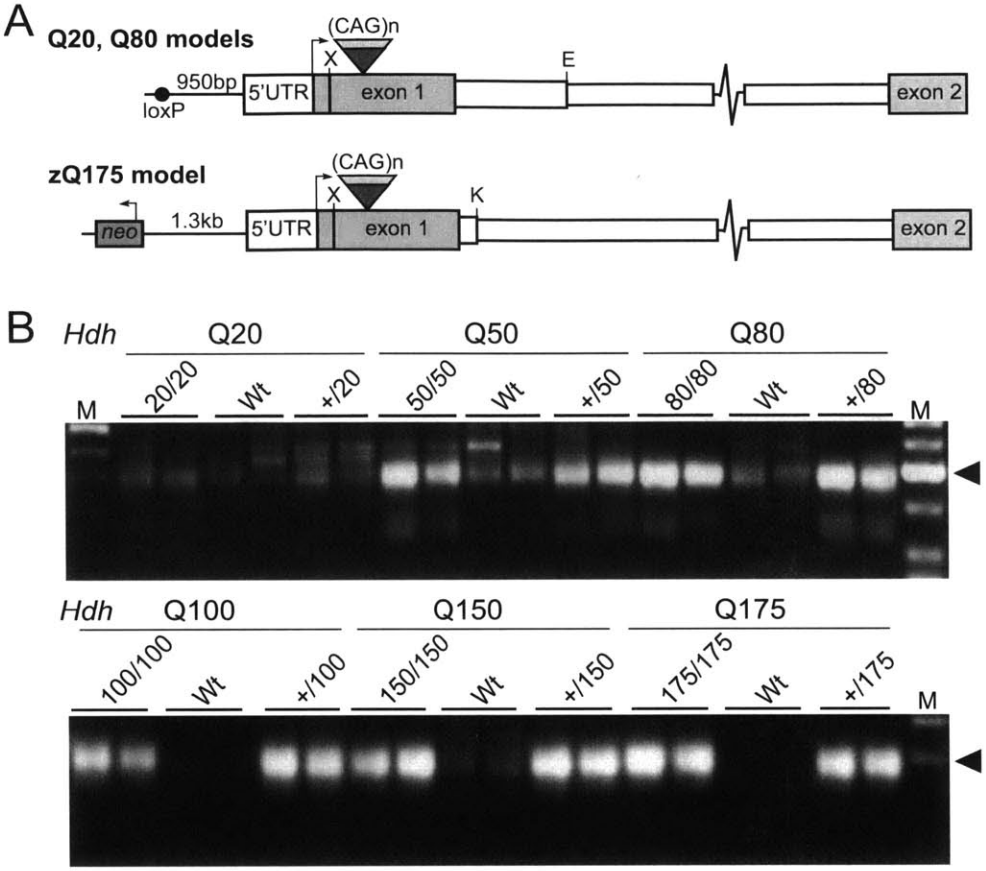

Figure 3-6: 3'RACE product in all expanded polyQ mouse lines. (A) Schematic representations of chimeric human-mouse *Htt* genes in the *Hdh*Q20, *Hdh*Q80, and zQ175 lines. The 5'UTR and first 28 bp of exon 1 are always of mouse origin, whereas the remaining exon 1 sequence is human. The *Hdh*Q20 and *Hdh*Q80 lines contain 268 bp of human intron 1, 124 bp of mouse intron 1 is deleted, and there is a loxP site 5' to the ATG. Line zQ175 contains 10 bp of human intron 1 with 94 bp of mouse intron 1 deleted and an intact neo-cassette 1.3-kb 5' to the ATG. X, XmnI; E, EcoRV; K, KpnI; ♦, cryptic polyadenylation signal. (B) 3'RACE product is present in all lines except *Hdh*Q20.

Mouse *Htt* Sequence Only	
Mouse Line	**Repeat Size**
*Hdh*Q50	59 ± 0.62
*Hdh*Q100	110 ± 1.34
*Hdh*Q150	167 ± 8.18

Human-mouse chimeric *Htt*	
Mouse Line	**Repeat Size**
*Hdh*Q20	17 ± 0.46
*Hdh*Q80	81 ± 0.72
zQ175	189 ± 7.85

Table 3-1: CAG repeat sizes of different HD knock-in mouse models.

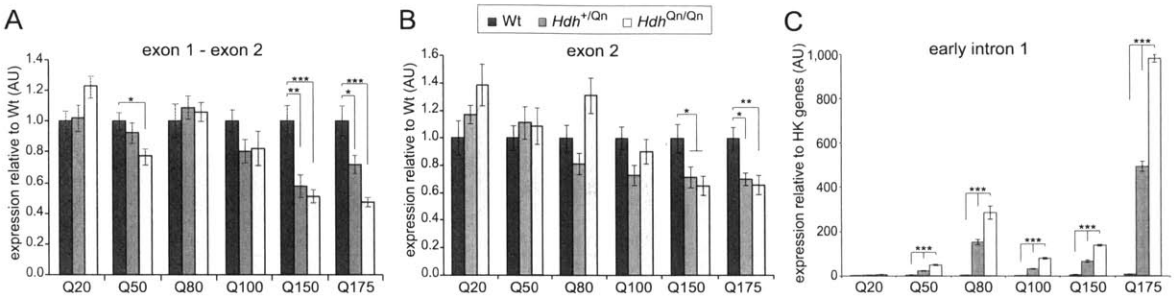

Figure 3-7: The levels of the (A) spliced exon 1-exon 2 and (B) exon 2 transcripts are shown relative to wildtype. (C) The expression level of early intron 1 transcripts is shown relative to the geometrical mean of three housekeeping genes (*Atp5b*, *Eif4a3*, *Sdha*). n = 8/genotype; *P $<$ 0.05; **P $<$ 0.01; ***P $<$ 0.001. Data are mean ± SEM.

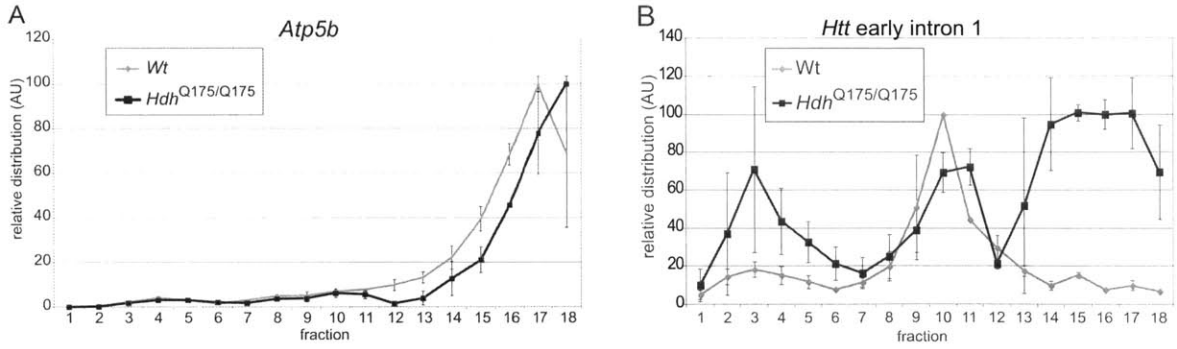

Figure 3-8: Polysome gradients showing the relative distribution of (A) *Atp5b* and (B) early *Htt* intron 1 transcripts. Data are mean ± SEM, n=2.

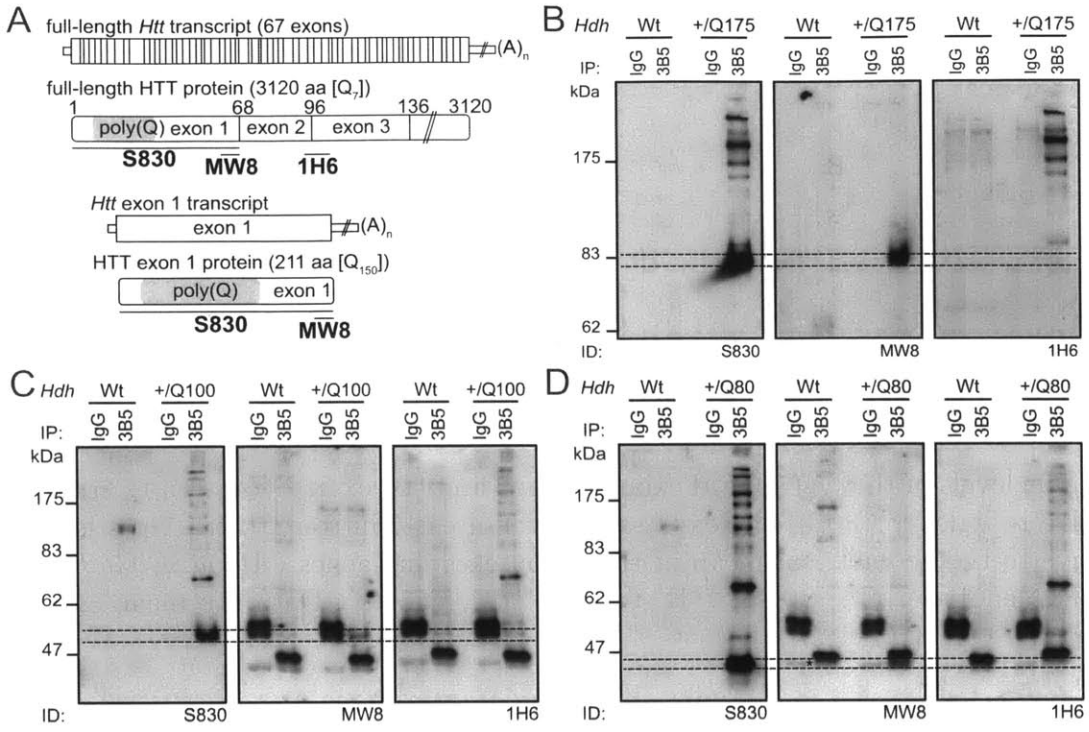

Figure 3-9: An exon 1 Htt protein is found in expanded polyQ mouse lines. (A) Schematic shows the position of the Htt antibody epitopes. (B-D) Htt proteins were immunoprecipitated with 3B5H10- or IgG-coupled magnetic beads from wildtype and (B) zQ175, (C) *Hdh*Q100, and (D) *Hdh*Q80 mice and western immunoblots were immunoprobed with S830, MW8, and 1H6 antibodies. Dotted lines indicate the gel migration of the exon 1 Htt proteins; due to the polyglutamine tract these do not migrate as predicted by their molecular weight.

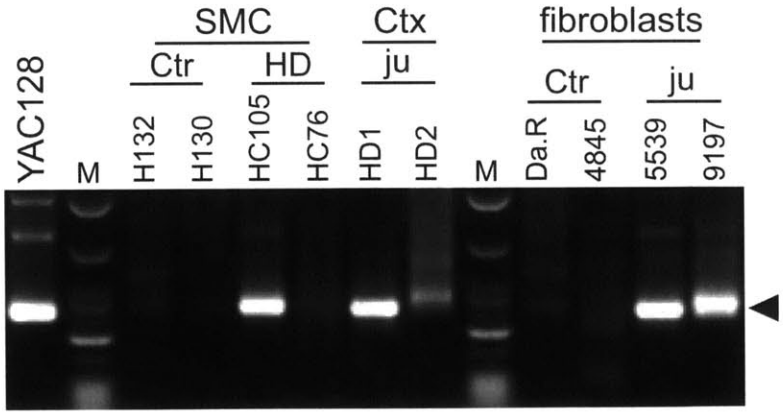

Figure 3-10: 3'RACE of human *HTT*. The expected RACE product size is about 260 bp; Ctr, control subject; Ctx, cortex; HD, adult onset HD; ju, juvenile-onset HD; M, low-molecular-weight markers (New England Biolabs); SMC, sensory motor cortex.

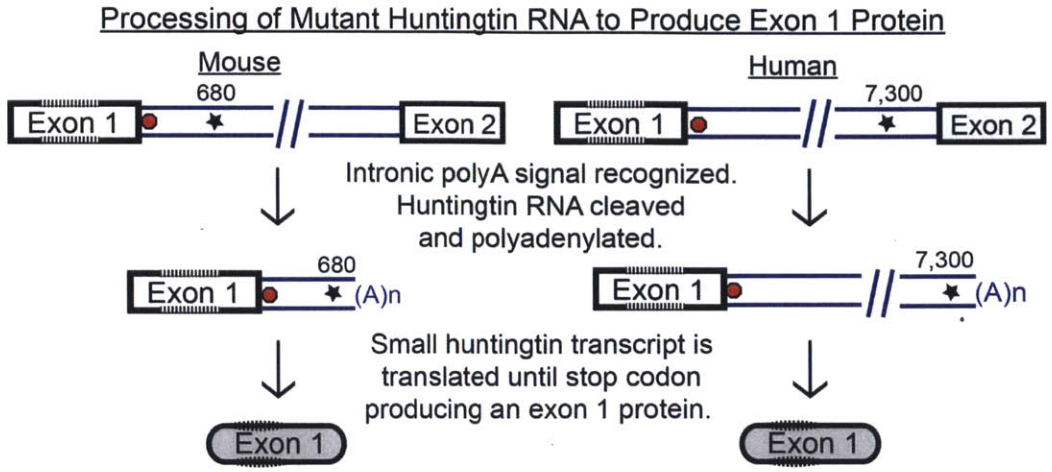

Figure 3-11: Diagram of aberrant splicing of mouse and human mutant huntingtin. Both mouse and human huntingtin RNA have a stop codon (red octagon) immediately in intron 1. There is a cryptic polyA signal ($\star$) 680 bases into mouse intron 1 and 7,300 bases into human intron 1.

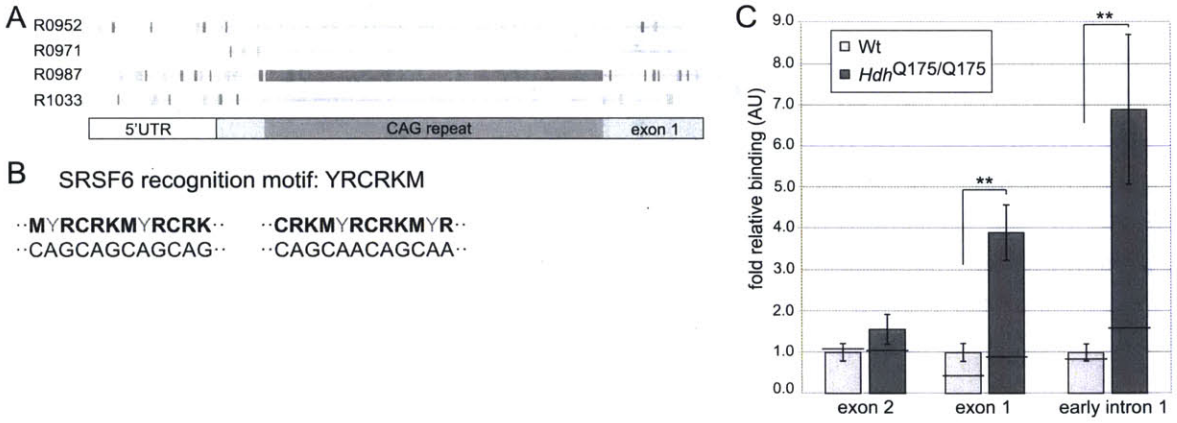

Figure 3-12: The splicing factor SRSF6 binds to expanded CAG repeats in *Htt* transcripts. (A) RegRNA predicts a cluster of R0987 regulatory motifs (CTGN) in the expanded CAG repeat of *Htt*. Using ESEfinder 3.0, this motif was mapped to the binding site of SRSF6. (B) The RNA recognition motif of SRSF6 is YRCRKM, closely resembling a CAG or CAGCAA repeat. Nucleotide abbreviations: Y, T or C; R, A or G; K, G or T; M, A or C. (C) RNA-IP of SRSF6 from zQ175 brain resulted in the coprecipitation of higher levels of early intronic and exon 1 transcripts compared with wildtype. In contrast, the coprecipitated levels of zQ175 and wildtype exon 2 transcripts were not significantly different. n = 6/ genotype. Horizontal bar, IgG control immunoprecipitation. Data are mean $\pm$ SEM; **P $<$ 0.01.

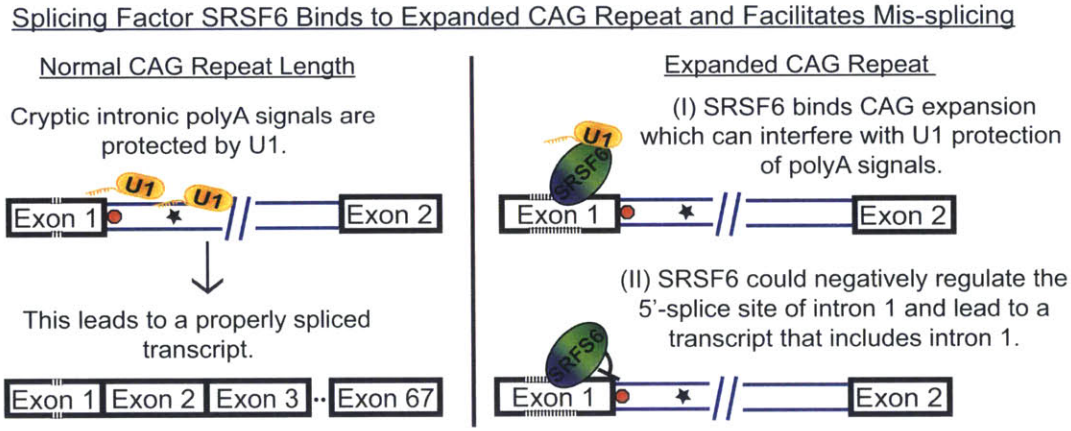

Figure 3-13: Involvement of SRSF6 in *HTT* mis-splicing. We propose that SRSF6 binds to the expanded CAG repeat (hash marks). Two possible scenarios could arise from this: SRSf6 binding could interfere with U1 snRNP protection of the cryptic polyA signals in intron 1 by depleting the local pool of U1 snRNP by direct interaction; or SRSF6 binding interferes with the assembly of a stable and productive spliceosome at the 5'-splice site.

Chapter 4

Mis-splicing in CAG Repeat Disorders

I would like to thank Andreas Neueder, Annie Sittler, and Andrew Lieberman for their generous contribution of tissue samples, sequencing data, and discussion to this study and Charlotte Albright for assistance in RNA-Seq library preparation. This work was supported by the Cure Huntingtin's Disease Initiative and Hereditary Disease Foundation.

4.1 Introduction

After identifying the mis-spliced mutant *HTT* transcript, we began to think on a genome-wide level about mis-splicing in CAG repeat disorders. We had RNA-Seq data available on skeletal muscle from the R6/2 HD mouse model as well as mouse models for two other CAG repeat disorders: Spinocerebellar ataxia 7 (SCA7) and Spinal-bulbar muscular atrophy (SBMA). Skeletal muscle wasting, as will be discussed below, is a severe peripheral symptom in most CAG disorders and proper muscle function is highly reliant on a specific program of alternative splicing. All three polyQ proteins involved in these disorders have been implicated in general splicing alterations, but an in-depth examination of splicing has not been performed. By examining all three disorders in parallel we can determine what disease specific splicing alterations may

exist and what splicing alterations may be a general polyQ consequence.

4.2 SCA7 and SBMA

Long CAG repeats occur at several sites throughout the genome outside of the *HTT* locus and are prone to expansion. As in HD, these expanded repeats often result in pathogenic disturbances. In total, there are nine disorders that are attributed to pathogenic expansion of CAG repeats; these are summarized in Table 4-1. Here we focus on Spinocerebellar ataxia 7 (SCA7) and Spinal-bulbar muscular atrophy (SBMA).

SCA7 is a neurodegenerative disorder characterized by ataxic (uncoordinated) gait, dysarthria (unclear speech), dysphagia (difficulty swallowing), and muscle atrophy (David et al., 1998; Johansson, 1998; Benton et al., 1998). The cause is a CAG repeat expansion in the ataxin-7 (*ATXN7*) gene, with $(CAG)_{\geqq 37}$ alleles fully penetrant (Johansson, 1998). The normal *ATXN7* gene encodes a component of the STAGA transcriptional activator complex (Helmlinger et al., 2004) and is expressed throughout many tissues (Cancel et al., 2000; Jonasson et al., 2002). The mutant ATXN7 protein does misfold and causes intranuclear inclusions similar to HTT (Holmberg, 1998). Despite many tissues expressing the mutant *ATXN7* gene, only the cerebellum, brainstem, and retina demonstrate severe degeneration (Martin et al., 1994).

SBMA, similar to SCA7, is characterized by dysarthria and dysphagia, but is accompanied by more extensive weakness of facial muscles. In addition, individuals with SBMA experience twitching, cramping, and weakness in the arms and legs as well as hormonal abnormalities (Sperfeld et al., 2002; Dejager et al., 2002; Katsuno et al., 2006). The causal mutation is a CAG expansion in the androgen receptor (*AR*) gene on the X chromosome and affects only men. Alleles of $(CAG)_{\geqq 40}$ are fully penetrant. Upon binding by hormone ligand, the normal androgen receptor translocates into the nucleus and binds DNA, regulating transcription of androgen responsive genes (Bolton et al., 2007). The mutant androgen receptor unfolds upon ligand binding

and forms intranuclear inclusions (Katsuno et al., 2002; Takeyama et al., 2002). As noted in the previous CAG disorders, despite widespread expression of the mutant polyQ protein, cellular degeneration is restricted to specific tissues. For SBMA, these regions include the brainstem and spinal cord (Lieberman & Fischbeck, 2000).

To summarize, HD, SCA7, and SBMA are three of nine CAG repeat expansion disorders. Mutant polyQ proteins misfold, form inclusions, and disrupt many cellular processes through both gain and loss of function mechanisms. Interestingly, all three of the affected genes are involved in transcriptional regulation, and, naturally, transcriptional dysregulation is a common molecular consequence of the polyQ expansion. The genetic context of the CAG expansion determines specific regions within the CNS that degenerate. Although cell death only occurs in CNS regions, peripheral tissues do exhibit significant dysfunction in all three disorders.

4.3 Severe Muscle Pathology, An Early And Severe Symptom

In many CAG disorders, the bulk of research has focused on CNS pathology because the CNS is the site of extensive degeneration and strongly linked to phenotypic manifestations of the disease. Recently, however, an effort has been made to study CAG disorders from a systemic perspective. An emerging peripheral phenotype common to the CAG disorders is severe muscular dysfunction.

Muscle dysfunction is an early feature in HD. Muscle from pre-symptomatic HD individuals shows a one-third decrease in ATP generation (Lodi et al., 2001). One pre-symptomatic individual, a marathon runner, developed severe muscle fatigue and pain prior to choreic manifestation (Kosinski et al., 2007), suggesting additional stress can expedite the deterioration of muscle. Muscle biopsies from HD patients with a clinical diagnosis exhibit an even more significant impairment in ATP generation than pre-symptomatic individuals (Lodi et al., 2001). Gene expression studies from these muscle biopsies demonstrate a transition from fast-twitch to slow-twitch fiber com-

position (Strand et al., 2005). Muscle cultures from patients exhibit HTT aggregates (Ciammola et al., 2006), elongated and morphologically compromised mitochondria (Ciammola et al., 2011), and impaired PGC-1α activity (Chaturvedi et al., 2009). Both transgenic and knock-in mouse models faithfully recapitulate these disease processes (Ribchester et al., 2004; Chaturvedi et al., 2009; Gizatullina et al., 2006; van der Burg et al., 2009; Zielonka et al., 2014).

Muscle has not been extensively studied in SCA7 despite commonly observed muscle atrophy in patients. Muscle biopsies that have been examined from individuals with SCA7 do display intranuclear inclusions, autophagic vacuoles, mislocalized mitochondria, and impaired activity of mitochondria complex IV and I activity (Forsgren et al., 1996; Ansorge et al., 2004). SCA7 model mice do suffer from early muscle wasting (Yoo et al., 2003) and have abnormal muscle mitochondria (Han et al., 2010).

Early signs of SBMA are muscle cramping and elevated creatine kinase levels in the serum. Muscle biopsies from SBMA patients exhibit both hypertrophic and atrophic fibers. Fibers have structural changes such as fiber splitting and nuclei clumping, and even replacement of muscle fibers with adipose tissue is observed (Sobue et al., 1989). The AR113Q SBMA knock-in mouse model recapitulates these myopathic changes around 10-13 weeks, long before degeneration of the spinal cord is evident at $\sim$24 months (Yu et al., 2006). For example, hind-limb muscle of AR113Q mice has large rounded muscle fibers with central nuclei. Intranuclear inclusions comprised of mutant AR are visible. A reduction of neurotrophic factors NT-4 and GDNF is found in the muscle of mutant animals. Together, these early myopathic and neurotrophic changes may facilitate spinal cord neuron dysfunction and degeneration in a non-cell autonomous manner (Yu et al., 2006).

4.4 The Therapeutic Benefit of Rescuing Muscle in CAG Expansion Disorders

A testament to the intrinsic and severe nature of muscle pathology in CAG expansion disorders is the therapeutic benefit from therapies administered peripherally in disease models. For example, using a knock-in model of SBMA, Lieberman et al. demonstrated that subcutaneous administration of antisense oligonucleotides suppressing mutant *AR* expression could rescue deficits in muscle weight, fiber size, grip strength, and muscle transcriptional dysregulation, as well as extend lifespan (Lieberman et al., 2014). SBMA mouse phenotype can also be improved with peripheral overexpression or administration of IGF-1, suggesting trophic support in the muscles slows degeneration of spinal cord neurons (Rinaldi et al., 2012; Palazzolo et al., 2009).

A similar phenotypic rescue was observed in transgenic HD mice expressing another transgene - mutant heat shock transcription factor 1 (*HSF1*). *HSF1* induces expression of many heat shock genes and signals a cellular program to prevent abnormal protein folding and aggregation. The *HSF1* mutant in the HD transgenic mice was more readily activatable due to a mutation in a domain that suppressed trimerization, a necessary step for DNA binding. The double transgenics (mutant *HTT* / mutant *HSF1*) had reduced aggregates in muscle, reduced muscle weight loss, and reduced muscle fiber structural defects compared to the single mutant *HTT* transgenics. Interestingly, the lifespan of these mice was significantly improved even though the active *HSF1* was only expressed in the heart, stomach, spleen, muscle, and testis (Fujimoto et al., 2005).

These findings do not suggest that muscle pathology is completely intrinsic. But the therapeutic rescue illustrates that a considerable contribution to muscle pathology comes from peripheral disturbances by mutant huntingtin.

4.5 The Role of Splicing in Muscle

Proper muscle structure and function relies on an extensive alternative splicing program. More than 90% of human genes have alternative splicing (Wang et al., 2008) and most of the alternative events are regulated by tissue type. Muscle, brain, testis, and heart display the most alternative splicing events, consistent with their very specialized functions. The muscle-specific splicing program consists of $>$ 1,000 alternative splicing events (Castle et al., 2008). And the muscle splicing signature is largely retained across mammals and is even found in chicken (Merkin et al., 2012).

Alternative splicing is a delicately coordinated process and there are several tissue specific splicing factors known to be important regulators of the alternative splicing in muscle. Deep sequencing of a conditional *Rbfox1* knockout mouse identified 209 mis-splicing events in muscle. Many genes in which these events occur are involved in calcium regulation and cytoskeleton maintenance. These mice displayed reduced myofiber size, I-band disorganization, perturbed calcium homeostasis, and reduced force generation (Pedrotti et al., 2015). Other important muscle splicing factors include RBM24 (Yang et al., 2014) and the muscleblind-like proteins (Konieczny et al., 2014).

4.6 Mutant PolyQ Proteins and Splicing

Our RNA-Seq data on HD muscle has shown transcriptional dysregulation of two alternative splicing factors (Figure 4-1A). On the protein level, RNA-binding proteins are amongst the interacting partners that have disrupted interactions with mutant Htt and are sequestered in intracellular aggregates. A summary table of identified aberrant interactions between splicing involved proteins and mutant Htt are listed in Table 4-2. Of note, the splicing protein Fus is one of the dominant components of aggregates in an HD cell model and is found in intranuclear inclusions in R6/2 mouse and human patient tissue (Doi et al., 2008); furthermore, mutations in Fus have been implicated in amyotrophic lateral sclerosis (Zhou et al., 2013; Orozco &

Edbauer, 2013; Daigle et al., 2013). A yeast two-hybrid screen using the N-terminus of Htt identified interactions with two other splicing related proteins: Prpf40a and Prpf40b (Faber et al., 1998). Follow-up studies on Prpf40a have demonstrated a greater binding affinity to Htt with an expanded repeat as well as sequestration of the normally nuclear splicing factor in the cytoplasm. Splicing efficiency of a reporter gene was shown to be reduced in the presence of mutant Htt and mediated through Prpf40a loss of function (Jiang et al., 2011).

Yu et al. has shown that SBMA model mice have increased expression of the RNA-binding protein *Cugbp1* and mis-splicing of two Cugbp1 regulated genes, chloride channel 1 *Clcn1* and muscleblind-like protein 1 *Mbnl1* (Yu et al., 2009). The authors also tested a non-Cugbp1 regulated mini-gene, calcitonin/calcitonin gene-related peptide (CT/CGRP), and observed a significant shift in the ratio of CT to CGRP transcripts (Yu et al., 2009), suggesting the mutant AR receptor disturbs RNA splicing both through Cugbp1 and other splicing factors. While we did not observe Cugbp1 transcriptional dysregulation in our SBMA mouse muscle, we did observe a significant decrease in *Mbnl1* (Figure 4-1B).

Splicing in SCA7 has been unexplored. However, it was demonstrated that the transcriptional STAGA complex (which contains ATXN7) may interact with the SF3b splicing complex (Martinez et al., 2001), which is not surprising given RNA synthesis and RNA splicing are coordinated (Maniatis & Reed, 2002). As in HD, it is also possible for RNA-binding proteins to be in aggregates, although this is still an open question. In addition, we found transcriptional dysreguation of several alternative splicing factors (Figure 4-1C).

Given the aberrant expression and activity of splicing machinery in HD, SBMA, and SCA7, we hypothesized that mutant polyQ proteins may impact the splicing process in muscle on a genome-wide level and this could be a cause of muscle atrophy. We evaluated our RNA-sequencing data for perturbation of splicing genome-wide. Briefly, we investigated splicing in HD transgenic mice (R6/2), knock-in SBMA mice (113Q), and knock-in SCA7 mice (100Q). We evaluated five types of splicing events: skipped exons (SE), mutually exclusive exons (MXE), retained introns (RI), alterna-

tive 5' splice sites (A5SS), and alternative 3' splice sites (A3SS); these event types are summarized in Figure 4-2.

4.7 Method of Global Splicing Analysis in CAG Expansion Disorders

We utilized the mixture-of-isoforms (MISO) framework (Katz et al., 2010) to analyze splicing in our HD, SBMA, and SCA7 datasets. MISO calculates Percent Spliced In (PSI Ψ) values - the fraction of mRNAs that represent the inclusion isoform for an event. Default parameters for sampling were used: burn_in=500, lag=10, num_iters=5000. We only included events in our analysis that met the following inclusion criteria: events were supported by a minimum of 40 reads, the PSI value confidence intervals for a given event did not span > 0.4 (40% range), and events were expressed in at least 2 animals / genotype, across all genotypes.

4.7.1 Annotations

Splicing events were obtained from the MISO annotations page: `http://genes.mit.edu/burgelab/miso/docs/annotation.html`. Annotations were version 2, compiled June 2013. A summary of their derivation, as stated in the MISO documentation:

> "These annotations were derived by considering all transcripts annotated in Ensemble genes, knowGenes (UCSC) and RefSeq genes. The flanking exons to alternative exons were chosen by taking the shortest stretches of flanking that are most common among the annotated transcripts for a gene."

Gene symbols and accession identifiers for events were included in the provided annotations.

4.7.2 Differential Splicing Analysis

We first assessed the consistency of biological samples. A metric we termed SigDiff was calculated to incorporate both the difference between wildtype and mutant samples and variance within each genotype. We also wanted to assess if a calculated SigDiff score could be the result of chance, so we generated a SigDiff score for each possible combination of genotypes and calculated a Z-score for the correct SigDiff. Below is an example calculation for one gene for a set of 2 wildtype and 2 mutant samples:

1. Calculate a delta vector: absolute value of each pairwise delta (Δ) PSI (Ψ)

$$Delta = \{|wt1\Psi - mut1\Psi|, |wt1\Psi - mut2\Psi|, |wt2\Psi - mut1\Psi|, |wt2\Psi - mut2\Psi|, \\ |wt1\Psi - wt2\Psi|, |mut1\Psi - mut2\Psi|\}$$

or written as

$$Delta = \{|\Delta wt1\Psi, mut1\Psi|, |\Delta wt1\Psi, mut2\Psi|, |\Delta wt2\Psi, mut1\Psi|, |\Delta wt2\Psi, mut2\Psi|, \\ |\Delta wt1\Psi, wt2\Psi|, |\Delta mut1\Psi, mut2\Psi|\}$$

2. Calculate the SigDiff value: Average of deltas (Δs) between wildtype and mutant samples minus the average of deltas (Δs) within wildtype and mutant genotypes

$$SigDiff = \langle \Delta\Psi \textit{ between genotypes} \rangle - \langle \Delta\Psi \textit{ within genotypes} \rangle$$

or written as

$$SigDiff = \langle \Delta wt\Psi, mut\Psi \rangle - \langle \Delta wt\Psi, wt\Psi, \Delta mut\Psi, mut\Psi \rangle$$

3. Calculate the SigDiff for every combination of genoptypes to generate the range

of SigDiff scores possible by chance for selected gene

$$Random = SigDiff({}^{4\ samples}C_{2\ samples\ per\ genotype})$$

4. Generate Z-score to assess if SigDiff above random background

$$Z - score = \frac{SigDiff - \langle Random \rangle}{sd(Random)}$$

Events were filtered as follows:

- An event needed to have a biologically interesting difference between wildtype and mutant PSI Ψ values. We set this at a 15% difference, slightly more stringent than thresholds used in literature (Katz et al., 2014; Wang et al., 2008; Pedrotti et al., 2015). As an example, in our SCA7 dataset, of the 16,354 events with sufficient coverage, 473 had an average Ψ difference of 15% between genotypes.

- An event was required to have a SigDiff metric $\geqq 0.075$ to ensure that the difference between genotypes is considerably greater than the difference within genotypes. This was an arbitrary threshold we chose based on a blinded assessment of events that would be called. In our SCA7 dataset, this further restricted significant events to 380.

- Lastly, we required the Z-score of an event to be $\geqq 2$. We desired this restriction as a safeguard against an event being called significant due to a favorable chance distribution of a moderately variable Ψ value. A threshold of 2 can be thought of as follows for our SCA7 dataset which has 4 wildlype and 4 mutant samples: If all SigDiff values are calculated for every combination of 8 samples into 2 genotypes, the SigDiff value for the correct grouping of samples was 2 standard deviations above the mean for the entire distribution. In our SCA7 dataset, the Z-score threshold filtered out an additional 19 events. As an example, the following event met the average $\Delta\Psi$ and SigDiff thresholds but not the Z-score

threshold.

gsymbol	event	wt1	wt2	wt3	wt4	mut1	mut2	mut3	mut4	zscores	SigDiff	Avg Δψ
Obfc2a	A5SS	0.17	0.22	0.07	0.11	0.22	0.21	0.52	0.5	1.79	0.0779	0.22

4.8 Identified Mis-Splicing Events in CAG Expansion Disorders

4.8.1 Differential Splicing in HD Muscle

The HD muscle RNA-Seq dataset was from the quadriceps of 4 wildtype animals and 4 R6/2 animals, all 12weeks of age. These samples were sequenced to a depth of 53 million, 40 base reads. We identified 191 differential splicing events between wildtype and mutant muscle. These events are listed in Appendix Table C-1. The PSIΨ values for the differential events are plotted in a heatmap in Figure 4-3A. The top of the heatmap shows events that have higher inclusion (warmer color) in wildtype animals, while the bottom of the heatmap shows the opposite pattern. To assess the validity of our differentially spliced events, we grouped the 8 samples into every combination of 4 'wildtype' and 4 'mutant' (a total of 35 groupings) and called differential splicing (Figure 4-3B). The correct group of samples, indicated by a red diamond, was clearly above the conservative background of the other groupings, suggesting our differential splicing calls are truly attributed to the HD mutation.

Genes that were mis-spliced were grouped to indicate which biological processes may be most affected (Figure 4-3C). Many genes were involved in cytoskeletal and mitochondrial organization. As an example, mis-spliced mitochondria genes are plotted in Figure 4-4. Genes *Mff*, *Mul1*, and *Opa1* are of interest because they regulate the fission-fusion balance of mitochondria and excessive mitochondria fission is observed in HD (Guo et al., 2013). The *Mul1* mis-splicing event appears to regulate inclusion of the domain that targets Mul1 to mitochondria, which would have significant consequences on functional activity (Attaix & Taillandier, 2012; Lokireddy et al., 2012;

Jenkins et al., 2013). Another interesting gene, *Rhot1* (also known as *Miro1*) is an adapter on the outer mitochondria membrane that binds the Kif5 motor in response to calcium signaling to facilitate mitochondria localization (MacAskill et al., 2009; Cai & Sheng, 2009). This rapid and timely transport of mitochondria throughout projections is critical to synapse activity (Cai & Sheng, 2009).

4.8.2 Differential Splicing in SCA7 Muscle

The SCA7 muscle RNA-Seq dataset was from the quadriceps of 4 wildtype animals and 4 homozygous knock-in (*ATXN7* 100Q) animals, all ~6months of age. These mutant animals were in the advanced stages of a SCA7-like phenotype, with significant weight loss, visual impairment, locomotor deficits, curvature of the spine, and muscle atrophy; their average lifespan is ~7months. These samples were sequenced to a depth of 103 million, 80 base reads. We identified 361 differential splicing events between wildtype and mutant muscle. These events are listed in Appendix Table C-2. As in the previous section, PSIΨ values for the differential events are plotted in a heatmap in Figure 4-5A. The top of the heatmap shows events that have higher inclusion in wildtype animals, while the bottom of the heatmap shows the opposite pattern. Our number of identified differentially spliced events was highly above the conservative background of events called when samples were randomly grouped (Figure 4-5B). And as seen in HD, many of the events are in genes involved in cytoskeletal and mitochondrial organization (Figure 4-5C), including the fission-fusion genes *Mff*, *Mul1*, and *Opa1*.

4.8.3 Differential Splicing in SBMA Muscle

Our SBMA dataset was more complex. We had RNA-Seq from the quadriceps of 3 wildtype mice and 3 SBMA homozygous knock-in (AR113) mice. In addition, we had RNA-Seq from the quadriceps of mice with suppressed *AR* expression through subcutaneous administration of antisense oligonucleotides complementary to the *AR* transcript. The antisense oligonucleotide treatment in these mice rescued deficits in

muscle weight, fiber size, and grip strength, reversed changes in muscle gene expression, and extended lifespan. Lastly, we had RNA-Seq from the quadriceps of AR113 animals that harbored additional mutations. In addition to the polyQ expansion in the androgen receptor, these mice also had mutations that substituted two arginines for two lysines (K385, K518) in the androgen receptor protein. These KRKR mutations prevent AR from being sumoylated. Sumoylation represses the transcription factor activity of AR, so these additional mutations should rescue the transcriptional dysregulation in AR113 animals. However, these mice actually demonstrated more severe transcriptional dysregulation in quadriceps (Lieberman et al., 2014). For that reason, we considered their RNA-Seq data as representative of a more extreme mutant phenotype.

These samples were sequenced to a depth of 43 million, 101 base reads. We identified 65 differential splicing events between wildtype and mutant muscle. These events are listed in Appendix Table C-3. PSIΨ values for the differential events are plotted in a heatmap in Figure 4-6A. We performed spearman hierarchical clustering on the samples based on the PSIΨ values of the differentially spliced genes. As can be seen in the heatmap, the rescue samples cluster with the wildtype samples and all of the ARQ113 samples cluster together. However, one can see that events identified as differentially spliced between wildtype and mutant animals are only marginally above the 15% difference threshold. This can be best appreciated by comparing the intensity difference between wildtype and mutant PSIΨ values in the heatmap for SBMA (Figure 4-6A) and the heatmap for SCA7 (Figure 4-5A). The number of splicing events was not considerably above background (Figure 4-6B) either. Similar to HD and SCA7, many mis-spliced genes are involved in cytoskeletal organization (Figure 4-6C).

Of the 65 differentially spliced events, 21 are rescued when we call differential splicing between rescue samples and mutant samples. If we relax our criteria to only a 10% average PSIΨ rescue, then 37 of the 65 events are rescued. We are excited to examine these 37 events more critically to determine what distinguishes them from the remaining 28 non-rescued events. We also would like to see if a common motif is

found near the alternative splicing events that are rescued, possibly even a Cugbp1 or Fus binding site as previous research and transcriptional dysregulation would suggest. In addition, this dataset had low power due to the small number of replicates. If we down-sample our two other datasets it would be interesting to see if a similar number of dysregulated splicing events are called. Our inclination is that SBMA splicing is not as dysregulated as HD and SCA7 and we will see considerable mis-splicing even when these two datasets are down-sampled. This is based on the degree of mis-splicing of events common to all disorders, which show minimal dysregulation in SBMA, moderate dysregulation in HD, and severe dysregulation in SCA7, as will be discussed below. Lastly, we have pelvic muscle tissue from SBMA animals to process; pelvic muscle has higher *AR* expression than quadriceps, thus we may see more dramatic splicing changes in this muscle tissue.

4.8.4 Commonly Mis-spliced Events

The lists of dysregulated splicing events for the three disorders were compared (Figure 4-7). Four splicing events were found to be mis-spliced in the same direction for all three disorders. These four events were skipped exons in the genes *Camk2b*, *Rapgef1*, *Uspl1*, and *Rtn4*. The skipped exon in *Uspl1*, which stands for ubiquitin specific peptidase like 1, caught our interest as several studies have shown that inclusion of exon 2 is significantly increased in the muscle of Spinal Muscular Atrophy model mice (Bäumer et al., 2009; Zhang et al., 2008b). Inclusion increases with symptoms and is more pronounced in muscle than other affected tissues (spinal cord and kidney) (Bäumer et al., 2009). The skipped exon is demonstrated in Figure 4-8. SCA7 and HD muscle have a ~40% increase in exon 2 inclusion compared to wildtype; SBMA muscle has a more subtle increase of 23% which is more extreme in the KRKR mutant and rescued with *AR* knock-down. Uspl1 is a sumo ligating enzyme and exon 2 contains the canonical start codon. Exclusion of this exon leads to a longer 5' UTR with translation initiation occurring in exon 4. The resulting proteins differ by ~200 amino acids. We are excited to assess Uspl1 protein in mutant muscle and study the different N-termini. It appears that the N-terminal amino acids are critical for an

essential, non-catalytic function of Uspl1 in cajal bodies (Schulz et al., 2012; Hutten et al., 2014)

4.9 Summary and Future Directions

Severe muscle atrophy is a common peripheral symptom of polyQ disorders. Rescue of peripheral symptoms has demonstrated overall therapeutic efficacy in mouse models of polyQ disorders. An alternative splicing program is critical to proper muscle structure and function. We find that quadriceps of HD and SCA7 mouse models exhibit widespread mis-splicing while quadriceps of SBMA exhibit more mild splicing impairment. The mis-splicing in SBMA is largely rescued by *AR* knock-down. We are excited to validate mis-spliced events of interest at the protein level and strategically analyze the sequence surrounding alternative events to determine splicing factors that may be contributing to mis-splicing.

4.10 Additional Methods

For the HD dataset, RNA-Seq libraries were sequenced at the MIT Biomicrocenter on the Illumina HiSeq, with 40b reads. For the SCA7 dataset, RNA-Seq libraries were also sequenced at the MIT Biomicrocenter on the Illumina NextSeq, with 80b-85b reads. RNA-Seq libraries for the SBMA dataset were generated at the University of Michigan using the Illumina Hi-Seq with reads of 101 bases.

Illumina fastq files were filtered with FastX *fast_quality_filter -q 30 -p 50* to remove low quality reads. Read pairs were combined and analyzed as single end. For SCA7, there was a disproportionate sequencing depth among samples, so fastq files were sampled using 'Seqtk: Toolkit for processing sequences in FASTA/Q formats' with source code from `https://github.com/lh3/seqtk`. Reads were mapped to the mm9 genome (downloaded from Ilumina UCSC files 7/26/2014) using bowtie 2.2.3 (Langmead et al., 2009), samtools 0.1.19 (Li et al., 2009), and tophat 2.0.12 (Trapnell et al., 2012). Tophat options *-a 6 –read-realign-edit-dist 0* were used for all datasets.

Tophat options *–segment-length 20 –segment-mismatches 1* were also used for the HD dataset due to the shorter read length.

Heatmaps of dysregulated splicing events were generated using GENE-E: `http://www.broadinstitute.org/cancer/software/GENE-E/index.html`. Sashimi plot was used for displaying *Uspl1* read coverage (Katz et al., 2015). For the isoform plots made with Sashimi plot, we pooled biological replicates and called PSI values again. The venn diagram in Figure 4-7 was created using the Venny software (Oliveros, 2015). Genes were grouped into biological processes using the GOTermMapper from Princeton University, which can be found at `http://go.princeton.edu/cgi-bin/GOTermMapper`.

For each dataset, the splicing event composition for dysregulated events was compared to the splicing event composition for all events in the dataset with coverage to determine if the polyQ proteins led to dysregulation of a particular type of splicing event. PolyQ proteins did not affect a specific type of splicing event, as can be observed in Appendix Figure C-1.

4.11 Figures and Tables

Table 4-1: CAG repeat expansion disorders. Adapted from (Cummings & Zoghbi, 2000).

Disorder	Signature Phenotype	Gene	Gene Locus	Normal Repeat #	Disease Repeat #
Spinal-bulbar muscular atrophy	Muscular atrophy, hormonal abnormalities	Androgen Receptor	Xq11-12	6-39	40-63
Huntington's disease	Chorea, psychiatric disturbances, cognitive decline	Huntingtin	4p16.3	6-34	36-121
Spinocerebellar ataxia 1	Ataxia	Ataxin-1	6p22-23	8-44	39-83
Spinocerebellar ataxia 2	Ataxia	Ataxin-2	12q23-24	13-33	32-77
Spinocerebellar ataxia 3	Ataxia	Ataxin-3	14q24-31	12-40	54-89
Spinocerebellar ataxia 6	Ataxia	CACNA1A	19p3	4-18	19-33
Spinocerebellar ataxia 7	Ataxia, retinal degeneration	Ataxin-7	3p12-21	4-35	37-306
Spinocerebellar ataxia 17	Ataxia	TBP	2q13	29-42	47-55
Dentatorubral-pallidouysian atrophy	Epilepsy, ataxia, dementia	ATN1	12q	6-36	49-84

Table 4-2: RNA binding proteins with altered mutant HTT interactions.

Gene_Description	Interaction with huntingtin		Citation
	cytoplasmic fraction	membrane fraction	
Ddx1 ATP-dependent RNA helicase DDX1	normal<<expanded	NA	Culver 2012
Ddx5 Probable ATP-dependent RNA helicase DDX5	normal<<expanded	normal>expanded	Culver 2012
Dhx15 Putative pre-mRNA-splicing factor ATP-dependent RNA helicase DHX15	normal<<expanded	NA	Culver 2012
Fus RNA-binding protein FUS	normal<<expanded	NA	Culver 2012
Sf3a3 Splicing factor 3A subunit 3	normal<<expanded	NA	Culver 2012
Sfpq Splicing factor, proline- and glutamine-rich	normal<<expanded	NA	Culver 2012
Sfrs1 Isoform 1 of Splicing factor, arginine/serine-rich 1	normal<<expanded	NA	Culver 2012
Sfrs3 Isoform Long of Splicing factor, arginine/serine-rich 3	only expanded	NA	Culver 2012
Rbmx RNA binding motif protein, X chromosome	normal<<expanded	NA	Culver 2012
D1Pas1 Putative ATP-dependent RNA helicase PI10	NA	normal<<expanded	Culver 2012
Ddx3x ATP-dependent RNA helicase DDX3X	NA	normal<<expanded	Culver 2012
Dhx57 Isoform 1 of Putative ATP-dependent RNA helicase DHX57	NA	normal<<expanded	Culver 2012
Prpf40a pre-mRNA-processing factor 40 homolog A	yeast two-hybrid		Faber 1998, Jiang 2011
Prpf40b pre-mRNA processing factor 40 homolog B	yeast two-hybrid		Faber 1998
TDP-43	in aggregates		Schwab 2008
Fus RNA-binding protein	in aggregates		Doi 2008

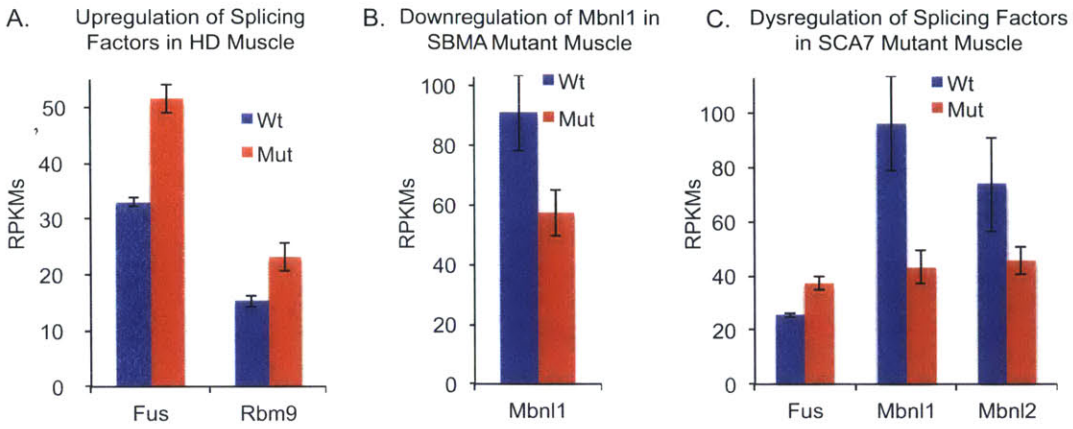

Figure 4-1: Upregulation of splicing genes in polyQ muscle.

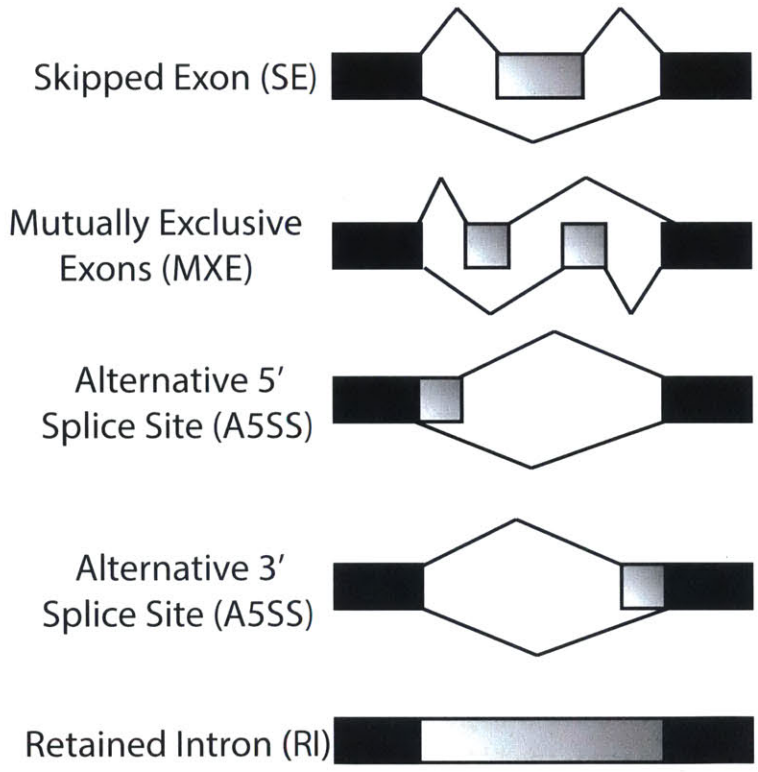

Figure 4-2: Different types of alternative splicing events.

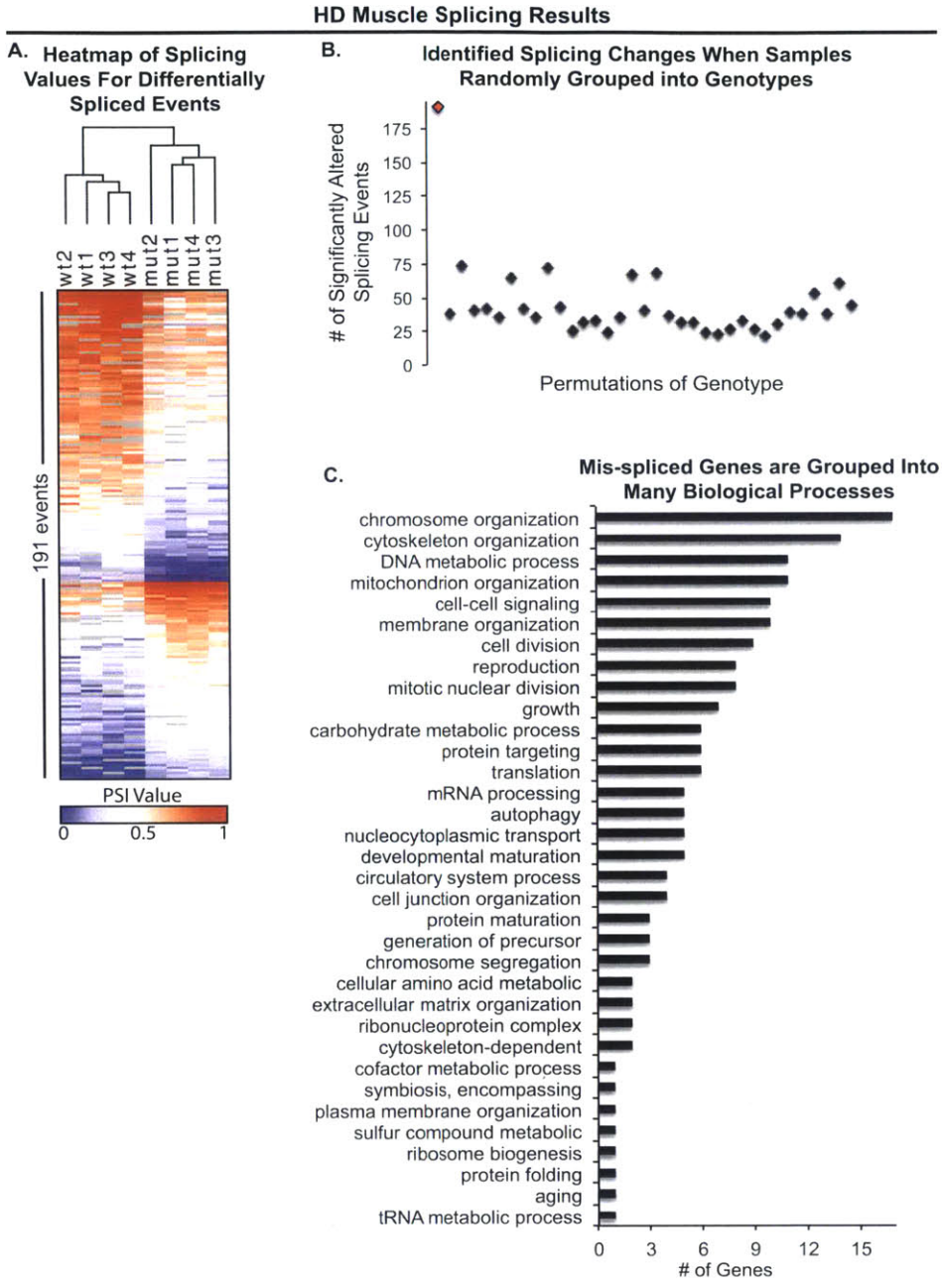

Figure 4-3: Splicing analysis of **HD** muscle. A) The 191 mis-spliced events are plotted in a heatmap, with dark red indicating 100% inclusion of the event and dark blue indicating 0% inclusion. Inclusion values were very consistent across genotype. There was a bias towards events with decreased inclusion values in the mutant condition. B) The number of significant splicing events identified was compared to a conservative background. Samples were grouped into two genotypes and differential splicing was called. The correct grouping of samples, indicated by the red diamond, resulted in a significantly higher number of differential splicing calls. C) Mis-spliced genes were grouped to indicate which biological processes may be most affected.

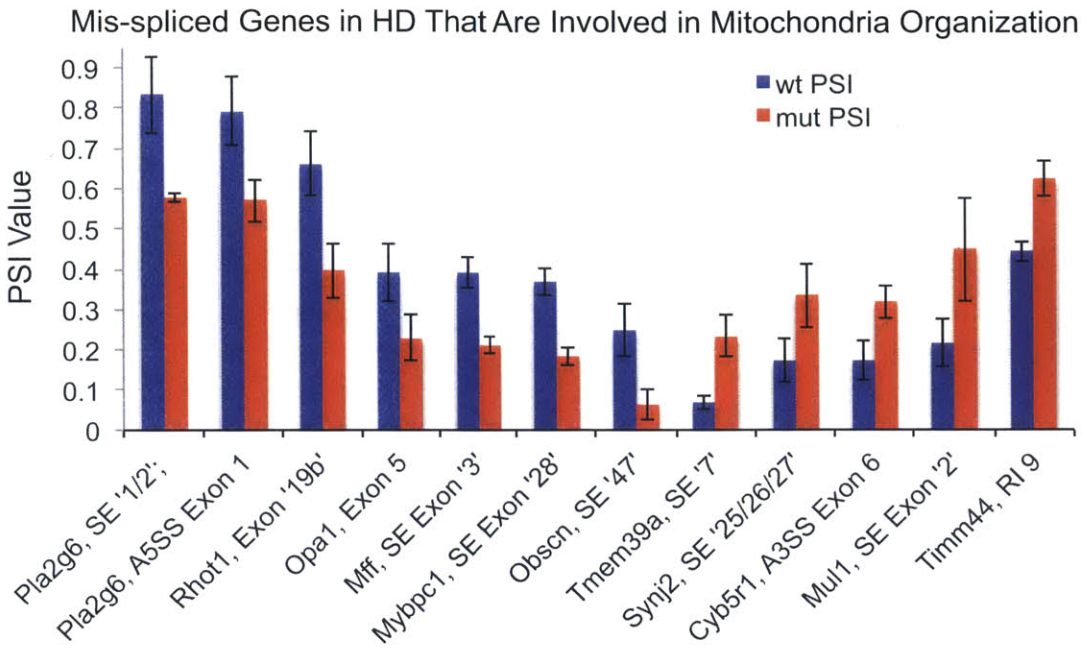

Figure 4-4: Mitochondrial genes that are mis-spliced in HD muscle.

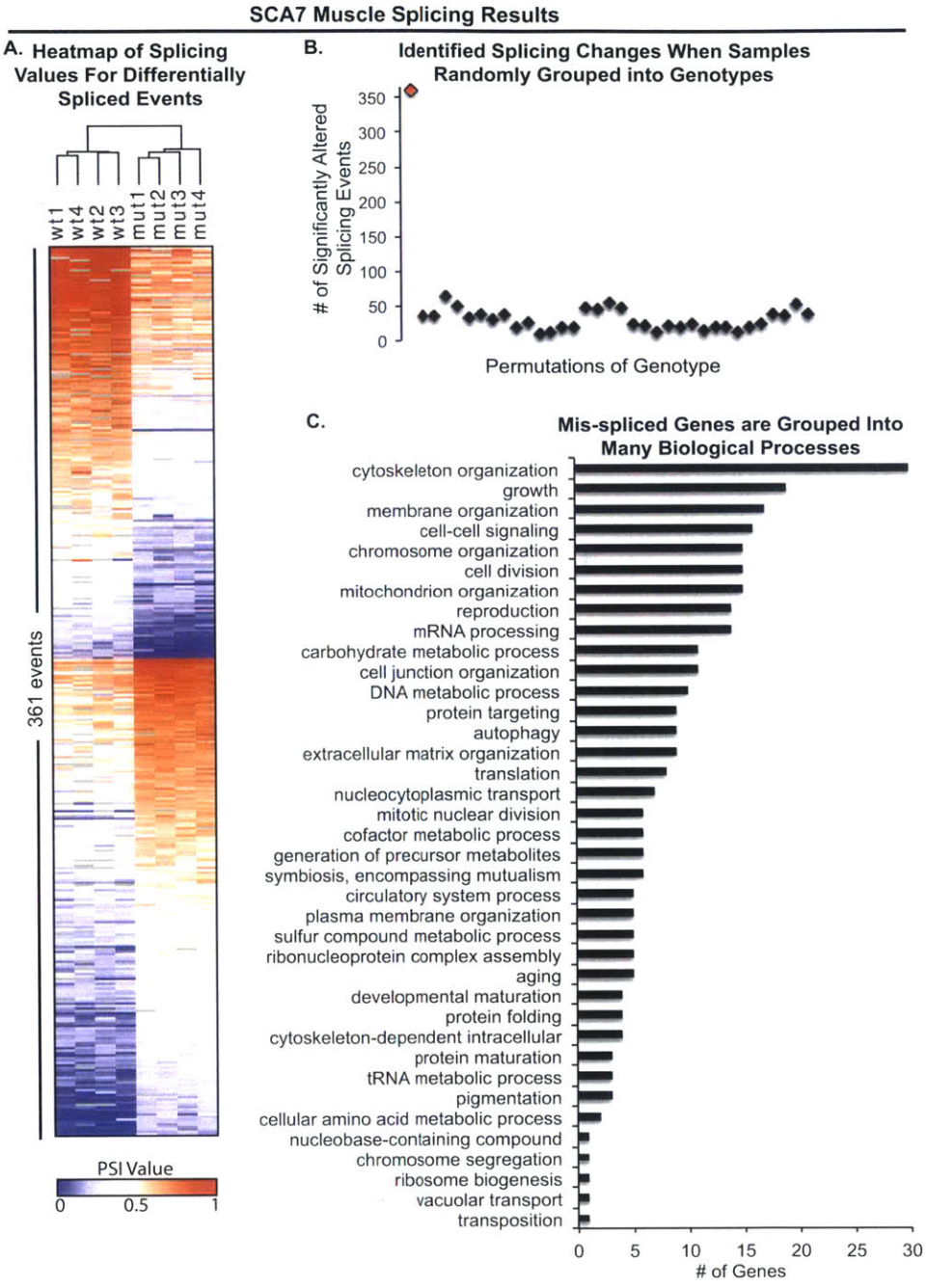

Figure 4-5: Splicing analysis of **SCA7** muscle. A) The 361 mis-spliced events are plotted in a heatmap, with dark red indicating 100% inclusion of the event and dark blue indicating 0% inclusion. Inclusion values were very consistent across genotype. There was a bias towards events with increased inclusion values in the mutant condition. B) The number of significant splicing events identified was compared to a conservative background. Samples were grouped into two genotypes and differential splicing was called. The number of differential splicing calls with the correct grouping of samples, indicated by the red diamond, was significantly above background. C) Mis-spliced genes were grouped to indicate which biological processes may be most affected.

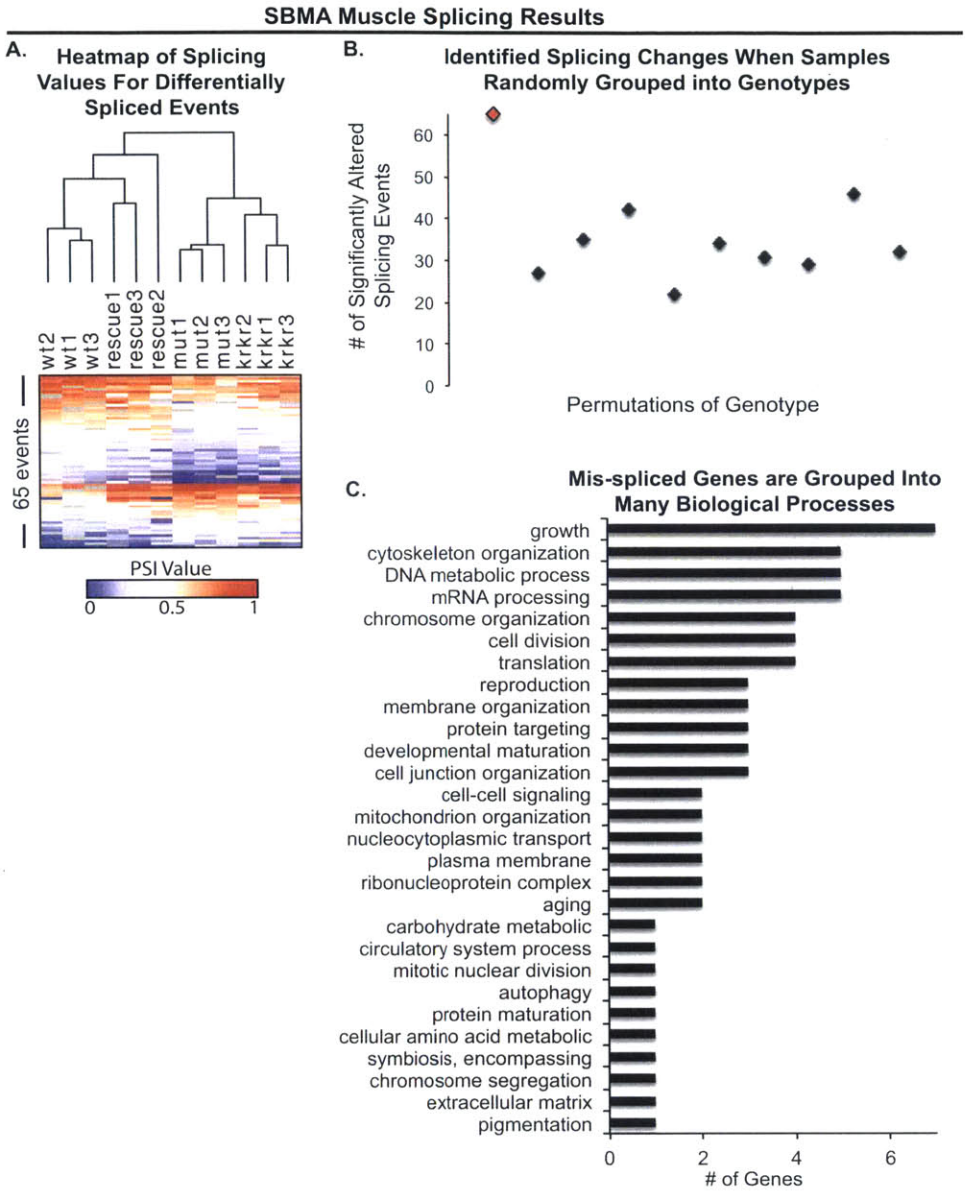

Figure 4-6: Splicing analysis of **SBMA** muscle. A) The 65 mis-spliced events are plotted in a heatmap, with dark red indicating 100% inclusion of the event and dark blue indicating 0% inclusion. Inclusion values were very consistent across genotype, but differences between genotype are largely not much higher than threshold (mutant animal PSIs were only a shade different than wildtype). The antisense oligonucleotide animals do cluster with wildtype animals while the KRKR/AR113Q mutants cluster with the single AR113Q mutants. B) The number of significant splicing events identified was compared to a conservative background. Samples were grouped into two genotypes and differential splicing was called. The correct grouping of samples, indicated by the red diamond, was marginally above background. C) Mis-spliced genes were grouped to indicate which biological processes may be most affected.

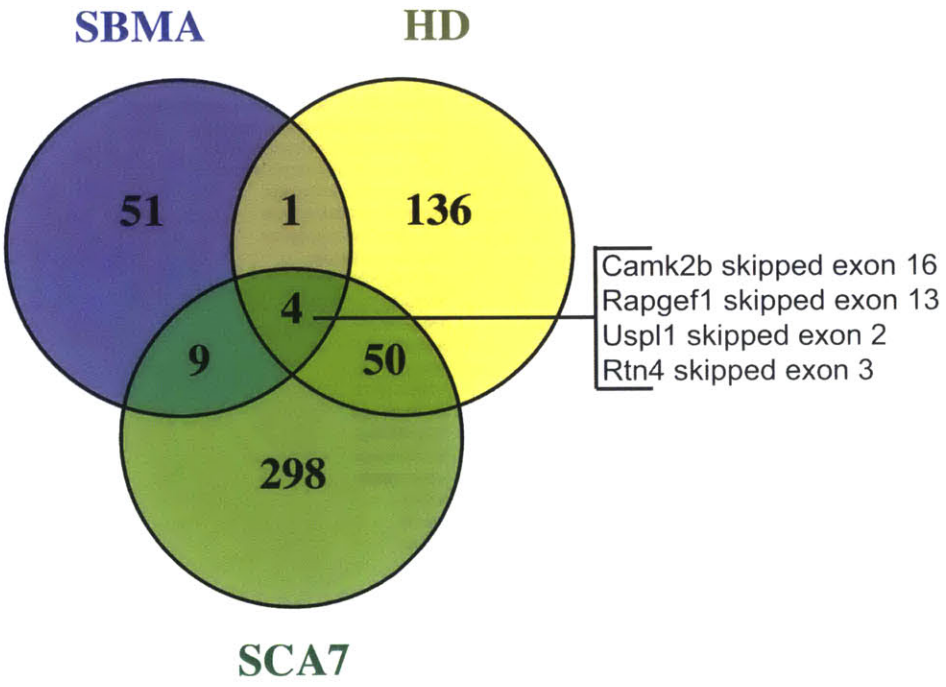

Figure 4-7: Overlap of differential splicing events from HD, SBMA, and SCA7. HD and SCA7 share many differential splicing events. Four SE events are common to all three disorders.

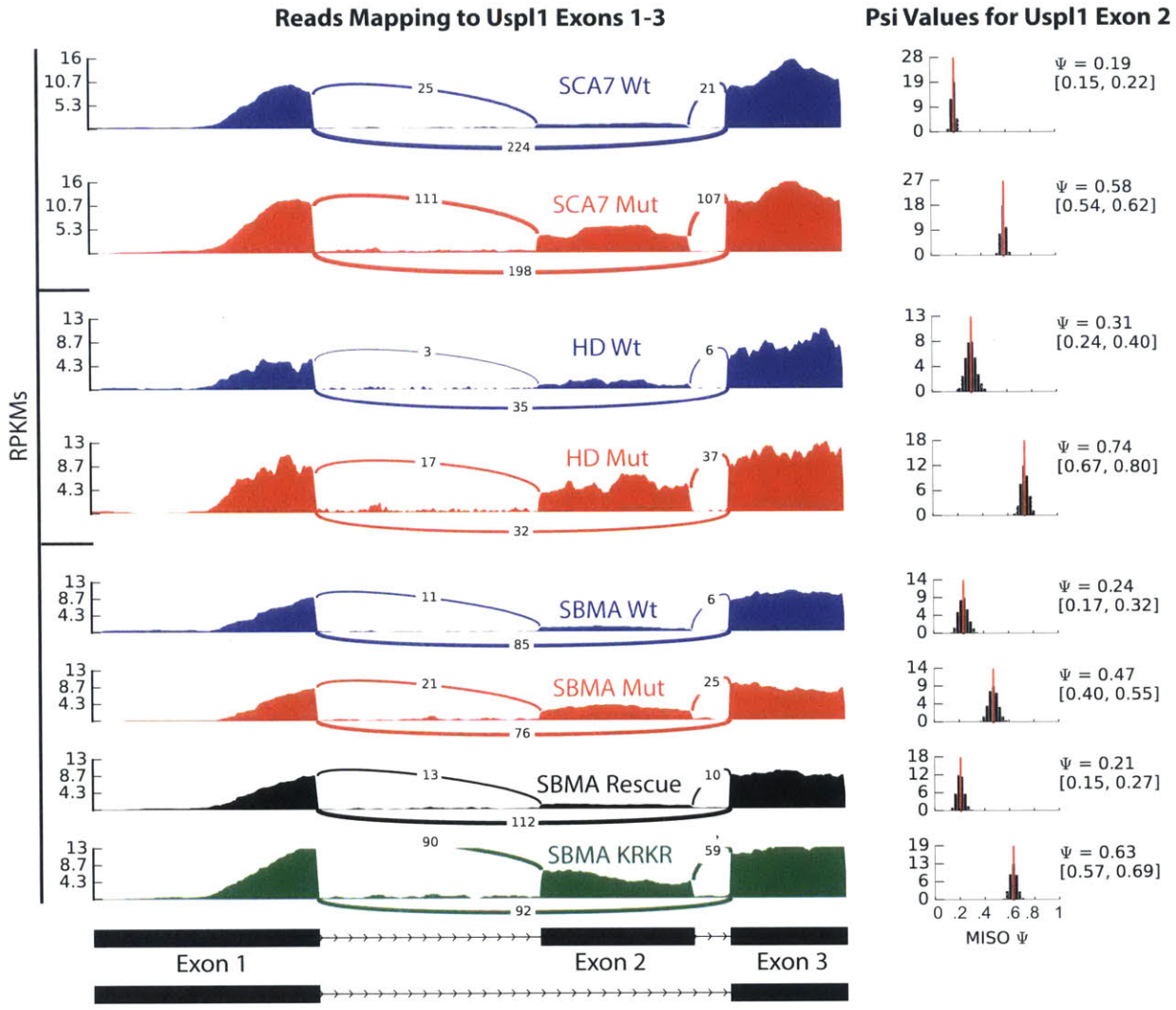

Figure 4-8: Reads mapping to *Uspl1* exons 1-3 are shown on the left. The corresponding PSI Ψ values are shown on the right. For all three disorders, mutant samples have at least a 20% increase in Ψ levels. For SBMA, the antisense oligonucleotide rescue does restore *Uspl1* exon 2 inclusion to wildtype levels and the KRKR / AR113Q mutants have more extensive mis-splicing than the single AR113Q mutants.

Chapter 5

Conclusions and Future Directions

5.1 Transcriptional Dysregulation

Microarray studies have demonstrated that transcriptional dysregulation in the brain is a key feature of HD. The dysregulation observed in human postmortem brain tissue is largely recapitulated in HD mouse models, especially the R6/2 mouse model. We performed RNA-Seq to extend our knowledge on dysregulated genes. Our RNA-Seq data confirmed canonically dysregulated genes in the cortex and striatum but also revealed new insights. Most intriguingly, we found an upregulated genetic signature of an interferon 1 response. This signature is found in SCA7 mouse models as well (Chort et al., 2013), suggesting a possibility that the RNA hairpins formed from the CAG repeat may be triggering a viral dsRNA response. In the future, it would be interesting to explore publicly available datasets from other neurodegenerative disorders to see if interferon 1 upregulation is unique to CAG disorders.

The transcriptional dysregulation in HD is strikingly skewed toward downregulation and we explored the possibility of an epigenetic influence facilitating this pattern. We examined the H3K4me3 mark, which has critical functions in the brain. We found a significant overlap of genes with decreased H3K4me3 occupancy and genes with decreased expression in HD. To investigate the H3K4me3 mark more rigorously, we used k-means clustering to identify five predominant patterns of H3K4me3 that occur in both wildtype and R6/2 mice. Intriguingly, there is a specific H3K4me3 profile, one

that extends into the gene body, in wildtype mice marking a very large fraction of genes that will be downregulated in the presence of mutant HTT. This profile is enriched in genes with critical neuronal function. In R6/2 mice, the H3K4me3 profile is maintained, but has decreased overall levels. Increasing these methylation levels in HD flies through genetic reduction of a demethylase is neuroprotective, indicating lower H3K4me3 facilitates a reduction in transcription for the HD downregulated genes.

We suggest that H3K4me3 architecture is part of a fundamental epigenetic feature controlling expression levels, and in HD, it determines a response to *HTT* exon 1 expression. We would like to compile ensembles of several epigenetic marks and determine if there is a broader epigenetic pattern at *HTT* sensitive promoters. It is also important to repeat previous experiments that explored wildtype and mutant HTT binding to chromatin with more precise technologies. This would indicate if HTT interaction with these promoters or if mutant HTT activates a cell signaling pathway that impacts the epigenetic profile at these target sites.

5.2 Mis-splicing of Mutant *HTT*

We identified a small exon 1-intron 1 polyadenylated mRNA transcript in the brains of HD mouse models expressing either mutant *Htt* (mouse) or *HTT* (human). The same transcript was also present in fibroblast lines derived from HD patients and in postmortem HD brains. Our data show an increased association of the splicing factor SRSF6 with expanded CAG repeats, which could account for the CAG repeat length dependent production of the exon 1-intron 1 transcript. Translation of this transcript produces an exon 1 Htt/HTT protein.

We know that an exon 1 HTT protein is highly pathogenic. Expression of HTT exon 1 in R6/2 transgenic mice results in the most severe HD-like pathology that exists among the widely used mouse models of HD. It would be interesting though to see how this small fragment contributes to HD-like onset in knock-in mice. We have considered an experiment to address this question. First, we can design several

siRNAs that target the first 1200 bases of Htt intron 1. These could be tested in the Q111 mouse striatal cell line for ability to knockdown the exon 1 / intron 1 transcript (which is present in this cell line (Ng et al., 2013)). If successful, siRNAs could be intrastriatally injected into knock-in mice. Both molecular and behavorial phenotypes could be examined to determine if knockdown of the small exon 1 *HTT* delayed disease onset. It would also be interesting to alter the levels of either U1 or SRSF6 in the Q111 striatal cell line and measure any changes in *Htt* exon 1/ intron 1 splicing frequency as a confirmation of the mis-splicing mechanism.

It is also critical to study the exon 1 fragment in the context of human HD. Exon 1 HTT protein, which originally stimulated our investigation, is found in postmortem HD human brain (Lunkes et al., 2002; Difiglia, 1997). A detailed and quantitative investigation of the relationship between the presence of these fragments and the mis-splicing of the human *HTT* gene is now essential. Given the extreme pathogenicity of the exon 1 HTT protein, we would expect that the frequency of mis-splicing must occur at a very low level in adult-onset HD. Our mouse data indicate that repeat size plays a critical role in frequency of mis-splicing, consistent with our working model in which the length of the repeat dictates the association of SRSF6 and *HTT* exon 1. Indeed, although a low level of mis-splicing was found in the knock-in line carrying 50 CAGs, which would be at the higher end of the repeat length present in most adult-onset HD patients, we were not able to detect the corresponding protein by immunoprecipitation and western blotting. In contrast, the exon 1 proteins produced via mis-splicing events in knock-in mice carrying between 80 and 190 glutamines were readily identifiable. This discrepancy is likely to be a combination of both a low level of mis-splicing in the 50Q mice and the polyQ length-related binding kinetics of polyQ-specific antibodies. Technical considerations for identifying the mis-spliced products in human tissues can be predicted to be yet more challenging. Thus far, we have been able to detect the presence of the short mRNA by 3'RACE in postmortem brain from two HD individuals. We were unsuccessful in two additional human brain samples, possibly due to the poor quality of the RNA. The successful 3'RACE experiments support the prediction that the mis-spliced *HTT* transcripts in

human HD brains are approximately 7300 bp. This adds another level of difficulty, as the isolation of intact polyadenylated transcripts of this length from postmortem brain tissue is extremely difficult. This, in combination with the GC-rich sequence in this region has meant that we have been unable to show increased levels of intron 1 transcripts in RNA extracted from HD postmortem brain through RNA-Seq.

In order to quantify the level of mis-splicing at the exon1-intron 1 boundary, we plan to use ribosome protection assays followed by deep sequencing to detect ribosome-protected RNA fragments. This approach will give a clean look at all the brain transcripts that were being actively translated, permitting us to determine the level at which mis-splicing occurs in human HD brain.

The pathogenic contribution of the exon 1 protein produced would be expected to be a factor of both the frequency of the mis-splicing event and the half-life of the protein fragment. Even if frequency of the mis-splicing event is comparatively low in the adult-onset HD brain, the accumulation of a highly pathogenic protein species that is resistant to degradation would still be expected to have a strong pathogenic impact.

The demonstration that the production of the *HTT* exon 1 occurs at a pathologically relevant scale in human brain will be directly relevant to therapeutic strategies now under development for HD. One major approach is targeting *HTT* RNA for degradation using either antisense oligonucleotides or RNAi technologies (Lu & Yang, 2012; Harper, 2009; Sah & Aronin, 2011). Therapies targeting *HTT* RNA downstream of exon 1 will only reduce levels of a full-length *HTT* transcript leaving the exon 1 mis-spliced transcript untouched. We suggest an optimal strategy for HD therapeutics will target the RNA at the 5'UTR or in exon 1 in order to reduce levels of both the full-length and the short mis-spliced exon 1 *HTT* transcript. We briefly explored a method for targeting RNA at the 5' UTR or in exon 1. We used small oligonucleotides that would bind upstream or downstream of two stable RNA hairpins - one in the 5' UTR and one comprised of the CAG repeat in exon 1. We successfully showed these could reduce translation of HTT *in vitro*. We also designed a morpholino to bind the very 5' terminus of *HTT* RNA, a strategy that has been

shown to reduce translational initiation (Summerton, 1999). It would be exciting to continue using these oligonucleotide approaches in cell culture and if successful *in vivo*.

5.3 Muscle Pathology

After identifying mis-splicing of the mutant *HTT* transcript, we began to think on a genome-wide level about mis-splicing in CAG repeat disorders. A common pathological feature of several CAG repeat disorders is extreme muscle atrophy. Proper muscle function and health is dependent on an extensive alternative splicing program. We developed a pipeline for calling differential splicing and used it to analyze RNA-Seq data from skeletal muscle of the R6/2 transgenic HD mouse model, the 113Q knock-in SBMA model, and the 100Q knock-in SCA7 mouse model. The alternative splicing program in the HD and SCA7 muscle samples was largely perturbed, with many common splicing events affected. Interestingly, many of the mis-spliced events are in genes involved in mitochondria structure and localization and cytoskeletal organization. The mitochondria genes are especially interesting given the extremely compromised state of mitochondria in diseased muscle. Mis-splicing in SBMA was markedly less severe, but was rescued with peripheral knockdown of the causative mutation. Several splicing events were common to all disorders. The *Uspl1* skipped exon is of interest because it has been noted in other disorders and would result in a considerable protein difference.

Through statistical analysis we will be assessing any motif enrichment for splicing factors to determine the mechanism of mis-splicing. We would also like to examine splicing events of interest at the protein level to have a better indication of how differential splicing may be affecting the HD phenotype.

5.4 Additional Sequencing Analyses

5.4.1 Proper mRNA Transport in HD Neurons

While many systems are dependent on local translation, this spatial feature is especially critical in the projections of neurons. A pool of RNAs are transported to synapses where they are translationally repressed. Upon appropriate stimulation, these RNAs can be immediately translated into protein, negating the need and time it takes for the signal to travel to the soma before a response initiates.

It has been well established that Htt associates with motor complexes that transport vesicles inter- and intra-cellularly. More recently, Htt was shown to localize to dendritic RNA granules and P-bodies and possibly modulate RNA localization through Ago2 (Savas et al., 2010). As a confirmation at the single RNA level, the authors followed up showing that Htt is associated with the transport of *β-actin* RNA along dendrites and that transport is dependent on a ZBP1 (an RNA transport protein) targeting sequence in the 3' UTR (Ma et al., 2011). Given these roles of Htt in cellular transport and RNA localization, we would like to ask whether there exists genome-wide dysregulated mRNA transport in the brains of HD model mice; specifically, is the transport from soma to synapses disrupted? The experiment to address this question would involve fractionation of soma and synapses followed by RNA-Seq of each fraction in HD and wildtype mice. We believe there will be many synapse RNAs present in wildtype neurons that will be retained in the soma of HD neurons.

Fractionation of neurons in mouse brain has been routinely done in an effort to understand protein composition in different cellular locations. We have begun to establish a protocol in which we can efficiently isolate **high quality RNA** from synaptosomes. We have developed an efficient fractionation protocol which is depicted in Figure 5-1. We homogenize brain regions and clarify homogenate of cell debris in a low speed spin. Homogenate is spun at 16,000g to separate cytosol from the crude synaptosome pellet. The synaptosome pellet is purified through a sucrose gradient. Both protein and RNA are isolated from homogenate, cytosol, and synaptosome

fractions. We will asses fraction purity through western blotting of fractions with synaptic marker SNAP-25, nuclear markers H3 and MCM3, and ubiquitous spectrin. Several of these markers have been shown to be robust in HD isolated synaptosomes (Valencia et al., 2013). RNA quality will be assessed with an Agilent Bioanalyzer and RNA with RINs >7.5 will be used for RNA-Seq preparations. We will compare the ratio of cytoplasmic to synaptosomal reads for all genes. The homogenate will be used as a control for dysregulated gene expression between the wildtype and mutant conditions. If a group of mRNAs does seem to have a higher cytoplasmic/synaptosome ratio in mutant animals, it would be interesting to see if it is enriched for the ZBP1 binding sequence that was identified in Htt associated dendritic transport of *β-actin* RNA.

5.4.2 Assessing Translational Efficiency in HD Neurons

As mentioned in the introduction, Ribo-Seq follows a similar protocol to RNA-Seq, but only isolates RNA that is bound by a ribosome, yielding a profile of all RNAs being translated. When this is compared to the transcriptional profile from the same tissue, one can calculate the translational efficiency for all RNAs measured. Ignolia et al. pioneered this strategy in yeast and we have been adapting it for mouse brain. The protocol involves digesting unprotected RNA, pelleting ribosomes, isolating protected RNA that is approximately 30b, and preparing and sequencing small cDNA libraries from those RNAs. The largest hurdle is to subtract out contaminating rRNA fragments, because unlike RNA-Seq, it is not possible to separate out based on the polyA tail. As an example, data published on mouse cell lines show between 60-80% of reads maping to rRNA genes (Katz et al., 2014). We initially had similar levels of rRNA contamination in our Ribo-Seq preparations. The Gilbert lab at MIT found that tighter size selection when preparing Ribo-Seq reads for yeast resulted in lower rRNA contamination (personal communication). With our mammalian samples, we found different distributions of read lengths for reads originating from mRNA verse rRNA (Figure 5-2). A tighter cut of protected RNA coupled with the epicenter Ribo-Zero proprietary rRNA subtraction has reduced our rRNA reads by approximately

40% (Figure 5-3).

With this adapted protocol, we would like to perform concurrent RNA- and Ribo-Seq on cortex and striatum of an HD mouse model and determine if there are specific transcripts with altered translational efficiency.

5.5 Final Summary

The dramatic improvement in the speed and cost of DNA sequencing has enabled the development of many techniques to study the cell at a genome-wide level. By applying several of these techniques to the study of Huntington's disease we have given insight into the role of epigenetics and splicing in disease pathogenesis. We are prepared to extend our genome-wide studies to RNA localization and translational efficiency. By expanding our understanding of the HD disease process, we hope to enhance the development of optimal therapeutics and biomarkers for therapeutic efficacy for HD and related disorders.

5.6 Chapter 5 - Figures

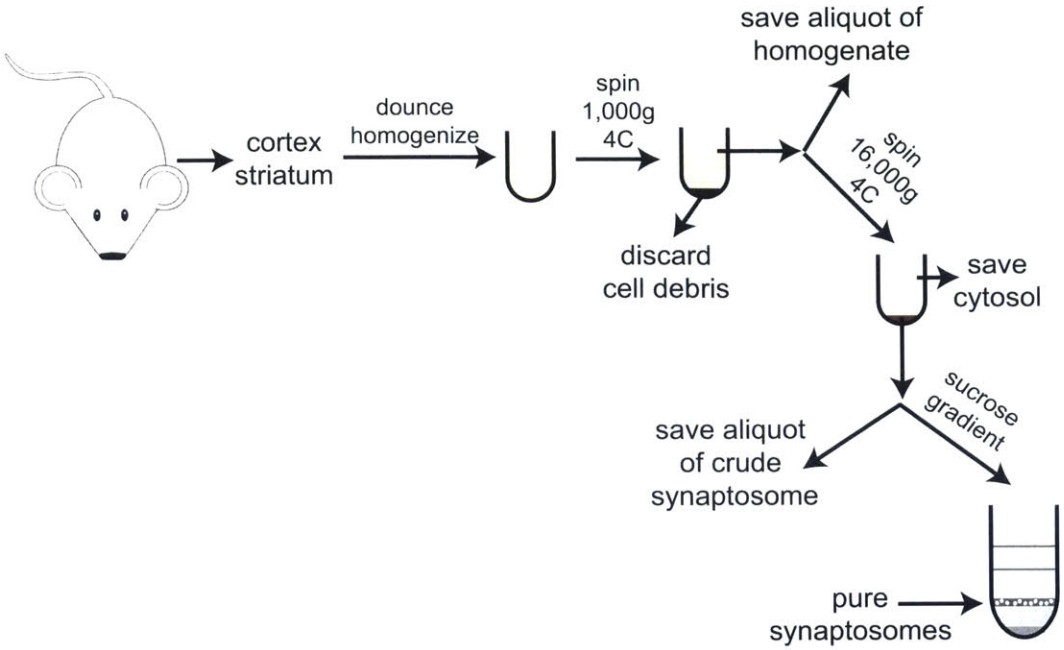

Figure 5-1: Our protocol for isolating RNA and protein from neuronal compartments.

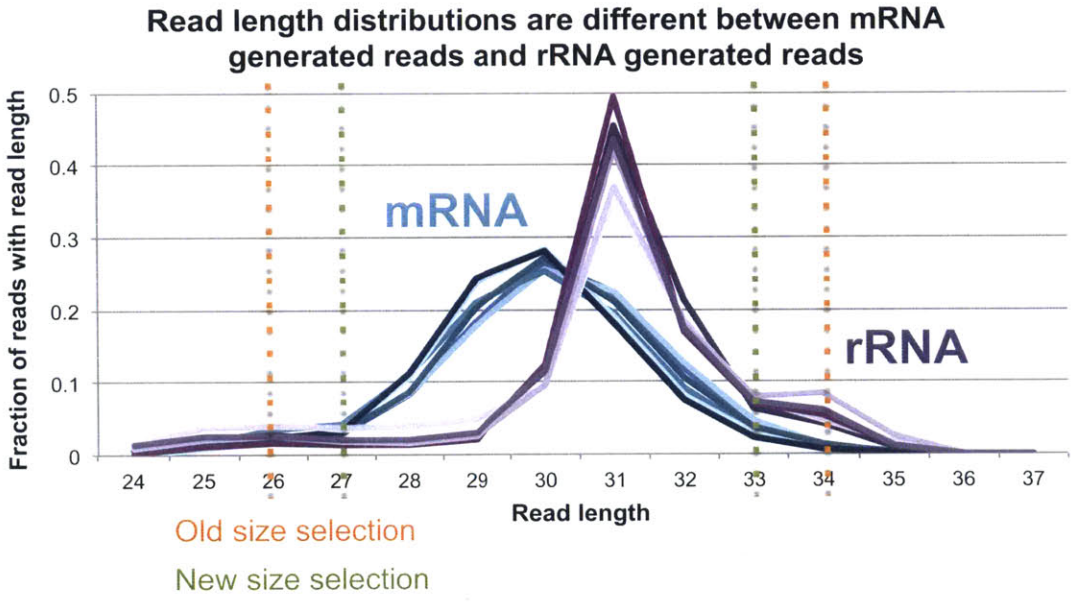

Figure 5-2: Read length distribution is different for reads generated from mRNA verse rRNA. A tighter size selection of protected fragments, especially on the higher end, will reduce the amount of rRNA generated reads. We do not want to cut much shorter than 33 bases because the mammalian ribosome takes on a conformation at stop codons that protects about 32-33 bases.

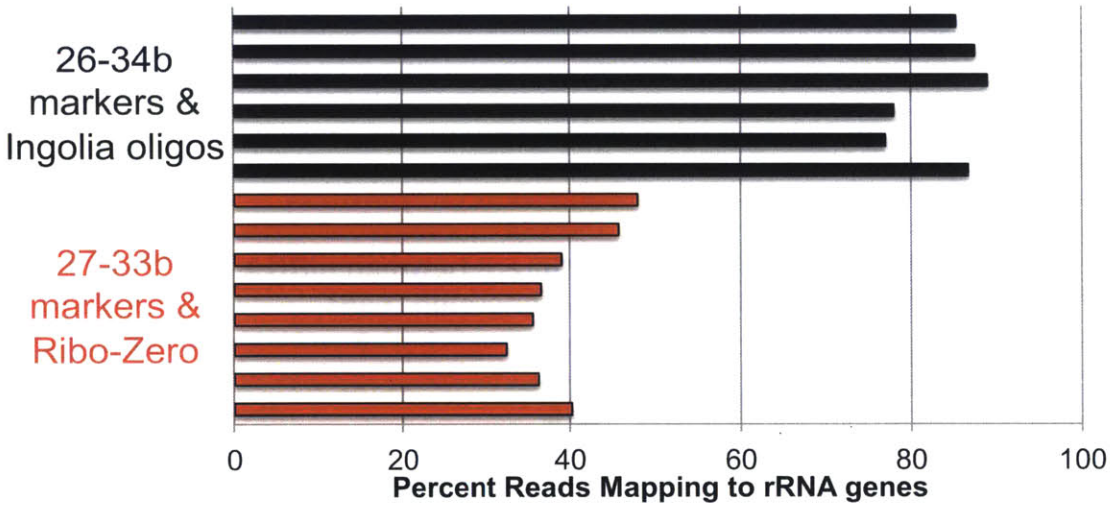

Figure 5-3: Improvement in rRNA subtraction in Ribo-Seq.

Appendix A - Supplement for Chapter 2

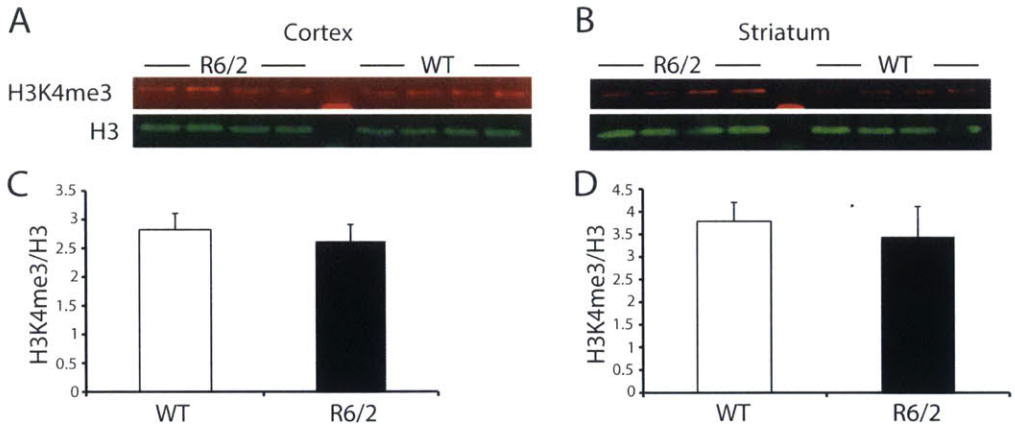

Figure A-1: H3K4me3 levels were quantified in total protein lysates from cortex and striatum of four 12wk Wt and R6/2 mice. (A and B) Western analysis of (A) cortex and (B) striatum samples using Odyssey LiCOR chemiluminescence. Total H3 levels were used as a loading control. (C and D) Quantitation was performed using Odyssey IR imager, and one-way ANOVA was performed for statistical analysis. No statistically significant differences were observed in either brain regions.

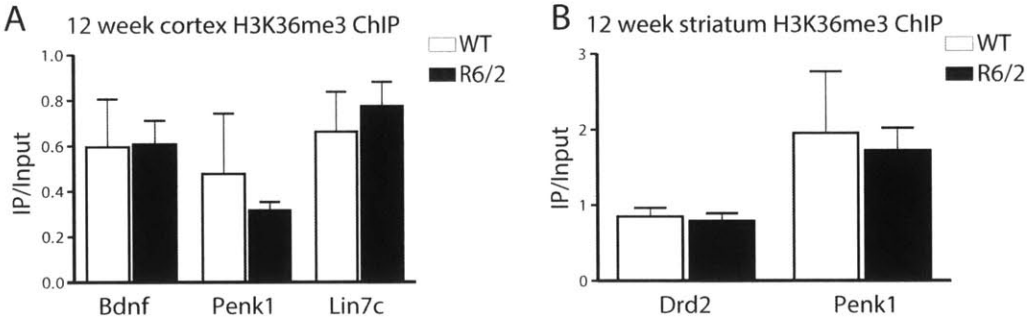

Figure A-2: H3K36me3 occupancy in coding regions was compared between 12wk old WT and R6/2 mice by ChIP. There were no statistically significant differences in H3K36me3 levels in the coding region of preproenkephalin (*Penk1*), brain-derived neurotrophic factor (*Bdnf*), and *Lin7c* genes in the (A) cortex and *Penk1* and dopamine receptor 2 (*Drd2*) in the (B) striatum (n = 4 in each group)

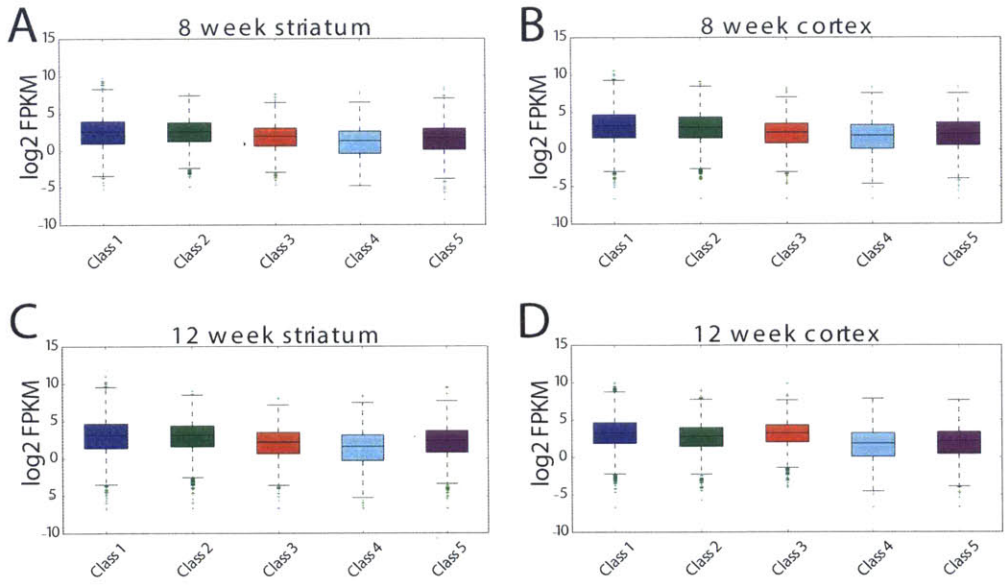

Figure A-3: Box-and-whisker plots of log2 FPKM distributions for the five classes of H3K4me3 profiles in wildtype mice in (A) 8wk striatum, (B) 8wk cortex, (C) 12wk striatum, and (D) 12wk cortex show that class membership is not tightly associated with absolute gene expression levels.

Table A-1: Dysregulated genes in 8wk striatum.

Gene	ESM181	ESM184	ESM192	ESW176	ESW180	ESW183	gene_symbol	gene_desc	padj	DESeq Delta
14419	0.23	0.00	0.09	0.00	6.38	3.97	Gal	galanin	1.76E-06	31.77
75512	0.07	0.00	0.51	1.09	3.72	2.55	Gpx6	glutathione peroxidase 6	4.12E-06	12.63
13654	0.41	0.37	0.37	2.89	5.60	5.26	Egr2	early growth response 2	8.96E-17	11.97
320712	0.15	0.23	0.23	3.37	1.56	2.03	Abi3bp	ABI gene family, member 3 (NESH) binding protein	1.15E-11	11.47
27220	1.76	0.27	0.29	2.37	9.75	11.30	Cartpt	cocaine and amphetamine regulated transcript	2.99E-10	10.04
14174	0.03	0.14	0.20	0.94	1.02	1.35	Fgf3	fibroblast growth factor 3	0.02694611	8.66
12311	0.43	0.00	0.05	0.17	2.01	1.60	Calcr	calcitonin receptor isoform a precursor	6.58E-08	7.75
12918	0.67	0.04	0.22	1.85	2.18	2.08	Crh	corticotropin releasing hormone	0.00098846	6.49
73284	0.76	0.37	1.13	6.34	2.20	4.35	Ddit4l	DNA-damage-inducible transcript 4-like	5.33E-09	5.78
170676	4.91	1.34	1.65	7.15	19.05	15.61	Peg10	paternally expressed 10 isoform RF1/RF2	2.87E-19	5.30
329421	0.18	0.44	0.46	1.94	1.24	1.00	Myo3b	myosin IIIB	0.00207636	3.91
320139	0.22	0.63	0.65	2.23	1.36	2.00	Ptpn7	protein tyrosine phosphatase, non-receptor type,protein tyrosine phosphatase, non-receptor type,	0.0105492	3.75
399548	14.42	51.44	58.13	157.95	137.81	154.10	Scn4b	sodium channel, type IV, beta	0.00023733	3.65
219134	0.53	0.12	0.63	1.58	1.30	1.67	Tmem46	transmembrane protein 46	0.01456257	3.57
12405	1.40	0.47	0.54	3.10	3.04	2.33	Cbln2	cerebellin 2 precursor protein,cerebellin 2 precursor protein,cerebellin 2 precursor protein,cerebellin 2 precursor protein,	0.00198994	3.55
232413	0.23	0.48	0.75	1.73	1.34	2.07	Clec12a	C-type lectin domain family 12, member a	0.06956506	3.53
22771	9.12	3.11	0.98	16.77	16.41	12.31	Zic1	Zic family member 1,Zic family member 1,	6.12E-10	3.49
192199	0.47	0.58	0.43	1.14	2.49	1.37	Rspo1	thrombospondin type 1 domain containing	0.08397745	3.41
14313	0.34	0.45	0.89	3.25	1.44	0.98	Fst	follistatin,follistatin,	0.04874246	3.41
18619	100.86	194.89	186.04	643.27	463.09	500.74	Penk1	preproenkephalin 1,preproenkephalin 1,	0.00079315	3.36
59046	139.18	132.13	194.09	836.11	349.47	349.68	Arpp19	cAMP-regulated phosphoprotein 19,cAMP-regulated phosphoprotein 19,	1.44E-05	3.35
12509	1.94	1.91	2.52	11.61	4.57	4.76	Cd59a	CD59a antigen	0.00130813	3.34
16543	0.23	0.39	0.53	1.21	0.77	1.85	Mdfic	MyoD family inhibitor domain containing protein,MyoD family inhibitor domain containing protein,	0.05072155	3.34
238680	0.66	0.61	0.93	1.77	2.13	3.15	Cntnap3	contactin associated protein-like 3,contactin associated protein-like 3,	0.00463014	3.22
74513	7.67	5.85	8.76	31.91	17.47	18.84	Neto2	neuropilin- and tolloid-like protein 2,neuropilin- and tolloid-like protein 2,neuropilin- and tolloid-like protein 2,	8.69E-05	3.10
20190	0.40	0.79	0.29	1.37	1.75	1.29	Ryr1	ryanodine receptor 1, skeletal muscle	0.00106985	3.00
246048	1.00	0.06	0.48	1.32	1.74	1.44	Chodl	chondrolectin,chondrolectin,	0.05746088	2.95
12308	16.85	0.53	0.49	17.92	21.55	11.17	Calb2	calbindin 2,calbindin 2,	1.98E-06	2.87
12484	1.85	0.88	2.85	4.53	6.08	5.05	Cd24a	CD24a antigen	0.02294754	2.82
15550	1.51	0.35	0.05	1.06	2.61	1.64	Htr1a	5-hydroxytryptamine (serotonin) receptor 1A	0.00242788	2.78
234912	2.05	0.95	0.93	4.15	2.55	4.02	9230110C19Rik	hypothetical protein LOC234912	0.04982221	2.76
64378	70.48	102.62	144.40	561.10	140.24	149.14	Gpr88	G-protein coupled receptor 88	0.03004881	2.73
18167	2.24	0.51	0.45	1.76	3.41	3.47	Npy2r	neuropeptide Y receptor Y2	0.00346364	2.71
66222	0.99	1.54	1.55	4.98	3.33	2.53	Serpinb1a	serine (or cysteine) proteinase inhibitor, clade,serine (or cysteine) proteinase inhibitor, clade,	0.07948828	2.70
22065	1.74	1.60	1.59	6.99	3.28	2.73	Trpc3	transient receptor potential cation channel,,transient receptor potential cation channel,,	0.00873665	2.68
20855	0.95	0.36	0.42	1.89	1.18	1.50	Stc1	stanniocalcin 1	0.04299876	2.66
101772	0.73	0.28	0.22	0.34	1.80	1.11	Tmem16a	transmembrane protein 16A,transmembrane protein 16A,	0.09534936	2.63
22036	1.58	1.74	1.38	4.64	3.53	4.04	Traip	TRAF-interacting protein	0.03360655	2.62
320116	1.60	0.84	1.22	1.32	4.31	3.98	C030019I05Rik	hypothetical protein LOC320116	0.04797325	2.61
13488	8.98	13.79	26.55	63.04	29.63	33.77	Drd1a	dopamine receptor D1A	0.01479246	2.60
67405	7.89	3.95	6.30	11.97	17.41	17.11	Nts	neurotensin	0.00948263	2.57
22068	1.14	0.74	0.56	3.36	1.17	1.68	Trpc6	transient receptor potential cation channel,,transient receptor potential cation channel,,	0.05990402	2.57
16592	3.52	2.45	2.31	12.91	5.48	2.43	Fabp5	fatty acid binding protein 5, epidermal	0.0766684	2.57
22421	1.31	1.64	1.17	2.99	3.90	3.49	Wnt7a	wingless-related MMTV integration site 7A	0.0324322	2.53
14281	6.73	2.10	1.83	7.93	10.73	8.14	Fos	FBJ osteosarcoma oncogene	0.00211501	2.53

74521	2.43	3.05	3.09	8.45	6.39	6.21	8430415E04Rik	HEAT-like repeat-containing protein,HEAT-like repeat-containing protein,	0.02000057	2.48
213121	1.11	0.36	0.41	1.76	1.12	1.71	Ankrd35	ankyrin repeat domain 35	0.06821363	2.45
19736	54.94	61.31	81.83	257.97	95.52	118.45	Rgs4	regulator of G-protein signaling 4	0.04243216	2.42
76459	2.60	5.46	4.25	9.38	6.48	13.67	Car12	carbonic anyhydrase 12,carbonic anyhydrase 12,	0.02294754	2.41
20348	2.35	1.39	1.15	5.14	3.18	3.30	Sema3c	semaphorin 3C,semaphorin 3C,	0.01253641	2.40
66259	137.07	107.36	184.43	621.28	176.53	213.66	Camk2n1	calcium/calmodulin-dependent protein kinase II	0.0931367	2.40
68028	14.17	5.51	14.75	43.79	15.90	21.49	Rpl22l1	ribosomal protein L22 like 1,ribosomal protein L22 like 1,	0.06784751	2.39
23984	16.51	36.77	38.11	82.49	65.58	66.63	Pde10a	phosphodiesterase 10A,phosphodiesterase 10A,phosphodiesterase 10A,	0.08038162	2.37
12504	2.42	5.82	7.20	12.41	10.78	13.05	Cd4	CD4 antigen,CD4 antigen,	0.04420391	2.36
14586	3.50	0.75	0.85	2.17	5.65	4.10	Gfra2	glial cell line derived neurotrophic factor,glial cell line derived neurotrophic factor,glial cell line derived neurotrophic factor,	0.0117411	2.34
70571	2.75	0.49	0.60	0.93	4.39	3.68	Tcerg1l	transcription elongation regulator 1-like	0.04797325	2.34
218341	2.67	1.00	2.27	7.63	2.55	3.43	Rfesd	Rieske (Fe-S) domain containing,Rieske (Fe-S) domain containing,	0.09363469	2.33
14608	4.43	4.85	6.77	15.78	9.59	11.68	Gpr83	G protein-coupled receptor 83	0.03443772	2.33
15904	33.60	29.97	35.69	92.61	58.66	77.90	Id4	inhibitor of DNA binding 4	0.02124713	2.33
12123	3.84	2.15	2.73	7.58	5.72	6.84	Hrk	harakiri	0.01260048	2.33
11838	6.47	14.67	6.78	13.21	29.52	21.82	Arc	activity regulated cytoskeletal-associated,activity regulated cytoskeletal-associated,	0.02493357	2.31
66291	7.14	2.56	9.24	25.69	8.97	8.31	1810030N24Rik	hypothetical protein LOC66291,hypothetical protein LOC66291,	0.07723621	2.31
18546	296.61	305.95	506.68	1263.82	576.06	668.55	Pcp4	Purkinje cell protein 4	0.08411849	2.29
12326	13.11	15.82	17.39	58.81	23.27	22.35	Camk4	calcium/calmodulin-dependent protein kinase IV	0.06676051	2.29
330941	19.66	16.31	21.47	69.85	29.79	29.62	AI593442	hypothetical protein LOC330941 isoform 2	0.03702028	2.29
269275	2.84	3.17	4.79	12.75	5.18	6.20	Acvr1c	activin A receptor, type IC	0.0414314	2.27
211612	2.83	1.76	3.17	9.81	3.44	4.02	Ptchd1	patched domain containing 1	0.02957098	2.26
11551	1.86	0.39	0.28	0.77	2.64	2.27	Adra2a	adrenergic receptor, alpha 2a	0.04797325	2.24
16497	35.36	41.98	59.26	160.07	65.53	75.99	Kcnab1	potassium voltage-gated channel, shaker-related,potassium voltage-gated channel, shaker-related,	0.07160414	2.24
19735	2.39	3.67	4.66	6.90	8.28	8.51	Rgs2	regulator of G-protein signaling 2	0.0797587	2.22
19711	36.65	8.97	6.14	15.13	61.55	38.10	Resp18	regulated endocrine-specific protein 18	0.00796221	2.22
12307	35.26	23.35	38.63	120.74	34.30	55.27	Calb1	calbindin-28K	0.04797325	2.20
68995	17.78	9.24	19.99	58.69	19.67	22.64	Mcts1	malignant T cell amplified sequence 1,malignant T cell amplified sequence 1,malignant T cell amplified sequence 1,	0.05518104	2.19
78771	14.32	12.99	26.83	60.58	23.35	32.24	Mctp1	multiple C2 domains, transmembrane 1,multiple C2 domains, transmembrane 1,multiple C2 domains, transmembrane 1,	0.08142527	2.18
12971	14.13	16.67	22.84	36.10	28.18	51.08	Crym	crystallin, mu	0.0735849	2.16
76206	2.61	0.66	0.80	0.76	4.60	3.41	Gpr165	G protein-coupled receptor 165	0.07108732	2.15
140723	3.49	0.56	1.01	2.44	4.58	3.77	Cacng5	calcium channel, voltage-dependent, gamma,calcium channel, voltage-dependent, gamma,calcium channel, voltage-dependent, gamma,	0.03209216	2.14
14806	10.17	6.94	9.76	29.83	11.76	14.82	Grik2	glutamate receptor, ionotropic, kainate 2 (beta,glutamate receptor, ionotropic, kainate 2 (beta,glutamate receptor, ionotropic, kainate 2 (beta,	0.04845914	2.13
15370	5.60	11.03	6.60	6.12	22.41	21.03	Nr4a1	nuclear receptor subfamily 4, group A, member 1	0.07335899	2.13
71436	4.68	4.92	8.47	17.68	8.89	11.06	Flrt3	fibronectin leucine rich transmembrane protein	0.0960741	2.11
99929	3.59	2.21	4.69	7.45	6.91	7.34	Tiparp	TCDD-inducible poly(ADP-ribose) polymerase	0.09285677	2.09
80334	13.73	4.81	10.62	33.80	12.09	13.81	Kcnip4	potassium channel interacting protein 4,potassium channel interacting protein 4,	0.04797325	2.08
12227	3.02	1.93	0.78	3.42	5.03	3.32	Btg2	B-cell translocation gene 2, anti-proliferative	0.07282092	2.07

108089	3.30	2.05	3.14	7.88	4.18	4.85	Rnf144a	ring finger protein 144	0.09850152	2.02
16426	6.29	5.26	3.54	4.11	17.43	8.83	Itih3	inter-alpha trypsin inhibitor, heavy chain 3	0.0882875	2.01
22774	2.58	0.56	0.07	1.40	3.20	1.80	Zic4	zinc finger protein of the cerebellum 4,zinc finger protein of the cerebellum 4,zinc finger protein of the cerebellum 4,zinc finger protein of the cerebellum 4,	0.0560064	2.01
244672	5.20	2.49	4.56	13.27	4.70	6.20	Cwf19l2	CWF19-like 2, cell cycle control,CWF19-like 2, cell cycle control,	0.0931367	2.01
18111	74.66	27.10	30.31	25.40	121.47	118.32	Nnat	neuronatin isoform alpha	0.04072009	2.00
15566	3.37	0.37	0.44	2.14	3.34	2.77	Htr7	5-hydroxytryptamine (serotonin) receptor 7	0.07297262	1.99
22773	2.41	0.36	0.53	1.40	2.86	2.23	Zic3	zinc finger protein of the cerebellum 3	0.09850152	1.98
108030	9.92	3.69	6.44	20.22	9.15	9.33	Lin7a	lin 7 homolog a isoform 1	0.07383948	1.96
407812	8.30	3.51	4.50	11.33	7.82	11.84	BC066028	hypothetical protein LOC407812	0.08708195	1.92
245386	11.30	1.32	2.16	3.34	14.93	9.97	6430550H21Rik	hypothetical protein LOC245386,hypothetical protein LOC245386,	0.0300027	1.91
14405	9.00	1.91	3.73	7.35	10.45	9.24	Gabrg1	gamma-aminobutyric acid A receptor, gamma 1,gamma-aminobutyric acid A receptor, gamma 1,	0.07980168	1.86
380702	2.49	0.40	0.28	2.37	2.38	0.97	Gm879	hypothetical protein LOC380702	0.07128942	1.82
26950	104.91	19.53	29.77	114.61	83.48	72.74	Vsnl1	visinin-like 1	0.09285677	1.78
20020	12.51	17.35	11.48	2.95	7.58	7.11	Polr2a	polymerase (RNA) II (DNA directed) polypeptide,polymerase (RNA) II (DNA directed) polypeptide,	0.0324322	0.43
241794	3.32	6.95	4.86	1.34	2.74	2.28	Kcng1	potassium voltage-gated channel, subfamily G,	0.07108732	0.42
71371	3.26	3.44	2.68	0.83	1.35	1.61	Arid5b	AT rich interactive domain 5B (Mrf1 like),AT rich interactive domain 5B (Mrf1 like),AT rich interactive domain 5B (Mrf1 like),	0.05746088	0.40
268482	5.41	6.40	3.70	1.53	1.34	0.56	A830036E02Rik	keratin complex 1, acidic, gene 12	0.00036319	0.22
14113	1.84	5.65	2.79	0.09	1.03	1.10	Fbl	fibrillarin	0.02294754	0.22
66898	2.06	0.66	3.23	0.21	0.28	0.49	Baiap2l1	BAI1-associated protein 2-like 1	4.47E-05	0.17

Table A-2: Dysregulated genes in 8wk cortex.

Gene	ECM184	ECM175	ECM181	ECW176	ECW178	ECW180	gene_symbol	gene_desc	padj	DESeq Delta
226896	0.09	0.00	0.06	2.17	1.49	0.00	Tcfap2d	transcription factor AP-2, delta	0.008346476	24.87
383787	0.24	1.45	0.27	6.63	5.02	2.07	Gm1337	hypothetical protein LOC383787	3.91E-09	7.02
18167	0.16	0.72	0.31	2.65	2.80	0.75	Npy2r	neuropeptide Y receptor Y2	0.012384401	5.15
15558	1.50	0.87	0.51	6.87	3.70	3.94	Htr2a	5-hydroxytryptamine (serotonin) receptor 2 A	0.001828899	4.97
213435	0.19	0.60	0.29	1.27	1.31	2.62	D830007F02Rik	myosin light chain kinase,myosin light chain kinase,myosin light chain kinase,	0.001267261	4.80
320609	1.96	2.92	1.20	14.03	9.89	5.08	D330017J20Rik	hypothetical protein LOC320609 isoform b,hypothetical protein LOC320609 isoform b,	3.75E-05	4.76
140781	0.24	0.36	0.22	0.97	1.22	1.52	Myh7	myosin, heavy polypeptide 7, cardiac muscle,	0.00443907	4.55
18187	0.93	1.64	0.32	4.57	4.58	3.43	Nrp2	neuropilin 2 isoform 1 precursor	0.00443907	4.36
228942	0.95	1.55	0.63	6.98	4.10	2.58	Cbln4	cerebellin 4 precursor	0.009422765	4.33
76459	0.40	1.10	0.37	3.25	4.09	0.63	Car12	carbonic anyhydrase 12,carbonic anyhydrase 12,	0.072788978	4.26
234912	0.81	1.66	1.44	6.85	6.25	3.55	9230110C19Rik	hypothetical protein LOC234912	0.015029856	4.23
15550	0.77	2.29	1.29	6.26	6.47	5.08	Htr1a	5-hydroxytryptamine (serotonin) receptor 1A	2.79E-05	4.07
22045	0.22	0.74	0.48	2.42	2.60	0.78	Trhr	thyrotropin releasing hormone receptor,thyrotropin releasing hormone receptor,	0.0449042	3.98
18232	0.23	0.79	1.04	2.92	3.96	1.24	Nxph2	neurexophilin 2	0.034463089	3.93
236285	0.59	1.04	0.53	4.07	2.94	1.41	Lancl3	LanC lantibiotic synthetase component C-like 3	0.034956042	3.88
239318	2.92	1.84	0.78	7.77	8.88	4.98	Plcxd3	phosphatidylinositol-specific phospholipase C, X	0.055349723	3.85
219134	0.15	0.63	0.42	2.80	1.27	0.58	Tmem46	transmembrane protein 46	0.092556991	3.82
19225	0.90	0.82	0.88	2.81	4.34	2.56	Ptgs2	prostaglandin-endoperoxide synthase 2	0.017686963	3.72
73284	2.11	2.28	1.94	6.32	7.93	9.48	Ddit4l	DNA-damage-inducible transcript 4-like	0.000321696	3.70
58175	6.31	9.90	7.34	25.54	43.82	17.06	Rgs20	regulator of G-protein signaling 20,regulator of G-protein signaling 20,	0.005230425	3.66
73707	0.42	0.89	0.87	2.83	2.04	3.10	Gucy2g	guanylate cyclase 2g,guanylate cyclase 2g,	0.003228908	3.64
75869	2.18	2.31	0.71	7.37	6.50	5.01	Arl5b	ADP-ribosylation factor-like 5B	0.013805601	3.59
76453	1.06	1.51	2.46	9.45	3.39	5.16	Prss23	protease, serine, 23,protease, serine, 23,	0.00078944	3.55
233271	26.77	19.99	14.23	77.97	96.81	39.76	Luzp2	leucine zipper protein 2,leucine zipper protein 2,	0.005342121	3.49
14405	3.51	4.89	3.33	17.79	17.08	6.05	Gabrg1	gamma-aminobutyric acid A receptor, gamma 1,gamma-aminobutyric acid A receptor, gamma 1,	0.009422765	3.47
18430	0.59	0.82	0.71	4.02	2.24	1.16	Oxtr	oxytocin receptor	0.066872403	3.46
208164	0.03	0.57	0.42	0.46	1.22	1.84	BC064033	hypothetical protein LOC208164	0.090922446	3.42
22042	8.64	17.10	9.28	46.35	49.13	23.83	Tfrc	transferrin receptor,transferrin receptor,transferrin receptor,	0.000774379	3.40
59012	0.60	0.67	0.94	2.53	3.16	1.84	Moxd1	monooxygenase, DBH-like 1	0.082942803	3.38
14219	2.79	3.19	9.40	12.61	26.48	12.84	Ctgf	connective tissue growth factor	0.000630858	3.34
19699	2.15	3.97	2.00	11.40	9.89	5.73	Reln	reelin precursor,reelin precursor,	0.002176939	3.32
21924	2.78	6.31	7.88	17.41	15.23	23.07	Tnnc1	troponin C, cardiac/slow skeletal	0.003238772	3.27
17171	0.95	2.07	1.89	7.11	6.81	2.21	Mas1	MAS1 oncogene,MAS1 oncogene,MAS1 oncogene,	0.082942803	3.27
19258	7.33	4.98	1.14	19.17	12.09	12.46	Ptpn4	protein tyrosine phosphatase, non-receptor type	0.016435367	3.25

72003	5.58	3.23	2.45	19.13	10.99	6.74	Synpr	synaptoporin,synaptoporin,	0.086260108	3.24
18619	9.56	49.98	16.60	99.12	101.95	44.40	Penk1	preproenkephalin 1,preproenkephalin 1,	0.001172514	3.23
217480	17.87	17.42	9.43	59.58	58.22	25.12	Dgkb	diacylglycerol kinase, beta,diacylglycerol kinase, beta,diacylglycerol kinase, beta,diacylglycerol kinase, beta,diacylglycerol kinase, beta,diacylglycerol kinase, beta,	0.015936583	3.19
12950	3.71	3.01	2.86	9.04	12.99	8.54	Hapln1	hyaluronan and proteoglycan link protein 1	0.009422765	3.15
240725	1.47	1.29	2.48	5.83	6.74	3.65	Sulf1	sulfatase 1,sulfatase 1,sulfatase 1,sulfatase 1,	0.026410737	3.08
320506	8.78	6.23	2.87	21.72	19.12	14.13	Lmbrd2	LMBR1 domain containing 2	0.038872697	3.07
17181	2.03	2.94	3.07	10.97	8.13	5.33	Matn2	matrilin 2,matrilin 2,matrilin 2,	0.022307642	3.03
228432	13.83	10.37	2.30	30.39	19.57	28.75	Tmem16c	hypothetical protein LOC228432	0.017669579	3.01
268670	1.38	2.37	1.69	5.88	7.29	3.24	Zfp759	zinc finger protein 759	0.064425458	3.00
216578	1.61	2.38	0.72	5.77	4.72	3.53	Papolg	poly(A) polymerase gamma,poly(A) polymerase gamma,	0.087309951	2.99
319239	0.08	0.40	1.48	2.84	1.63	1.33	Npsr1	G protein-coupled receptor for asthma,G protein-coupled receptor for asthma,	0.03167767	2.95
229759	3.86	7.78	9.09	18.19	25.67	16.93	Olfm3	olfactomedin 3 isoform A	0.001521363	2.91
245684	29.61	28.94	12.15	75.01	81.28	48.08	Cnksr2	connector enhancer of kinase suppressor of Ras,connector enhancer of kinase suppressor of Ras,	0.02401168	2.88
14415	40.86	57.68	41.95	194.93	129.66	79.20	Gad1	glutamic acid decarboxylase 1,glutamic acid decarboxylase 1,glutamic acid decarboxylase 1,	0.009422765	2.87
170459	3.36	3.23	1.90	6.07	11.73	6.78	Stard4	StAR-related lipid transfer (START) domain,StAR-related lipid transfer (START) domain,	0.077692985	2.87
67498	15.95	14.00	10.95	35.46	54.22	28.46	Kcnv1	potassium channel Kv8.1 homolog,potassium channel Kv8.1 homolog,	0.023727841	2.85
20356	2.20	2.51	3.01	9.88	6.90	5.41	Sema5a	semaphorin 5A,semaphorin 5A,semaphorin 5A,semaphorin 5A,	0.009422765	2.85
11855	27.21	14.95	8.09	51.37	56.97	36.91	Arhgap5	Rho GTPase activating protein 5,Rho GTPase activating protein 5,	0.053504095	2.85
74513	7.01	9.62	7.44	27.45	25.83	15.09	Neto2	neuropilin- and tolloid-like protein 2,neuropilin- and tolloid-like protein 2,neuropilin- and tolloid-like protein 2,	0.015676707	2.82
240028	7.68	4.67	1.08	15.34	10.87	11.91	Lnpep	leucyl/cystinyl aminopeptidase,leucyl/cystinyl aminopeptidase,leucyl/cystinyl aminopeptidase,	0.05774093	2.82
14417	19.38	28.37	12.22	77.64	60.09	31.08	Gad2	glutamic acid decarboxylase 2,glutamic acid decarboxylase 2,	0.030321212	2.80
14348	9.18	12.65	8.39	27.43	30.23	27.33	Fut9	fucosyltransferase 9	0.002176939	2.78
12405	6.74	7.22	5.51	26.27	10.26	18.15	Cbln2	cerebellin 2 precursor protein,cerebellin 2 precursor protein,cerebellin 2 precursor protein,cerebellin 2 precursor protein,	0.011144686	2.78
22284	13.83	11.28	3.57	34.60	28.02	17.31	Usp9x	ubiquitin specific protease 9, X chromosome,ubiquitin specific protease 9, X chromosome,	0.074073855	2.77
12801	15.32	22.37	13.16	54.97	56.20	30.55	Cnr1	cannabinoid receptor 1 (brain)	0.017669579	2.76

67295	48.78	64.76	41.57	141.93	205.47	81.59	Rab3c	RAB3C, member RAS oncogene family,RAB3C, member RAS oncogene family,	0.041226789	2.74
11829	18.13	11.13	11.64	37.37	49.05	27.23	Aqp4	aquaporin 4,aquaporin 4,aquaporin 4,aquaporin 4,	0.047929563	2.74
21847	3.46	6.51	6.27	15.05	17.87	11.82	Klf10	Kruppel-like factor 10	0.012623511	2.73
20348	5.10	6.42	4.13	20.99	12.35	9.39	Sema3c	semaphorin 3C,semaphorin 3C,	0.041388927	2.72
19283	18.38	12.40	7.06	37.07	39.37	26.90	Ptprz1	protein tyrosine phosphatase, receptor type Z,,protein tyrosine phosphatase, receptor type Z,,	0.053504095	2.71
74521	2.87	3.72	1.73	8.30	8.08	6.11	8430415E04Rik	HEAT-like repeat-containing protein,HEAT-like repeat-containing protein,	0.085161249	2.71
19386	17.32	15.98	7.33	46.18	43.62	20.72	Ranbp2	RAN binding protein 2	0.090922446	2.70
22353	16.67	14.77	17.88	37.96	65.18	30.51	Vip	vasoactive intestinal polypeptide	0.057785075	2.69
241514	3.04	4.77	3.55	15.65	10.03	5.12	Zfp804a	zinc finger protein 804A,zinc finger protein 804A,	0.082634809	2.69
12123	3.38	5.06	4.50	9.19	17.68	8.21	Hrk	harakiri	0.034463089	2.68
233726	36.96	37.32	17.02	99.50	96.63	46.80	Ipo7	importin 7	0.089025168	2.68
68861	6.48	9.94	7.68	28.88	24.24	11.88	1190002N15Rik	hypothetical protein LOC68861	0.046683945	2.68
71912	0.69	0.37	1.33	0.90	1.04	4.56	Jsrp1	JP-45 protein	0.090411965	2.68
235072	133.92	188.82	214.52	511.15	635.23	280.68	6-Sep	cell division cycle 10 homolog	0.019074644	2.65
269109	15.03	14.14	6.80	33.59	39.11	21.77	Dpp10	dipeptidyl peptidase 10	0.090922446	2.63
20512	97.28	89.91	63.80	224.52	300.50	136.58	Slc1a3	solute carrier family 1 (glial high affinity,solute carrier family 1 (glial high affinity,	0.082634809	2.61
381511	18.55	18.04	17.09	46.07	57.27	38.42	Ppm2c	protein phosphatase 2C, magnesium dependent,	0.023727841	2.61
227059	21.70	19.62	12.88	42.59	58.15	41.72	Slc39a10	solute carrier family 39 (zinc transporter),,solute carrier family 39 (zinc transporter),,	0.032106955	2.60
26570	3.21	3.52	1.98	7.24	10.25	5.36	Slc7a11	solute carrier family 7 (cationic amino acid,solute carrier family 7 (cationic amino acid,	0.093384826	2.60
18162	0.47	2.08	0.96	3.50	2.64	3.01	Npr3	natriuretic peptide receptor 3 isoform a	0.01460696	2.60
99887	8.47	7.99	4.14	18.06	22.09	13.85	Tmem56	transmembrane protein 56,transmembrane protein 56,transmembrane protein 56,transmembrane protein 56,	0.077058376	2.60
26878	6.59	7.06	7.91	20.48	17.67	18.39	B3galt2	UDP-Gal:betaGlcNAc beta	0.009880573	2.59
12064	3.84	4.92	5.24	11.93	16.76	7.94	Bdnf	brain derived neurotrophic factor isoform 2	0.074073855	2.59
100129	1.53	1.78	1.56	5.06	3.61	4.02	Gpr153	G protein-coupled receptor 153	0.081619006	2.58
11789	25.75	27.83	17.12	72.65	64.60	46.97	Apc	adenomatosis polyposis coli	0.034972277	2.58
14608	1.62	3.04	2.24	4.00	7.92	6.02	Gpr83	G protein-coupled receptor 83	0.073423735	2.58
13179	1.23	2.27	5.32	4.31	10.63	7.98	Dcn	decorin,decorin,	0.029818744	2.58
18795	37.11	42.91	32.16	108.95	115.00	66.07	Plcb1	phospholipase C, beta 1,phospholipase C, beta 1,phospholipase C, beta 1,	0.03853806	2.58
17896	3.78	5.18	11.03	16.10	11.47	24.14	Myl4	myosin, light polypeptide 4,myosin, light polypeptide 4,	0.011957034	2.57
64706	2.68	2.86	2.16	7.03	7.29	5.59	Scube1	signal peptide, CUB domain, EGF-like 1,signal peptide, CUB domain, EGF-like 1,	0.054127886	2.57
74782	2.63	3.31	1.88	6.61	4.31	9.19	Glt8d2	glycosyltransferase 8 domain containing 2	0.03853806	2.56
110075	1.44	1.17	1.89	3.11	2.81	5.68	Bmp3	bone morphogenetic protein 3,bone morphogenetic protein 3,	0.043175365	2.54
72585	10.56	17.25	12.90	12.63	49.92	41.47	Lypd1	Ly6/Plaur domain containing 1,Ly6/Plaur domain containing 1,	0.005839858	2.53

242474	1.84	2.17	0.66	4.00	3.49	4.44	D730040F13Rik	hypothetical protein LOC242474	0.05774093	2.53
109294	5.38	4.45	3.05	8.32	15.27	9.32	C030045D06Rik	hypothetical protein LOC109294	0.093384826	2.52
20713	29.51	21.69	15.06	73.92	49.61	41.96	Serpini1	serine (or cysteine) proteinase inhibitor, clade	0.0954841	2.48
14609	54.56	46.57	39.80	118.73	143.94	90.32	Gja1	gap junction membrane channel protein alpha 1,gap junction membrane channel protein alpha 1,gap junction membrane channel protein alpha 1,gap junction membrane channel protein alpha 1,gap junction membrane channel protein alpha 1,gap junction membrane channel protein alpha 1,gap junction membrane channel protein alpha 1,	0.066763081	2.47
59046	280.77	249.88	348.57	673.79	740.18	752.53	Arpp19	cAMP-regulated phosphoprotein 19,cAMP-regulated phosphoprotein 19,	0.016559386	2.47
20254	42.41	55.11	51.40	192.37	102.64	75.18	Scg2	secretogranin II,secretogranin II,	0.043143726	2.46
73288	14.68	18.32	13.47	42.00	45.27	26.63	Ccdc132	coiled-coil domain containing 132,coiled-coil domain containing 132,coiled-coil domain containing 132,	0.076663722	2.46
53623	37.14	45.33	27.75	111.37	101.63	57.88	Gria3	glutamate receptor, ionotropic, AMPA3 (alpha,glutamate receptor, ionotropic, AMPA3 (alpha,glutamate receptor, ionotropic, AMPA3 (alpha,glutamate receptor, ionotropic, AMPA3 (alpha,	0.085161249	2.44
19378	0.08	1.65	1.54	1.70	2.30	4.01	Aldh1a2	aldehyde dehydrogenase family 1, subfamily A2	0.035914083	2.44
17968	17.66	10.29	3.82	28.69	18.17	30.13	Ncam2	neural cell adhesion molecule 2	0.087063219	2.43
27528	26.41	37.11	26.00	66.43	54.80	97.16	D0H4S114	neuronal protein 3.1	0.002693702	2.41
236920	2.62	2.65	1.90	5.89	5.41	6.16	Stard8	START domain containing 8	0.076134594	2.41
108030	14.01	13.88	12.34	36.01	38.66	22.87	Lin7a	lin 7 homolog a isoform 1	0.091231654	2.40
14265	13.07	18.87	13.98	43.17	42.10	24.97	Fmr1	fragile X mental retardation protein 1,fragile X mental retardation protein 1,fragile X mental retardation protein 1,fragile X mental retardation protein 1,fragile X mental retardation protein 1,	0.074073855	2.39
14401	40.24	46.03	39.04	104.90	128.12	67.28	Gabrb2	gamma-aminobutyric acid (GABA-A) receptor,	0.09046635	2.37
211739	16.12	23.19	18.77	49.41	54.07	35.27	Vstm2a	V-set and transmembrane domain containing 2A	0.053504095	2.37
269831	4.12	6.33	7.98	14.90	18.40	10.60	Tspan12	tetraspanin 12	0.090417372	2.37
207227	9.66	13.97	9.59	29.36	30.17	19.64	Stxbp5l	syntaxin binding protein 5-like,syntaxin binding protein 5-like,	0.054127886	2.37
19878	35.59	34.79	26.10	84.42	81.34	60.62	Rock2	Rho-associated coiled-coil forming kinase 2,Rho-associated coiled-coil forming kinase 2,	0.082634809	2.33
234353	52.26	53.09	29.27	103.10	111.64	102.42	Psd3	pleckstrin and Sec7 domain containing 3 isoform,pleckstrin and Sec7 domain containing 3 isoform,	0.058452156	2.33
19419	52.42	77.28	51.75	148.71	150.33	117.81	Rasgrp1	RAS guanyl releasing protein 1	0.046252429	2.28
80718	4.45	6.72	4.09	11.87	13.65	9.56	Rab27b	RAB27b, member RAS oncogene family	0.095383468	2.28

72117	11.70	20.13	18.50	40.24	51.45	23.46	Nat13	Mak3p homolog,Mak3p homolog,Mak3p homolog,	0.09831577	2.27
242362	5.93	7.02	6.78	15.83	16.45	12.89	Manea	mannosidase, endo-alpha	0.08721296	2.27
18573	59.59	50.09	18.81	79.94	94.83	114.20	Pde1a	phosphodiesterase 1A, calmodulin-dependent,phosphodiesterase 1A, calmodulin-dependent,phosphodiesterase 1A, calmodulin-dependent,	0.076663722	2.26
227580	24.03	51.71	50.11	105.90	107.73	70.98	C1ql3	C1q-like 3	0.034321153	2.25
399548	5.00	17.75	5.01	20.41	24.68	17.02	Scn4b	sodium channel, type IV, beta	0.062906041	2.23
17155	2.85	5.38	3.20	7.59	9.25	8.47	Man1a	mannosidase, alpha, class 1A, member 1,mannosidase, alpha, class 1A, member 1,mannosidase, alpha, class 1A, member 1,	0.09046635	2.20
102866	32.61	48.67	45.00	95.77	117.64	64.89	Pls3	plastin 3 precursor,plastin 3 precursor,plastin 3 precursor,	0.097942344	2.20
243755	0.00	2.32	0.98	0.98	3.24	2.88	Slc13a4	solute carrier family 13 (sodium/sulfate,solute carrier family 13 (sodium/sulfate,	0.095383468	2.15
16497	11.86	27.06	19.41	32.77	55.02	34.00	Kcnab1	potassium voltage-gated channel, shaker-related,potassium voltage-gated channel, shaker-related,	0.096362218	2.08
20442	1.37	2.59	2.20	5.04	2.91	4.96	St3gal1	ST3 beta-galactoside alpha-2,3-sialyltransferase,ST3 beta-galactoside alpha-2,3-sialyltransferase,	0.069657812	2.08
16485	11.47	16.54	17.12	35.67	28.90	27.63	Kcna1	potassium voltage-gated channel subfamily A	0.085161249	2.02
211770	1.89	2.49	2.85	3.19	3.43	7.85	Trib1	tribbles homolog 1,tribbles homolog 1,	0.038875402	1.98
16011	17.17	15.66	22.59	32.18	31.09	46.64	Igfbp5	insulin-like growth factor binding protein 5	0.04248993	1.96
12227	5.07	4.62	5.04	7.47	7.55	14.02	Btg2	B-cell translocation gene 2, anti-proliferative	0.087620042	1.94
14586	4.89	12.07	8.01	14.32	12.10	21.82	Gfra2	glial cell line derived neurotrophic factor,glial cell line derived neurotrophic factor,glial cell line derived neurotrophic factor,	0.034463089	1.92
381280	14.36	6.13	7.30	5.10	3.91	3.09	6430706D22Rik	hypothetical protein LOC381280	0.019831597	0.43
381983	34.46	53.17	31.21	14.08	14.94	20.61	Lmtk3	lemur tyrosine kinase 3,lemur tyrosine kinase 3,	0.093384826	0.41
17025	20.69	14.98	27.38	6.60	12.09	6.43	Alad	aminolevulinate, delta-, dehydratase,aminolevulinate, delta-, dehydratase,	0.05774093	0.40
56506	45.79	22.48	28.67	13.15	11.83	13.63	Cib2	calcium and integrin binding family member 2	0.090922446	0.40
72699	8.35	14.81	11.89	4.84	5.31	3.86	Lime1	Lck interacting transmembrane adaptor 1,Lck interacting transmembrane adaptor 1,	0.08721296	0.40
54196	110.10	130.78	154.83	51.80	46.39	49.96	Pabpn1	poly(A) binding protein, nuclear 1,poly(A) binding protein, nuclear 1,poly(A) binding protein, nuclear 1,	0.03167767	0.37
79044	33.70	24.90	47.74	8.89	11.17	17.00	Mrps34	mitochondrial ribosomal protein S34	0.082942803	0.34
66481	212.81	92.49	264.01	38.64	55.51	94.77	Rps21	ribosomal protein S21,ribosomal protein S21,ribosomal protein S21,	0.09046635	0.34
234388	92.79	85.09	174.81	28.62	32.10	59.97	Ccdc124	coiled-coil domain containing 124	0.06832941	0.34
214917	36.75	31.98	61.08	10.45	13.84	17.45	BC008155	hypothetical protein LOC214917,hypothetical protein LOC214917,hypothetical protein LOC214917,	0.040398095	0.32

14325	70.64	37.72	110.32	12.27	19.16	38.41	Ftl1	ferritin light chain 1	0.044978849	0.32
20637	87.34	213.18	124.90	45.25	33.25	44.53	Snrp70	U1 small nuclear ribonucleoprotein 70 kDa	0.001826313	0.29
76917	13.21	7.17	22.21	2.73	2.77	4.98	Flywch2	FLYWCH family member 2	0.061156523	0.24
68490	4.01	5.82	5.35	0.64	0.69	2.37	Zfp579	zinc finger protein 579	0.090922446	0.24
243529	16.71	18.04	34.28	1.33	1.84	13.65	H1fx	H1 histone family, member X	0.095383468	0.24
69871	9.28	5.97	10.72	0.77	0.56	3.88	2010007H12Rik	hypothetical protein LOC69871	0.090231897	0.20
30052	59.40	40.58	97.59	1.20	2.06	36.17	Pcsk1n	proprotein convertase subtilisin/kexin type 1	0.003777041	0.20
67445	66.75	47.70	100.89	2.79	2.15	37.17	C1qtnf4	C1q and tumor necrosis factor related protein 4	0.002693702	0.19
68209	17.43	13.57	29.41	1.75	1.33	8.17	Rnaseh2c	AYP1 protein	0.033645024	0.18
54123	1.90	1.08	3.68	0.21	0.14	0.36	Irf7	interferon regulatory factor 7,interferon regulatory factor 7,interferon regulatory factor 7,	0.014131146	0.11
620779	1.82	0.99	0.80	0.00	0.04	0.00	LOC620779	hypothetical LOC620779	0.00011239	0.01

Table A-3: Dysregulated genes in 12wk striatum.

Gene	TSM492	TSM482	TSM490	TSW478	TSW479	TSW491	gene_symbol	gene_desc	padj	DESeq Delta
233080	0.00	0.00	0.00	0.39	2.15	1.13	Ffar3	free fatty acid receptor 3	1.04E-06	Inf
68527	0.00	0.00	0.00	0.00	0.94	3.22	1110017I16Rik	hypothetical protein LOC68527,hypothetical protein LOC68527,	0.004629433	Inf
76974	0.00	0.00	0.00	1.21	3.76	0.97	1190003J15Rik	HIU hydrolase	0.000387897	Inf
75512	0.18	0.00	0.00	9.67	3.00	12.72	Gpx6	glutathione peroxidase 6	1.45E-20	137.29
230098	0.00	0.00	0.12	1.26	0.83	1.48	E130306D19Rik	hypothetical protein LOC230098	0.001068226	28.07
380683	0.21	0.07	0.19	1.72	2.76	2.81	Sec14l3	SEC14-like 3	0.001318874	15.62
103149	0.17	0.10	0.00	0.95	1.90	1.19	Upb1	ureidopropionase, beta	0.040581344	15.29
399548	45.46	16.45	22.63	419.04	371.23	479.77	Scn4b	sodium channel, type IV, beta	8.85E-41	14.81
378435	0.22	0.00	0.13	2.85	0.09	1.05	Mafa	Mafa homolog	0.05687955	11.16
319239	0.06	0.20	0.37	1.94	3.00	1.55	Npsr1	G protein-coupled receptor for asthma,G protein-coupled receptor for asthma,	1.12E-07	10.10
71878	0.01	0.03	0.36	1.00	1.41	1.57	2310007D09Rik	hypothetical protein LOC71878	0.001116801	9.78
14174	0.70	0.00	0.17	2.82	2.82	3.02	Fgf3	fibroblast growth factor 3	0.018459409	9.71
380728	0.63	0.29	0.68	5.43	5.05	5.02	LOC380728	similar to potassium voltage-gated channel,	1.25E-10	9.63
232413	0.18	0.98	0.21	2.79	4.32	5.32	Clec12a	C-type lectin domain family 12, member a	4.22E-08	8.99
211232	0.59	0.33	0.20	4.00	3.84	1.53	Cpne9	copine-like protein	0.000538305	8.39
20190	0.36	0.33	0.58	3.12	3.97	3.15	Ryr1	ryanodine receptor 1, skeletal muscle	1.69E-17	8.08
627191	24.81	7.87	13.73	139.62	87.32	147.02	Tmem90a	capucin,capucin,	1.34E-18	7.96
13924	0.48	0.10	0.36	2.03	2.37	3.03	Ptprv	protein tyrosine phosphatase, receptor type, V	5.06E-06	7.94
320139	1.04	0.12	0.33	4.28	2.39	5.11	Ptpn7	protein tyrosine phosphatase, non-receptor type,protein tyrosine phosphatase, non-receptor type,	2.82E-05	7.79
320712	0.89	0.34	0.33	2.43	2.06	6.75	Abi3bp	ABI gene family, member 3 (NESH) binding protein	0.000214963	7.35
12504	7.95	1.59	2.34	27.67	20.48	39.96	Cd4	CD4 antigen,CD4 antigen,	6.92E-15	7.34
244562	0.33	0.00	0.12	0.77	1.18	1.32	Abcc12	ATP-binding cassette, sub-family C (CFTR/MRP),,ATP-binding cassette, sub-family C (CFTR/MRP),,	0.02877883	7.24
73284	1.43	0.92	1.00	8.50	6.31	9.75	Ddit4l	DNA-damage-inducible transcript 4-like	1.03E-08	7.21
16323	2.80	1.38	2.05	12.11	11.39	20.77	Inhba	inhibin beta A	2.26E-08	7.04
240216	0.10	0.33	0.12	1.24	0.12	2.48	E230025N22Rik	hypothetical protein LOC240216	0.014951068	6.96
59289	0.45	0.26	0.08	1.87	1.16	2.31	Ccbp2	chemokine binding protein 2,chemokine binding protein 2,	0.006093038	6.65
19739	38.58	12.35	21.34	140.13	121.02	203.13	Rgs9	regulator of G-protein signaling 9,regulator of G-protein signaling 9,regulator of G-protein signaling 9,	1.32E-11	6.46
23984	31.31	16.75	21.37	118.25	173.11	160.73	Pde10a	phosphodiesterase 10A,phosphodiesterase 10A,phosphodiesterase 10A,	1.88E-10	6.45
18005	0.13	0.20	0.29	1.07	0.65	2.18	Nek2	NIMA (never in mitosis gene a)-related expressed,NIMA (never in mitosis gene a)-related expressed,	0.002664772	6.34
16909	0.65	0.53	0.38	2.04	3.30	4.55	Lmo2	LIM domain only 2	0.012972107	6.28
18619	250.34	166.19	168.00	1241.14	900.62	1510.07	Penk1	preproenkephalin 1,preproenkephalin 1,	6.15E-12	6.17
140741	5.44	1.55	2.53	22.22	11.49	25.28	Gpr6	G protein-coupled receptor 6	1.06E-06	6.11
13655	3.74	0.48	3.23	17.89	13.33	14.67	Egr3	early growth response 3,early growth response 3,	3.98E-06	6.10
11540	24.70	7.61	14.08	92.26	79.36	114.07	Adora2a	adenosine A2a receptor	3.79E-11	6.08
241303	0.87	0.31	0.38	2.37	4.72	2.54	A130092J06Rik	hypothetical protein LOC241303,hypothetical protein LOC241303,	0.000812067	6.05
18387	0.57	0.73	0.63	3.54	5.10	3.14	Oprk1	opioid receptor, kappa 1,opioid receptor, kappa 1,opioid receptor, kappa 1,	0.004306958	6.05
12810	14.89	3.56	5.85	26.18	69.24	51.22	Coch	coagulation factor C homolog (Limulus,coagulation factor C homolog (Limulus,	2.14E-07	6.00

269582	1.29	0.25	0.52	4.02	2.81	5.24	Clspn	claspin,claspin,claspin,	8.06E-05	5.83
72500	1.69	0.00	0.90	6.93	1.02	7.38	Ier5l	immediate early response 5-like	0.002199754	5.83
12904	0.32	1.03	0.26	4.12	0.88	4.24	Crabp2	cellular retinoic acid binding protein II	0.019083186	5.66
73598	0.00	0.12	0.59	1.84	0.58	1.59	1700001O22Rik	hypothetical protein LOC73598	0.052137058	5.57
16402	0.88	0.50	0.38	3.51	2.02	4.19	Itga5	integrin alpha 5,integrin alpha 5,	0.000344556	5.52
219170	0.01	0.27	0.38	0.00	2.55	1.10	AU021034	hypothetical protein LOC219170	0.028812197	5.47
270150	0.42	0.34	1.35	0.48	5.18	5.77	BC038167	hypothetical protein LOC270150	0.024261264	5.44
59046	294.35	277.06	230.45	1236.64	1872.51	1236.21	Arpp19	cAMP-regulated phosphoprotein 19,cAMP-regulated phosphoprotein 19,	5.71E-10	5.43
224129	43.88	23.60	33.21	187.80	158.06	196.04	Adcy5	adenylate cyclase 5	3.00E-09	5.34
58234	3.11	1.10	3.68	19.89	11.17	10.77	Shank3	SH3/ankyrin domain gene 3	7.47E-09	5.27
18124	0.49	0.13	0.78	2.26	4.35	0.63	Nr4a3	nuclear receptor subfamily 4, group A, member 3,nuclear receptor subfamily 4, group A, member 3,nuclear receptor subfamily 4, group A, member 3,	0.056252687	5.18
19662	4.38	1.98	1.66	18.76	11.63	10.93	Rbp4	retinol binding protein 4, plasma,retinol binding protein 4, plasma,	0.002822469	5.14
11838	11.61	2.43	6.52	44.59	35.75	26.31	Arc	activity regulated cytoskeletal-associated,activity regulated cytoskeletal-associated,	5.23E-07	5.11
235130	0.16	0.28	0.27	0.87	1.19	1.57	Adamts15	a disintegrin-like and metalloprotease	0.00111446	5.10
14403	13.58	3.93	8.71	42.90	39.46	50.96	Gabrd	gamma-aminobutyric acid (GABA-A) receptor,	3.22E-07	5.07
99296	9.49	2.98	5.29	42.75	15.90	32.01	Hrh3	histamine receptor H 3	2.37E-08	5.03
74720	0.24	0.48	0.33	2.13	0.04	3.13	4930511J11Rik	hypothetical protein LOC74720	0.036228747	5.01
170952	3.52	1.03	1.90	10.53	13.00	8.22	Prima1	proline rich membrane anchor 1 precursor	0.015359354	4.93
15551	1.52	0.66	1.59	8.41	5.02	5.25	Htr1b	5-hydroxytryptamine (serotonin) receptor 1B	0.005770116	4.89
15370	5.66	2.40	3.18	22.41	24.37	8.25	Nr4a1	nuclear receptor subfamily 4, group A, member 1	6.87E-05	4.85
74100	233.18	128.18	121.73	619.41	883.47	788.79	Arpp21	cyclic AMP-regulated phosphoprotein, 21 isoform,cyclic AMP-regulated phosphoprotein, 21 isoform,cyclic AMP-regulated phosphoprotein, 21 isoform,cyclic AMP-regulated phosphoprotein, 21 isoform,	4.30E-07	4.82
19395	19.23	5.72	11.98	59.21	50.15	67.06	Rasgrp2	RAS, guanyl releasing protein 2,RAS, guanyl releasing protein 2,	2.89E-07	4.81
228852	1.56	0.72	2.08	9.84	6.43	4.80	Ppp1r16b	protein phosphatase 1, regulatory (inhibitor),protein phosphatase 1, regulatory (inhibitor),protein phosphatase 1, regulatory (inhibitor),	6.33E-07	4.80
13857	1.44	0.92	1.32	5.47	4.76	7.53	Epor	erythropoietin receptor,erythropoietin receptor,	0.001825563	4.79
243385	0.92	0.62	1.69	4.40	7.81	3.21	Gprin3	GPRIN family member 3	0.000498885	4.71
17896	0.52	0.42	2.79	8.90	6.66	1.93	Myl4	myosin, light polypeptide 4,myosin, light polypeptide 4,	0.026971201	4.70
13489	15.63	7.49	9.61	63.74	30.35	59.84	Drd2	dopamine receptor 2	1.90E-07	4.69
93842	0.21	0.21	0.67	1.01	2.21	1.88	Igsf9	immunoglobulin superfamily, member 9,immunoglobulin superfamily, member 9,	0.006842219	4.69
12672	6.93	4.30	6.34	29.68	22.11	29.79	Chrm4	cholinergic receptor, muscarinic 4	1.12E-07	4.59
269016	1.49	0.44	0.57	3.54	4.23	3.84	Sh3rf2	SH3 domain containing ring finger 2,SH3 domain containing ring finger 2,	0.002632921	4.57
70435	29.94	9.08	21.40	108.57	72.00	95.55	2610204M08Rik	formin, inverted,formin, inverted,	1.34E-07	4.56
329421	0.57	0.33	0.53	1.89	1.63	2.97	Myo3b	myosin IIIB	0.001479548	4.52
18574	124.72	47.64	67.80	348.50	268.96	469.45	Pde1b	phosphodiesterase 1B, Ca2+-calmodulin dependent,phosphodiesterase 1B, Ca2+-calmodulin dependent,	5.30E-07	4.52

21414	1.14	0.57	1.25	3.01	6.05	4.33	Tcf7	transcription factor 7, T-cell specific,transcription factor 7, T-cell specific,	0.009392024	4.49
238680	0.84	1.00	1.15	2.24	5.02	6.19	Cntnap3	contactin associated protein-like 3,contactin associated protein-like 3,	7.13E-05	4.48
11553	3.56	2.29	4.65	19.24	11.01	17.06	Adra2c	adrenergic receptor, alpha 2c	2.53E-07	4.46
107656	8.18	5.42	6.33	35.56	18.06	35.71	Krt9	keratin complex 1, acidic, gene 9	1.52E-07	4.44
218630	0.25	0.36	0.59	1.84	0.85	2.66	Ccno	cyclin O	0.027385702	4.43
76969	2.28	1.26	2.73	14.23	4.48	9.11	Chst1	carbohydrate (keratan sulfate Gal-6),carbohydrate (keratan sulfate Gal-6),	1.37E-05	4.39
13842	0.40	0.33	0.61	2.00	1.47	2.34	Epha8	Eph receptor A8	0.003295101	4.36
192199	0.32	1.29	0.56	2.83	2.28	4.48	Rspo1	thrombospondin type 1 domain containing	0.003208135	4.35
71529	7.21	4.50	10.12	34.96	36.23	22.57	9030409G11Rik	hypothetical protein LOC71529	0.000812067	4.31
329934	1.49	1.13	1.95	9.22	3.78	6.76	Foxo6	forkhead box O6	0.000138439	4.28
268934	3.23	1.36	2.03	11.97	6.59	9.91	Grm4	glutamate receptor, metabotropic 4	0.000194103	4.27
12123	5.43	2.48	4.09	15.96	14.90	20.96	Hrk	harakiri	2.45E-06	4.26
20511	19.73	16.71	27.88	115.38	101.43	55.09	Slc1a2	excitatory amino acid transporter 2 isoform 2	5.23E-07	4.21
13170	7.03	2.15	6.97	34.99	10.61	22.95	Dbp	D site albumin promoter binding protein	1.46E-05	4.21
16438	42.62	25.73	32.76	136.00	148.19	140.37	Itpr1	inositol 1,4,5-triphosphate receptor 1,inositol 1,4,5-triphosphate receptor 1,	1.16E-05	4.19
11847	0.65	0.79	0.61	1.57	3.23	3.78	Arg2	arginase type II	0.077649882	4.18
22761	1.10	0.65	2.18	8.52	3.73	4.14	Zfpm1	zinc finger protein, multitype 1	0.000174634	4.16
18386	1.43	0.20	1.20	4.80	3.87	3.16	Oprd1	opioid receptor, delta 1	0.004924529	4.14
18810	0.70	0.09	1.17	3.86	3.17	1.05	Plec1	plectin 1 isoform 4	0.000193565	4.12
16512	8.44	1.36	7.10	27.65	17.72	24.13	Kcnh3	potassium voltage-gated channel, subfamily H,potassium voltage-gated channel, subfamily H,	2.82E-05	4.10
231801	7.48	1.65	4.88	18.54	18.71	19.53	Hrbl	HIV-1 Rev-binding protein-like protein isoform,HIV-1 Rev-binding protein-like protein isoform,HIV-1 Rev-binding protein-like protein isoform,HIV-1 Rev-binding protein-like protein isoform,	0.085914824	4.10
228432	19.04	8.77	12.17	39.86	79.40	42.92	Tmem16c	hypothetical protein LOC228432	0.000364459	4.10
80981	16.28	5.55	7.94	28.63	41.82	53.08	Arl4d	ADP-ribosylation factor-like 4D	0.000206249	4.09
18626	3.20	1.49	2.61	12.71	11.37	5.83	Per1	period homolog 1,period homolog 1,period homolog 1,	0.00026862	4.09
16985	0.33	1.05	1.07	5.47	4.00	0.58	Lsp1	lymphocyte specific 1,lymphocyte specific 1,lymphocyte specific 1,lymphocyte specific 1,lymphocyte specific 1,lymphocyte specific 1,	0.044625187	4.07
72324	0.67	0.42	0.51	3.03	1.50	1.98	Plxdc1	plexin domain containing 1	0.041218274	4.04
56458	1.58	1.14	1.26	6.22	3.91	6.14	Foxo1	forkhead box O1	7.55E-05	4.04
54610	3.21	1.64	2.71	9.39	11.53	9.70	Tbc1d8	TBC1 domain family, member 8,TBC1 domain family, member 8,	0.0002303	4.03
15930	7.06	3.45	2.78	13.21	23.77	16.60	Indo	indoleamine-pyrrole 2,3 dioxygenase	0.004444779	4.02
20650	0.71	0.39	0.62	1.75	3.66	1.56	Sntb2	syntrophin, basic 2	0.024545473	4.01
242667	33.05	10.05	24.83	115.76	54.49	101.52	Dlgap3	disks large-associated protein 3,disks large-associated protein 3,	2.35E-06	3.97
76459	6.86	4.07	2.54	14.65	16.42	22.98	Car12	carbonic anyhydrase 12,carbonic anyhydrase 12,	9.70E-05	3.96
57816	47.87	14.61	20.54	116.43	84.85	120.49	Tesc	tescalcin,tescalcin,	0.000146051	3.92
212706	0.65	1.24	1.34	5.65	3.57	3.51	C330016O10Rik	Nedd4 binding protein 3	0.001259438	3.91
15444	472.77	134.34	209.67	1166.72	658.19	1405.26	Hpca	hippocalcin,hippocalcin,hippocalcin,	7.10E-05	3.91
22068	0.73	1.02	0.64	3.05	4.20	2.07	Trpc6	transient receptor potential cation channel,,transient receptor potential cation channel,,	0.012214237	3.86
11472	14.26	2.88	6.51	34.56	24.23	31.95	Actn2	actinin alpha 2	0.000322898	3.86
51791	6.20	3.36	6.28	23.02	13.36	24.33	Rgs14	regulator of G-protein signaling 14,regulator of G-protein signaling 14,	6.33E-05	3.83
75668	3.13	0.28	1.29	9.81	2.89	5.47	Rasl10a	RAS-related on chromosome 22	0.085187423	3.82

230872	2.08	0.79	2.42	8.50	5.06	6.61	Crocc	ciliary rootlet coiled-coil, rootletin,ciliary rootlet coiled-coil, rootletin,ciliary rootlet coiled-coil, rootletin,	0.000177634	3.81
14573	0.10	0.68	0.45	1.67	1.67	1.39	Gdnf	glial cell line derived neurotrophic factor,glial cell line derived neurotrophic factor,	0.006291359	3.80
19679	2.56	1.43	3.12	10.33	8.54	8.25	Pitpnm2	phosphatidylinositol transfer protein,,phosphatidylinositol transfer protein,,phosphatidylinositol transfer protein,,phosphatidylinositol transfer protein,,	7.13E-05	3.79
16010	5.49	8.63	7.42	30.01	17.88	34.48	Igfbp4	insulin-like growth factor binding protein 4	5.43E-07	3.79
12971	18.63	39.46	18.33	63.57	102.52	125.18	Crym	crystallin, mu	3.17E-07	3.79
237403	8.00	4.17	6.52	24.30	18.99	27.98	BC072620	hypothetical protein LOC237403	4.14E-05	3.76
228550	23.85	5.89	14.05	62.59	43.26	59.13	Itpka	inositol 1,4,5-trisphosphate 3-kinase A	0.000193565	3.75
68337	15.05	8.84	18.68	57.22	42.36	58.65	Crip2	LIM only protein HLP	2.96E-05	3.71
243634	4.69	3.09	2.68	10.94	12.91	14.50	Tmem16b	transmembrane protein 16B	0.00064275	3.66
20732	0.89	0.54	0.90	2.06	3.30	3.23	Spint1	Kunitz-type protease inhibitor 1 precursor,Kunitz-type protease inhibitor 1 precursor,	0.068171892	3.66
20980	2.88	3.56	3.05	13.11	9.12	12.69	Syt2	synaptotagmin II,synaptotagmin II,	5.52E-05	3.64
13488	31.52	26.32	19.36	66.39	108.41	110.37	Drd1a	dopamine receptor D1A	7.92E-05	3.64
225872	1.95	0.17	1.13	1.03	4.96	5.94	Npas4	neuronal PAS domain protein 4	0.051150122	3.63
225870	8.72	2.53	5.42	20.25	17.07	23.69	Rin1	Ras and Rab interactor 1	0.00035656	3.63
380921	1.99	0.91	2.14	3.82	10.56	3.78	Dgkh	diacylglycerol kinase, eta,diacylglycerol kinase, eta,	0.018150366	3.61
13371	5.48	3.70	5.16	16.46	25.57	10.00	Dio2	deiodinase, iodothyronine, type II	0.000812067	3.58
78779	9.63	1.80	5.64	21.96	17.76	22.07	Spata2L	spermatogenesis associated 2-like,spermatogenesis associated 2-like,	0.001775002	3.58
268980	11.52	10.37	11.04	33.82	43.64	40.60	Strn	striatin, calmodulin binding protein,striatin, calmodulin binding protein,	7.10E-05	3.56
12654	0.42	0.53	1.11	2.38	2.24	2.77	Chi3l1	chitinase 3-like 1	0.085595171	3.56
241638	38.97	19.05	28.17	122.32	79.44	106.12	Prosapip1	ProSAPiP1 protein	7.10E-05	3.53
68070	2.68	2.31	2.19	7.48	8.97	9.13	Pdzd2	PDZ domain containing 2	0.0001076	3.53
18546	848.64	513.52	466.41	2288.44	1931.13	2262.32	Pcp4	Purkinje cell protein 4	0.000283241	3.52
240185	16.10	10.31	11.71	46.24	45.14	44.35	9430020K01Rik	hypothetical protein LOC240185	0.00012606	3.51
237211	0.23	1.18	0.63	0.92	5.10	1.20	Fancb	Fanconi anemia, complementation group B,Fanconi anemia, complementation group B,	0.052998612	3.49
229599	2.59	1.59	2.42	10.74	4.83	7.44	Gm129	hypothetical protein LOC229599,hypothetical protein LOC229599,	0.0181828	3.46
71907	11.13	6.03	4.12	25.00	22.11	26.79	Serpina9	serine (or cysteine) proteinase inhibitor, clade	0.00246788	3.43
74136	24.19	12.20	20.59	73.56	49.72	72.39	Sec14l1	SEC14-like 1,SEC14-like 1,SEC14-like 1,	9.11E-05	3.43
74096	0.83	0.37	1.25	2.94	1.25	4.28	Hvcn1	hydrogen voltage-gated channel 1	0.026331135	3.43
668940	0.54	0.27	0.58	2.42	0.71	1.64	Myh7b	RIKEN cDNA 0610038P03	0.025001193	3.43
216166	0.93	1.20	1.26	3.54	1.99	6.09	6330514A18Rik	hypothetical protein LOC216166,hypothetical protein LOC216166,	0.019624614	3.42
65112	9.59	8.39	8.36	24.14	29.72	36.41	Tmepai	transmembrane prostate androgen-induced protein	0.000122666	3.38
12348	78.38	13.80	54.80	212.15	79.99	202.55	Car11	carbonic anhydrase 11	0.000138439	3.38
233071	19.42	7.21	14.12	54.27	30.52	53.04	Snx26	sorting nexin 26,sorting nexin 26,sorting nexin 26,	0.000147263	3.37
16538	0.95	0.35	1.35	3.85	1.82	3.28	Kcns1	K+ voltage-gated channel, subfamily S, 1	0.028870079	3.36
56018	20.60	9.06	17.70	61.06	43.57	54.53	Stard10	START domain containing 10,START domain containing 10,	0.000847085	3.35
330119	2.89	1.97	1.81	6.82	7.65	7.68	Adamts3	a disintegrin-like and metalloprotease	0.004444779	3.30
20450	0.34	1.82	0.48	2.48	2.74	3.60	St8sia2	ST8 alpha-N-acetyl-neuraminide	0.000270862	3.29

20519	1.04	1.08	1.21	3.64	3.09	4.33	Slc22a3	solute carrier family 22 (organic cation	0.009681101	3.29
245038	12.46	6.26	9.08	28.04	22.24	41.65	Dclk3	doublecortin-like kinase 3	0.000323518	3.27
14555	12.23	5.43	10.45	38.07	18.71	35.44	Gpd1	glycerol-3-phosphate dehydrogenase 1 (soluble),glycerol-3-phosphate dehydrogenase 1 (soluble),	0.000320263	3.25
16520	29.90	6.03	19.14	66.56	46.99	67.88	Kcnj4	potassium inwardly-rectifying channel J4	0.001237786	3.25
140743	10.15	7.23	5.50	21.41	20.87	32.81	Rem2	rad and gem related GTP binding protein 2	0.001456642	3.24
14813	2.15	0.83	3.25	9.79	4.23	6.15	Grin2c	glutamate receptor, ionotropic, NMDA2C (epsilon	0.001267142	3.21
19736	140.10	87.61	90.19	281.08	374.15	374.16	Rgs4	regulator of G-protein signaling 4	0.001767903	3.20
14708	129.68	64.56	76.60	320.45	225.87	327.62	Gng7	guanine nucleotide binding protein (G protein),	0.000875482	3.18
243374	0.42	0.79	0.31	1.37	0.83	2.66	Gimap8	GTPase, IMAP family member 8	0.033550158	3.17
53972	103.79	29.85	58.54	213.58	159.67	236.37	Ngef	neuronal guanine nucleotide exchange factor	0.00112097	3.16
16497	60.83	62.65	52.00	136.67	235.37	185.40	Kcnab1	potassium voltage-gated channel, shaker-related,potassium voltage-gated channel, shaker-related,	0.000874967	3.15
78514	4.69	4.08	4.01	11.27	12.73	15.89	Arhgap10	Rho GTPase activating protein 10,Rho GTPase activating protein 10,	0.00297154	3.13
23876	0.32	0.60	0.26	1.34	0.97	1.43	Fbln5	fibulin 5	0.030004299	3.12
192678	3.50	5.63	4.79	12.07	15.93	15.93	Rassf3	Ras association (RalGDS/AF-6) domain family 3	0.000437397	3.12
12575	3.56	1.54	3.92	10.35	6.61	11.51	Cdkn1a	cyclin-dependent kinase inhibitor 1A (P21),cyclin-dependent kinase inhibitor 1A (P21),	0.010431616	3.12
56219	4.43	2.70	3.32	14.76	10.35	7.77	Extl1	exostoses (multiple)-like 1	0.003922746	3.11
269019	4.56	5.37	3.12	10.56	14.90	15.40	Stk32a	serine/threonine kinase 32A	0.001733126	3.10
73728	37.57	15.96	28.19	95.87	65.58	92.75	Psd	pleckstrin and Sec7 domain containing homolog,pleckstrin and Sec7 domain containing homolog,	0.000699026	3.10
207911	4.62	1.90	3.27	9.73	9.34	11.41	Mchr1	melanin-concentrating hormone receptor 1	0.065825284	3.08
58226	1.14	0.56	1.77	3.87	3.76	3.05	Cacna1h	calcium channel alpha13.2 subunit	0.006660522	3.08
58994	17.64	8.95	12.07	43.14	30.46	46.30	Smpd3	sphingomyelin phosphodiesterase 3, neutral,sphingomyelin phosphodiesterase 3, neutral,sphingomyelin phosphodiesterase 3, neutral,	0.00080265	3.07
243911	0.89	0.86	1.18	3.38	3.23	2.34	Kirrel2	kin of IRRE-like 2	0.05464033	3.06
14538	18.89	9.43	9.09	33.00	41.16	41.86	Gcnt2	glucosaminyl (N-acetyl) transferase 2 isoform B	0.004538403	3.05
76453	0.32	0.70	1.40	3.46	2.51	1.41	Prss23	protease, serine, 23,protease, serine, 23,	0.019653451	3.02
277973	2.60	1.55	3.37	9.35	5.54	7.94	Slc9a5	solute carrier family 9 (sodium/hydrogen	0.002105262	3.01
330695	77.11	26.24	53.88	200.13	88.34	190.07	Ctxn1	cortexin 1	0.000802036	3.01
108071	2.44	2.06	2.67	5.69	10.18	5.94	Grm5	glutamate receptor, metabotropic 5,glutamate receptor, metabotropic 5,	0.005484091	3.01
58200	23.39	9.19	15.43	56.21	30.99	57.30	Ppp1r1a	protein phosphatase 1, regulatory (inhibitor)	0.003275931	3.00
20564	1.90	0.59	1.95	6.10	3.56	3.56	Slit3	slit homolog 3	0.024745481	2.99
67972	92.62	57.88	52.11	167.60	243.39	201.01	Atp2b1	plasma membrane calcium ATPase 1	0.007903466	2.99
74521	4.11	3.75	3.88	8.94	13.87	12.32	8430415E04Rik	HEAT-like repeat-containing protein,HEAT-like repeat-containing protein,	0.006169175	2.99
13849	4.99	3.42	6.90	17.80	9.74	18.20	Ephx1	epoxide hydrolase 1, microsomal	0.004632102	2.98
21828	0.47	0.09	2.36	2.41	3.64	2.61	Thbs4	thrombospondin 4	0.058297541	2.97
108100	75.21	28.33	58.03	160.57	142.16	172.39	Baiap2	brain-specific angiogenesis inhibitor	0.002573177	2.96
23882	1.80	1.06	5.02	6.09	7.00	10.34	Gadd45g	growth arrest and DNA-damage-inducible 45 gamma	0.043068902	2.96
18610	25.02	16.31	7.41	43.79	51.97	49.56	Pdyn	beta-neoendorphin-dynorphin preproprotein,beta-neoendorphin-dynorphin preproprotein,	0.019624614	2.94

108069	11.01	9.53	9.25	22.19	39.11	27.22	Grm3	glutamate receptor, metabotropic 3	0.004924529	2.94
13653	37.28	21.56	30.21	91.31	101.36	70.68	Egr1	early growth response 1	0.004349553	2.92
217124	107.98	58.10	93.00	339.68	169.82	252.49	Ppp1r9b	protein phosphatase 1, regulatory subunit 9B,protein phosphatase 1, regulatory subunit 9B,	0.001456642	2.91
13134	7.42	8.35	5.72	17.32	20.22	25.72	Dach1	dachshund 1 isoform 1	0.001116801	2.91
75659	4.69	2.70	4.42	10.57	9.72	13.89	Wdr54	D3Mm3e protein,D3Mm3e protein,	0.052275431	2.90
20183	17.98	8.03	10.11	47.79	22.65	34.70	Rxrg	retinoid X receptor gamma,retinoid X receptor gamma,	0.006842219	2.90
19259	93.09	41.59	55.57	189.08	145.40	219.84	Ptpn5	protein tyrosine phosphatase, non-receptor type,protein tyrosine phosphatase, non-receptor type,	0.002248921	2.90
12326	15.74	18.88	18.74	38.50	59.37	58.60	Camk4	calcium/calmodulin-dependent protein kinase IV	0.00132503	2.90
319477	29.17	10.68	23.22	76.15	44.04	64.09	6030419C18Rik	hypothetical protein LOC319477,hypothetical protein LOC319477,	0.002410644	2.89
13875	8.52	2.53	5.59	17.90	10.96	19.71	Erf	Ets2 repressor factor	0.006660522	2.88
16011	5.67	10.60	17.61	41.83	30.74	25.92	Igfbp5	insulin-like growth factor binding protein 5	0.000102814	2.88
104099	1.87	1.12	1.49	3.99	4.08	4.94	Itga9	integrin alpha 9,integrin alpha 9,	0.022923125	2.88
80889	5.37	5.48	4.24	18.04	12.49	13.54	Mesdc1	mesoderm development candidate 1	0.00220833	2.88
54377	13.28	7.31	8.66	29.20	28.27	27.19	Cacng4	voltage-dependent calcium channel gamma-4	0.025001193	2.87
110279	24.05	16.90	20.93	62.95	52.80	63.32	Bcr	breakpoint cluster region homolog	0.001456642	2.87
12373	1.46	1.08	1.05	2.01	2.03	6.32	Casq2	calsequestrin 2	0.07843178	2.86
20238	2.27	1.72	2.65	5.24	9.87	4.11	Atxn1	ataxin 1	0.023872452	2.86
171180	7.18	4.88	4.41	14.52	14.18	18.85	Syt12	synaptotagmin XII	0.006660522	2.86
17433	82.63	74.29	271.52	636.64	257.61	327.11	Mobp	myelin-associated oligodendrocytic basic protein	0.000144652	2.85
66425	159.02	81.41	94.82	277.94	281.71	407.68	Pcp4l1	Purkinje cell protein 4-like 1	0.003304056	2.85
14367	0.36	0.78	0.48	0.60	2.95	1.14	Fzd5	frizzled 5 precursor	0.072562051	2.85
20370	42.22	17.92	28.09	87.29	61.08	104.59	Sez6	seizure related gene 6,seizure related gene 6,seizure related gene 6,	0.002192077	2.85
209225	0.98	0.27	1.07	2.52	1.93	2.24	Zfp710	zinc finger protein 710,zinc finger protein 710,	0.098543507	2.85
231842	3.83	1.08	3.24	8.12	7.31	7.90	6530401C20Rik	archaemetzincin-1,archaemetzincin-1,	0.044055144	2.84
110891	37.65	9.73	22.95	88.62	45.00	67.33	Slc8a2	solute carrier family 8 (sodium/calcium	0.003925871	2.83
110862	3.49	1.94	3.74	8.15	11.89	5.90	Kcnq3	potassium voltage-gated channel, subfamily Q,	0.055100048	2.82
14998	4.21	4.74	4.01	9.38	8.80	18.38	H2-DMa	histocompatibility 2, class II, locus DMa,histocompatibility 2, class II, locus DMa,	0.056576015	2.80
71007	0.97	3.11	2.92	4.48	6.61	8.67	4933400E14Rik	hypothetical protein LOC71007	0.00493898	2.80
29863	23.73	24.04	15.53	43.14	66.46	69.25	Pde7b	phosphodiesterase 7B	0.003185937	2.80
18143	5.37	2.14	3.79	10.91	8.37	12.23	Npas2	neuronal PAS domain protein 2	0.014962751	2.78
117148	29.16	11.48	20.58	65.42	38.52	64.78	Efcbp2	neuronal calcium-binding protein 2	0.005353926	2.75
229722	3.55	1.82	2.38	6.88	7.17	7.30	5330417C22Rik	hypothetical protein LOC229722	0.052106047	2.75
26556	32.65	14.25	19.95	59.15	55.01	68.58	Homer1	homer homolog 1 isoform S	0.060173947	2.75
218772	16.33	20.76	11.70	32.14	53.90	49.44	Rarb	retinoic acid receptor, beta,retinoic acid receptor, beta,	0.004111318	2.75
235604	110.72	49.66	83.87	239.21	182.86	252.21	Camkv	CaM kinase-like vesicle-associated	0.004599723	2.74
140781	0.50	0.60	0.66	2.08	1.24	1.49	Myh7	myosin, heavy polypeptide 7, cardiac muscle,	0.065825284	2.74
11515	2.91	1.37	3.14	7.53	6.64	6.25	Adcy9	adenylate cyclase 9,adenylate cyclase 9,	0.022020087	2.73
217480	46.58	61.81	45.88	84.40	196.99	142.79	Dgkb	diacylglycerol kinase, beta,diacylglycerol kinase, beta,diacylglycerol kinase, beta,diacylglycerol kinase, beta,diacylglycerol kinase, beta,diacylglycerol kinase, beta,	0.006762881	2.73
217166	14.10	6.95	10.11	34.58	21.02	30.13	Nr1d1	nuclear receptor subfamily 1, group D, member 1	0.006842219	2.73

68918	2.88	3.31	5.63	9.79	9.04	13.49	1190005I06Rik	RIKEN cDNA 1190005I06	0.07843178	2.73
78339	2.78	1.36	3.23	9.23	5.99	4.88	Ttyh3	tweety 3	0.019083186	2.72
56613	6.39	4.06	6.28	16.33	13.51	15.66	Rps6ka4	ribosomal protein S6 kinase, polypeptide 4	0.010597459	2.72
68810	75.15	38.11	33.72	104.89	154.92	140.72	Nexn	nexilin,nexilin,nexilin,	0.016821231	2.71
207592	3.33	2.85	3.24	8.98	10.04	6.73	Tbc1d16	TBC1 domain family, member 16,TBC1 domain family, member 16,	0.031755141	2.71
241118	22.60	6.14	8.21	34.15	23.62	43.02	Accn4	amiloride-sensitive cation channel 4, pituitary	0.017751099	2.71
52662	5.59	3.32	4.56	9.68	18.57	8.58	D18Ertd653e	hypothetical protein LOC52662	0.066795404	2.71
246710	14.66	7.22	11.66	33.71	26.92	30.85	Rhobtb2	Rho-related BTB domain containing 2,Rho-related BTB domain containing 2,	0.006386064	2.70
15904	21.92	56.61	41.00	66.39	127.23	132.17	Id4	inhibitor of DNA binding 4	0.000616671	2.70
108655	29.04	15.43	18.31	53.99	52.01	62.37	Foxp1	forkhead box P1,forkhead box P1,forkhead box P1,forkhead box P1,forkhead box P1,forkhead box P1,	0.010030555	2.69
230868	6.93	2.88	4.80	19.24	10.48	9.75	Igsf21	immunoglobin superfamily, member 21	0.043382647	2.69
19735	7.61	6.54	5.34	15.82	19.85	17.38	Rgs2	regulator of G-protein signaling 2	0.014270009	2.69
229595	0.58	0.82	1.54	2.96	3.31	1.68	Adamtsl4	ADAMTS-like 4,ADAMTS-like 4,	0.065401289	2.69
67731	4.35	4.40	6.07	11.73	16.00	12.32	Fbxo32	F-box protein 32	0.013396638	2.68
20361	16.79	6.01	11.53	43.70	18.66	30.11	Sema7a	semaphorin 7A	0.00693591	2.68
98970	0.96	1.43	1.00	3.39	3.07	2.71	Fibcd1	fibrinogen C domain containing 1	0.029407348	2.67
69534	5.76	4.13	4.72	13.64	10.25	15.41	Avpi1	Esau protein	0.067635168	2.67
102644	2.31	0.90	3.04	7.86	3.65	5.29	Oaf	out at first	0.052542267	2.66
140904	30.71	21.30	23.48	69.32	63.23	69.65	Caln1	calneuron 1,calneuron 1,	0.00709267	2.65
225724	8.87	5.62	6.05	17.32	14.72	22.99	Mapk4	mitogen-activated protein kinase 4	0.007489285	2.65
103534	6.82	4.10	5.64	16.58	12.96	14.25	Mgat4b	mannoside acetylglucosaminyltransferase 4,	0.02521284	2.64
72844	51.61	14.64	32.64	100.17	76.07	85.97	Kctd17	potassium channel tetramerisation domain,potassium channel tetramerisation domain,	0.017036478	2.64
110351	39.96	23.05	34.24	100.22	63.08	92.66	Rap1gap	Rap1 GTPase-activating protein,Rap1 GTPase-activating protein,	0.003781936	2.64
269615	1.51	0.88	2.68	4.49	4.99	3.83	Plch2	phospholipase C, eta 2	0.097359353	2.63
56484	1.84	0.42	2.42	6.38	3.08	2.98	Foxo3a	forkhead box O3a,forkhead box O3a,forkhead box O3a,forkhead box O3a,	0.091222826	2.63
68617	7.09	5.04	6.95	19.17	16.12	15.43	1110012J17Rik	hypothetical protein LOC68617	0.006776159	2.63
58227	2.08	1.42	1.65	4.68	3.29	5.66	9630031F12Rik	hypothetical protein LOC58227,hypothetical protein LOC58227,	0.040271068	2.63
105653	109.48	40.78	74.07	232.96	124.01	238.72	Phyhip	phytanoyl-CoA hydroxylase interacting protein	0.005572299	2.63
68339	3.52	1.13	3.20	6.97	6.78	6.91	Ccdc88c	coiled-coil domain containing 88C	0.033550158	2.62
383787	15.01	9.72	9.56	28.74	25.55	37.03	Gm1337	hypothetical protein LOC383787	0.006842219	2.62
21916	15.69	10.93	14.09	26.80	41.78	38.79	Tmod1	tropomodulin 1	0.014270009	2.62
223626	16.14	6.04	12.20	33.00	26.85	31.16	4930572J05Rik	mesenchymal stem cell protein DSCD75 homolog	0.026906088	2.62
13638	9.50	4.11	8.14	20.33	15.87	20.84	Efna3	ephrin A3	0.050557615	2.61
14608	6.16	9.11	7.72	17.54	18.16	24.81	Gpr83	G protein-coupled receptor 83	0.004276599	2.60
20743	45.49	15.04	37.56	120.36	71.26	64.56	Spnb3	spectrin beta 3	0.011255092	2.60
80906	54.37	38.24	29.36	95.58	92.00	122.54	Kcnip2	Kv channel-interacting protein 2 isoform a	0.019555259	2.60
12323	24.18	9.94	19.98	54.59	35.89	50.48	Camk2b	calcium/calmodulin-dependent protein kinase II,,calcium/calmodulin-dependent protein kinase II,,calcium/calmodulin-dependent protein kinase II,,calcium/calmodulin-dependent protein kinase II,,	0.007584496	2.60
18751	121.17	107.26	99.07	288.32	265.87	306.74	Prkcb1	protein kinase C, beta 1,protein kinase C, beta 1,	0.015624137	2.60
12294	35.54	25.59	22.57	65.07	69.19	80.26	Cacna2d3	calcium channel, voltage-dependent, alpha2/delta	0.008288574	2.59

231125	9.66	2.92	5.48	15.56	13.74	17.85	Zfyve28	zinc finger, FYVE domain containing 28	0.032808579	2.59
51801	23.60	6.90	18.57	52.95	17.17	57.40	Ramp1	receptor-activity modifying protein 1	0.049033054	2.59
64378	201.71	192.76	137.69	391.27	502.88	502.71	Gpr88	G-protein coupled receptor 88	0.017557343	2.59
218194	154.47	94.47	104.71	305.78	256.12	361.56	Phactr1	phosphatase and actin regulator 1 isoform 1,phosphatase and actin regulator 1 isoform 1,	0.011198475	2.58
14697	73.07	32.67	49.65	122.95	120.65	150.89	Gnb5	guanine nucleotide-binding protein, beta-5,guanine nucleotide-binding protein, beta-5,	0.018150366	2.57
109652	5.28	3.98	3.73	12.58	5.54	14.86	Acy1	aminoacylase 1	0.075155639	2.57
99010	23.33	6.02	15.11	50.67	27.87	35.10	Agpat7	acyltransferase like 3,acyltransferase like 3,	0.027689606	2.57
19045	137.87	78.92	114.38	301.55	213.71	335.99	Ppp1ca	protein phosphatase 1, catalytic subunit, alpha	0.005556515	2.56
72003	7.16	5.40	6.50	15.20	14.76	19.37	Synpr	synaptoporin,synaptoporin,	0.019468144	2.56
55984	14.67	9.37	11.53	33.78	23.17	34.55	Camkk1	calcium/calmodulin-dependent protein kinase	0.008205593	2.56
12295	18.95	11.08	18.23	50.01	33.96	38.06	Cacnb1	calcium channel, voltage-dependent, beta 1	0.029187317	2.55
11652	9.02	3.48	5.35	17.39	12.10	16.07	Akt2	thymoma viral proto-oncogene 2,thymoma viral proto-oncogene 2,thymoma viral proto-oncogene 2,	0.04098494	2.54
382253	6.73	3.33	5.98	13.07	17.36	10.28	Cdkl5	cyclin-dependent kinase-like 5	0.064874237	2.53
11790	8.78	1.81	12.89	25.71	14.44	18.98	Speg	SPEG complex locus isoform 1	0.097618237	2.53
69675	2.87	1.17	2.41	5.91	5.89	4.57	Pxdn	peroxidasin,peroxidasin,	0.089507831	2.53
18755	8.57	9.21	4.63	16.60	18.13	22.25	Prkch	protein kinase C, eta	0.014382103	2.52
13848	7.44	3.47	5.11	17.52	11.31	11.66	Ephb6	Eph receptor B6,Eph receptor B6,	0.034999028	2.51
66259	439.45	272.94	289.39	699.17	929.87	923.40	Camk2n1	calcium/calmodulin-dependent protein kinase II	0.055842	2.51
67800	26.31	14.46	18.68	48.75	44.12	57.28	Dgat2	diacylglycerol O-acyltransferase 2	0.016864224	2.51
246104	2.97	5.36	6.24	10.91	12.87	13.03	Rhbdl3	rhomboid, veinlet-like 4	0.005770116	2.50
11769	154.77	64.49	100.42	296.75	178.22	330.57	Ap1s1	adaptor protein complex AP-1, sigma 1	0.009392024	2.50
381126	2.90	1.94	2.99	5.54	7.50	6.76	Gm944	hypothetical protein LOC381126	0.044055144	2.50
73086	5.08	6.69	6.13	9.82	22.10	13.16	Rps6ka5	ribosomal protein S6 kinase, polypeptide 5,ribosomal protein S6 kinase, polypeptide 5,	0.023872452	2.50
74563	5.68	2.73	5.11	9.96	9.76	14.00	Rasgef1c	RasGEF domain family, member 1C	0.064613934	2.49
216527	21.75	11.93	18.36	47.23	35.94	46.66	Ccm2	cerebral cavernous malformation 2 homolog,cerebral cavernous malformation 2 homolog,	0.018459409	2.49
20393	13.34	14.01	23.30	55.56	27.88	41.93	Sgk	serum/glucocorticoid regulated kinase,serum/glucocorticoid regulated kinase,	0.00800213	2.49
67784	4.55	1.31	3.80	6.46	10.14	7.45	Plxnd1	plexin D1	0.085187423	2.49
17912	4.61	4.89	4.79	8.68	15.16	11.69	Myo1b	myosin IB,myosin IB,myosin IB,	0.026414066	2.48
67326	25.51	17.49	16.51	54.21	42.04	52.09	1700037H04Rik	hypothetical protein LOC67326,hypothetical protein LOC67326,	0.023213384	2.48
74513	9.59	20.40	12.13	28.68	41.40	35.42	Neto2	neuropilin- and tolloid-like protein 2,neuropilin- and tolloid-like protein 2,neuropilin- and tolloid-like protein 2,	0.004076308	2.47
71960	4.25	2.48	6.22	13.71	8.72	9.54	Myh14	myosin, heavy polypeptide 14,myosin, heavy polypeptide 14,	0.012411395	2.47
81840	7.93	3.89	5.97	17.87	11.36	14.69	Sorcs2	VPS10 domain receptor protein SORCS 2,VPS10 domain receptor protein SORCS 2,	0.02148708	2.46
170835	5.96	3.45	3.77	13.12	8.33	11.14	Pib5pa	phosphatidylinositol (4,5) bisphosphate	0.04098494	2.46
207728	30.57	11.11	23.82	60.95	46.19	52.87	Pde2a	phosphodiesterase 2A, cGMP-stimulated,phosphodiesterase 2A, cGMP-stimulated,phosphodiesterase 2A, cGMP-stimulated,phosphodiesterase 2A, cGMP-stimulated,	0.021735742	2.46

56149	18.84	4.65	7.43	27.36	10.35	38.55	Grasp	GRP1 (general receptor for phosphoinositides	0.037342126	2.45
12484	0.78	3.90	2.76	2.10	11.11	5.20	Cd24a	CD24a antigen	0.0584824	2.45
80891	3.00	4.90	3.46	13.38	5.56	9.12	Msr2	macrophage scavenger receptor 2,macrophage scavenger receptor 2,	0.020165753	2.45
240514	6.37	2.74	6.22	19.51	6.04	12.46	n/a	n/a	0.012484894	2.45
211652	12.07	8.42	11.45	29.45	21.68	26.70	Wwc1	WW, C2 and coiled-coil domain containing 1,WW, C2 and coiled-coil domain containing 1,	0.015927613	2.44
16492	10.18	8.85	7.18	14.66	26.11	23.98	Kcna4	potassium voltage-gated channel, shaker-related	0.028812197	2.44
22174	28.14	12.43	16.19	49.76	39.19	49.90	Tyro3	TYRO3 protein tyrosine kinase 3,TYRO3 protein tyrosine kinase 3,	0.024773816	2.44
276952	88.41	45.31	57.84	175.23	94.16	202.44	Rasl10b	RAS-like, family 10, member B,RAS-like, family 10, member B,	0.009725161	2.43
16554	1.60	0.90	3.29	6.52	5.14	2.34	Kif13b	kinesin family member 13B,kinesin family member 13B,	0.057277668	2.42
24064	15.90	11.73	17.36	34.57	40.42	34.87	Spry2	sprouty homolog 2	0.026200525	2.41
13731	4.10	3.64	4.44	8.83	12.76	8.10	Emp2	epithelial membrane protein 2	0.058691492	2.41
268510	8.46	4.19	8.38	19.04	12.23	19.58	Mgat5b	mannoside acetylglucosaminyltransferase 5,	0.01941923	2.40
29861	17.06	8.58	12.04	34.10	21.44	35.26	Neud4	neuronal d4 domain family member	0.026331135	2.40
15898	31.03	7.23	22.51	60.12	33.51	53.02	Icam5	intercellular adhesion molecule 5,	0.026200525	2.40
13643	1.34	1.75	3.24	5.99	4.74	4.53	Efnb3	ephrin B3	0.035614175	2.39
57776	51.47	17.20	45.07	105.23	85.87	78.36	Ttyh1	tweety 1 isoform 2,tweety 1 isoform 2,	0.03847362	2.39
207565	32.35	10.09	15.89	56.17	30.03	53.43	Camkk2	calcium/calmodulin-dependent protein kinase,calcium/calmodulin-dependent protein kinase,calcium/calmodulin-dependent protein kinase,calcium/calmodulin-dependent protein kinase,	0.032522977	2.39
72898	15.98	6.58	15.53	36.05	25.69	29.87	Asphd2	aspartate beta-hydroxylase domain containing 2	0.040581344	2.38
72902	61.07	130.19	88.39	171.22	296.04	205.02	Spock3	sparc/osteonectin, cwcv and kazal-like domains,sparc/osteonectin, cwcv and kazal-like domains,	0.011641241	2.38
233552	6.37	2.40	3.37	11.34	7.78	9.88	Gdpd5	glycerophosphodiester phosphodiesterase domain,glycerophosphodiester phosphodiesterase domain,	0.098779552	2.38
68178	0.99	1.11	1.33	3.09	2.52	2.61	Cgnl1	cingulin-like 1	0.052275431	2.38
94047	6.74	2.49	4.89	11.35	11.06	11.56	Cecr6	cat eye syndrome chromosome region, candidate 6	0.065737487	2.37
50781	18.31	14.72	18.30	47.02	43.16	32.78	Dkk3	dickkopf homolog 3,dickkopf homolog 3,	0.023171045	2.37
330941	27.33	30.88	24.65	55.89	68.97	74.01	AI593442	hypothetical protein LOC330941 isoform 2	0.014075514	2.37
245684	19.10	22.09	18.26	36.50	69.94	35.40	Cnksr2	connector enhancer of kinase suppressor of Ras,connector enhancer of kinase suppressor of Ras,	0.03979673	2.37
22003	171.91	69.59	85.28	261.39	238.26	256.29	Tpm1	tropomyosin 1, alpha,tropomyosin 1, alpha,tropomyosin 1, alpha,	0.062353445	2.37
68458	7.74	4.91	29.01	57.90	16.30	24.26	Ppp1r14a	protein phosphatase 1, regulatory (inhibitor)	0.029929246	2.36
11857	14.66	6.74	9.79	25.74	17.85	30.30	Arhgdib	Rho, GDP dissociation inhibitor (GDI) beta,Rho, GDP dissociation inhibitor (GDI) beta,	0.08833366	2.36
58208	36.18	30.50	27.28	58.54	74.06	92.48	Bcl11b	B-cell leukemia/lymphoma 11B isoform b	0.021152216	2.36
19699	7.06	6.03	5.80	12.16	18.46	14.09	Reln	reelin precursor,reelin precursor,	0.036019097	2.36
210135	9.97	8.02	8.87	20.83	16.57	26.57	Zfp180	zinc finger protein 180	0.017909129	2.35
16559	4.25	2.49	2.46	5.35	4.24	12.16	Kif17	kinesin family member 17,kinesin family member 17,	0.065737487	2.35
23936	34.95	35.64	33.84	104.73	58.85	84.96	Lynx1	Ly6/neurotoxin 1	0.006842219	2.35

12815	1.22	0.93	2.54	5.31	2.25	3.32	Col11a2	procollagen, type XI, alpha 2,procollagen, type XI, alpha 2,procollagen, type XI, alpha 2,	0.057158613	2.35
78771	20.37	42.62	21.64	44.51	98.77	57.14	Mctp1	multiple C2 domains, transmembrane 1,multiple C2 domains, transmembrane 1,multiple C2 domains, transmembrane 1,	0.019083186	2.35
360013	13.25	8.08	14.62	33.72	22.78	27.86	Myo18a	myosin XVIIIa,myosin XVIIIa,myosin XVIIIa,myosin XVIIIa,myosin XVIIIa,	0.015190615	2.34
66725	5.42	5.76	5.69	10.94	15.47	13.16	Lrrk2	leucine-rich repeat kinase 2	0.026200525	2.34
381353	5.65	2.36	6.05	13.74	8.56	10.92	Gm996	hypothetical protein LOC381353	0.035045469	2.34
246317	7.61	6.18	5.91	13.09	19.37	13.91	Neto1	neuropilin- and tolloid-like protein 1	0.068970947	2.33
330914	10.96	4.02	9.65	21.91	21.08	14.98	Grit	Rho GTPase-activating protein	0.064349245	2.33
118445	18.77	10.76	13.18	32.06	20.61	47.51	Klf16	Kruppel-like factor 16	0.02091643	2.31
224090	6.44	5.42	5.88	18.30	10.09	13.08	Tmem44	transmembrane protein 44,transmembrane protein 44,	0.022400726	2.31
14313	0.46	3.53	0.63	2.80	3.04	5.01	Fst	follistatin,follistatin,	0.028929133	2.31
75216	1.23	1.90	1.23	2.73	3.11	4.30	4930534B04Rik	hypothetical protein LOC75216,hypothetical protein LOC75216,hypothetical protein LOC75216,	0.071461814	2.30
216439	79.42	29.60	58.56	154.21	100.79	133.73	Centg1	centaurin, gamma 1,centaurin, gamma 1,	0.033700993	2.30
20312	89.48	40.83	67.20	181.39	120.35	158.63	Cx3cl1	chemokine (C-X3-C motif) ligand 1	0.028501569	2.30
17119	4.01	4.24	4.56	9.56	11.23	8.97	Mxd1	MAX dimerization protein 1,MAX dimerization protein 1,	0.04098494	2.30
11941	56.20	34.43	41.52	113.50	94.42	97.94	Atp2b2	plasma membrane calcium ATPase 2 isoform 1,plasma membrane calcium ATPase 2 isoform 1,	0.035614175	2.29
18951	115.91	48.13	82.79	245.72	142.17	178.82	4-Sep	septin 5	0.029407348	2.29
216963	24.58	15.47	27.10	69.78	36.61	47.75	Git1	G protein-coupled receptor kinase-interactor 1	0.015624137	2.29
21802	16.59	11.78	10.62	29.01	27.27	33.83	Tgfa	transforming growth factor alpha	0.036019097	2.28
12801	22.63	25.90	19.51	47.83	62.79	46.78	Cnr1	cannabinoid receptor 1 (brain)	0.031513803	2.28
98170	22.78	10.64	17.00	46.85	26.43	42.30	Tmem132a	heat shock 70kDa protein 5 binding protein 1	0.028929133	2.27
22342	31.76	14.69	28.34	68.55	45.26	54.98	Lin7b	lin 7 homolog b	0.081236016	2.27
17748	58.60	32.38	75.14	165.28	78.33	134.48	Mt1	metallothionein 1,metallothionein 1,	0.021735742	2.27
66355	14.21	10.04	13.89	26.01	25.77	34.93	Gmpr	guanosine monophosphate reductase	0.052106047	2.27
211187	10.45	7.19	9.85	21.27	17.48	24.37	Lrtm2	leucine-rich repeats and transmembrane domains,leucine-rich repeats and transmembrane domains,	0.028929133	2.27
23972	3.42	6.32	3.96	6.69	15.51	9.15	Papss2	3'-phosphoadenosine 5'-phosphosulfate synthase,3'-phosphoadenosine 5'-phosphosulfate synthase,3'-phosphoadenosine 5'-phosphosulfate synthase,	0.057277668	2.26
21336	3.17	4.28	2.90	7.16	8.46	8.06	Tacr1	tachykinin receptor 1,tachykinin receptor 1,	0.03993717	2.26
77590	10.06	5.80	5.87	14.45	15.64	19.56	4631426J05Rik	N-acetylgalactosamine 4-sulfate,N-acetylgalactosamine 4-sulfate,	0.067916608	2.26
93898	3.52	2.33	5.47	10.52	6.34	8.82	Lass1	longevity assurance homolog 1,longevity assurance homolog 1,	0.05912982	2.25
76900	18.94	5.31	17.69	41.21	17.22	34.02	Ssbp4	single stranded DNA binding protein 4	0.078608074	2.25
666704	8.45	5.91	8.95	19.44	12.51	20.94	Samd1	sterile alpha motif domain containing 1	0.042170727	2.25
24001	9.33	4.56	7.46	15.24	13.16	19.77	Tiam2	T-cell lymphoma invasion and metastasis 2,T-cell lymphoma invasion and metastasis 2,T-cell lymphoma invasion and metastasis 2,	0.04511554	2.24
235431	23.91	15.07	19.58	52.19	29.33	50.84	Coro2b	coronin, actin binding protein, 2B	0.021994288	2.24
50932	49.06	19.14	40.33	90.34	54.03	98.45	Mink1	misshapen-like kinase 1 isoform 1,misshapen-like kinase 1 isoform 1,	0.026253393	2.24

243725	37.23	47.19	36.23	74.92	112.44	86.15	Ppp1r9a	protein phosphatase 1, regulatory (inhibitor),protein phosphatase 1, regulatory (inhibitor),protein phosphatase 1, regulatory (inhibitor),protein phosphatase 1, regulatory (inhibitor),	0.04405325	2.24
66222	1.94	3.45	3.54	5.73	7.34	7.09	Serpinb1a	serine (or cysteine) proteinase inhibitor, clade,serine (or cysteine) proteinase inhibitor, clade,	0.099353012	2.24
12647	1.87	3.46	2.60	5.12	5.81	6.95	Chat	choline acetyltransferase,choline acetyltransferase,	0.068082698	2.24
226922	9.03	8.48	7.56	16.96	20.62	19.16	Kcnq5	potassium voltage-gated channel, subfamily Q,	0.04047368	2.24
268445	8.07	3.03	7.77	16.86	10.89	14.19	Ankrd13b	ankyrin repeat domain 13b	0.078548127	2.22
217082	19.91	25.20	16.71	40.61	50.39	47.41	Hlf	hepatic leukemia factor,hepatic leukemia factor,hepatic leukemia factor,hepatic leukemia factor,	0.029214818	2.21
219151	2.42	2.05	3.66	6.19	4.92	6.96	Scara3	scavenger receptor class A, member 3	0.072701844	2.20
72148	6.80	7.68	5.37	11.64	15.31	17.31	2610019F03Rik	hypothetical protein LOC72148	0.064868851	2.20
108699	395.23	226.32	286.26	708.58	654.68	625.69	Chn1	chimerin (chimaerin) 1 isoform 1,chimerin (chimaerin) 1 isoform 1,	0.056960688	2.20
19659	1.29	2.05	1.77	3.37	2.02	5.94	Rbp1	retinol binding protein 1, cellular	0.09022736	2.20
57740	32.68	9.24	21.54	54.99	32.93	51.15	Stk32c	serine/threonine kinase 32C	0.084862511	2.19
227753	9.07	7.36	15.82	29.86	20.11	20.73	Gsn	gelsolin,gelsolin,gelsolin,gelsolin,	0.031474616	2.19
100986	18.07	20.72	18.72	33.17	55.48	38.31	Akap9	A kinase (PRKA) anchor protein (yotiao) 9	0.057158613	2.19
227737	4.28	2.75	6.37	14.90	5.18	9.43	9130404D14Rik	hypothetical protein LOC227737	0.034400943	2.19
26941	11.77	4.87	11.48	29.89	12.87	19.08	Slc9a3r1	solute carrier family 9 (sodium/hydrogen	0.071631183	2.18
268709	44.66	45.02	46.49	107.60	100.62	92.66	BC055107	downregulated in renal cell carcinoma,downregulated in renal cell carcinoma,downregulated in renal cell carcinoma,	0.031657442	2.18
320292	16.67	13.09	12.51	27.48	34.13	31.14	Rasgef1b	RasGEF domain family, member 1B isoform 1	0.07843178	2.18
77938	1.84	1.85	2.49	5.07	4.62	3.91	A930008G19Rik	hypothetical protein LOC77938,hypothetical protein LOC77938,hypothetical protein LOC77938,hypothetical protein LOC77938,	0.092270598	2.18
22421	2.92	3.11	2.28	5.66	4.17	8.49	Wnt7a	wingless-related MMTV integration site 7A	0.080958014	2.17
382018	16.55	5.26	14.72	30.47	26.33	21.99	Unc13a	unc-13 homolog A	0.098097409	2.17
53625	19.37	18.15	16.39	33.72	45.01	40.11	B3gnt2	UDP-GlcNAc:betaGal,UDP-GlcNAc:betaGal,UDP-GlcNAc:betaGal,	0.061985432	2.17
230775	25.38	9.42	22.67	50.09	31.67	42.79	Bai2	brain-specific angiogenesis inhibitor 2,brain-specific angiogenesis inhibitor 2,brain-specific angiogenesis inhibitor 2,brain-specific angiogenesis inhibitor 2,brain-specific angiogenesis inhibitor 2,	0.049307131	2.17
56213	15.84	10.53	14.84	34.26	24.28	31.21	Htra1	HtrA serine peptidase 1,HtrA serine peptidase 1,	0.058536345	2.16
52187	34.74	41.64	30.06	50.40	106.25	76.26	Rragd	Ras-related GTP binding D,Ras-related GTP binding D,	0.072991661	2.16
76157	10.46	13.63	8.15	17.49	27.66	25.32	Slc35d3	solute carrier family 35, member D3	0.062504665	2.15
24105	17.32	9.57	16.78	34.57	28.35	31.23	Rbck1	RanBP-type and C3HC4-type zinc finger containing	0.081236016	2.15
327958	5.28	3.32	4.65	11.90	7.72	9.13	Pitpnm3	Pitpnm family member 3 isoform 2	0.064914524	2.15
231148	30.47	14.51	19.98	52.38	35.51	52.08	Ablim2	actin-binding LIM protein 2,actin-binding LIM protein 2,actin-binding LIM protein 2,actin-binding LIM protein 2,	0.060316935	2.15
69202	418.08	257.73	311.94	909.96	459.77	762.89	Ptms	parathymosin	0.035229636	2.15

12331	74.04	52.76	55.80	129.56	121.75	142.08	Cap1	CAP, adenylate cyclase-associated protein 1,CAP, adenylate cyclase-associated protein 1,CAP, adenylate cyclase-associated protein 1,CAP, adenylate cyclase-associated protein 1,	0.050970379	2.15
243914	4.55	3.23	5.37	9.81	7.35	11.26	Lgi4	leucine-rich repeat LGI family, member 4	0.07187772	2.14
544963	1.80	2.70	2.10	4.74	2.33	7.10	Iqgap2	IQ motif containing GTPase activating protein 2,IQ motif containing GTPase activating protein 2,	0.030843972	2.14
15461	89.36	51.65	48.81	132.58	95.61	178.38	Hras1	Harvey rat sarcoma virus oncogene 1,Harvey rat sarcoma virus oncogene 1,	0.065961875	2.14
433938	6.89	4.36	5.94	11.91	12.51	12.84	Mn1	meningioma 1	0.086511954	2.14
54524	18.44	16.93	11.90	31.26	36.25	34.67	Syt6	synaptotagmin 6,synaptotagmin 6,synaptotagmin 6,synaptotagmin 6,	0.067530464	2.13
11519	14.66	6.91	16.45	33.38	26.52	21.21	Add2	adducin 2 (beta),adducin 2 (beta),adducin 2 (beta),adducin 2 (beta),adducin 2 (beta),	0.090853222	2.13
70083	7.17	6.53	9.92	19.65	14.37	16.49	Metrn	meteorin	0.097359353	2.12
27528	17.49	39.53	21.45	33.93	75.35	58.79	D0H4S114	neuronal protein 3.1	0.03593848	2.11
54403	13.01	11.51	11.54	23.84	29.58	22.81	Slc4a4	solute carrier family 4 (anion exchanger),,solute carrier family 4 (anion exchanger),,	0.099353012	2.11
230863	29.87	15.65	13.97	33.71	29.78	63.46	Sh2d5	SH2 domain containing 5,SH2 domain containing 5,	0.067916608	2.11
53321	24.22	11.70	19.27	48.73	31.04	37.28	Cntnap1	contactin associated protein 1	0.06425103	2.11
18417	25.29	58.68	96.36	125.82	134.18	120.17	Cldn11	claudin 11	0.012411395	2.09
241589	12.07	8.60	9.48	21.40	22.90	19.40	D430041D05Rik	hypothetical protein LOC241589,hypothetical protein LOC241589,hypothetical protein LOC241589,	0.094552922	2.09
20741	10.72	7.26	10.60	22.91	18.99	18.20	Spnb1	spectrin beta 1,spectrin beta 1,	0.065562768	2.09
13385	135.86	64.08	103.16	253.95	153.79	225.60	Dlg4	postsynaptic density protein 95,postsynaptic density protein 95,	0.06264956	2.08
56461	28.46	11.02	18.20	51.17	27.22	42.77	Kcnip3	calsenilin, presenilin-binding protein, EF hand	0.094492706	2.08
17158	2.13	4.09	3.38	4.35	9.85	5.97	Man2a1	mannosidase 2, alpha 1	0.090853222	2.08
23948	29.35	10.37	18.58	49.45	27.96	44.13	Mmp17	matrix metallopeptidase 17	0.095841752	2.07
239556	9.21	3.75	6.40	15.51	9.37	15.30	Cacna1i	calcium channel, voltage-dependent, alpha 1I	0.086768121	2.06
17153	41.14	68.79	105.45	142.53	148.41	154.91	Mal	myelin and lymphocyte protein, T-cell	0.022441189	2.05
238130	9.52	12.48	10.74	17.10	27.62	22.68	Dock4	dedicator of cytokinesis 4,dedicator of cytokinesis 4,dedicator of cytokinesis 4,	0.067916608	2.05
22065	2.37	3.90	2.37	6.64	4.77	6.52	Trpc3	transient receptor potential cation channel,,transient receptor potential cation channel,,	0.080201738	2.05
320111	11.34	12.91	23.64	43.83	21.96	32.98	Prr18	proline rich region 18	0.02000858	2.04
68203	33.25	21.57	25.09	65.04	50.57	49.41	Diras2	DIRAS family, GTP-binding RAS-like 2	0.095480914	2.04
12349	23.79	35.76	63.12	109.56	76.32	65.00	Car2	carbonic anhydrase 2	0.023213384	2.03
17304	32.16	24.48	30.44	69.95	48.09	60.08	Mfge8	milk fat globule-EGF factor 8 protein isoform 1	0.065562768	2.03
83797	28.87	11.50	21.58	48.41	28.86	48.22	Smarcd1	SWI/SNF related, matrix associated, actin	0.099804371	2.01
83997	32.36	42.37	32.31	56.17	91.83	67.77	Slmap	sarcolemma associated protein,sarcolemma associated protein,sarcolemma associated protein,sarcolemma associated protein,	0.099353012	2.00
77113	48.10	62.32	58.53	99.25	124.09	116.99	Klhl2	kelch-like 2, Mayven,kelch-like 2, Mayven,	0.062027315	2.00
27276	10.13	15.98	28.03	52.16	26.85	29.62	Plekhb1	pleckstrin homology domain containing, family B,pleckstrin homology domain containing, family B,	0.026978093	1.99

19317	13.74	25.76	28.88	48.21	59.94	28.94	Qk	quaking protein,quaking protein,quaking protein,quaking protein,	0.07843178	1.99
74206	2.68	2.85	3.46	6.99	4.40	6.64	Sipa1l3	signal-induced proliferation-associated 1 like,signal-induced proliferation-associated 1 like,signal-induced proliferation-associated 1 like,signal-induced proliferation-associated 1 like,signal-induced proliferation-associated 1 like,	0.064914524	1.99
107449	2.47	2.69	4.02	7.98	4.09	6.05	Unc5b	unc-5 homolog B,unc-5 homolog B,unc-5 homolog B,	0.071631183	1.96
17136	30.04	29.55	65.77	106.43	63.25	68.71	Mag	myelin-associated glycoprotein,myelin-associated glycoprotein,myelin-associated glycoprotein,	0.052925605	1.90
23945	25.53	20.17	23.81	54.76	27.65	49.74	Mgll	monoglyceride lipase,monoglyceride lipase,monoglyceride lipase,	0.081236016	1.88
215303	3.32	6.96	3.75	9.50	5.08	11.79	Camk1g	calcium/calmodulin-dependent protein kinase I	0.095299326	1.86
23964	5.88	11.99	6.42	12.25	13.46	19.47	Odz2	odd Oz/ten-m homolog 2 isoform 1,odd Oz/ten-m homolog 2 isoform 1,	0.058571824	1.84
338521	4.08	6.08	10.53	15.17	8.54	14.12	Fa2h	fatty acid 2-hydroxylase,fatty acid 2-hydroxylase,	0.087278116	1.82
319317	182.62	153.02	255.94	70.16	212.97	67.02	A930034L06Rik	hypothetical protein LOC319317	0.07843178	0.59
18647	25.74	31.72	31.13	15.99	22.29	10.39	Pftk1	PFTAIRE protein kinase 1,PFTAIRE protein kinase 1,PFTAIRE protein kinase 1,	0.097800464	0.54
56070	45.82	57.52	39.69	18.13	30.66	24.62	Tcerg1	transcription elongation regulator 1 (CA150),transcription elongation regulator 1 (CA150),transcription elongation regulator 1 (CA150),	0.057158613	0.51
67298	159.23	313.89	171.17	93.28	131.90	102.62	Gprasp1	G protein-coupled receptor associated sorting,G protein-coupled receptor associated sorting,	0.092144587	0.50
231279	10.34	16.99	14.45	4.71	9.63	6.48	Guf1	GUF1 GTPase homolog,GUF1 GTPase homolog,	0.094948887	0.49
320472	17.92	23.59	26.51	12.23	13.62	7.91	Ppm1e	protein phosphatase 1E (PP2C domain containing)	0.051932192	0.49
67500	51.76	70.67	44.62	23.90	33.26	25.06	Ccar1	cell division cycle and apoptosis regulator 1,cell division cycle and apoptosis regulator 1,	0.039718821	0.49
18573	41.26	30.70	26.14	23.73	14.56	9.32	Pde1a	phosphodiesterase 1A, calmodulin-dependent,phosphodiesterase 1A, calmodulin-dependent,phosphodiesterase 1A, calmodulin-dependent,	0.092755927	0.49
57743	25.39	31.19	28.59	11.79	17.34	12.52	Sec61a2	Sec61, alpha subunit 2	0.065527974	0.49
16981	23.22	43.25	24.11	10.90	21.45	12.16	Lrrn3	leucine rich repeat protein 3, neuronal	0.042170727	0.48
54561	31.31	78.21	36.51	18.91	33.43	19.20	Nap1l3	nucleosome assembly protein 1-like 3	0.051416316	0.48
381280	12.64	6.41	4.17	2.83	2.26	6.24	6430706D22Rik	hypothetical protein LOC381280	0.090531785	0.48
14394	41.42	133.83	69.11	35.33	48.15	33.72	Gabra1	gamma-aminobutyric acid (GABA-A) receptor,	0.063641983	0.47
109205	22.75	15.67	14.17	8.13	9.25	7.62	Sobp	sine oculis-binding protein homolog,sine oculis-binding protein homolog,	0.020760121	0.47
13839	13.79	15.49	15.15	6.64	8.84	5.47	Epha5	Eph receptor A5,Eph receptor A5,Eph receptor A5,Eph receptor A5,Eph receptor A5,Eph receptor A5,	0.023849801	0.47
14199	38.67	61.87	47.80	18.98	25.06	25.13	Fhl1	four and a half LIM domains 1 isoform 3	0.045640321	0.46
57775	11.69	32.33	13.17	6.14	10.05	10.35	Usp29	ubiquitin specific peptidase 29	0.057158613	0.46
268390	11.00	17.44	11.75	4.48	9.03	4.83	Ahsa2	RIKEN cDNA 1110064P04	0.031122376	0.45
217517	9.08	33.48	18.80	8.85	11.72	7.35	Stxbp6	syntaxin binding protein 6 (amisyn)	0.064914524	0.45
72852	7.77	20.09	13.49	4.43	8.22	6.16	2900024O10Rik	hypothetical protein LOC72852	0.062627052	0.45
14783	13.27	28.28	15.41	7.81	8.49	9.54	Grb10	growth factor receptor bound protein 10,growth factor receptor bound protein 10,	0.05965615	0.45

268345	5.74	15.43	8.82	5.61	6.29	1.74	Kcnc2	potassium voltage gated channel, Shaw-related,potassium voltage gated channel, Shaw-related,	0.043382647	0.45
74868	26.62	50.40	30.32	16.49	15.69	16.11	Tmem65	hypothetical protein LOC74868	0.037808228	0.44
245670	29.79	82.99	38.48	16.32	27.04	24.51	Rragb	Ras-related GTP binding B	0.045739583	0.44
56496	8.65	28.16	12.33	3.80	13.42	4.66	Tspan6	tetraspanin 6	0.067916608	0.44
76740	15.17	36.95	26.10	12.19	15.41	7.00	C920006C10Rik	RIKEN cDNA C920006C10	0.022923125	0.44
26950	119.84	261.08	165.69	104.46	94.78	43.17	Vsnl1	visinin-like 1	0.018002496	0.44
14702	31.52	70.28	46.78	30.52	22.41	12.91	Gng2	guanine nucleotide binding protein (G protein),	0.028812197	0.44
84652	5.81	10.93	8.51	3.13	4.35	3.61	Drctnnb1a	down-regulated by Ctnnb1, a	0.048718733	0.43
15560	21.58	51.23	26.56	9.63	19.67	13.63	Htr2c	5-hydroxytryptamine (serotonin) receptor 2C,5-hydroxytryptamine (serotonin) receptor 2C,	0.012172159	0.43
20257	175.65	173.26	149.73	84.21	68.23	61.97	Stmn2	stathmin-like 2	0.008203307	0.43
15980	20.69	10.02	14.42	6.92	4.04	8.38	Ifngr2	interferon gamma receptor 2	0.042376987	0.43
217125	9.44	7.61	11.38	4.06	4.33	3.79	Samd14	sterile alpha motif domain containing 14 isoform	0.038249772	0.42
211739	19.89	74.13	42.79	15.84	23.75	19.20	Vstm2a	V-set and transmembrane domain containing 2A	0.02949593	0.42
27062	45.33	67.29	46.17	23.11	24.28	20.44	Cadps	Ca<2+>dependent activator protein for secretion,Ca<2+>dependent activator protein for secretion,	0.010377122	0.42
56527	5.91	4.79	7.76	4.61	1.69	1.50	Mast1	microtubule associated serine/threonine kinase	0.07591265	0.42
18389	10.54	19.73	11.49	5.82	4.93	7.00	Opfl1	opioid receptor-like 1,opioid receptor-like 1,opioid receptor-like 1,opioid receptor-like 1,	0.063372885	0.42
54712	5.33	12.85	7.16	2.68	4.37	3.65	Plxnc1	plexin C1	0.033840146	0.42
228662	19.73	35.75	26.65	11.04	14.15	9.32	Btbd3	BTB/POZ domain containing protein 3 isoform 2	0.010377122	0.42
66573	11.90	26.04	17.30	6.57	10.66	5.76	Dzip1	DAZ interacting protein 1,DAZ interacting protein 1,DAZ interacting protein 1,DAZ interacting protein 1,	0.013341774	0.41
380686	38.07	51.97	34.37	18.33	17.47	15.98	1500041B16Rik	hypothetical protein LOC380686	0.016821231	0.41
70536	8.01	24.91	12.53	5.40	7.81	5.51	Qpct	glutaminyl-peptide cyclotransferase (glutaminyl,glutaminyl-peptide cyclotransferase (glutaminyl,	0.079003069	0.41
227325	31.94	74.50	62.87	22.38	28.19	18.61	Dner	delta/notch-like EGF-related receptor,delta/notch-like EGF-related receptor,	0.008461476	0.40
12140	54.26	118.22	46.52	30.89	26.69	30.45	Fabp7	fatty acid binding protein 7, brain	0.032294362	0.40
216197	7.73	6.64	8.80	3.86	2.85	2.60	Ckap4	cytoskeleton-associated protein 4	0.037116397	0.40
320865	12.91	12.63	7.63	5.32	4.11	3.83	Cdh18	cadherin 18,cadherin 18,cadherin 18,	0.024475703	0.40
270028	37.11	27.39	28.70	15.85	9.39	12.16	Tmem28	transmembrane protein 28	0.005877729	0.40
214240	30.93	46.59	37.19	19.29	14.22	12.35	Disp2	dispatched homolog 2	0.005572299	0.39
243339	93.37	188.06	112.39	56.23	53.24	47.34	Tmem130	hypothetical protein LOC243339	0.005820579	0.39
77630	5.22	0.59	4.95	0.99	1.33	1.95	Prdm8	PR domain containing 8	0.06206971	0.39
245595	4.65	9.01	5.48	2.87	1.98	2.76	Zfp711	zinc finger protein 711,zinc finger protein 711,	0.065737487	0.39
18761	7.17	9.56	9.26	3.84	3.08	3.28	Prkcq	protein kinase C, theta,protein kinase C, theta,protein kinase C, theta,	0.047542686	0.39
226830	24.41	15.80	21.37	10.67	6.64	6.62	Smyd2	SET and MYND domain containing 2	0.023872452	0.39
71687	9.05	5.04	8.10	4.30	1.62	2.76	Tmem25	transmembrane protein 25,transmembrane protein 25,	0.064518025	0.39
52552	6.24	9.80	6.74	2.79	3.17	2.83	Parp8	poly (ADP-ribose) polymerase family, member 8,poly (ADP-ribose) polymerase family, member 8,poly (ADP-ribose) polymerase family, member 8,	0.071631183	0.39
72605	14.38	21.71	14.96	13.17	3.52	3.01	Car10	carbonic anhydrase 10,carbonic anhydrase 10,carbonic anhydrase 10,	0.022773859	0.38
16922	67.91	141.51	80.36	43.37	37.70	29.68	Phyh	phytanoyl-CoA hydroxylase	0.005956315	0.38
15481	85.40	61.45	69.63	43.78	13.91	24.97	Hspa8	heat shock protein 8,heat shock protein 8,	0.004599723	0.38

56747	14.12	12.89	15.52	8.06	4.10	3.98	Sez6l	seizure related 6 homolog like,seizure related 6 homolog like,seizure related 6 homolog like,seizure related 6 homolog like,	0.00493898	0.38
16519	8.72	6.26	7.83	5.40	1.02	2.16	Kcnj3	potassium inwardly-rectifying channel, subfamily	0.098543507	0.37
17470	50.49	115.49	58.45	25.83	33.28	24.98	Cd200	Cd200 antigen	0.002289624	0.37
55936	6.99	15.01	8.62	3.78	4.49	3.03	Ctps2	cytidine 5'-triphosphate synthase 2,cytidine 5'-triphosphate synthase 2,cytidine 5'-triphosphate synthase 2,cytidine 5'-triphosphate synthase 2,	0.025001193	0.37
106957	13.04	25.99	14.64	6.35	7.54	5.83	Slc39a6	solute carrier family 39 (metal ion	0.004349553	0.36
52906	85.96	199.31	115.07	38.81	64.81	43.07	Ahi1	Abelson helper integration site	0.000812067	0.36
228911	4.06	9.19	7.36	2.74	2.01	2.76	Tshz2	teashirt zinc finger family member 2,teashirt zinc finger family member 2,teashirt zinc finger family member 2,teashirt zinc finger family member 2,teashirt zinc finger family member 2,	0.024261264	0.36
83669	23.45	29.02	36.08	12.36	10.60	8.96	Wdr6	WD repeat domain 6	0.001465463	0.36
66151	22.60	34.21	23.97	8.94	10.56	9.59	Prr13	proline rich 13,proline rich 13,proline rich 13,proline rich 13,	0.00826669	0.36
215789	3.77	4.71	6.38	2.39	1.59	1.29	Phactr2	phosphatase and actin regulator 2,phosphatase and actin regulator 2,phosphatase and actin regulator 2,phosphatase and actin regulator 2,	0.0923627	0.35
70357	10.53	23.53	12.17	6.08	5.02	5.19	Kcnip1	Kv channel-interacting protein 1,Kv channel-interacting protein 1,	0.028304646	0.35
234515	1.83	5.01	3.90	0.98	1.50	1.19	Inpp4b	inositol polyphosphate-4-phosphatase, type II,inositol polyphosphate-4-phosphatase, type II,inositol polyphosphate-4-phosphatase, type II,inositol polyphosphate-4-phosphatase, type II,inositol polyphosphate-4-phosphatase, type II,	0.080699514	0.34
78593	24.91	49.67	22.85	14.08	9.30	10.11	Nrip3	nuclear receptor interacting protein 3,nuclear receptor interacting protein 3,	0.00138066	0.34
225182	2.76	4.16	2.08	0.96	1.45	0.65	Rbbp8	retinoblastoma binding protein 8,retinoblastoma binding protein 8,retinoblastoma binding protein 8,	0.06700426	0.34
268354	16.33	17.22	19.11	3.78	5.56	8.50	AI851790	TAFA2 protein,TAFA2 protein,	0.001034218	0.34
18548	8.08	13.36	7.59	4.32	3.74	1.73	Pcsk1	proprotein convertase subtilisin/kexin type 1,proprotein convertase subtilisin/kexin type 1,	0.01269459	0.33
215378	5.41	8.58	4.67	2.25	1.45	2.59	B830045N13Rik	DBCCR1-like,DBCCR1-like,DBCCR1-like,	0.038293151	0.33
219257	5.40	9.65	7.25	1.91	3.48	2.13	Pcdh20	protocadherin 20	0.003901319	0.33
19418	4.39	2.11	5.08	1.50	1.18	1.13	Rasgrf2	RAS protein-specific guanine	0.048818531	0.33
13865	11.31	18.26	20.05	7.09	5.90	3.51	Nr2f1	nuclear receptor subfamily 2, group F, member 1	0.002984696	0.33
232560	3.20	5.51	4.24	0.90	2.03	1.36	Caprin2	caprin family member 2,caprin family member 2,	0.028414786	0.33
15959	6.19	10.16	7.74	1.92	3.79	2.28	Ifit3	interferon-induced protein with	0.014568199	0.33
15572	25.74	19.37	19.99	12.79	1.91	6.64	Elavl4	ELAV-like 4 isoform a,ELAV-like 4 isoform a,	0.041640843	0.33
11514	2.10	3.99	2.88	1.20	0.75	1.00	Adcy8	adenylate cyclase 8,adenylate cyclase 8,	0.053274074	0.32
73341	3.49	7.37	3.37	1.72	1.20	1.73	Arhgef6	Rac/Cdc42 guanine nucleotide exchange factor 6,Rac/Cdc42 guanine nucleotide exchange factor 6,	0.027416972	0.32
12814	1.17	1.89	2.54	0.37	1.02	0.41	Col11a1	procollagen, type XI, alpha 1	0.04760262	0.32
102278	6.20	3.00	11.59	3.20	1.24	2.29	Cpne7	copine 7 protein	0.038249772	0.32
12405	3.33	10.37	4.56	3.85	1.19	0.95	Cbln2	cerebellin 2 precursor protein,cerebellin 2 precursor protein,cerebellin 2 precursor protein,cerebellin 2 precursor protein,	0.09022736	0.32

83398	3.21	3.24	2.32	0.79	1.36	0.70	Ndst3	N-deacetylase/N-sulfotransferase (heparan,N-deacetylase/N-sulfotransferase (heparan,	0.007557633	0.32
20846	7.77	10.54	10.29	2.92	3.33	3.00	Stat1	signal transducer and activator of transcription,signal transducer and activator of transcription,signal transducer and activator of transcription,signal transducer and activator of transcription,signal transducer and activator of transcription,	0.001465463	0.32
245468	4.03	8.02	6.25	2.16	2.07	1.68	Pnma3	paraneoplastic antigen MA3	0.012127895	0.32
105440	5.11	13.86	6.55	3.53	1.69	2.96	Kctd9	potassium channel tetramerisation domain	0.022003277	0.32
100637	13.40	28.07	10.83	4.44	6.39	5.94	B230342M21Rik	hypothetical protein LOC100637,hypothetical protein LOC100637,	0.003300314	0.32
243771	2.13	5.12	3.94	0.94	1.27	1.25	Parp12	poly (ADP-ribose) polymerase family, member 12	0.055111323	0.31
57915	2.82	3.30	2.78	1.45	0.30	0.99	Tbc1d1	TBC1 domain family, member 1,TBC1 domain family, member 1,TBC1 domain family, member 1,TBC1 domain family, member 1,	0.028812197	0.30
77629	12.13	14.15	13.74	4.87	4.63	2.73	4930544G21Rik	sphingosine kinase type 1-interacting protein,sphingosine kinase type 1-interacting protein,	4.73E-05	0.30
16391	6.63	7.69	6.82	1.20	2.95	2.22	Isgf3g	interferon dependent positive acting,interferon dependent positive acting,interferon dependent positive acting,	0.007302389	0.30
239133	5.22	13.35	8.34	2.49	2.90	2.64	Dleu7	deleted in lymphocytic leukemia, 7	0.036718244	0.29
56470	12.39	11.50	11.75	3.82	2.33	4.14	Rgs19	regulator of G-protein signaling 19,regulator of G-protein signaling 19,regulator of G-protein signaling 19,regulator of G-protein signaling 19,regulator of G-protein signaling 19,	0.008348244	0.29
237213	10.90	20.85	12.02	4.92	3.79	3.89	Glra2	glycine receptor, alpha 2 subunit	0.000812067	0.28
64580	1.68	2.87	1.41	0.51	0.87	0.34	Ndst4	N-deacetylase/N-sulfotransferase (heparin,N-deacetylase/N-sulfotransferase (heparin,N-deacetylase/N-sulfotransferase (heparin,	0.061513352	0.28
13132	1.36	5.02	1.81	0.72	0.87	0.75	Dab2	disabled homolog 2 isoform b	0.06612411	0.28
54598	1.90	4.84	3.09	1.23	0.48	1.07	Calcrl	calcitonin receptor-like,calcitonin receptor-like,	0.029340442	0.28
22418	1.51	1.15	1.69	0.36	0.19	0.67	Wnt5a	wingless-related MMTV integration site 5A,wingless-related MMTV integration site 5A,	0.090853222	0.28
269437	0.78	2.94	1.90	0.72	0.26	0.57	Plch1	phospholipase C, eta 1,phospholipase C, eta 1,phospholipase C, eta 1,	0.067962094	0.27
13180	9.67	21.06	6.68	3.31	0.53	6.40	Pcbd1	pterin 4 alpha carbinolamine	0.086768121	0.27
18187	3.16	2.43	3.06	1.00	0.74	0.62	Nrp2	neuropilin 2 isoform 1 precursor	0.021984375	0.27
353282	1.42	1.46	1.60	0.42	0.50	0.27	Sfmbt2	Scm-like with four mbt domains 2,Scm-like with four mbt domains 2,Scm-like with four mbt domains 2,Scm-like with four mbt domains 2,	0.007489285	0.26
56506	30.97	23.71	17.50	7.57	4.70	6.61	Cib2	calcium and integrin binding family member 2	0.004191904	0.26
224344	3.36	7.52	4.93	1.62	0.93	1.58	Rbm11	RNA binding motif protein 11	0.012484894	0.26
76142	3.09	8.20	5.07	1.99	0.54	1.66	Ppp1r14c	PKC-potentiated PP1 inhibitory protein	0.0188757	0.25
110058	4.79	4.00	4.35	1.09	1.45	0.73	Syt17	synaptotagmin XVII,synaptotagmin XVII,synaptotagmin XVII,synaptotagmin XVII,	0.024031392	0.25
59058	3.29	1.77	5.31	0.91	0.05	1.52	Bhlhb5	basic helix-loop-helix domain containing, class	0.010377122	0.24
71562	3.61	2.29	3.03	0.43	1.15	0.49	Afmid	arylformamidase	0.012009344	0.23

11989	2.60	7.82	4.15	1.79	0.82	0.80	Slc7a3	solute carrier family 7 (cationic amino acid,solute carrier family 7 (cationic amino acid,	0.021046316	0.23
245403	0.90	1.59	1.28	0.10	0.53	0.25	Wdr40c	WD repeat domain 40C	0.094766641	0.23
12122	2.73	2.44	4.13	1.19	0.00	0.91	Bid	BH3 interacting domain death agonist	0.077948764	0.23
19039	7.80	7.17	8.59	2.33	0.84	2.04	Lgals3bp	lectin, galactoside-binding, soluble, 3 binding	0.000709144	0.22
18430	2.55	1.50	1.84	0.61	0.36	0.31	Oxtr	oxytocin receptor	0.002248921	0.21
56016	2.40	3.42	2.22	0.74	0.45	0.51	Hebp2	heme binding protein 2,heme binding protein 2,	0.045849503	0.21
230073	1.16	2.14	1.78	0.54	0.03	0.47	Ddx58	DEAD/H box polypeptide RIG-I,DEAD/H box polypeptide RIG-I,DEAD/H box polypeptide RIG-I,	0.02552819	0.20
77318	1.43	3.38	1.33	0.40	0.26	0.59	Ankrd55	ankyrin repeat domain 55,ankyrin repeat domain 55,	0.09022736	0.20
19106	1.13	1.55	1.20	0.48	0.10	0.21	Eif2ak2	eukaryotic translation initiation factor 2-alpha	0.045513142	0.20
15944	4.30	7.23	5.67	1.40	0.34	1.73	Irgm	immunity-related GTPase family, M	0.002289624	0.20
210417	1.12	2.19	0.87	0.51	0.14	0.16	Thsd7b	thrombospondin, type I, domain containing 7B,thrombospondin, type I, domain containing 7B,	0.010377122	0.19
70918	3.00	1.79	3.96	0.37	0.47	0.85	Nsun7	NOL1/NOP2/Sun domain family, member 7,NOL1/NOP2/Sun domain family, member 7,NOL1/NOP2/Sun domain family, member 7,	0.009798624	0.19
16145	1.67	3.99	2.04	0.53	0.00	0.90	Igtp	interferon gamma induced GTPase	0.060298996	0.18
20513	3.41	4.56	5.15	1.48	0.00	0.93	Slc1a6	solute carrier family 1 (high affinity	0.010689147	0.18
108058	23.68	40.95	35.50	6.13	5.89	5.42	Camk2d	calcium/calmodulin-dependent protein kinase II,,calcium/calmodulin-dependent protein kinase II,,calcium/calmodulin-dependent protein kinase II,,	3.68E-18	0.17
11819	6.99	19.72	17.10	3.09	3.13	1.41	Nr2f2	nuclear receptor subfamily 2, group F, member 2	2.29E-11	0.17
14706	28.32	26.80	34.93	5.47	6.08	3.98	Gng4	guanine nucleotide binding protein (G protein),	9.22E-13	0.17
209200	1.42	2.53	1.81	0.36	0.00	0.61	Dtx3l	deltex 3-like,deltex 3-like,	0.00220833	0.17
98303	1.96	3.31	1.99	0.34	0.31	0.47	D630023F18Rik	hypothetical protein LOC98303,hypothetical protein LOC98303,	0.015970391	0.15
14805	2.78	8.07	3.86	0.93	0.48	0.77	Grik1	glutamate receptor, ionotropic, kainate 1,glutamate receptor, ionotropic, kainate 1,glutamate receptor, ionotropic, kainate 1,glutamate receptor, ionotropic, kainate 1,	1.38E-05	0.15
77220	2.24	5.56	3.25	0.81	0.49	0.32	C030003D03Rik	hypothetical protein LOC77220,hypothetical protein LOC77220,	2.35E-06	0.14
246709	3.97	0.16	2.44	0.20	0.27	0.43	Rgs13	regulator of G-protein signaling 13,regulator of G-protein signaling 13,	0.022401776	0.14
114875	1.26	0.89	2.05	0.07	0.32	0.16	Plcz1	phospholipase C, zeta 1	0.049033054	0.13
66931	2.26	1.33	1.56	0.51	0.06	0.11	1700010I14Rik	hypothetical protein LOC66931	0.048260993	0.13
320460	2.65	6.20	2.76	0.40	0.34	0.66	A830006F12Rik	hypothetical protein LOC320460,hypothetical protein LOC320460,	1.43E-08	0.12
64242	2.67	7.55	5.37	0.73	0.00	0.99	Ngb	neuroglobin	0.000400554	0.11
14255	0.94	1.04	1.03	0.14	0.00	0.19	Flt3	FMS-like tyrosine kinase 3	0.035230682	0.11
11516	2.24	2.66	3.61	0.76	0.00	0.15	Adcyap1	adenylate cyclase activating polypeptide 1,adenylate cyclase activating polypeptide 1,	0.001465463	0.11
320265	3.89	4.00	4.27	0.56	0.23	0.50	C630007B19Rik	TAFA1 protein,TAFA1 protein,	5.66E-09	0.10
23962	1.87	4.13	4.13	0.30	0.00	0.54	Oasl2	2'-5' oligoadenylate synthetase-like 2	1.73E-07	0.08
22268	1.25	0.91	1.78	0.00	0.00	0.30	Upk1b	uroplakin 1B	0.043590421	0.07
320500	0.64	2.11	1.14	0.19	0.05	0.03	A930001M12Rik	hypothetical protein LOC320500	0.001113129	0.07
15957	4.90	12.07	6.24	0.41	0.00	0.84	Ifit1	interferon-induced protein with	2.14E-16	0.05
24110	2.06	1.89	2.39	0.00	0.00	0.32	Usp18	ubiquitin specific peptidase 18	0.00220833	0.05
110304	1.15	3.06	2.39	0.00	0.12	0.14	Glra3	glycine receptor, alpha 3 subunit	0.002664772	0.04
17116	0.63	2.20	1.67	0.00	0.00	0.02	Mab21l1	mab-21-like 1	1.21E-09	0.00

Table A-4: Dysregulated genes in 12wk cortex.

Gene	TCM9452	TCM9450	TCM9453	TCW9451	TCW9457	TCW9469	gene_symbol	gene_desc	padj	DESeq Delta
269589	0.11	0.01	0.00	1.32	1.47	1.08	Sytl1	synaptotagmin-like 1	4.96E-11	31.00
11686	0.12	0.20	0.14	1.82	1.68	1.48	Alox12b	arachidonate 12-lipoxygenase, 12R type	4.34E-12	10.56
192199	0.38	0.34	0.48	4.45	5.25	2.92	Rspo1	thrombospondin type 1 domain containing	4.53E-22	10.42
71912	0.35	0.39	0.12	2.57	3.20	3.13	Jsrp1	JP-45 protein	4.23E-12	10.21
386454	0.20	0.28	0.13	2.78	2.60	0.86	Rnf39	ring finger protein 39	7.83E-12	10.20
72500	0.40	1.13	0.17	7.04	4.03	5.05	Ier5l	immediate early response 5-like	2.37E-20	9.34
110751	0.28	0.21	0.08	1.33	1.89	1.24	Adam33	a disintegrin and metallopeptidase domain 33,a disintegrin and metallopeptidase domain 33,	1.06E-09	8.08
21924	3.24	1.25	2.36	13.86	23.10	14.12	Tnnc1	troponin C, cardiac/slow skeletal	4.70E-16	7.47
243967	0.36	0.37	0.31	2.94	1.83	3.02	Gm484	hypothetical protein LOC243967,hypothetical protein LOC243967,	1.40E-10	7.44
73598	0.13	0.25	0.50	2.67	1.92	1.83	1700001O22Rik	hypothetical protein LOC73598	2.78E-12	7.21
67077	0.93	1.21	0.54	6.38	6.80	5.13	1700019N12Rik	hypothetical protein LOC67077	2.68E-10	6.80
216166	0.68	1.22	0.38	7.39	3.53	4.11	6330514A18Rik	hypothetical protein LOC216166,hypothetical protein LOC216166,	5.88E-16	6.60
14313	0.22	0.24	0.16	0.89	2.19	0.75	Fst	follistatin,follistatin,	1.88E-06	6.22
85030	0.72	0.73	0.34	3.57	3.93	3.39	Tnfrsf25	tumor necrosis factor receptor superfamily,,tumor necrosis factor receptor superfamily,,	3.46E-12	6.04
74230	0.35	0.30	0.68	2.83	2.97	2.05	1700016K19Rik	hypothetical protein LOC74230	1.88E-06	5.87
353287	0.78	0.71	0.40	3.52	4.05	3.14	Mrcl	mannose receptor-like,mannose receptor-like,	4.34E-12	5.71
19416	0.50	0.80	0.08	2.24	2.24	3.40	Rasd1	RAS, dexamethasone-induced 1	1.47E-08	5.68
13654	0.62	0.47	0.23	2.57	2.75	1.78	Egr2	early growth response 2	1.23E-11	5.32
20190	0.48	0.47	0.37	2.16	2.39	2.25	Ryr1	ryanodine receptor 1, skeletal muscle	2.70E-23	5.16
72795	1.41	6.00	0.24	11.47	14.85	12.66	Ttc19	tetratricopeptide repeat domain 19 isoform 1,tetratricopeptide repeat domain 19 isoform 1,	4.64E-05	5.09
229214	0.11	0.37	0.24	1.56	1.07	1.00	Gpr103	G protein-coupled receptor 103	3.23E-05	4.98
100102	0.10	0.43	0.15	1.85	0.69	0.87	Pcsk9	proprotein convertase subtilisin/kexin type 9	2.14E-09	4.98
16855	0.38	0.29	0.10	1.39	1.22	1.15	Lgals4	lectin, galactose binding, soluble 4,lectin, galactose binding, soluble 4,	0.009922161	4.93
18292	0.23	0.33	0.22	1.22	1.58	1.08	Sebox	SEBOX homeobox	0.001565039	4.87
353499	0.42	0.39	0.18	2.18	1.22	1.39	Tmc4	transmembrane channel-like gene family 4,transmembrane channel-like gene family 4,transmembrane channel-like gene family 4,	3.53E-06	4.82
12615	0.16	0.45	0.15	1.19	1.05	1.45	Cenpa	centromere protein A	0.001780591	4.80
73284	2.01	1.03	0.83	5.65	6.49	6.60	Ddit4l	DNA-damage-inducible transcript 4-like	3.81E-16	4.77
13857	0.48	0.79	0.32	2.80	2.53	2.31	Epor	erythropoietin receptor,erythropoietin receptor,	3.79E-08	4.75
76161	25.37	13.44	21.28	93.78	115.03	72.67	6330527O06Rik	6330527O06Rik protein	5.78E-36	4.64
399548	5.75	7.99	4.40	27.73	29.57	26.36	Scn4b	sodium channel, type IV, beta	3.97E-31	4.56
59289	0.23	0.37	0.20	0.95	1.28	1.40	Ccbp2	chemokine binding protein 2,chemokine binding protein 2,	1.58E-05	4.51
230735	0.47	1.94	0.84	6.55	3.82	4.30	Epha10	Eph receptor A10	3.70E-11	4.50
73707	0.57	0.46	0.38	2.07	2.65	1.62	Gucy2g	guanylate cyclase 2g,guanylate cyclase 2g,	7.70E-10	4.48
73327	0.42	0.46	0.32	1.46	1.92	1.79	1700040I03Rik	hypothetical protein LOC73327,hypothetical protein LOC73327,	0.021847002	4.27
16528	1.13	1.31	0.99	5.72	5.36	3.10	Kcnk4	TRAAK	1.12E-09	4.10
12931	0.33	0.33	0.35	0.70	0.92	2.46	Crlf1	cytokine receptor-like factor 1	0.004094018	4.03
27261	0.78	0.94	0.92	4.82	2.76	2.99	Dok3	docking protein 3	5.33E-08	3.97
21393	1.21	0.63	1.18	3.30	5.32	3.37	Tcap	titin-cap	0.000120602	3.93
11838	14.82	17.31	21.17	63.26	79.33	65.53	Arc	activity regulated cytoskeletal-associated,activity regulated cytoskeletal-associated,	1.08E-25	3.86
52815	1.18	1.21	1.18	4.80	4.44	4.38	Ldhd	D-lactate dehydrogenase	6.12E-10	3.79
71760	1.08	1.63	0.81	2.42	5.58	5.27	Agxt2l1	alanine-glyoxylate aminotransferase 2-like 1	2.02E-08	3.75
14586	5.41	3.78	7.31	21.80	24.09	14.95	Gfra2	glial cell line derived neurotrophic factor,glial cell line derived neurotrophic factor,glial cell line derived neurotrophic factor,	2.96E-18	3.65
12831	0.62	0.88	1.07	3.38	2.72	3.12	Col5a1	procollagen, type V, alpha 1	3.18E-14	3.60

103551	5.88	6.54	9.01	27.91	26.49	23.19	E130012A19Rik	hypothetical protein LOC103551	1.39E-19	3.58
100129	1.96	2.51	1.44	8.99	7.04	5.01	Gpr153	G protein-coupled receptor 153	6.00E-14	3.52
11550	2.65	2.46	2.66	11.60	9.22	6.82	Adra1d	adrenergic receptor, alpha 1d	1.60E-15	3.51
74782	1.47	1.56	1.96	6.33	6.73	4.47	Glt8d2	glycosyltransferase 8 domain containing 2	1.22E-11	3.50
234912	0.93	1.47	0.73	3.24	3.25	4.55	9230110C19Rik	hypothetical protein LOC234912	1.91E-05	3.50
27220	1.27	2.68	0.65	5.50	5.93	4.51	Cartpt	cocaine and amphetamine regulated transcript	0.000329813	3.44
15550	1.01	1.45	1.32	4.25	3.59	5.17	Htr1a	5-hydroxytryptamine (serotonin) receptor 1A	1.03E-13	3.40
75668	4.72	6.83	4.83	24.34	14.81	16.70	Rasl10a	RAS-related on chromosome 22	1.03E-13	3.38
99296	6.60	8.20	5.55	23.82	17.82	26.14	Hrh3	histamine receptor H 3	4.30E-21	3.29
12659	0.44	0.93	0.62	2.17	2.29	2.08	Ovgp1	oviductal glycoprotein 1	3.28E-05	3.28
13170	4.12	6.03	2.49	14.08	13.26	14.42	Dbp	D site albumin promoter binding protein	2.37E-12	3.28
12608	0.94	1.55	0.68	4.03	3.45	2.93	Cebpb	CCAAT/enhancer binding protein beta	2.71E-05	3.27
56222	0.73	0.96	0.69	3.25	2.30	2.24	Cited4	Cbp/p300-interacting transactivator, with	0.000509487	3.24
83762	1.08	2.35	0.95	5.78	3.46	4.98	Otof	otoferlin isoform 1	5.10E-14	3.23
78617	0.13	0.65	0.24	1.13	0.77	1.40	Cstad	CSA-conditional, T cell activation-dependent	0.084501597	3.18
15565	0.15	0.72	0.35	1.88	1.15	0.90	Htr6	5-hydroxytryptamine (serotonin) receptor 6	0.005240973	3.18
19225	0.63	0.83	0.71	2.43	2.14	2.29	Ptgs2	prostaglandin-endoperoxide synthase 2	5.33E-08	3.15
236920	3.38	2.04	2.41	9.50	9.21	6.19	Stard8	START domain containing 8	8.12E-15	3.15
22068	1.29	1.13	1.47	3.47	3.84	5.06	Trpc6	transient receptor potential cation channel,,transient receptor potential cation channel,,	1.52E-08	3.15
76459	1.37	1.77	1.58	4.52	3.78	6.66	Car12	carbonic anyhydrase 12,carbonic anyhydrase 12,	5.24E-11	3.14
232933	1.02	0.96	0.93	3.12	3.18	2.76	C530028I08Rik	hypothetical protein LOC232933	0.000235846	3.12
66259	183.73	173.66	199.07	507.78	725.54	516.65	Camk2n1	calcium/calmodulin-dependent protein kinase II	7.75E-14	3.11
225642	3.00	1.80	1.28	5.31	5.46	8.22	Grp	gastrin releasing peptide	0.001055655	3.10
22761	2.58	3.37	3.94	11.68	8.78	10.34	Zfpm1	zinc finger protein, multitype 1	1.72E-16	3.09
54141	1.72	1.48	1.74	5.59	4.86	4.78	Spag5	sperm associated antigen 5	8.16E-10	3.08
18159	0.73	0.92	0.56	2.63	1.95	2.24	Nppc	natriuretic peptide precursor type C	0.008806181	3.06
228550	18.65	17.59	25.45	66.30	66.03	56.44	Itpka	inositol 1,4,5-trisphosphate 3-kinase A	2.97E-16	3.04
13070	0.49	0.56	0.80	2.10	1.96	1.58	Cyp11a1	cytochrome P450, family 11, subfamily a,	0.001971804	3.03
319239	0.14	0.87	0.27	1.52	0.94	1.37	Npsr1	G protein-coupled receptor for asthma,G protein-coupled receptor for asthma,	5.08E-05	3.02
60425	2.68	0.90	1.16	5.03	6.23	2.92	Doc2g	double C2, gamma	0.001648893	3.00
320265	2.38	4.94	2.95	11.22	11.65	8.15	C630007B19Rik	TAFA1 protein,TAFA1 protein,	1.54E-12	3.00
21886	1.46	2.28	2.82	8.15	4.93	6.62	Tle2	transducin-like enhancer protein 2,transducin-like enhancer protein 2,transducin-like enhancer protein 2,	1.95E-10	2.99
68498	0.82	0.54	0.41	1.44	2.30	1.58	Tspan11	tetraspanin 11	0.000362294	2.98
67622	3.46	1.96	1.87	5.18	9.39	7.29	Mxra7	matrix-remodelling associated 7,matrix-remodelling associated 7,	2.27E-05	2.97
12918	1.42	0.84	0.83	3.66	2.90	2.60	Crh	corticotropin releasing hormone	0.002667828	2.93
21955	2.62	1.08	1.73	4.13	6.50	4.81	Tnnt1	troponin T1, skeletal, slow,troponin T1, skeletal, slow,	0.023020872	2.91
217154	10.59	7.87	12.59	32.31	33.44	24.34	Stac2	SH3 and cysteine rich domain 2	2.34E-14	2.88
56742	1.01	0.98	1.69	3.88	3.22	3.53	Psrc1	proline/serine-rich coiled-coil 1,proline/serine-rich coiled-coil 1,	0.000123185	2.88
19049	22.36	42.29	19.97	64.54	72.44	103.83	Ppp1r1b	protein phosphatase 1, regulatory (inhibitor),protein phosphatase 1, regulatory (inhibitor),	6.11E-14	2.83
19227	0.48	0.58	0.29	1.01	1.12	1.67	Pthlh	parathyroid hormone-like peptide precursor,parathyroid hormone-like peptide precursor,	0.058910386	2.80
225872	2.18	2.33	1.32	5.82	4.33	6.32	Npas4	neuronal PAS domain protein 4	5.37E-08	2.80
239405	2.23	1.92	2.10	5.32	6.10	5.97	Rspo2	R-spondin 2 homolog,R-spondin 2 homolog,	5.41E-08	2.76
243277	0.48	0.45	0.41	1.69	1.35	0.62	Gpr133	G protein-coupled receptor 133	0.000447397	2.71
20300	1.49	0.74	0.94	2.50	2.59	3.48	Ccl25	chemokine (C-C motif) ligand 25	0.04018504	2.69
50782	4.78	3.84	3.28	14.29	8.02	9.47	Rgs11	regulator of G-protein signaling 11,regulator of G-protein signaling 11,regulator of G-protein signaling 11,	8.80E-08	2.68
14403	10.15	9.45	6.93	28.97	21.81	20.40	Gabrd	gamma-aminobutyric acid (GABA-A) receptor,	1.71E-10	2.67
216976	2.91	2.10	2.22	5.93	7.36	5.87	BC030499	hypothetical protein LOC216976	0.005860846	2.67

68854	0.55	0.88	0.65	1.81	1.81	1.93	Asb11	ankyrin repeat and SOCS box-containing protein	0.036634186	2.66
12919	4.50	3.69	6.12	13.34	11.84	12.87	Crhbp	corticotropin releasing hormone binding protein	1.41E-08	2.64
235086	2.46	2.92	1.66	8.36	6.58	3.63	Igsf9b	immunoglobulin superfamily, member 9B	4.06E-06	2.64
71733	0.84	0.77	0.63	2.76	1.77	1.37	Susd2	sushi domain containing 2	0.000932157	2.63
14608	1.60	3.33	1.82	8.55	5.04	4.25	Gpr83	G protein-coupled receptor 83	5.30E-08	2.62
16891	0.50	0.80	0.47	2.08	1.62	0.93	Lipg	lipase, endothelial,lipase, endothelial,	0.000518017	2.61
16323	3.12	1.17	2.06	4.69	8.36	3.55	Inhba	inhibin beta A	0.00214325	2.59
11548	2.61	1.68	2.40	6.62	5.85	5.04	Adra1b	adrenergic receptor, alpha 1b,adrenergic receptor, alpha 1b,adrenergic receptor, alpha 1b,	4.54E-07	2.58
83922	0.58	0.86	0.71	2.00	1.43	2.10	Tsga14	testis specific gene A14	0.000644946	2.56
26568	0.46	0.45	0.42	1.15	1.04	1.18	Slc27a3	solute carrier family 27 member 3	0.04018504	2.55
14555	14.17	9.89	12.75	28.85	29.41	36.49	Gpd1	glycerol-3-phosphate dehydrogenase 1 (soluble),glycerol-3-phosphate dehydrogenase 1 (soluble),	6.24E-10	2.55
268709	38.80	36.85	37.47	74.07	106.33	109.96	BC055107	downregulated in renal cell carcinoma,downregulated in renal cell carcinoma,downregulated in renal cell carcinoma,	9.51E-11	2.54
18610	1.63	5.50	2.41	9.72	8.23	6.29	Pdyn	beta-neoendorphin-dynorphin preproprotein,beta-neoendorphin-dynorphin preproprotein,	0.000478587	2.53
212706	1.53	1.66	1.61	4.69	4.02	3.49	C330016O10Rik	Nedd4 binding protein 3	4.14E-05	2.52
18991	3.59	4.59	3.77	8.00	10.15	12.18	Pou3f1	POU domain, class 3, transcription factor 1	9.05E-08	2.50
668940	1.30	0.63	1.03	2.35	3.05	1.99	Myh7b	RIKEN cDNA 0610038P03	0.000220061	2.49
16478	9.33	19.93	6.47	34.78	24.73	30.20	Jund1	jun D proto-oncogene	8.13E-11	2.49
74580	0.47	0.51	0.31	0.92	0.92	1.38	4833409A17Rik	hypothetical protein LOC74580	0.03811683	2.48
22353	6.85	6.12	7.15	18.97	18.94	12.19	Vip	vasoactive intestinal polypeptide	1.40E-07	2.48
16010	14.42	6.50	13.60	28.58	33.57	24.38	Igfbp4	insulin-like growth factor binding protein 4	1.50E-08	2.48
72168	15.19	8.83	13.94	29.96	34.01	29.63	Aifm3	apoptosis-inducing factor like,apoptosis-inducing factor like,	9.44E-09	2.47
12819	0.48	0.36	0.49	1.22	1.20	0.85	Col15a1	procollagen, type XV	0.00539328	2.47
216019	3.46	1.00	2.66	5.72	7.38	4.58	Hkdc1	hexokinase domain containing 1	4.96E-05	2.47
211770	1.98	2.13	1.44	4.90	5.53	3.43	Trib1	tribbles homolog 1,tribbles homolog 1,	7.10E-06	2.47
114606	0.28	0.56	0.69	1.43	0.97	1.37	Tle6	transducin-like enhancer protein 6,transducin-like enhancer protein 6,transducin-like enhancer protein 6,	0.025840207	2.47
64706	3.97	3.64	3.89	12.06	9.58	6.94	Scube1	signal peptide, CUB domain, EGF-like 1,signal peptide, CUB domain, EGF-like 1,	6.00E-11	2.46
12575	3.07	5.62	2.41	11.03	9.72	6.78	Cdkn1a	cyclin-dependent kinase inhibitor 1A (P21),cyclin-dependent kinase inhibitor 1A (P21),	2.02E-06	2.46
109857	0.25	1.20	0.33	1.80	1.42	1.15	Cbr3	carbonyl reductase 3	0.0645028	2.45
383787	1.41	4.02	1.55	6.29	6.09	4.79	Gm1337	hypothetical protein LOC383787	2.36E-08	2.44
17965	13.18	6.39	5.80	25.71	16.18	20.65	Nbl1	neuroblastoma, suppression of tumorigenicity 1	5.96E-07	2.43
12227	2.06	2.90	1.78	4.68	4.22	7.69	Btg2	B-cell translocation gene 2, anti-proliferative	1.50E-05	2.43
72014	2.55	2.69	2.44	7.03	5.23	6.58	1500005I02Rik	hypothetical protein LOC72014	1.15E-05	2.42
12823	1.76	2.40	1.96	4.01	6.31	4.63	Col19a1	procollagen, type XIX, alpha 1,procollagen, type XIX, alpha 1,	9.61E-08	2.42
52443	6.40	2.06	15.58	10.46	28.88	18.55	Mrpl48	mitochondrial ribosomal protein L48,mitochondrial ribosomal protein L48,	0.000172662	2.41
51801	10.56	9.32	8.30	16.30	29.62	22.07	Ramp1	receptor-activity modifying protein 1	0.00284842	2.40
12348	29.84	33.78	32.56	77.56	80.86	72.95	Car11	carbonic anhydrase 11	1.02E-09	2.40
381511	13.77	17.80	14.31	37.56	49.15	23.78	Ppm2c	protein phosphatase 2C, magnesium dependent,	2.18E-09	2.38
207565	27.82	23.69	29.01	59.67	87.01	45.72	Camkk2	calcium/calmodulin-dependent protein kinase,calcium/calmodulin-dependent protein kinase,calcium/calmodulin-dependent protein kinase,calcium/calmodulin-dependent protein kinase,	1.26E-08	2.38
14221	7.59	9.15	6.58	19.12	17.68	19.12	Fjx1	four jointed box 1	5.83E-08	2.37
68404	57.86	42.80	64.18	117.81	149.22	126.95	Nrn1	neuritin 1	3.90E-09	2.36
114249	3.51	1.83	3.51	6.19	8.47	6.40	Npnt	nephronectin isoform a,nephronectin isoform a,	1.73E-05	2.36

16512	14.05	15.85	14.56	47.09	30.09	28.35	Kcnh3	potassium voltage-gated channel, subfamily H,potassium voltage-gated channel, subfamily H,	4.96E-11	2.36
277432	7.87	16.65	8.86	33.52	20.88	24.69	Vstm2l	V-set and transmembrane domain containing	4.50E-09	2.35
64385	0.98	0.55	0.83	1.21	1.74	2.62	Cyp4f14	cytochrome P450, family 4, subfamily f,,cytochrome P450, family 4, subfamily f,,cytochrome P450, family 4, subfamily f,,	0.055951136	2.35
171180	6.10	4.48	6.05	13.12	16.01	10.35	Syt12	synaptotagmin XII	4.92E-07	2.35
237928	0.76	0.95	1.05	2.10	2.68	1.76	Phospho1	phosphatase, orphan 1	0.013648647	2.35
13446	4.56	6.67	5.20	16.60	11.43	10.83	Doc2a	double C2, alpha	3.17E-08	2.35
29857	1.70	1.00	1.04	2.68	3.34	2.75	Mapk12	mitogen-activated protein kinase 12,mitogen-activated protein kinase 12,	0.029267444	2.34
16499	11.03	6.98	10.17	21.55	25.62	18.91	Kcnab3	potassium voltage-gated channel, shaker-related,potassium voltage-gated channel, shaker-related,potassium voltage-gated channel, shaker-related,	5.60E-07	2.34
15558	1.65	2.59	1.36	5.06	4.93	3.23	Htr2a	5-hydroxytryptamine (serotonin) receptor 2 A	0.000105166	2.33
72324	1.26	1.20	1.26	3.66	2.85	2.24	Plxdc1	plexin domain containing 1	0.001346187	2.33
51800	4.69	5.42	5.84	13.50	13.13	10.79	Bok	Bcl-2-related ovarian killer protein	1.51E-05	2.33
13656	2.25	6.09	1.12	10.96	5.95	5.31	Egr4	early growth response 4	3.53E-06	2.33
210741	0.65	2.00	0.92	3.77	2.57	2.00	Kcnk12	potassium channel, subfamily K, member 12	0.001439983	2.32
233271	10.45	15.93	13.29	23.81	38.73	29.86	Luzp2	leucine zipper protein 2,leucine zipper protein 2,	4.32E-08	2.31
432763	4.54	9.61	2.00	14.22	10.44	12.73	Prr7	proline rich 7 (synaptic)	6.55E-05	2.30
27528	16.97	12.24	14.68	30.24	42.18	29.38	D0H4S114	neuronal protein 3.1	1.88E-06	2.29
19201	2.15	1.97	2.13	3.66	5.26	5.40	Pstpip2	proline-serine-threonine phosphatase-interacting	0.003560871	2.29
68385	4.54	3.67	4.64	8.45	9.76	11.43	Tlcd1	TLC domain containing 1,TLC domain containing 1,	0.0006968	2.29
11766	0.53	0.95	0.64	1.45	1.38	2.01	Ap1g2	adaptor protein complex AP-1, gamma 2 subunit,adaptor protein complex AP-1, gamma 2 subunit,	0.032472549	2.28
20893	13.11	13.65	15.25	34.72	38.63	23.00	Bhlhb2	basic helix-loop-helix domain containing, class	2.39E-08	2.27
76900	11.72	22.44	14.30	46.33	32.51	30.29	Ssbp4	single stranded DNA binding protein 4	4.64E-08	2.27
13371	9.25	6.75	9.63	16.79	24.22	17.59	Dio2	deiodinase, iodothyronine, type II	6.29E-07	2.26
106648	1.67	1.96	1.27	2.43	3.37	5.28	Cyp4f15	cytochrome P450, family 4, subfamily f,,cytochrome P450, family 4, subfamily f,,	0.015167895	2.26
12424	155.82	126.29	118.56	339.01	291.88	278.18	Cck	cholecystokinin	3.28E-08	2.26
269295	3.85	7.45	3.97	15.76	10.35	8.62	Rtn4rl2	reticulon 4 receptor-like 2	2.34E-05	2.25
330695	56.44	95.15	50.01	212.78	124.36	121.31	Cbxn1	cortexin 1	3.11E-10	2.25
214253	0.64	0.76	0.77	1.62	1.75	1.54	Etnk2	ethanolamine kinase 2	0.032891721	2.25
78088	2.63	1.98	2.46	6.34	5.84	3.90	Ankrd56	ankyrin repeat domain 56	2.39E-05	2.24
20351	5.53	7.35	6.09	17.65	14.00	10.95	Sema4a	sema domain, immunoglobulin domain (Ig),,sema domain, immunoglobulin domain (Ig),,	1.89E-07	2.23
211232	7.44	4.59	5.89	14.58	13.87	11.46	Cpne9	copine-like protein	2.30E-05	2.23
57914	1.83	1.59	2.00	4.62	3.89	3.59	Tpte2	transmembrane phosphoinositide 3-phosphatase and,transmembrane phosphoinositide 3-phosphatase and,transmembrane phosphoinositide 3-phosphatase and,	0.018245912	2.23
109648	55.44	35.45	53.05	97.44	81.07	142.21	Npy	neuropeptide Y	2.20E-06	2.23
12123	3.53	5.04	4.08	10.21	8.10	10.10	Hrk	harakiri	1.24E-07	2.22
231293	0.72	0.65	0.51	1.08	1.52	1.58	C130090K23Rik	hypothetical protein LOC231293	0.098929585	2.22
68337	19.03	20.13	19.59	52.84	39.48	38.61	Crip2	LIM only protein HLP	8.44E-08	2.22
22317	12.65	12.92	18.78	37.61	37.34	23.24	Vamp1	vesicle-associated membrane protein 1 isoform b	0.000273326	2.21
225870	6.06	8.49	5.19	14.90	14.73	14.17	Rin1	Ras and Rab interactor 1	1.32E-06	2.20
229599	2.55	1.95	1.70	3.72	4.88	5.05	Gm129	hypothetical protein LOC229599,hypothetical protein LOC229599,	0.032962219	2.19
68895	0.63	1.08	0.85	2.10	1.11	2.41	Rasl11a	RAS-like family 11 member A,RAS-like family 11 member A,	0.087488056	2.18
230872	3.68	4.67	5.56	10.89	9.53	10.00	Crocc	ciliary rootlet coiled-coil, rootletin,ciliary rootlet coiled-coil, rootletin,ciliary rootlet coiled-coil, rootletin,	1.17E-07	2.18
666048	0.99	0.39	0.51	1.29	1.44	1.44	MUSG0000000	hypothetical protein LOC666048	0.013337651	2.17

57266	21.15	18.66	20.44	40.19	39.86	52.12	Cxcl14	kidney-expressed chemokine CXC	2.58E-06	2.17
64011	324.54	300.65	409.58	696.11	906.98	662.75	Nrgn	neurogranin	1.22E-06	2.17
22174	22.12	22.66	21.75	59.83	47.75	37.38	Tyro3	TYRO3 protein tyrosine kinase 3,TYRO3 protein tyrosine kinase 3,	2.30E-08	2.17
66477	5.81	13.43	7.80	11.27	20.10	26.58	Usmg5	upregulated during skeletal muscle growth 5	0.051250001	2.16
12862	0.95	1.56	2.63	2.86	2.73	5.55	Cox6a2	cytochrome c oxidase, subunit VI a, polypeptide	0.079144445	2.15
50500	0.33	0.59	0.58	0.72	1.42	1.13	Ttpa	tocopherol (alpha) transfer protein,tocopherol (alpha) transfer protein,	0.074969096	2.15
19894	61.46	49.42	59.44	126.26	127.24	114.11	Rph3a	rabphilin 3A,rabphilin 3A,	4.54E-07	2.15
50722	7.15	5.33	8.09	19.30	10.61	14.51	Dkkl1	dickkopf-like 1	0.00032919	2.15
244216	5.94	10.36	2.70	14.47	12.35	14.25	Zfp771	zinc finger protein 771	0.000691545	2.14
240514	4.37	7.44	2.66	13.12	9.48	8.70	n/a	n/a	2.62E-06	2.14
17181	2.81	3.29	2.91	6.44	5.49	7.41	Matn2	matrilin 2,matrilin 2,matrilin 2,	0.000157643	2.14
381633	7.50	13.72	1.00	23.81	10.57	12.71	Gm1673	hypothetical protein LOC381633,hypothetical protein LOC381633,hypothetical protein LOC381633,	0.015646634	2.14
16848	2.62	4.07	1.77	4.47	7.64	6.03	Lfng	lunatic fringe gene homolog,lunatic fringe gene homolog,	0.005269869	2.14
16157	2.14	1.92	1.79	5.11	4.34	3.04	Il11ra1	interleukin 11 receptor, alpha chain 1,interleukin 11 receptor, alpha chain 1,interleukin 11 receptor, alpha chain 1,interleukin 11 receptor, alpha chain 1,	0.015349733	2.13
70435	18.66	15.55	19.39	40.88	42.28	31.76	2610204M08Rik	formin, inverted,formin, inverted,	6.02E-07	2.13
215303	5.63	5.15	6.56	13.69	12.66	10.78	Camk1g	calcium/calmodulin-dependent protein kinase I	2.87E-05	2.13
213391	0.64	0.66	0.39	1.36	1.44	0.83	Rassf4	Ras association (RalGDS/AF-6) domain family 4,Ras association (RalGDS/AF-6) domain family 4,	0.011967526	2.12
13875	4.22	4.33	5.51	10.07	10.96	9.16	Erf	Ets2 repressor factor	1.50E-05	2.12
12950	1.71	2.04	2.14	3.44	5.10	4.12	Hapln1	hyaluronan and proteoglycan link protein 1	0.000327479	2.12
210029	1.02	1.00	1.12	2.46	1.82	2.47	Metrnl	meteorin, glial cell differentiation	0.012954749	2.12
232440	6.20	5.28	5.50	11.45	13.28	11.70	H2afj	H2A histone family, member J	0.00039502	2.12
12426	9.40	9.75	9.72	26.97	20.81	13.97	Cckbr	cholecystokinin B receptor	8.43E-07	2.12
235402	30.50	37.71	39.54	98.57	70.73	60.73	Lingo1	leucine rich repeat and Ig domain containing 1,leucine rich repeat and Ig domain containing 1,	1.40E-08	2.11
18301	3.48	3.02	3.74	8.09	6.31	7.12	Fxyd5	FXYD domain-containing ion transport regulator,FXYD domain-containing ion transport regulator,FXYD domain-containing ion transport regulator,	0.041039097	2.11
66733	1.04	0.60	0.71	1.44	2.34	1.23	Kcng4	potassium voltage-gated channel, subfamily G,	0.044957353	2.10
268481	5.65	6.48	6.57	11.55	15.59	12.41	Krt222	RIKEN cDNA 6330509G02,RIKEN cDNA 6330509G02,	9.50E-05	2.10
239096	0.75	0.99	0.74	2.31	1.28	1.64	Cdh24	cadherin-like 24	0.018931618	2.10
17748	30.00	65.80	48.18	116.28	74.14	112.35	Mt1	metallothionein 1,metallothionein 1,	2.65E-07	2.09
21827	1.19	1.50	1.22	2.70	2.08	3.40	Thbs3	thrombospondin 3	0.009814657	2.09
21835	6.75	3.21	5.81	8.24	11.00	14.04	Thrsp	thyroid hormone-responsive protein	0.009950818	2.08
79362	2.83	4.61	3.27	8.42	6.90	7.15	Bhlhb3	basic helix-loop-helix domain containing, class	0.001992241	2.08
233335	2.07	3.07	1.84	4.08	5.05	5.53	Dmn	desmuslin isoform M,desmuslin isoform M,	0.040011177	2.08
104418	58.10	56.44	63.62	156.06	104.63	109.02	Dgkz	diacylglycerol kinase zeta,diacylglycerol kinase zeta,diacylglycerol kinase zeta,	6.12E-08	2.08
223626	10.70	8.63	9.89	24.53	19.06	17.91	4930572J05Rik	mesenchymal stem cell protein DSCD75 homolog	4.90E-05	2.08
56213	16.08	12.03	14.24	23.20	29.42	36.02	Htra1	HtrA serine peptidase 1,HtrA serine peptidase 1,	0.000160151	2.08
74762	1.79	1.35	1.58	3.42	3.22	3.23	Mdga1	MAM domain containing	0.000329813	2.07
242721	1.63	1.52	1.57	3.08	2.96	3.83	Klhdc7a	kelch domain containing 7A	0.00062552	2.07
16517	3.39	4.51	4.02	6.12	8.23	10.54	Kcnj16	potassium inwardly-rectifying channel J16,potassium inwardly-rectifying channel J16,	0.00026972	2.06
271305	1.45	1.45	1.44	3.59	2.94	2.51	Phf21b	PHD finger protein 21B,PHD finger protein 21B,PHD finger protein 21B,	0.002407936	2.06
210622	2.24	2.24	3.16	6.21	5.25	4.41	E430002G05Rik	regeneration associated muscle protease,regeneration associated muscle protease,	0.000452943	2.06
12531	3.07	2.40	2.34	5.79	5.56	4.82	Cdc25b	cell division cycle 25 homolog B,cell division cycle 25 homolog B,	0.002968928	2.06

241638	27.96	28.52	30.76	58.04	64.13	59.63	Prosapip1	ProSAPiP1 protein	3.99E-06	2.06
15205	1.31	3.67	2.07	3.67	5.09	5.84	Hes1	hairy and enhancer of split 1	0.015349733	2.06
12156	0.45	0.59	0.54	1.20	1.06	1.05	Bmp2	bone morphogenetic protein 2	0.083079526	2.06
18121	1.33	1.59	1.30	3.27	2.96	2.54	Nog	noggin	0.019155893	2.06
170716	1.51	1.39	1.20	2.77	3.00	2.63	Cyp4f13	cytochrome P450, family 4, subfamily f,	0.085744681	2.06
217166	16.18	17.43	13.53	37.59	29.80	30.36	Nr1d1	nuclear receptor subfamily 1, group D, member 1	7.21E-06	2.06
98363	3.91	3.19	3.97	6.78	5.97	10.25	Efhd1	EF hand domain containing 1	0.002424986	2.06
268934	1.91	3.37	2.47	7.82	4.22	4.01	Grm4	glutamate receptor, metabotropic 4	7.38E-05	2.06
100163	1.74	1.22	0.93	3.33	2.41	2.31	Pafah2	platelet-activating factor acetylhydrolase 2,platelet-activating factor acetylhydrolase 2,platelet-activating factor acetylhydrolase 2,	0.014148914	2.06
232146	1.35	2.62	1.07	3.75	2.98	3.70	Tmem166	hypothetical protein LOC232146	0.017914065	2.05
22229	0.95	0.60	0.73	1.37	0.92	2.44	Ucp3	uncoupling protein 3 (mitochondrial, proton	0.093305179	2.05
109904	0.69	0.86	0.92	1.61	1.80	1.63	Mcf2	mcf.2 transforming,mcf.2 transforming,	0.033950792	2.04
22360	98.40	94.71	95.25	176.33	209.06	208.10	Nrsn1	neurensin 1	2.58E-05	2.04
12193	1.53	1.99	1.73	3.42	2.99	4.41	Zfp36l2	zinc finger protein 36, C3H type-like 2	0.001964674	2.03
226777	16.71	9.99	12.30	24.57	35.90	19.69	C130074G19Rik	hypothetical protein LOC226777	0.000404798	2.03
226412	34.48	42.09	36.54	75.00	90.72	64.15	R3hdm1	R3H domain (binds single-stranded nucleic,R3H domain (binds single-stranded nucleic,R3H domain (binds single-stranded nucleic,	1.20E-05	2.03
19018	4.28	13.06	0.80	16.20	6.26	14.47	Scand1	paroxisome proliferative activated receptor,	0.003842042	2.02
17153	20.14	18.20	25.87	44.35	38.68	48.27	Mal	myelin and lymphocyte protein, T-cell	3.17E-06	2.02
18386	2.10	2.72	2.35	5.70	5.54	3.40	Oprd1	opioid receptor, delta 1	0.000366011	2.02
241303	0.92	0.70	0.69	1.95	1.52	1.23	A130092J06Rik	hypothetical protein LOC241303,hypothetical protein LOC241303,	0.020585842	2.01
12671	6.27	6.22	6.18	14.80	14.76	8.26	Chrm3	cholinergic receptor, muscarinic 3, cardiac	9.85E-05	2.01
12496	1.28	1.67	1.25	2.91	2.51	3.04	Entpd2	ectonucleoside triphosphate diphosphohydrolase	0.041917051	2.01
15370	8.95	14.00	11.54	26.38	22.02	21.26	Nr4a1	nuclear receptor subfamily 4, group A, member 1	9.80E-06	2.00
11553	1.45	3.79	1.77	5.24	4.40	4.56	Adra2c	adrenergic receptor, alpha 2c	0.000624396	2.00
213649	1.85	2.00	2.42	4.29	3.73	4.62	Arhgef19	Rho guanine nucleotide exchange factor (GEF) 19	0.002095076	2.00
12322	261.59	276.30	268.14	521.04	570.88	536.99	Camk2a	calcium/calmodulin-dependent protein kinase II	0.000235846	2.00
15939	9.34	10.67	9.17	23.58	23.74	11.67	Ier5	immediate early response 5	2.97E-05	2.00
237761	6.69	13.56	6.51	16.64	14.00	23.34	Ankrd43	ankyrin repeat domain 43	4.04E-05	2.00
22070	0.69	3.18	1.98	5.92	3.68	2.12	Tpt1	tumor protein, translationally-controlled 1	0.045712738	2.00
78514	4.09	3.61	4.17	8.33	9.48	5.74	Arhgap10	Rho GTPase activating protein 10,Rho GTPase activating protein 10,	0.00152286	1.99
12351	6.03	4.74	6.04	9.61	10.68	13.23	Car4	carbonic anhydrase 4	0.007892676	1.99
67916	34.77	30.92	33.52	59.70	59.59	80.23	Ppap2b	phosphatidic acid phosphatase type 2B	4.61E-05	1.99
232334	4.11	4.61	3.93	8.05	6.88	10.40	Vgll4	vestigial like 4,vestigial like 4,vestigial like 4,	0.008722144	1.99
64074	1.83	2.59	2.34	4.47	2.90	6.07	Smoc2	SPARC related modular calcium binding 2,SPARC related modular calcium binding 2,	0.00284842	1.98
12654	1.84	1.27	1.81	3.40	2.28	4.10	Chi3l1	chitinase 3-like 1	0.05111586	1.98
12490	12.49	8.24	12.54	23.76	26.90	15.20	Cd34	CD34 antigen,CD34 antigen,	0.001565039	1.98
14645	315.40	177.35	274.15	408.58	549.44	571.54	Glul	glutamine synthetase	0.000877592	1.97
237397	1.36	1.22	0.99	2.82	2.44	1.90	4932409I22Rik	hypothetical protein LOC237397,hypothetical protein LOC237397,	0.002486651	1.97
16956	2.02	5.14	3.83	5.28	9.93	6.60	Lpl	lipoprotein lipase,lipoprotein lipase,	0.000624396	1.97
70472	1.26	1.25	1.06	1.89	3.20	1.98	Atad2	ATPase family, AAA domain containing 2	0.020317566	1.97
15937	1.72	2.49	1.42	4.81	3.14	3.22	Ier3	immediate early response 3	0.052711302	1.96
225724	8.72	7.52	6.98	16.67	17.17	12.27	Mapk4	mitogen-activated protein kinase 4	0.000206383	1.96
26559	3.09	2.32	2.10	4.43	4.88	5.55	Hunk	hormonally upregulated Neu-associated kinase	0.003819964	1.96
13609	20.63	19.52	20.09	36.10	39.17	44.10	Edg1	endothelial differentiation sphingolipid	0.00012919	1.96
76969	5.49	4.53	3.77	8.75	11.21	7.29	Chst1	carbohydrate (keratan sulfate Gal-6),carbohydrate (keratan sulfate Gal-6),	0.003933029	1.95
210719	4.29	2.99	4.14	5.89	10.81	5.82	Mkx	mohawk	0.005937098	1.95

235320	5.31	7.16	5.36	11.56	13.92	9.61	Zbtb16	zinc finger and BTB domain containing 16,zinc finger and BTB domain containing 16,zinc finger and BTB domain containing 16,	0.000233467	1.95
21847	6.09	5.73	5.46	11.07	14.69	8.30	Klf10	Kruppel-like factor 10	0.001234638	1.95
26556	38.60	41.35	36.06	78.69	80.89	66.09	Homer1	homer homolog 1 isoform S	0.001452056	1.95
18682	3.00	3.28	4.12	5.96	5.24	9.22	Phkg1	phosphorylase kinase gamma 1	0.002746257	1.95
216795	2.60	1.88	2.50	4.84	5.42	3.47	Wnt9a	wingless-type MMTV integration site 9A	0.004886347	1.95
71803	15.61	13.56	17.10	30.62	24.13	35.51	Slc25a18	solute carrier family 25 (mitochondrial	0.000313895	1.95
54713	2.69	2.14	2.29	4.61	4.58	4.78	Fezf2	Fez family zinc finger 2,Fez family zinc finger 2,	0.015102273	1.94
67445	21.82	43.45	20.86	73.81	41.99	53.27	C1qtnf4	C1q and tumor necrosis factor related protein 4	6.41E-06	1.94
216835	0.46	0.45	0.82	1.36	0.89	1.15	Usp43	ubiquitin specific protease 43,ubiquitin specific protease 43,	0.022517021	1.94
17304	40.62	28.96	44.11	72.48	58.92	91.11	Mfge8	milk fat globule-EGF factor 8 protein isoform 1	4.78E-05	1.94
76051	0.90	1.41	1.14	2.30	2.11	2.36	Ganc	glucosidase, alpha; neutral C,glucosidase, alpha; neutral C,	0.008463788	1.94
56149	10.97	10.65	8.11	21.99	18.54	17.59	Grasp	GRP1 (general receptor for phosphoinositides	0.000553434	1.94
19094	14.72	11.89	14.06	29.19	28.71	21.39	Mapk11	mitogen-activated protein kinase 11	0.000216493	1.94
104079	5.23	3.82	7.02	12.19	10.24	9.08	Nxph3	neurexophilin 3	0.000453539	1.94
13864	3.25	5.32	3.19	9.67	5.24	8.05	Nr2f6	nuclear receptor subfamily 2, group F, member 6	0.000770356	1.93
235584	6.45	8.74	7.41	18.10	13.58	12.48	Dusp7	dual specificity phosphatase 7	4.72E-05	1.93
109042	4.13	7.31	4.30	13.90	6.53	10.29	Prkcdbp	protein kinase C, delta binding protein	0.002547542	1.93
23936	57.99	43.77	54.30	103.44	104.04	97.85	Lynx1	Ly6/neurotoxin 1	0.00012053	1.93
16782	1.62	1.76	1.35	4.16	2.44	2.59	Lamc2	laminin, gamma 2	0.001903547	1.93
70083	7.29	8.29	8.75	18.99	13.20	15.13	Metrn	meteorin	0.000529341	1.93
52829	2.73	2.82	2.78	3.98	6.20	6.03	D4Bwg0951e	hypothetical protein LOC52829	0.034347933	1.93
20650	1.31	1.67	0.95	2.57	3.14	1.94	Sntb2	syntrophin, basic 2	0.0174418	1.93
544963	4.64	4.01	3.93	6.59	8.18	9.48	Iqgap2	IQ motif containing GTPase activating protein 2,IQ motif containing GTPase activating protein 2,	0.001949549	1.93
52897	31.01	38.09	36.35	66.71	73.99	61.42	D11Bwg0517e	DNA segment, Chr 11, Brigham & Women's Genetics,DNA segment, Chr 11, Brigham & Women's Genetics,DNA segment, Chr 11, Brigham & Women's Genetics,	0.000151837	1.92
243914	5.69	3.85	5.25	9.40	6.96	12.41	Lgi4	leucine-rich repeat LGI family, member 4	0.000911846	1.92
108069	10.40	9.56	11.08	21.30	19.22	19.84	Grm3	glutamate receptor, metabotropic 3	0.000134064	1.92
17171	2.43	2.85	1.76	4.60	4.34	4.69	Mas1	MAS1 oncogene,MAS1 oncogene,MAS1 oncogene,	0.018781556	1.92
217082	17.49	18.01	19.47	30.92	44.49	31.38	Hlf	hepatic leukemia factor,hepatic leukemia factor,hepatic leukemia factor,hepatic leukemia factor,	0.000240781	1.92
224090	9.98	8.14	10.52	17.34	19.27	18.82	Tmem44	transmembrane protein 44,transmembrane protein 44,	0.000328594	1.92
12606	0.87	1.18	0.92	2.00	2.01	1.72	Cebpa	CCAAT/enhancer binding protein alpha	0.056474714	1.91
232855	1.72	1.15	1.52	3.53	2.42	2.55	BC023179	hypothetical protein LOC232855	0.018998032	1.91
56349	2.74	4.67	2.22	5.48	8.06	5.00	Net1	neuroepithelial cell transforming gene 1 isoform	0.008053664	1.91
242667	27.88	38.98	40.64	72.45	65.74	69.09	Dlgap3	disks large-associated protein 3,disks large-associated protein 3,	1.10E-05	1.91
12192	2.23	2.28	2.36	3.39	4.48	5.41	Zfp36l1	zinc finger protein 36, C3H type-like 1	0.013329354	1.91
16476	6.30	8.37	7.20	13.35	9.06	19.89	Jun	Jun oncogene	0.000220061	1.91
67603	2.26	3.82	3.76	8.20	5.88	4.87	Dusp6	dual specificity phosphatase 6	0.00035989	1.91
73340	85.66	92.85	89.74	191.36	156.58	169.10	Nptxr	neuronal pentraxin receptor	8.99E-05	1.90
217517	8.94	10.64	8.93	19.07	20.37	15.42	Stxbp6	syntaxin binding protein 6 (amisyn)	0.000240781	1.90
67122	3.98	5.04	3.36	5.82	7.03	11.02	Nrarp	Notch-regulated ankyrin repeat protein	0.006892972	1.90
20361	21.91	18.15	23.28	44.12	49.89	27.31	Sema7a	semaphorin 7A	0.000152126	1.90
15483	4.50	2.76	5.19	5.87	6.96	11.02	Hsd11b1	hydroxysteroid 11-beta dehydrogenase 1	0.038471738	1.90
76376	22.99	31.95	26.96	57.20	62.53	37.26	Slc24a2	solute carrier family 24,solute carrier family 24,solute carrier family 24,solute carrier family 24,	8.02E-05	1.90
27984	44.39	30.12	48.29	83.49	93.19	58.81	Efhd2	EF hand domain containing 2	0.00015024	1.90
22417	2.95	2.61	4.65	7.72	6.10	5.66	Wnt4	wingless-related MMTV integration site 4	0.018620322	1.90
243312	4.09	3.00	3.71	7.62	5.46	7.66	A930017N06Rik	hypothetical protein LOC243312	0.001276798	1.89
64136	4.74	4.37	2.83	10.47	7.02	5.27	Sdf2l1	stromal cell-derived factor 2-like 1	0.022517021	1.89

76539	3.35	3.61	2.84	4.52	8.09	5.98	D19Ertd737e	hypothetical protein LOC76539	0.041717048	1.89
237831	2.39	1.88	1.75	3.46	3.35	4.63	Slc13a5	solute carrier family 13 (sodium-dependent	0.026987208	1.88
11676	203.35	146.10	175.75	291.00	267.16	436.92	Aldoc	aldolase 3, C isoform,aldolase 3, C isoform,	0.000516696	1.88
53376	12.30	14.87	11.90	23.85	24.39	25.75	Usp2	ubiquitin-specific protease 2 isoform Usp2-69	0.000539432	1.88
14184	12.10	14.43	14.75	23.88	22.39	31.91	Fgfr3	fibroblast growth factor receptor 3,fibroblast growth factor receptor 3,fibroblast growth factor receptor 3,fibroblast growth factor receptor 3,	0.000206383	1.88
109594	1.84	2.23	2.33	5.15	1.83	5.11	Lmo1	LIM domain only 1	0.048565583	1.88
12667	3.94	5.05	5.29	9.93	7.83	9.12	Chrd	chordin,chordin,chordin,	0.000725705	1.88
243529	7.47	12.57	9.88	20.13	12.33	24.23	H1fx	H1 histone family, member X	0.000995518	1.87
192678	7.57	5.94	7.71	11.25	18.06	10.78	Rassf3	Ras association (RalGDS/AF-6) domain family 3	0.003312362	1.87
381677	43.53	62.70	52.35	105.99	120.94	72.27	Vgf	VGF nerve growth factor inducible	0.000121063	1.87
210673	4.18	7.84	4.43	13.03	9.83	8.13	Prrt3	proline-rich transmembrane protein 3,proline-rich transmembrane protein 3,proline-rich transmembrane protein 3,proline-rich transmembrane protein 3,proline-rich transmembrane protein 3,	0.000303276	1.87
504193	98.14	102.64	102.63	208.31	174.79	189.02	Npcd	neuronal pentraxin with chromo domain isoform 2	0.000216493	1.87
17691	1.64	2.58	0.93	3.03	3.15	3.48	Snf1lk	SNF1-like kinase	0.019026195	1.87
171171	8.27	8.53	7.81	16.21	11.23	18.76	Ntng2	netrin G2 isoform b	0.00246101	1.86
26941	11.32	9.34	14.23	16.64	19.13	29.76	Slc9a3r1	solute carrier family 9 (sodium/hydrogen	0.001779808	1.86
320292	8.81	10.55	8.72	17.42	18.33	16.71	Rasgef1b	RasGEF domain family, member 1B isoform 1	0.00119531	1.86
56089	4.17	2.68	4.13	8.72	7.06	4.81	Ramp3	receptor activity modifying protein 3	0.023324559	1.86
19736	79.30	68.77	73.85	117.86	172.20	125.88	Rgs4	regulator of G-protein signaling 4	0.001392808	1.86
12890	224.22	151.05	220.76	288.99	356.87	474.73	Cplx2	complexin 2	0.003842042	1.86
16485	11.59	15.00	12.34	22.91	30.11	19.97	Kcna1	potassium voltage-gated channel subfamily A	0.000479233	1.85
54376	3.20	3.73	4.06	7.38	7.02	6.18	Cacng3	voltage-dependent calcium channel gamma-3	0.014022231	1.85
11878	3.13	3.14	2.28	5.92	4.63	5.43	Arx	aristaless related homeobox gene,aristaless related homeobox gene,	0.011417678	1.85
15936	1.53	1.65	2.76	4.65	3.07	3.38	Ier2	immediate early response 2	0.021037353	1.85
14813	5.55	5.15	5.12	9.65	9.04	10.80	Grin2c	glutamate receptor, ionotropic, NMDA2C (epsilon	0.001536179	1.85
23945	33.97	29.04	34.71	61.83	55.54	64.85	Mgll	monoglyceride lipase,monoglyceride lipase,monoglyceride lipase,	0.000284007	1.84
58200	18.94	18.84	19.20	40.20	24.77	40.73	Ppp1r1a	protein phosphatase 1, regulatory (inhibitor)	0.000539432	1.84
19679	8.20	11.58	9.26	22.65	16.01	15.24	Pitpnm2	phosphatidylinositol transfer protein,,phosphatidylinositol transfer protein,,phosphatidylinositol transfer protein,,	5.59E-05	1.84
20148	3.84	1.87	2.29	4.89	4.01	6.00	Dhrs3	dehydrogenase/reductase (SDR family) member 3,dehydrogenase/reductase (SDR family) member 3,	0.045109835	1.84
74186	1.76	1.97	1.30	3.81	2.96	2.60	Ccdc3	coiled-coil domain containing 3	0.030320262	1.84
225049	0.95	1.20	0.99	2.38	1.61	1.83	Ttc7	tetratricopeptide repeat domain 7,tetratricopeptide repeat domain 7,	0.020317566	1.84
14219	3.27	3.78	3.93	9.49	6.28	4.61	Ctgf	connective tissue growth factor	0.001779808	1.84
14066	9.38	10.58	10.41	14.01	16.45	25.79	F3	coagulation factor III	0.003941278	1.84
233071	16.62	24.58	18.17	46.30	28.09	35.21	Snx26	sorting nexin 26,sorting nexin 26,sorting nexin 26,	3.77E-05	1.84
20350	0.36	1.08	0.92	2.15	1.04	1.16	Sema3f	sema domain, immunoglobulin domain (Ig), short,sema domain, immunoglobulin domain (Ig), short,sema domain, immunoglobulin domain (Ig), short,	0.022773808	1.84
14415	45.37	57.61	35.17	88.80	83.82	81.26	Gad1	glutamic acid decarboxylase 1,glutamic acid decarboxylase 1,glutamic acid decarboxylase 1,	0.000518017	1.83
56188	21.57	11.86	22.46	28.53	20.62	50.88	Fxyd1	phospholemman precursor	0.071241904	1.83
320924	1.01	0.39	0.67	1.26	1.13	1.44	Ccbe1	collagen and calcium binding EGF domains 1,collagen and calcium binding EGF domains 1,	0.099792525	1.83
319520	1.59	2.20	1.74	3.83	3.88	2.50	Dusp4	dual specificity phosphatase 4	0.030922945	1.83

269831	2.46	4.01	3.83	5.22	8.45	5.28	Tspan12	tetraspanin 12	0.013567799	1.83
329934	1.41	2.47	1.93	3.51	2.68	4.54	Foxo6	forkhead box O6	0.017768998	1.83
74521	3.05	3.79	2.90	5.27	6.93	5.60	8430415E04Rik	HEAT-like repeat-containing protein,HEAT-like repeat-containing protein,	0.013974644	1.83
17750	23.59	30.95	26.37	54.35	40.84	53.34	Mt2	metallothionein 2	0.001964674	1.83
68458	9.10	7.07	10.52	16.88	12.78	19.30	Ppp1r14a	protein phosphatase 1, regulatory (inhibitor)	0.045015897	1.83
216963	42.16	47.05	52.21	104.48	71.45	83.40	Git1	G protein-coupled receptor kinase-interactor 1	4.72E-05	1.82
18142	2.12	1.50	1.90	4.02	2.62	3.46	Npas1	neuronal PAS domain protein 1	0.06042145	1.82
11554	3.58	6.03	4.71	11.38	8.58	6.41	Adrb1	adrenergic receptor, beta 1	0.000932157	1.82
233552	4.10	4.52	3.45	9.39	5.85	6.86	Gdpd5	glycerophosphodiester phosphodiesterase domain,glycerophosphodiester phosphodiesterase domain,	0.002128112	1.82
14180	3.94	3.45	3.31	6.71	7.14	5.81	Fgf9	fibroblast growth factor 9,fibroblast growth factor 9,	0.037739036	1.82
30878	4.67	4.45	6.53	8.58	11.11	9.09	Apln	apelin	0.003045533	1.82
16504	9.82	11.93	10.75	20.23	19.58	19.88	Kcnc3	potassium voltage gated channel, Shaw-related,potassium voltage gated channel, Shaw-related,	0.000539432	1.82
52838	1.35	1.82	0.99	2.53	2.84	2.26	D2Bwg1335e	hypothetical protein LOC52838	0.078777654	1.82
17132	2.62	3.77	3.14	5.15	8.26	4.08	Maf	avian musculoaponeurotic fibrosarcoma (v-maf),avian musculoaponeurotic fibrosarcoma (v-maf),	0.009822247	1.81
80889	2.48	4.29	2.85	6.69	5.13	5.80	Mesdc1	mesoderm development candidate 1	0.001889032	1.81
77125	0.87	0.65	1.50	1.81	1.32	2.38	Il33	interleukin 33,interleukin 33,	0.078003447	1.81
77627	1.43	2.17	1.33	3.33	2.97	2.67	Efcab3	CAP-binding protein complex interacting protein,CAP-binding protein complex interacting protein,CAP-binding protein complex interacting protein,	0.064453962	1.81
74015	10.35	12.81	12.80	26.80	20.51	17.75	Fcho1	FCH domain only 1	0.000313895	1.81
19418	10.69	13.20	11.32	21.28	23.69	18.75	Rasgrf2	RAS protein-specific guanine	0.001518045	1.81
16011	19.80	9.95	19.69	26.39	27.65	36.81	Igfbp5	insulin-like growth factor binding protein 5	0.00152286	1.81
12443	8.36	5.49	6.06	11.07	11.53	13.86	Ccnd1	cyclin D1	0.006807929	1.81
11484	5.38	3.32	4.39	7.60	6.88	9.39	Aspa	aspartoacylase (aminoacylase) 2,aspartoacylase (aminoacylase) 2,	0.0397987	1.81
12064	4.11	3.85	4.93	7.34	9.88	6.36	Bdnf	brain derived neurotrophic factor isoform 2	0.004989366	1.81
20511	148.47	99.42	145.52	177.95	263.25	271.33	Slc1a2	excitatory amino acid transporter 2 isoform 2	0.00306716	1.81
18628	4.25	6.23	4.44	10.58	9.07	7.44	Per3	period homolog 3,period homolog 3,period homolog 3,period homolog 3,	0.000728697	1.80
63953	1.39	1.18	1.60	2.26	2.67	2.67	Dusp10	dual specificity phosphatase 10	0.079370531	1.80
21916	14.69	10.95	11.40	22.96	21.39	22.80	Tmod1	tropomodulin 1	0.003081515	1.80
381678	1.71	1.55	2.57	3.10	3.44	3.95	Zcwpw1	zinc finger, CW type with PWWP domain 1	0.073212544	1.80
18162	0.91	1.04	1.12	1.89	2.03	1.69	Npr3	natriuretic peptide receptor 3 isoform a	0.016296056	1.80
330790	10.63	16.34	18.20	31.88	32.32	17.62	Hapln4	brain link protein 2	0.000140241	1.79
104099	0.89	0.97	0.98	1.40	1.57	2.16	Itga9	integrin alpha 9,integrin alpha 9,	0.063208766	1.79
277973	3.34	3.95	3.06	7.00	6.96	4.67	Slc9a5	solute carrier family 9 (sodium/hydrogen	0.003931173	1.79
56177	392.08	326.01	367.70	731.58	555.03	657.84	Olfm1	olfactomedin 1 isoform d	0.000518235	1.79
78408	53.42	42.99	55.90	96.22	96.86	81.69	2900046G09Rik	hypothetical protein LOC78408	0.000806314	1.79
73230	1.41	1.35	1.13	2.29	2.45	2.26	Bmper	crossveinless 2	0.078003447	1.79
102614	4.06	4.42	4.31	8.42	7.41	7.30	Rpp25	ribonuclease P 25kDa subunit	0.02423148	1.79
267019	3.81	3.63	5.95	6.54	11.21	6.39	Rps15a	ribosomal protein S15a	0.004076343	1.79
16538	2.61	2.95	3.27	5.40	6.04	4.44	Kcns1	K+ voltage-gated channel, subfamily S, 1	0.014524488	1.78
20682	5.12	4.23	6.87	8.06	9.11	12.13	Sox9	SRY-box containing gene 9	0.003238969	1.78
76282	3.86	3.16	5.18	7.37	6.93	7.49	Gpt1	glutamic pyruvic transaminase 1, soluble	0.02266439	1.78
66949	1.92	1.68	2.87	4.32	3.88	3.46	Trim59	mouse RING finger 1,mouse RING finger 1,	0.013033268	1.78
19293	35.46	14.68	42.47	43.75	66.26	56.01	Pvalb	parvalbumin,parvalbumin,parvalbumin,	0.007349585	1.78
208158	7.48	7.74	8.70	16.20	14.31	12.58	Map6d1	MAP6 domain containing 1	0.001259225	1.78
102595	2.92	1.88	3.54	4.99	5.12	4.86	Plekhq1	PH domain-containing protein homolog,PH domain-containing protein homolog,PH domain-containing protein homolog,	0.013990475	1.77

18951	193.38	139.35	188.39	327.42	267.94	334.31	4-Sep	septin 5	0.001024133	1.77
80708	7.43	5.66	7.74	14.66	12.55	9.87	Pacsin3	protein kinase C and casein kinase substrate in,protein kinase C and casein kinase substrate in,	0.007892676	1.77
63955	1.11	1.65	1.19	2.53	2.18	2.38	Cables1	Cdk5 and Abl enzyme substrate 1,Cdk5 and Abl enzyme substrate 1,	0.052125871	1.77
12921	4.29	4.34	3.48	10.19	6.40	4.98	Crhr1	corticotropin releasing hormone receptor 1	0.007524031	1.77
18751	101.70	94.56	109.86	155.63	217.35	175.18	Prkcb1	protein kinase C, beta 1,protein kinase C, beta 1,	0.006625169	1.77
57816	23.18	17.64	19.24	34.05	33.15	38.69	Tesc	tescalcin,tescalcin,	0.012347526	1.77
13842	0.79	1.09	0.90	1.83	1.44	1.68	Epha8	Eph receptor A8	0.048565583	1.77
74136	26.72	29.01	31.29	56.83	46.23	51.26	Sec14l1	SEC14-like 1,SEC14-like 1,SEC14-like 1,	0.00049996	1.77
76295	11.46	15.18	10.08	19.46	24.51	21.01	Atp11b	ATPase, Class VI, type 11B,ATPase, Class VI, type 11B,ATPase, Class VI, type 11B,	0.003846849	1.77
80891	5.61	3.32	5.11	9.03	7.04	8.97	Msr2	macrophage scavenger receptor 2,macrophage scavenger receptor 2,	0.018931618	1.77
12570	44.05	51.40	45.72	89.79	84.19	78.28	Cdk5r2	cyclin-dependent kinase 5, regulatory subunit 2	0.000806314	1.77
432530	39.96	41.64	42.83	77.95	78.32	65.59	Adcy1	adenylate cyclase 1	0.001619426	1.76
239827	1.31	1.48	1.22	2.94	2.51	1.70	Pigz	SMP3 mannosyltransferase	0.099453781	1.76
11816	465.26	306.54	485.23	584.50	659.38	993.31	Apoe	apolipoprotein E	0.004691765	1.76
18417	21.15	20.91	22.33	46.30	33.85	34.60	Cldn11	claudin 11	0.000779131	1.76
74229	11.45	16.97	13.22	26.92	22.92	24.31	Paqr8	progestin and adipoQ receptor family member,progestin and adipoQ receptor family member,	0.000624396	1.76
69551	1.80	2.05	2.57	3.18	2.56	5.70	2310022B05Rik	hypothetical protein LOC69551	0.019350928	1.76
66873	5.61	5.82	5.15	9.15	9.29	11.06	1200009O22Rik	hypothetical protein LOC66873	0.004998098	1.76
72585	9.71	23.68	11.66	28.56	15.67	35.62	Lypd1	Ly6/Plaur domain containing 1,Ly6/Plaur domain containing 1,	0.000628131	1.76
53412	9.75	7.68	10.94	14.22	17.81	18.38	Ppp1r3c	protein phosphatase 1, regulatory (inhibitor)	0.00698733	1.75
16438	57.59	52.44	56.02	93.86	107.50	90.35	Itpr1	inositol 1,4,5-triphosphate receptor 1,inositol 1,4,5-triphosphate receptor 1,	0.003330253	1.75
73728	51.48	49.74	56.25	105.70	74.01	97.75	Psd	pleckstrin and Sec7 domain containing homolog,pleckstrin and Sec7 domain containing homolog,	0.000463837	1.75
18099	14.69	15.25	14.15	26.27	31.26	20.28	Nlk	nemo like kinase,nemo like kinase,	0.002965258	1.75
15444	212.28	152.71	189.83	234.36	316.86	428.11	Hpca	hippocalcin,hippocalcin,hippocalcin,	0.008895604	1.75
19125	4.48	4.56	5.24	8.47	7.06	9.48	Prodh	proline dehydrogenase	0.014362151	1.74
70747	9.22	10.06	12.04	18.58	17.00	19.61	Tspan2	tetraspan 2	0.001339446	1.74
19734	1.89	1.44	2.29	3.34	3.04	3.51	Rgs16	regulator of G-protein signaling 16	0.067472291	1.74
223843	3.19	2.86	3.62	4.00	4.67	8.33	Dbx2	developing brain homeobox 2	0.051786299	1.74
29867	71.01	36.33	66.83	88.60	118.95	96.35	Cabp1	calcium binding protein 1	0.008274355	1.74
244418	3.45	3.36	3.49	7.45	5.31	5.36	D8Ertd82e	hypothetical protein LOC244418	0.003725563	1.74
56018	19.20	16.67	19.04	40.08	26.95	28.81	Stard10	START domain containing 10,START domain containing 10,	0.002930475	1.74
381353	9.39	14.29	9.23	23.02	16.03	18.71	Gm996	hypothetical protein LOC381353	0.000811367	1.74
217124	154.97	113.14	159.39	197.92	263.50	288.16	Ppp1r9b	protein phosphatase 1, regulatory subunit 9B,protein phosphatase 1, regulatory subunit 9B,	0.009398589	1.74
18626	4.89	8.22	4.96	12.25	9.36	9.88	Per1	period homolog 1,period homolog 1,period homolog 1,	0.002036746	1.74
67078	14.19	22.35	11.10	34.83	18.10	30.49	1700012G19Rik	hypothetical protein LOC67078	0.003384385	1.73
11744	1.46	2.22	1.66	4.50	2.75	2.04	Anxa11	annexin A11	0.043200336	1.73
56473	27.02	22.56	27.79	44.50	36.29	52.87	Fads2	fatty acid desaturase 2,fatty acid desaturase 2,	0.003777731	1.73
72475	31.23	28.35	30.70	44.77	59.86	52.22	Ssbp3	single-stranded DNA-binding protein isoform b	0.005937098	1.73
319832	6.07	8.68	7.23	10.96	14.22	13.23	6332401O19Rik	hypothetical protein LOC319832	0.005150689	1.73
70456	18.87	26.17	13.55	33.16	36.25	31.98	Brp44	brain protein 44	0.020310727	1.73
216961	13.79	12.03	11.23	24.65	18.23	21.13	Coro6	coronin, actin binding protein 6 isoform C,coronin, actin binding protein 6 isoform C,	0.011886757	1.73
330941	16.11	21.00	17.79	28.40	39.90	27.47	AI593442	hypothetical protein LOC330941 isoform 2	0.004083085	1.73
66673	7.51	6.95	8.67	12.68	13.56	13.89	Sorcs3	sortilin-related VPS10 domain containing	0.003926391	1.73
20608	1.69	3.81	1.87	5.98	3.78	3.07	Sstr4	somatostatin receptor 4	0.048729519	1.72
65112	6.94	6.14	6.62	11.83	12.73	9.81	Tmepai	transmembrane prostate androgen-induced protein	0.006588257	1.72
50754	57.00	42.32	50.18	77.37	96.45	84.88	Fbxw7	F-box and WD-40 domain protein 7, archipelago	0.007044471	1.72

14609	52.55	35.12	42.91	55.28	74.71	98.01	Gja1	gap junction membrane channel protein alpha 1,gap junction membrane channel protein alpha 1,gap junction membrane channel protein alpha 1,gap junction membrane channel protein alpha 1,gap junction membrane channel protein alpha 1,gap junction membrane channel protein alpha 1,gap junction membrane channel protein alpha 1,	0.013648647	1.72
233107	2.91	2.19	3.08	5.03	5.03	4.16	Kctd15	potassium channel tetramerisation domain,potassium channel tetramerisation domain,	0.047264337	1.72
58175	8.51	9.87	11.36	14.72	21.94	14.82	Rgs20	regulator of G-protein signaling 20,regulator of G-protein signaling 20,	0.024017843	1.72
108089	4.50	4.81	4.94	7.90	8.90	7.87	Rnf144a	ring finger protein 144	0.008053664	1.72
246228	3.97	2.62	3.69	6.23	6.28	5.34	Vwa1	von Willebrand factor A domain-related protein	0.026412089	1.72
170729	20.59	16.90	25.83	29.69	46.48	33.75	Scrt1	scratch homolog 1, zinc finger protein	0.006184468	1.72
20980	4.62	2.99	4.45	7.39	7.86	5.62	Syt2	synaptotagmin II,synaptotagmin II,	0.020054552	1.71
269615	11.46	11.25	10.59	18.96	20.03	18.03	Plch2	phospholipase C, eta 2	0.008950798	1.71
76267	37.92	28.58	40.48	56.81	59.27	68.72	Fads1	delta-5 desaturase,delta-5 desaturase,	0.003685999	1.71
269275	1.89	2.66	2.29	3.57	5.50	2.75	Acvr1c	activin A receptor, type IC	0.01359299	1.71
20674	7.75	8.02	8.40	10.48	17.04	14.24	Sox2	sex-determining region Y-box 2	0.024235109	1.71
67621	2.79	2.47	3.28	5.38	4.16	5.14	2310026E23Rik	hypothetical protein LOC67621	0.087822558	1.71
11459	2.43	2.53	2.84	5.60	2.87	4.94	Acta1	actin, alpha 1, skeletal muscle	0.075925033	1.71
12724	7.07	6.58	5.07	13.53	8.63	9.81	Clcn2	chloride channel 2	0.006934967	1.71
19739	6.15	10.23	3.81	9.88	9.08	15.47	Rgs9	regulator of G-protein signaling 9,regulator of G-protein signaling 9,regulator of G-protein signaling 9,	0.030414233	1.71
13121	7.60	8.36	8.16	12.39	15.92	13.19	Cyp51	cytochrome P450, family 51	0.009229184	1.71
17388	2.01	2.53	1.76	3.47	3.75	3.62	Mmp15	matrix metallopeptidase 15	0.043667086	1.70
228880	16.42	12.95	16.13	24.40	28.89	24.71	Prkcbp1	protein kinase C binding protein 1,protein kinase C binding protein 1,protein kinase C binding protein 1,protein kinase C binding protein 1,protein kinase C binding protein 1,protein kinase C binding protein 1,	0.006625169	1.70
11539	28.36	26.11	26.52	44.40	49.13	46.07	Adora1	adenosine A1 receptor	0.005516354	1.70
629378	22.45	33.09	19.89	49.89	39.87	39.82	Dact3	dapper homolog 3	0.002036746	1.70
319998	6.39	11.28	9.19	21.68	15.02	9.25	A230078I05Rik	hypothetical protein LOC319998,hypothetical protein LOC319998,	0.001202372	1.70
320158	5.67	6.03	5.71	9.78	11.11	8.93	Zmat4	zinc finger, matrin type 4	0.011714702	1.69
22421	2.62	1.70	2.67	3.36	3.78	4.89	Wnt7a	wingless-related MMTV integration site 7A	0.0726797	1.69
29861	13.45	11.31	11.65	21.18	22.39	18.29	Neud4	neuronal d4 domain family member	0.014022231	1.69
23972	2.12	1.91	2.13	2.66	2.71	5.13	Papss2	3'-phosphoadenosine 5'-phosphosulfate synthase,3'-phosphoadenosine 5'-phosphosulfate synthase,3'-phosphoadenosine 5'-phosphosulfate synthase,	0.082724998	1.69
68431	3.56	5.58	3.21	9.00	6.42	5.58	Fbxl15	F-box and leucine-rich repeat protein 15,F-box and leucine-rich repeat protein 15,	0.048565583	1.69
18011	4.63	9.77	5.54	13.76	8.17	12.01	Neurl	neuralized homolog,neuralized homolog,neuralized homolog,	0.002103487	1.69
18029	9.80	9.48	12.34	18.82	19.40	15.58	Nfic	nuclear factor I/C isoform b	0.003102132	1.68
53896	4.04	5.07	3.48	6.46	6.00	8.78	Slc7a10	solute carrier family 7 (cationic amino acid	0.073176309	1.68
99887	4.62	8.00	6.00	9.62	14.95	6.94	Tmem56	transmembrane protein 56,transmembrane protein 56,transmembrane protein 56,transmembrane protein 56,	0.009586662	1.68
214230	13.04	11.90	10.98	21.72	16.89	22.27	Pak6	p21 (CDKN1A)-activated kinase 6,p21 (CDKN1A)-activated kinase 6,	0.007044471	1.68
56219	8.54	8.00	10.08	17.38	16.94	10.70	Extl1	exostoses (multiple)-like 1	0.004264381	1.68
74205	21.48	18.05	20.70	24.08	37.92	39.54	Acsl3	acyl-CoA synthetase long-chain family member 3	0.022727081	1.68
75219	3.65	3.90	3.96	6.45	6.86	6.21	Dusp18	dual specificity phosphatase 18	0.015704048	1.68
228432	11.40	13.29	8.99	15.96	22.20	17.89	Tmem16c	hypothetical protein LOC228432	0.049885955	1.68
72605	25.24	21.08	26.70	37.24	53.48	32.60	Car10	carbonic anhydrase 10,carbonic anhydrase 10,carbonic anhydrase 10,	0.011870245	1.68
12326	14.30	13.09	16.25	20.81	32.28	20.85	Camk4	calcium/calmodulin-dependent protein kinase IV	0.011154574	1.68

12300	14.46	13.22	14.19	19.49	32.67	18.69	Cacng2	calcium channel, voltage-dependent, gamma	0.025107858	1.67
99326	17.75	18.53	17.14	33.53	30.32	25.16	Gaml3	GTPase activating RANGAP domain-like 3,GTPase activating RANGAP domain-like 3,GTPase activating RANGAP domain-like 3,GTPase activating RANGAP domain-like 3,	0.004989366	1.67
11682	0.64	0.81	0.91	1.54	1.20	1.20	Alk	anaplastic lymphoma kinase	0.073166564	1.67
230904	26.79	13.82	30.17	26.35	41.25	51.34	Fbxo2	F-box protein 2	0.034418304	1.67
75695	13.96	10.21	17.87	24.03	25.05	21.75	2900002H16Rik	hypothetical protein LOC75695	0.007271771	1.67
56461	29.10	23.00	22.40	48.68	39.19	37.66	Kcnip3	calsenilin, presenilin-binding protein, EF hand	0.006891442	1.67
12833	11.92	13.52	8.86	23.78	15.13	18.29	Col6a1	procollagen, type VI, alpha 1	0.005085649	1.67
26878	4.09	5.74	4.64	7.03	9.21	8.12	B3galt2	UDP-Gal:betaGlcNAc beta	0.019066135	1.67
17289	5.83	7.68	6.38	10.00	10.47	12.78	Mertk	c-mer proto-oncogene tyrosine kinase	0.016490464	1.67
241764	2.14	2.99	2.33	4.94	3.50	3.92	L3mbtl	l(3)mbt-like	0.062618921	1.66
15460	4.76	3.46	4.81	7.22	9.06	5.53	Hr	hairless protein	0.023414885	1.66
68525	2.21	2.19	2.49	3.57	3.71	4.19	Evc2	Ellis van Creveld syndrome 2 homolog,Ellis van Creveld syndrome 2 homolog,	0.056211833	1.66
18217	34.11	24.92	29.36	47.34	34.77	66.06	Ntsr2	neurotensin receptor 2	0.011870245	1.66
244745	15.01	14.49	13.54	25.69	25.05	21.06	Dpy19l1	dpy-19-like 1,dpy-19-like 1,dpy-19-like 1,	0.008103109	1.66
13998	1.21	1.75	1.27	2.09	2.18	2.80	Fgd6	FYVE, RhoGEF and PH domain containing 6	0.041039097	1.66
68070	2.59	4.00	2.56	6.05	4.88	4.37	Pdzd2	PDZ domain containing 2	0.004254361	1.66
59090	5.67	8.59	5.63	14.09	11.10	8.01	Midn	midnolin,midnolin,midnolin,midnolin,	0.005658881	1.65
104582	15.72	17.08	16.91	29.82	29.56	23.76	Rprml	reprimo-like	0.016296056	1.65
70615	4.97	5.00	4.10	8.69	6.40	8.26	Ankrd24	ankyrin repeat domain 24,ankyrin repeat domain 24,	0.022748432	1.65
106877	4.90	3.23	4.07	7.39	8.36	4.44	Afap1l1	actin filament associated protein 1-like 1	0.053411056	1.65
68027	22.71	20.91	25.42	43.46	42.08	29.48	Tmem178	hypothetical protein LOC68027	0.006982773	1.65
242662	16.95	15.43	21.07	33.44	29.33	25.64	Rims3	regulating synaptic membrane exocytosis 3,regulating synaptic membrane exocytosis 3,	0.013990475	1.65
16835	2.68	2.66	2.34	4.72	3.99	4.07	Ldlr	low density lipoprotein receptor,low density lipoprotein receptor,low density lipoprotein receptor,low density lipoprotein receptor,	0.038872791	1.65
67712	3.61	5.89	3.48	6.89	8.38	6.33	Slc25a37	solute carrier family 25, member 37	0.027031561	1.65
217692	45.08	42.93	42.44	72.24	78.63	65.72	Sipa1l1	signal-induced proliferation-associated 1 like,signal-induced proliferation-associated 1 like,signal-induced proliferation-associated 1 like,signal-induced proliferation-associated 1 like,	0.009814657	1.65
18143	4.87	6.93	6.43	11.04	8.94	10.21	Npas2	neuronal PAS domain protein 2	0.006588257	1.65
16513	34.60	23.56	27.40	42.72	47.07	53.15	Kcnj10	potassium inwardly-rectifying channel J10	0.020054552	1.65
72309	6.84	15.47	6.30	17.24	17.61	12.67	Tmem158	Ras-induced senescence 1	0.017927343	1.65
19055	263.09	237.36	234.29	320.54	479.90	410.49	Ppp3ca	protein phosphatase 3, catalytic subunit, alpha,protein phosphatase 3, catalytic subunit, alpha,protein phosphatase 3, catalytic subunit, alpha,	0.030599954	1.65
320343	4.14	3.86	4.91	6.59	7.01	7.84	Lypd6	LY6/PLAUR domain containing 6,LY6/PLAUR domain containing 6,	0.028056656	1.64
51791	7.28	8.87	7.50	15.56	9.70	13.68	Rgs14	regulator of G-protein signaling 14,regulator of G-protein signaling 14,	0.011665825	1.64
20401	3.03	3.38	4.40	8.10	4.57	5.02	Sh3bp1	SH3-domain binding protein 1,SH3-domain binding protein 1,SH3-domain binding protein 1,SH3-domain binding protein 1,	0.040216585	1.64
66234	14.50	21.85	15.06	31.14	31.63	22.10	Sc4mol	sterol-C4-methyl oxidase-like	0.010851437	1.64
67516	4.09	3.97	3.69	4.79	5.88	8.84	Kctd4	potassium channel tetramerisation domain	0.081628276	1.64
18636	3.60	3.81	4.26	7.29	6.09	5.83	Cfp	complement factor properdin	0.08679196	1.64
238377	1.66	2.07	1.89	3.66	3.06	2.59	Gpr68	G protein-coupled receptor 68,G protein-coupled receptor 68,	0.072090673	1.64
70729	22.11	16.93	20.72	35.70	40.78	20.45	Nos1ap	C-terminal PDZ domain ligand of neuronal nitric	0.068765191	1.64
18719	3.24	4.32	2.88	5.59	4.62	6.90	Pip5k1b	phosphatidylinositol-4-phosphate 5-kinase, type	0.078714542	1.63
98170	33.24	27.98	44.17	68.65	59.00	46.05	Tmem132a	heat shock 70kDa protein 5 binding protein 1	0.00243023	1.63

277414	14.80	15.84	11.15	29.27	16.45	23.15	Trp53i11	transformation related protein 53 inducible,transformation related protein 53 inducible,transformation related protein 53 inducible,	0.006891442	1.63
83398	3.53	3.16	2.93	6.21	3.41	6.25	Ndst3	N-deacetylase/N-sulfotransferase (heparan,N-deacetylase/N-sulfotransferase (heparan,	0.018277417	1.63
58238	3.09	4.43	4.19	6.36	6.70	6.27	A830059I20Rik	hypothetical protein LOC58238	0.059026999	1.63
73032	40.17	32.47	43.47	79.80	54.12	57.24	Ttc9b	tetratricopeptide repeat domain 9B	0.005329063	1.63
66860	2.80	3.40	2.67	4.00	3.56	7.02	Tanc1	TPR domain, ankyrin-repeat and,TPR domain, ankyrin-repeat and,	0.0293263	1.63
26950	156.45	137.73	185.45	252.13	290.66	247.49	Vsnl1	visinin-like 1	0.010114331	1.63
12856	28.09	31.55	42.17	43.86	66.79	55.63	Cox17	cytochrome c oxidase subunit XVII assembly	0.048729324	1.63
104174	6.11	4.59	5.00	7.17	7.56	10.91	Gldc	glycine decarboxylase,glycine decarboxylase,	0.063312877	1.63
240185	11.44	16.11	11.57	22.81	25.65	15.96	9430020K01Rik	hypothetical protein LOC240185	0.009054726	1.63
11941	77.64	70.41	74.65	124.63	150.93	90.39	Atp2b2	plasma membrane calcium ATPase 2 isoform 1,plasma membrane calcium ATPase 2 isoform 1,	0.017892776	1.63
74182	11.67	19.09	12.51	21.82	26.52	21.78	Prei4	preimplantation protein 4 isoform 3	0.028198554	1.63
12450	11.21	15.22	14.51	19.95	28.64	18.67	Ccng1	cyclin G1	0.015704048	1.63
68939	16.96	15.14	18.29	29.65	28.81	24.42	Rasl11b	RAS-like, family 11, member B	0.014258979	1.63
246104	3.29	3.17	2.24	4.86	4.04	5.40	Rhbdl3	rhomboid, veinlet-like 4	0.078677224	1.63
50781	56.88	40.01	61.42	102.11	90.31	67.82	Dkk3	dickkopf homolog 3,dickkopf homolog 3,	0.005090492	1.63
328232	12.97	13.01	13.00	22.48	21.39	20.34	Gfod1	glucose-fructose oxidoreductase domain	0.009140118	1.63
226641	9.18	8.80	7.96	13.55	16.55	12.46	Atf6	activating transcription factor 6	0.022773808	1.63
20927	3.30	3.67	3.02	6.19	5.05	4.97	Abcc8	ATP-binding cassette, sub-family C (CFTR/MRP),,ATP-binding cassette, sub-family C (CFTR/MRP),,ATP-binding cassette, sub-family C (CFTR/MRP),,	0.030960591	1.62
192976	4.32	4.31	3.13	7.57	7.01	4.67	BC046404	hypothetical protein LOC192976,hypothetical protein LOC192976,	0.090232803	1.62
118452	60.05	51.98	58.95	94.38	84.32	102.46	Baalc	brain and acute leukemia, cytoplasmic isoform	0.009841983	1.62
237403	3.64	5.80	3.91	8.91	7.04	5.96	BC072620	hypothetical protein LOC237403	0.014333742	1.62
217219	8.38	15.56	9.23	25.42	12.89	15.99	BC025575	hypothetical protein LOC217219	0.001993513	1.62
18546	212.52	137.33	225.36	221.25	363.56	353.92	Pcp4	Purkinje cell protein 4	0.034530316	1.62
319555	4.55	4.38	4.31	7.73	6.98	6.91	Nwd1	NACHT and WD repeat domain containing 1,NACHT and WD repeat domain containing 1,	0.032546376	1.62
14348	4.85	9.55	6.02	11.06	15.49	6.85	Fut9	fucosyltransferase 9	0.010713755	1.62
231070	9.12	8.41	6.87	11.06	15.16	13.70	Insig1	insulin induced gene 1	0.07642712	1.62
20378	4.26	4.45	3.84	6.98	7.90	5.62	Frzb	frizzled-related protein	0.06327488	1.62
170676	1.84	2.36	1.92	3.01	3.30	3.72	Peg10	paternally expressed 10 isoform RF1/RF2	0.047347188	1.62
76982	99.80	72.91	115.69	134.60	192.06	144.83	3110035E14Rik	hypothetical protein LOC76982	0.021737995	1.62
12709	125.93	122.22	133.88	278.18	163.94	178.93	Ckb	creatine kinase, brain	0.00185222	1.62
80906	32.90	29.87	29.86	42.30	52.97	51.89	Kcnip2	Kv channel-interacting protein 2 isoform a	0.078714542	1.62
105859	21.15	21.97	18.54	37.76	29.87	32.92	Csdc2	RNA-binding protein pippin	0.012019507	1.61
20614	731.65	576.67	722.42	975.78	1374.25	946.61	Snap25	synaptosomal-associated protein 25	0.057273043	1.61
245049	10.27	10.73	12.52	16.89	21.27	16.23	Myrip	myosin VIIA and Rab interacting protein	0.0174418	1.61
106931	27.05	19.16	24.69	38.14	41.67	35.50	Kctd1	potassium channel tetramerisation domain,potassium channel tetramerisation domain,potassium channel tetramerisation domain,	0.029309261	1.61
216049	93.66	97.42	103.78	146.24	179.04	154.46	Zfp365	zinc finger protein 365,zinc finger protein 365,	0.019839524	1.61
16527	4.76	4.81	3.97	8.86	7.34	5.84	Kcnk3	potassium channel, subfamily K, member 3	0.027031561	1.61
68203	45.19	38.24	42.04	67.10	73.59	63.66	Diras2	DIRAS family, GTP-binding RAS-like 2	0.018616437	1.61
69908	6.05	6.96	8.60	12.68	8.46	13.99	Rab3b	RAB3B, member RAS oncogene family,RAB3B, member RAS oncogene family,	0.008103109	1.61
76886	47.12	41.68	43.14	71.37	78.31	64.15	6430514L14Rik	hypothetical protein LOC76886	0.018200413	1.61
18810	5.76	6.36	5.85	10.71	10.23	8.22	Plec1	plectin 1 isoform 4	0.009841983	1.61
18125	2.99	3.83	3.18	4.70	3.90	7.53	Nos1	nitric oxide synthase 1, neuronal,nitric oxide synthase 1, neuronal,	0.051494816	1.61
22393	11.72	16.47	12.73	26.78	15.06	24.44	Wfs1	Wolfram syndrome 1 protein homolog	0.004454985	1.60
243274	4.10	4.08	4.04	7.44	7.90	4.42	Tmem132d	hypothetical protein LOC243274	0.035626497	1.60

227059	18.21	27.42	18.70	38.36	40.39	25.08	Slc39a10	solute carrier family 39 (zinc transporter),,solute carrier family 39 (zinc transporter),,	0.009887243	1.60
13602	454.34	255.88	459.22	454.79	621.56	811.81	Sparcl1	SPARC-like 1 (mast9, hevin)	0.073176309	1.60
171469	33.79	32.34	31.11	56.07	44.80	56.49	Gpr37l1	G protein-coupled receptor 37-like 1	0.013179586	1.60
12313	467.97	516.60	491.62	720.42	852.15	805.07	Calm1	calmodulin 1	0.06326969	1.59
16524	30.11	22.07	29.98	43.30	51.70	37.44	Kcnj9	potassium inwardly-rectifying channel subfamily,potassium inwardly-rectifying channel subfamily,	0.024255932	1.59
11549	1.29	1.35	1.34	2.75	2.06	1.62	Adra1a	adrenergic receptor, alpha 1a,adrenergic receptor, alpha 1a,adrenergic receptor, alpha 1a,adrenergic receptor, alpha 1a,adrenergic receptor, alpha 1a,	0.091943043	1.59
17131	4.20	3.31	2.95	6.13	5.82	4.89	Smad7	MAD homolog 7,MAD homolog 7,	0.071941819	1.59
17433	176.42	79.48	189.56	178.50	199.67	329.18	Mobp	myelin-associated oligodendrocytic basic protein	0.050188052	1.59
107831	35.66	44.05	37.65	75.33	57.16	54.87	Bai1	brain-specific angiogenesis inhibitor 1,brain-specific angiogenesis inhibitor 1,brain-specific angiogenesis inhibitor 1,brain-specific angiogenesis inhibitor 1,brain-specific angiogenesis inhibitor 1,	0.005658881	1.59
14789	3.90	3.70	3.95	7.02	5.57	5.82	Leprel2	leprecan-like 2	0.063815794	1.59
14260	1.55	1.72	1.46	2.46	3.02	2.10	Fmn1	formin 1 isoform 1	0.059550424	1.59
22065	2.49	3.24	2.45	5.05	4.86	3.18	Trpc3	transient receptor potential cation channel,,transient receptor potential cation channel,,	0.067692885	1.59
71795	9.88	9.13	8.22	13.97	15.54	14.13	Pitpnc1	phosphatidylinositol transfer protein,,phosphatidylinositol transfer protein,,phosphatidylinositol transfer protein,,	0.036697079	1.59
226922	7.85	10.70	8.68	14.82	17.16	11.58	Kcnq5	potassium voltage-gated channel, subfamily Q,	0.018449394	1.58
70430	14.73	17.61	15.19	19.56	24.71	30.63	Tbce	tubulin-specific chaperone e,tubulin-specific chaperone e,	0.062964859	1.58
66725	4.50	6.46	4.52	7.95	9.78	6.83	Lrrk2	leucine-rich repeat kinase 2	0.031841629	1.58
67815	9.93	8.63	10.04	15.04	13.53	16.97	Sec14l2	SEC14-like 2	0.037739036	1.58
14805	2.38	3.03	2.57	4.06	3.74	4.91	Grik1	glutamate receptor, ionotropic, kainate 1,glutamate receptor, ionotropic, kainate 1,glutamate receptor, ionotropic, kainate 1,glutamate receptor, ionotropic, kainate 1,	0.09176987	1.58
68339	3.13	3.87	3.14	5.77	5.04	5.31	Ccdc88c	coiled-coil domain containing 88C	0.032546376	1.58
12716	71.95	59.31	71.02	108.65	100.70	111.66	Ckmt1	creatine kinase, mitochondrial 1, ubiquitous,creatine kinase, mitochondrial 1, ubiquitous,creatine kinase, mitochondrial 1, ubiquitous,	0.018329669	1.58
56405	13.75	14.27	14.60	31.17	20.83	16.05	Dusp14	dual specificity phosphatase 14,dual specificity phosphatase 14,dual specificity phosphatase 14,	0.012705031	1.58
269642	41.06	31.12	41.42	58.72	72.83	50.15	Nat8l	N-acetyltransferase 8-like	0.029779716	1.58
14394	31.58	58.62	38.04	62.96	95.91	44.74	Gabra1	gamma-aminobutyric acid (GABA-A) receptor,	0.022989582	1.58
15213	9.67	11.61	11.53	18.93	19.59	13.69	Hey1	hairy/enhancer-of-split related with YRPW motif	0.025271898	1.58
99010	19.50	21.66	18.69	39.27	31.86	23.25	Agpat7	acyltransferase like 3,acyltransferase like 3,	0.016437542	1.58
13653	53.25	44.79	51.19	89.09	95.43	53.51	Egr1	early growth response 1	0.019214159	1.58
56876	79.25	84.17	89.40	140.96	98.69	160.44	Nelf	nasal embryonic LHRH factor isoform B,nasal embryonic LHRH factor isoform B,	0.009310704	1.57
12354	5.49	5.86	5.16	11.14	7.25	7.69	Car7	carbonic anhydrase 7,carbonic anhydrase 7,carbonic anhydrase 7,	0.073323382	1.57
13803	84.76	93.28	79.10	151.35	144.77	112.58	Enc1	ectodermal-neural cortex 1	0.020390098	1.57
67784	5.15	7.43	5.16	12.87	7.44	7.68	Plxnd1	plexin D1	0.006653366	1.57
16012	11.10	7.36	13.59	20.45	16.21	14.15	Igfbp6	insulin-like growth factor binding protein 6	0.034523596	1.57
13196	20.33	18.60	22.73	32.41	38.10	26.37	Ddef1	development and differentiation enhancing,development and differentiation enhancing,development and differentiation enhancing,development and differentiation enhancing,development and differentiation enhancing,development and differentiation enhancing,	0.022773808	1.57
11922	24.35	19.31	27.52	28.76	45.64	38.53	Neurod6	neurogenic differentiation 6	0.061834199	1.57

84036	2.42	2.06	2.55	4.16	3.10	3.86	Kcnn1	potassium intermediate/small conductance,potassium intermediate/small conductance,potassium intermediate/small conductance,potassium intermediate/small conductance,	0.076322367	1.56
53623	30.62	36.77	28.79	48.70	64.23	38.48	Gria3	glutamate receptor, ionotropic, AMPA3 (alpha,glutamate receptor, ionotropic, AMPA3 (alpha,glutamate receptor, ionotropic, AMPA3 (alpha,glutamate receptor, ionotropic, AMPA3 (alpha,	0.035221977	1.56
15902	31.89	30.34	33.16	48.13	56.16	46.22	Id2	inhibitor of DNA binding 2	0.041039097	1.56
19395	3.26	6.38	3.16	7.51	4.95	7.55	Rasgrp2	RAS, guanyl releasing protein 2,RAS, guanyl releasing protein 2,	0.085856642	1.56
18479	99.97	92.95	107.71	160.14	171.02	141.16	Pak1	p21 (CDKN1A)-activated kinase 1	0.021737995	1.56
77582	11.08	21.16	11.07	31.27	20.20	16.70	Leng4	leukocyte receptor cluster (LRC) member 4	0.006891442	1.56
23948	29.32	30.36	33.39	57.67	45.73	43.16	Mmp17	matrix metallopeptidase 17	0.009493925	1.56
195646	9.78	11.46	8.77	18.89	16.01	12.43	Hs3st2	heparan sulfate D-glucosaminyl	0.032342646	1.56
268445	11.74	13.76	15.25	24.46	18.05	21.44	Ankrd13b	ankyrin repeat domain 13b	0.010914756	1.56
55984	22.97	20.55	23.08	36.72	35.79	31.86	Camkk1	calcium/calmodulin-dependent protein kinase	0.02458778	1.56
380684	17.79	10.33	18.50	21.27	26.19	26.09	Nefh	neurofilament, heavy polypeptide	0.051786299	1.56
20512	89.28	74.00	87.42	102.30	128.71	163.18	Slc1a3	solute carrier family 1 (glial high affinity,solute carrier family 1 (glial high affinity,	0.058228885	1.56
14086	40.70	47.45	45.96	86.98	66.82	57.06	Fscn1	fascin homolog 1, actin bundling protein	0.008053664	1.56
240058	4.72	5.72	4.84	9.74	7.24	6.89	Cpne5	copine V,copine V,	0.027031561	1.55
22239	6.50	7.87	7.84	12.10	11.98	10.75	Ugt8a	UDP galactosyltransferase 8A,UDP galactosyltransferase 8A,UDP galactosyltransferase 8A,UDP galactosyltransferase 8A,	0.031577138	1.55
12349	36.86	27.32	48.97	62.06	51.64	63.26	Car2	carbonic anhydrase 2	0.01415092	1.55
71393	11.51	11.90	10.38	15.57	17.69	19.67	Kctd6	potassium channel tetramerisation domain,potassium channel tetramerisation domain,	0.097127711	1.55
14430	8.42	8.44	7.98	15.43	12.01	11.22	Galt	galactose-1-phosphate uridyl transferase,galactose-1-phosphate uridyl transferase,	0.051494816	1.55
16826	11.47	10.37	11.31	16.26	18.52	17.05	Ldb2	LIM domain binding 2 isoform 1	0.069419372	1.55
232947	24.19	25.02	31.47	47.32	38.45	39.94	BC024868	hypothetical protein LOC232947	0.01122158	1.55
58234	7.72	12.32	10.04	17.68	14.26	14.92	Shank3	SH3/ankyrin domain gene 3	0.010653008	1.55
116837	40.31	29.95	46.67	52.32	60.22	67.96	Rims1	regulating synaptic membrane exocytosis 1	0.03518217	1.54
53972	68.14	68.86	76.19	131.91	107.70	91.20	Ngef	neuronal guanine nucleotide exchange factor	0.011714702	1.54
57776	60.14	69.21	64.86	113.34	88.61	97.22	Ttyh1	tweety 1 isoform 2,tweety 1 isoform 2,tweety 1 isoform 2,	0.014711765	1.54
16332	5.96	4.63	5.26	8.67	7.24	8.61	Inppl1	inositol polyphosphate phosphatase-like 1,inositol polyphosphate phosphatase-like 1,inositol polyphosphate phosphatase-like 1,	0.06327488	1.54
320878	36.20	29.75	36.39	61.64	52.64	44.58	Mical2	flavoprotein oxidoreductase MICAL2,flavoprotein oxidoreductase MICAL2,flavoprotein oxidoreductase MICAL2,flavoprotein oxidoreductase MICAL2,	0.018389526	1.54
234353	34.94	51.34	38.04	59.45	68.84	65.30	Psd3	pleckstrin and Sec7 domain containing 3 isoform,pleckstrin and Sec7 domain containing 3 isoform,	0.036372936	1.54
13007	60.05	42.33	70.12	87.91	79.79	100.56	Csrp1	cysteine and glycine-rich protein 1	0.023730757	1.54
235604	74.74	85.05	82.25	131.83	109.85	133.53	Camkv	CaM kinase-like vesicle-associated	0.018449394	1.54
239556	8.49	8.93	8.65	13.71	17.14	9.47	Cacna1i	calcium channel, voltage-dependent, alpha 1I	0.042171146	1.54
245684	21.71	26.71	21.48	31.46	43.04	33.48	Cnksr2	connector enhancer of kinase suppressor of Ras,connector enhancer of kinase suppressor of Ras,	0.05499744	1.54
19419	45.60	71.56	56.61	101.69	98.49	68.46	Rasgrp1	RAS guanyl releasing protein 1	0.014505046	1.54
243621	21.62	19.40	21.77	32.87	30.04	34.42	Iqsec3	IQ motif and Sec7 domain 3,IQ motif and Sec7 domain 3,	0.029779716	1.53
208618	9.91	9.83	10.44	16.13	17.89	12.63	Etl4	enhancer trap locus 4,enhancer trap locus 4,enhancer trap locus 4,enhancer trap locus 4,enhancer trap locus 4,enhancer trap locus 4,	0.036322745	1.53

22784	26.48	22.30	29.11	43.85	45.26	31.09	Slc30a3	solute carrier family 30 (zinc transporter),	0.033676345	1.53
19291	20.26	25.89	23.75	35.64	36.20	36.46	Purb	purine rich element binding protein B	0.04568311	1.53
327958	10.98	12.99	10.56	22.05	17.17	14.02	Pitpnm3	Pitpnm family member 3 isoform 2	0.018200413	1.53
69017	43.79	46.77	43.74	73.90	79.41	54.05	1500031I19Rik	hypothetical protein LOC69017,hypothetical protein LOC69017,	0.033676345	1.53
105005	8.70	13.89	11.53	19.09	19.41	14.10	AW125753	expressed sequence AW125753	0.025432842	1.53
320027	4.53	4.44	3.41	8.17	6.41	4.38	Fstl4	follistatin-like 4	0.09726193	1.52
241656	9.12	9.35	10.47	13.84	20.59	10.05	Pak7	p21 (CDKN1A)-activated kinase 7,p21 (CDKN1A)-activated kinase 7,p21 (CDKN1A)-activated kinase 7,	0.071726428	1.52
29863	4.88	9.54	5.09	9.64	10.64	9.60	Pde7b	phosphodiesterase 7B	0.062004225	1.52
16874	3.00	3.87	4.27	5.75	5.39	5.94	Lhx6	LIM homeobox protein 6 isoform 4	0.081791943	1.52
246710	14.01	13.32	13.15	21.66	20.71	19.74	Rhobtb2	Rho-related BTB domain containing 2,Rho-related BTB domain containing 2,	0.045015897	1.52
19092	1.90	2.96	2.57	3.86	3.80	3.70	Prkg2	protein kinase, cGMP-dependent, type II	0.09122201	1.52
74596	19.81	17.67	20.71	30.84	33.60	24.57	Cds1	CDP-diacylglycerol synthase 1	0.044708623	1.52
12032	31.14	37.43	35.92	52.06	50.99	56.29	Bcan	brevican,brevican,	0.04018504	1.52
13349	15.20	15.51	16.18	25.15	24.02	22.54	Darc	Duffy blood group	0.078003447	1.51
20356	2.63	3.88	2.46	4.54	4.41	4.69	Sema5a	semaphorin 5A,semaphorin 5A,semaphorin 5A,semaphorin 5A,semaphorin 5A,	0.066954143	1.51
216874	40.20	38.60	44.08	63.04	57.16	65.92	Camta2	calmodulin binding transcription activator 2,calmodulin binding transcription activator 2,calmodulin binding transcription activator 2,calmodulin binding transcription activator 2,calmodulin binding transcription activator 2,	0.033380642	1.51
224997	83.27	70.00	66.38	126.85	103.59	102.53	Dlgap1	discs large homolog-associated protein 1 isoform,discs large homolog-associated protein 1 isoform,discs large homolog-associated protein 1 isoform,discs large homolog-associated protein 1 isoform,discs large homolog-associated protein 1 isoform,discs large homolog-associated protein 1 isoform,discs large homolog-associated protein 1 isoform,discs large homolog-associated protein 1 isoform,	0.044037542	1.51
52666	35.99	32.28	37.56	59.18	49.38	50.84	D10Ertd610e	RAC/CDC42 exchange factor,RAC/CDC42 exchange factor,	0.033169217	1.51
58188	8.85	12.72	9.32	17.11	12.24	17.56	Vstm2b	V-set and transmembrane domain containing 2B	0.074226903	1.50
12153	10.02	9.16	8.99	15.36	12.06	15.07	Bmp1	bone morphogenetic protein 1	0.064404819	1.50
18032	47.80	26.58	57.10	54.11	66.11	78.95	Nfix	nuclear factor I/X isoform 1	0.07265204	1.50
110886	10.14	13.42	10.88	15.50	13.59	22.99	Gabra5	gamma-aminobutyric acid (GABA-A) receptor,,gamma-aminobutyric acid (GABA-A) receptor,,	0.072305402	1.50
12569	48.38	58.24	51.03	77.48	86.06	75.93	Cdk5r1	cyclin-dependent kinase 5, regulatory subunit	0.051769317	1.50
29819	23.80	28.02	26.83	32.14	44.12	42.33	Stau2	staufen (RNA binding protein) homolog 2	0.083235933	1.50
67393	21.00	18.52	25.99	37.11	36.39	25.89	Cxxc5	CXXC finger 5,CXXC finger 5,	0.03598236	1.50
207777	24.12	24.78	25.29	40.52	38.71	32.75	Bzrap1	benzodiazapine receptor associated protein 1	0.036215983	1.50
16870	11.46	13.02	16.22	20.37	18.74	22.45	Lhx2	LIM homeobox protein 2,LIM homeobox protein 2,	0.043415255	1.50
319477	27.42	31.64	30.72	50.44	42.06	43.27	6030419C18Rik	hypothetical protein LOC319477,hypothetical protein LOC319477,	0.032472549	1.50
20250	138.42	150.94	144.60	221.95	199.96	234.12	Scd2	stearoyl-Coenzyme A desaturase 2	0.063406386	1.49
209011	10.14	9.29	10.72	16.23	12.60	16.39	Sirt7	sirtuin 7 (silent mating type information	0.093188917	1.49
56846	15.99	16.40	13.43	28.74	19.94	19.84	Apba2bp	amyloid beta (A4) precursor protein-binding,,amyloid beta (A4) precursor protein-binding,,	0.059938705	1.49
74100	99.26	104.25	99.09	160.42	144.31	142.73	Arpp21	cyclic AMP-regulated phosphoprotein, 21 isoform,cyclic AMP-regulated phosphoprotein, 21 isoform,cyclic AMP-regulated phosphoprotein, 21 isoform,cyclic AMP-regulated phosphoprotein, 21 isoform,	0.08198302	1.49
329828	5.39	5.21	6.30	7.68	7.80	10.02	AI464131	hypothetical protein LOC329828	0.093752451	1.49

74513	6.43	9.13	7.58	10.53	14.57	9.67	Neto2	neuropilin- and tolloid-like protein 2,neuropilin and tolloid-like protein 2,neuropilin- and tolloid-like protein 2,	0.087280105	1.49
170835	9.68	9.36	8.06	17.39	11.90	11.34	Pib5pa	phosphatidylinositol (4,5) bisphosphate	0.052588643	1.49
20312	115.55	130.48	118.35	245.61	156.06	147.09	Cx3cl1	chemokine (C-X3-C motif) ligand 1	0.018549262	1.49
58226	2.22	4.01	2.14	5.87	2.30	4.34	Cacna1h	calcium channel alpha13.2 subunit	0.023311348	1.49
18823	278.62	175.65	273.47	355.45	335.25	401.17	Plp1	proteolipid protein 1,proteolipid protein 1,	0.085744681	1.48
70638	7.69	11.57	7.26	15.31	11.30	13.10	5730507A09Rik	hypothetical protein LOC70638	0.043716343	1.48
223775	5.21	8.97	5.02	10.94	8.60	9.17	Pim3	proviral integration site 3	0.087935111	1.48
54194	40.45	32.30	41.98	55.96	55.47	58.86	Akap8l	A kinase (PRKA) anchor protein 8-like,A kinase (PRKA) anchor protein 8-like,	0.070979186	1.48
237979	1.37	2.52	1.68	3.42	2.58	2.24	Sdk2	sidekick 2,sidekick 2,	0.08886906	1.48
64297	4.47	4.03	4.52	7.89	5.23	6.40	Gprc5b	G protein-coupled receptor, family C, group 5,	0.065311366	1.48
77552	35.19	38.99	33.91	58.45	60.96	41.21	Tmem58	transmembrane protein 58	0.0801099	1.48
67468	39.19	62.23	51.34	68.86	82.51	75.62	Mmd	monocyte to macrophage,monocyte to macrophage,	0.056757921	1.47
16574	100.21	116.82	118.63	150.75	182.57	164.21	Kif5c	kinesin family member 5C	0.094986397	1.47
26457	14.47	15.31	12.47	23.02	17.55	21.93	Slc27a1	solute carrier family 27, member 1,solute carrier family 27, member 1,solute carrier family 27, member 1,solute carrier family 27, member 1,	0.078003447	1.47
100072	21.06	27.49	19.45	31.16	38.07	31.46	n/a	n/a	0.098929585	1.47
56224	48.09	43.01	45.32	71.34	77.73	53.00	Tspan5	tetraspanin 5	0.081428165	1.47
68041	21.26	18.69	32.89	36.61	31.59	40.03	Mid1ip1	MID1 interacting G12-like protein,MID1 interacting G12-like protein,	0.038834598	1.47
269060	10.41	12.01	12.07	21.24	15.48	14.25	Dagla	diacylglycerol lipase, alpha	0.0293263	1.47
20249	3.46	3.02	3.65	5.67	3.21	6.18	Scd1	stearoyl-Coenzyme A desaturase 1	0.085744681	1.47
224022	8.87	11.48	8.06	16.63	13.19	12.26	Slc7a4	solute carrier family 7 (cationic amino acid	0.071241904	1.47
237847	12.59	11.00	12.75	19.62	18.62	15.67	Rtn4rl1	reticulon 4 receptor-like 1	0.083441337	1.46
11932	77.16	77.08	73.31	102.64	107.66	126.09	Atp1b2	Na+/K+ -ATPase beta 2 subunit	0.097751094	1.46
13848	19.29	13.36	19.94	29.72	27.89	19.79	Ephb6	Eph receptor B6,Eph receptor B6,	0.068765191	1.46
50914	17.35	21.37	17.88	33.39	21.47	29.01	Olig1	oligodendrocyte transcription factor 1	0.043732263	1.46
11758	35.56	38.71	36.17	56.51	50.04	56.64	Prdx6	peroxiredoxin 6	0.065518111	1.46
227580	24.25	39.82	24.74	48.31	47.86	35.05	C1ql3	C1q-like 3	0.055767842	1.46
12794	49.92	71.11	47.63	93.61	57.43	96.35	Cnih2	cornichon homolog 2	0.044748371	1.46
338521	4.37	3.60	5.12	8.94	3.81	6.53	Fa2h	fatty acid 2-hydroxylase,fatty acid 2-hydroxylase,	0.074226903	1.46
22042	8.08	13.32	10.84	15.19	18.69	13.37	Tfrc	transferrin receptor,transferrin receptor,transferrin receptor,	0.079144445	1.46
77938	3.67	3.96	3.95	7.58	4.78	4.69	A930008G19Rik	hypothetical protein LOC77938,hypothetical protein LOC77938,hypothetical protein LOC77938,hypothetical protein LOC77938,hypothetical protein LOC77938,	0.057419501	1.46
94047	9.73	9.00	9.64	15.97	16.01	9.77	Cecr6	cat eye syndrome chromosome region, candidate 6	0.08662639	1.45
54525	41.51	36.09	39.41	60.05	58.53	52.96	Syt7	synaptotagmin VII alpha isoform	0.091798959	1.45
11864	35.36	33.41	36.52	53.95	50.52	49.11	Arnt2	aryl hydrocarbon receptor nuclear translocator,aryl hydrocarbon receptor nuclear translocator,aryl hydrocarbon receptor nuclear translocator,	0.076068752	1.45
29873	83.30	71.53	91.10	115.00	122.40	121.91	Cspg5	chondroitin sulfate proteoglycan 5,chondroitin sulfate proteoglycan 5,chondroitin sulfate proteoglycan 5,chondroitin sulfate proteoglycan 5,	0.094005549	1.45
67252	43.95	43.25	47.05	68.98	73.82	52.72	Cap2	CAP, adenylate cyclase-associated protein, 2,CAP, adenylate cyclase-associated protein, 2,	0.080720964	1.45
67792	10.24	12.76	10.13	16.50	16.06	15.82	Rgs8	regulator of G-protein signalling 8	0.094986397	1.44
57780	25.83	34.60	34.43	53.84	37.66	45.59	Fxyd7	FXYD domain-containing ion transport regulator	0.077210652	1.44
225392	24.91	25.58	28.10	40.80	34.83	38.85	Rell2	RELT-like 2,RELT-like 2,	0.075302311	1.44
72754	6.52	6.06	7.19	11.44	8.74	8.47	Arhgef10l	Rho guanine nucleotide exchange factor (GEF),Rho guanine nucleotide exchange factor (GEF),Rho guanine nucleotide exchange factor (GEF),	0.081927519	1.44
97761	17.43	18.20	20.04	29.23	22.37	28.89	Sgsm2	RUN and TBC1 domain containing 1	0.059550424	1.44

211187	7.95	10.34	6.98	14.89	10.42	11.38	Lrtm2	leucine-rich repeats and transmembrane domains,leucine-rich repeats and transmembrane domains,	0.08141777	1.44
241727	33.66	44.16	40.44	63.54	47.31	60.87	Snph	syntaphilin,syntaphilin,syntaphilin,syntaphilin,	0.04568311	1.44
268480	25.68	25.86	24.78	39.83	32.17	38.16	Rapgefl1	Rap guanine nucleotide exchange factor	0.083079526	1.43
66972	59.59	82.39	62.85	106.53	79.56	109.58	Slc25a23	solute carrier family 25, member 23	0.062004225	1.43
27801	9.64	12.45	10.21	20.70	13.55	12.41	Zdhhc8	zinc finger, DHHC domain containing 8	0.043284069	1.43
21375	14.90	24.34	20.22	30.31	32.47	23.03	Tbr1	T-box brain gene 1	0.068745727	1.43
12217	22.15	29.07	23.95	43.91	36.73	27.72	Bsn	bassoon protein	0.06327488	1.43
380711	24.28	30.99	29.86	44.52	41.91	35.72	Gaml4	GTPase activating RANGAP domain-like 4,GTPase activating RANGAP domain-like 4,GTPase activating RANGAP domain-like 4,	0.065387975	1.42
13048	12.25	12.89	13.70	21.27	19.22	15.10	Cutl2	cut-like 2	0.081630474	1.42
216439	90.48	111.13	97.66	158.42	116.06	153.93	Centg1	centaurin, gamma 1,centaurin, gamma 1,	0.078447573	1.42
94090	21.14	29.51	21.07	47.62	27.45	27.53	Trim9	tripartite motif protein 9,tripartite motif protein 9,tripartite motif protein 9,tripartite motif protein 9,tripartite motif protein 9,tripartite motif protein 9,	0.043287947	1.42
268345	9.66	13.86	11.47	18.70	17.06	14.34	Kcnc2	potassium voltage gated channel, Shaw-related,potassium voltage gated channel, Shaw-related,	0.077068298	1.42
74351	49.93	25.38	48.10	26.18	30.20	30.47	Ddx23	DEAD (Asp-Glu-Ala-Asp) box polypeptide 23,DEAD (Asp-Glu-Ala-Asp) box polypeptide 23,	0.093305179	0.70
94184	31.61	24.75	20.97	13.25	17.39	22.78	Pdxdc1	pyridoxal-dependent decarboxylase domain,pyridoxal-dependent decarboxylase domain,	0.064782793	0.70
109754	46.01	25.45	39.46	22.92	26.19	28.69	Cyb5r3	diaphorase 1	0.078447573	0.70
67500	23.76	16.22	25.39	11.45	19.43	14.69	Ccar1	cell division cycle and apoptosis regulator 1,cell division cycle and apoptosis regulator 1,	0.057267786	0.69
66471	16.43	8.76	17.63	7.47	12.34	9.98	Anp32e	acidic (leucine-rich) nuclear phosphoprotein 32,acidic (leucine-rich) nuclear phosphoprotein 32,	0.062821591	0.69
216565	16.81	14.64	18.61	10.38	13.05	11.13	Ehbp1	EH domain binding protein 1,EH domain binding protein 1,EH domain binding protein 1,	0.09122201	0.69
14567	248.78	199.50	231.94	149.85	163.03	156.49	Gdi1	guanosine diphosphate (GDP) dissociation	0.072286889	0.69
22151	140.98	91.02	115.25	80.04	77.05	83.39	Tubb2a	tubulin, beta 2	0.061996966	0.69
105245	24.17	21.01	21.98	14.56	14.12	17.40	Txndc5	thioredoxin domain containing 5,thioredoxin domain containing 5,thioredoxin domain containing 5,thioredoxin domain containing 5,	0.09122201	0.68
243339	88.33	71.68	84.54	55.13	51.63	60.95	Tmem130	hypothetical protein LOC243339	0.070979186	0.68
76338	17.24	16.17	14.43	10.83	10.71	11.03	Rab2b	RAB2B protein,RAB2B protein,	0.089818463	0.67
52323	11.72	12.46	10.97	7.43	8.14	8.33	Klhl7	SBBI26 protein,SBBI26 protein,	0.092522167	0.67
231279	9.88	12.91	10.88	6.28	9.40	7.11	Guf1	GUF1 GTPase homolog,GUF1 GTPase homolog,	0.073166564	0.67
56070	23.43	22.73	23.34	13.57	18.26	15.15	Tcerg1	transcription elongation regulator 1 (CA150),transcription elongation regulator 1 (CA150),transcription elongation regulator 1 (CA150),	0.047155556	0.67
14199	39.68	39.92	34.48	26.23	24.53	26.59	Fhl1	four and a half LIM domains 1 isoform 3	0.069747717	0.67
20866	29.98	23.60	24.14	18.13	19.07	15.23	Stim1	stromal interaction molecule 1	0.049954216	0.67
18114	300.09	129.07	279.01	137.71	166.42	170.85	Rrp1	novel nuclear protein 1	0.029309261	0.67
320865	10.64	10.11	9.70	6.98	8.58	4.81	Cdh18	cadherin 18,cadherin 18,cadherin 18,	0.098674233	0.67
78323	8.88	7.43	7.06	5.13	4.96	5.63	2310046O06Rik	hypothetical protein LOC78323	0.096219162	0.66
214133	7.92	10.56	8.23	5.88	6.70	5.35	E130014J05Rik	hypothetical protein LOC214133,hypothetical protein LOC214133,	0.062004225	0.66
19090	4.59	5.38	4.48	2.79	3.37	3.41	Prkdc	protein kinase, DNA activated, catalytic	0.056883897	0.66
17984	90.52	105.78	106.46	38.27	67.68	95.98	Ndn	necdin	0.017139518	0.66
245468	7.47	7.18	6.66	4.19	5.08	4.95	Pnma3	paraneoplastic antigen MA3	0.07005384	0.66
14783	11.43	12.81	10.98	7.22	7.76	8.35	Grb10	growth factor receptor bound protein 10,growth factor receptor bound protein 10,	0.053411056	0.66
23856	16.79	16.11	17.98	10.70	12.72	10.30	Dido1	death inducer-obliterator 1 isoform 1,death inducer-obliterator 1 isoform 1,death inducer-obliterator 1 isoform 1,	0.091907902	0.66

12933	90.33	66.14	79.77	53.08	49.00	52.83	Crmp1	collapsin response mediator protein 1	0.045204376	0.66
66366	77.46	53.01	86.61	46.34	42.56	52.78	Ergic3	ERGIC and golgi 3,ERGIC and golgi 3,	0.07201235	0.66
23963	3.71	5.57	4.09	2.97	3.21	2.64	Odz1	odd Oz/ten-m homolog 1	0.095406269	0.66
15469	58.71	37.23	45.99	31.86	28.51	31.81	Prmt1	protein arginine N-methyltransferase 1,protein arginine N-methyltransferase 1,protein arginine N-methyltransferase 1,	0.052412365	0.65
103098	17.55	21.99	16.40	11.36	12.57	12.64	Slc6a15	solute carrier family 6, member 15,solute carrier family 6, member 15,	0.039245873	0.65
107503	11.46	8.37	16.17	6.71	9.62	7.21	Atf5	ativating transcription factor 5,ativating transcription factor 5,	0.09874322	0.65
11303	5.92	6.59	6.10	3.78	3.94	4.38	Abca1	ATP-binding cassette 1, sub-family A, member 1	0.045019153	0.65
13872	14.92	11.33	13.48	8.71	8.23	8.76	Ercc3	excision repair cross-complementing rodent	0.064547788	0.64
77630	12.73	11.54	12.18	7.42	8.17	8.12	Prdm8	PR domain containing 8	0.042898019	0.64
53885	14.23	8.20	11.47	5.74	7.14	8.72	Nphp1	nephronophthisis 1 (juvenile) homolog,nephronophthisis 1 (juvenile) homolog,nephronophthisis 1 (juvenile) homolog,	0.050501252	0.64
11815	75.32	38.25	61.18	36.54	26.80	49.40	Apod	apolipoprotein D,apolipoprotein D,apolipoprotein D,	0.020976219	0.64
12069	297.31	140.48	296.80	122.66	192.19	157.52	Bex2	brain expressed X-linked 2	0.007853226	0.64
170677	5.35	3.71	2.01	3.03	1.98	2.10	Pcdh21	protocadherin 21	0.092312037	0.64
104346	23.37	12.35	26.84	10.53	13.13	15.97	Gas8	growth arrest specific 8,growth arrest specific 8,	0.03811683	0.63
17222	6.96	9.47	7.44	5.16	4.97	5.03	Anapc1	anaphase promoting complex subunit 1,anaphase promoting complex subunit 1,	0.040192909	0.63
214552	7.32	7.57	6.59	4.73	4.48	4.41	Cep164	centrosomal protein 164,centrosomal protein 164,centrosomal protein 164,	0.047264337	0.63
14208	57.56	29.53	53.69	25.80	30.43	33.18	Ppm1g	protein phosphatase 1G (formerly 2C),	0.011967526	0.63
71648	13.29	10.59	14.89	7.42	6.96	10.08	Optn	optineurin,optineurin,optineurin,	0.058658296	0.63
80892	1.69	1.81	1.26	0.91	1.24	0.88	Zfhx4	zinc finger homeodomain 4	0.028768107	0.63
70025	134.59	88.92	131.27	91.24	67.51	62.88	Acot7	acyl-CoA thioesterase 7,acyl-CoA thioesterase 7,acyl-CoA thioesterase 7,	0.032472549	0.62
229584	19.17	16.16	17.60	12.25	10.47	10.34	Pogz	pogo transposable element with ZNF domain,pogo transposable element with ZNF domain,	0.022557806	0.62
71805	12.93	11.41	12.64	7.50	8.67	6.65	Nup93	nucleoporin 93,nucleoporin 93,nucleoporin 93,	0.033950792	0.62
12460	18.16	11.35	13.48	8.90	9.68	7.45	Ccs	copper chaperone for superoxide dismutase	0.064547788	0.61
56322	9.08	7.96	8.29	5.65	4.29	5.59	Timm22	translocase of inner mitochondrial membrane 22	0.042736008	0.61
14706	33.24	29.05	24.75	19.08	15.61	18.70	Gng4	guanine nucleotide binding protein (G protein),	0.009398589	0.61
70650	7.08	8.76	7.39	4.87	5.50	3.71	Zcchc8	zinc finger, CCHC domain containing 8,zinc finger, CCHC domain containing 8,	0.023577802	0.60
109900	12.11	10.35	12.62	6.22	5.78	8.78	Asl	argininosuccinate lyase	0.085744681	0.60
22670	10.65	7.76	12.22	6.18	6.93	5.40	Trim26	tripartite motif protein 26 isoform a	0.020271574	0.60
56045	4.72	5.09	4.17	3.08	2.31	3.03	Samhd1	SAM domain- and HD domain-containing protein 1,SAM domain- and HD domain-containing protein 1,SAM domain- and HD domain-containing protein 1,	0.060060796	0.60
17025	18.41	10.33	17.70	7.86	12.45	7.23	Alad	aminolevulinate, delta-, dehydratase,aminolevulinate, delta-, dehydratase,	0.026369658	0.60
107656	6.68	2.29	4.83	1.85	3.35	3.12	Krt9	keratin complex 1, acidic, gene 9	0.018975381	0.60
20019	6.12	6.94	7.21	4.07	3.96	4.09	Rpo1-4	RNA polymerase 1-4,RNA polymerase 1-4,RNA polymerase 1-4,RNA polymerase 1-4,	0.022773808	0.60
68272	20.11	17.83	20.45	10.30	11.65	12.95	Rbm28	RNA binding motif protein 28 isoform 2	0.005623588	0.59
22590	9.79	6.07	6.81	3.67	5.57	4.21	Xpa	xeroderma pigmentosum, complementation group A	0.097021617	0.59
54128	12.29	9.86	9.58	7.31	5.89	5.61	Pmm2	phosphomannomutase 2,phosphomannomutase 2,	0.04225927	0.59
100978	5.32	4.62	5.19	2.76	3.41	2.74	Nfxl1	ovarian zinc finger protein,ovarian zinc finger protein,	0.031100318	0.59
83669	29.63	38.22	27.97	21.49	12.74	22.74	Wdr6	WD repeat domain 6	0.010501485	0.59
14432	351.10	181.01	336.09	144.18	190.22	178.29	Gap43	growth associated protein 43	0.001109204	0.58
52668	21.06	23.55	22.54	13.00	14.84	11.38	D12Ertd647e	hypothetical protein LOC52668 isoform 3	0.045724525	0.58

231997	4.52	5.61	4.50	3.07	3.15	2.24	Fkbp14	FK506 binding protein 14	0.043978636	0.57
12675	8.97	10.91	9.72	5.29	6.55	5.11	Chuk	conserved helix-loop-helix ubiquitous kinase,conserved helix-loop-helix ubiquitous kinase,	0.009125725	0.57
17768	3.87	2.76	5.11	1.70	3.13	1.87	Mthfd2	methylenetetrahydrofolate dehydrogenase (NAD+	0.062004225	0.57
20846	5.53	6.59	6.94	3.63	3.64	3.59	Stat1	signal transducer and activator of transcription,signal transducer and activator of transcription,signal transducer and activator of transcription,signal transducer and activator of transcription,signal transducer and activator of transcription,	0.012213965	0.57
22240	14.53	14.28	15.80	9.16	5.10	10.90	Dpysl3	dihydropyrimidinase-like 3,dihydropyrimidinase-like 3,	0.032661436	0.56
12841	7.14	4.02	9.68	3.83	3.40	4.42	Col9a3	procollagen, type IX, alpha 3	0.050734849	0.56
215201	5.33	5.20	4.65	3.12	2.81	2.62	4732479N06Rik	hypothetical protein LOC215201,hypothetical protein LOC215201,	0.02266439	0.56
16777	4.94	4.67	5.41	2.34	2.03	4.00	Lamb1-1	laminin B1 subunit 1	0.007271771	0.56
15944	4.40	4.66	4.97	2.41	3.03	2.20	Irgm	immunity-related GTPase family, M	0.022367351	0.54
57434	2.37	2.58	2.21	1.53	1.35	1.02	Xrcc2	X-ray repair complementing defective repair in	0.058355561	0.54
75452	9.68	10.03	9.58	5.87	4.85	4.98	Ascc2	activating signal cointegrator 1 complex subunit	0.009229184	0.54
216459	16.91	12.79	17.85	10.68	7.88	6.98	Myl6b	myosin, light polypeptide 6B	0.027225203	0.54
16391	3.19	7.57	4.27	3.65	2.14	2.31	Isgf3g	interferon dependent positive acting,interferon dependent positive acting,interferon dependent positive acting,	0.081717822	0.53
12842	3.54	1.60	1.59	1.54	0.76	1.16	Col1a1	procollagen, type I, alpha 1	0.049927787	0.52
14964	9.25	3.08	8.32	1.90	4.49	4.51	H2-D1	histocompatibility 2, D region locus 1	0.002906502	0.52
19165	16.85	11.20	10.47	6.85	5.49	7.75	Psen2	presenilin 2,presenilin 2,presenilin 2,presenilin 2,	0.001392808	0.52
14972	11.42	7.88	9.16	4.86	4.27	5.75	H2-K1	histocompatibility 2, K1, K region isoform 1,histocompatibility 2, K1, K region isoform 1,	0.005522166	0.52
212627	4.56	2.79	4.38	1.85	1.34	2.93	Prpsap2	phosphoribosyl pyrophosphate,phosphoribosyl pyrophosphate,	0.060989896	0.52
20513	5.37	5.32	4.77	3.06	2.59	2.24	Slc1a6	solute carrier family 1 (high affinity	0.020507889	0.51
26436	1.83	2.23	2.16	0.77	1.28	1.13	Psg16	pregnancy specific glycoprotein 16	0.050188052	0.51
19277	6.09	5.83	5.08	3.25	2.20	3.22	Ptpro	protein tyrosine phosphatase, receptor type, O,protein tyrosine phosphatase, receptor type, O,protein tyrosine phosphatase, receptor type, O,protein tyrosine phosphatase, receptor type, O,	0.002212828	0.51
99586	1.73	1.84	1.54	0.84	0.52	1.24	Dpyd	dihydropyrimidine dehydrogenase	0.037656547	0.50
66141	11.26	6.99	6.75	4.68	3.72	4.25	Ifitm3	interferon induced transmembrane protein 3	0.043082537	0.50
56795	4.56	3.65	3.67	2.09	2.15	1.74	Arl10	ADP-ribosylation factor-like 10	0.086168661	0.50
380669	2.04	3.26	1.97	1.05	1.11	1.52	Lin28b	lin-28 homolog b	0.003554532	0.50
68695	28.53	20.72	29.56	17.01	5.80	16.56	Hddc3	HD domain containing 3	0.004989366	0.50
20020	20.26	23.15	17.34	10.73	10.58	8.91	Polr2a	polymerase (RNA) II (DNA directed) polypeptide,polymerase (RNA) II (DNA directed) polypeptide,	2.86E-05	0.50
243771	4.21	3.87	4.17	1.77	2.09	2.24	Parp12	poly (ADP-ribose) polymerase family, member 12	0.003170801	0.49
20716	6.59	8.22	6.51	3.13	2.38	5.11	Serpina3n	serine (or cysteine) proteinase inhibitor, clade	0.002931191	0.49
223267	20.81	14.78	16.41	9.74	6.18	9.72	BC006662	hypothetical protein LOC223267	0.001964674	0.49
80285	1.55	1.54	1.38	0.72	0.78	0.69	Parp9	B aggressive lymphoma,B aggressive lymphoma,	0.03518217	0.48
667370	2.83	2.04	2.72	1.06	1.73	0.92	LOC667370	similar to interferon-induced protein with,similar to interferon-induced protein with,	0.020507889	0.48
22352	13.49	9.01	9.33	5.62	4.72	5.09	Vim	vimentin	0.000724647	0.48
16913	4.17	1.89	3.44	1.70	0.98	1.81	Psmb8	proteosome (prosome, macropain) subunit, beta	0.083203161	0.47
15216	2.29	1.50	1.56	0.82	0.70	0.99	Hfe	hemochromatosis	0.080002788	0.47
209200	1.61	2.18	2.19	0.80	0.77	1.20	Dtx3l	deltex 3-like,deltex 3-like,	0.002833077	0.46

18044	11.79	10.22	9.26	5.61	4.67	4.06	Nfya	nuclear transcription factor-Y alpha,nuclear transcription factor-Y alpha,nuclear transcription factor-Y alpha,nuclear transcription factor-Y alpha,	1.20E-05	0.45
72748	7.58	4.12	6.78	2.41	3.44	2.61	Hdhd3	haloacid dehalogenase-like hydrolase domain	0.004187299	0.45
12159	2.84	1.39	1.96	1.33	0.38	1.12	Bmp4	bone morphogenetic protein 4	0.055054332	0.45
68126	13.62	10.71	12.00	6.40	4.78	5.17	Fahd2a	fumarylacetoacetate hydrolase domain containing	0.001384149	0.45
140703	5.75	4.79	5.04	2.42	2.30	2.25	Emid1	EMI domain containing 1,EMI domain containing 1,	0.004989366	0.45
55932	4.88	3.45	4.73	2.00	2.66	1.18	Gbp3	guanylate nucleotide binding protein 4,guanylate nucleotide binding protein 4,guanylate nucleotide binding protein 4,	0.000882412	0.44
66717	1.26	0.76	1.40	0.44	0.58	0.51	Ccdc96	coiled-coil domain containing 96	0.019839524	0.44
12840	1.32	1.59	2.88	0.69	0.90	0.96	Col9a2	procollagen, type IX, alpha 2	0.068765191	0.44
70951	1.39	1.93	1.76	0.53	0.99	0.68	Spata1	spermatogenesis associated 1	0.062825136	0.43
68828	1.40	1.23	1.56	0.74	0.49	0.57	Sync	syncoilin,syncoilin,	0.087488056	0.43
70110	2.40	1.84	1.71	0.92	1.07	0.54	Ifi35	interferon-induced protein 35	0.068510706	0.42
19039	5.32	8.92	8.71	4.34	3.03	2.34	Lgals3bp	lectin, galactoside-binding, soluble, 3 binding	0.000543129	0.42
56016	1.43	1.69	2.40	0.68	0.74	0.89	Hebp2	heme binding protein 2,heme binding protein 2,	0.032375197	0.41
22271	2.55	1.71	2.11	0.59	1.06	0.95	Upp1	uridine phosphorylase 1,uridine phosphorylase 1,uridine phosphorylase 1,	0.067690333	0.41
217069	1.88	1.98	1.62	0.83	0.66	0.76	Trim25	tripartite motif protein 25,tripartite motif protein 25,	0.000273326	0.40
53870	6.21	10.00	6.50	3.53	3.41	2.20	Cntn6	contactin 6	3.34E-06	0.40
71914	1.43	0.82	0.92	0.54	0.30	0.44	Antxr2	anthrax toxin receptor 2	0.019626164	0.40
226049	1.43	1.43	1.37	0.75	0.61	0.31	Dmrt2	terra	0.023833041	0.39
78781	1.38	1.60	1.33	0.46	0.52	0.70	Zc3hav1	zinc finger CCCH type, antiviral 1	0.009524668	0.39
353282	0.91	1.64	0.89	0.51	0.45	0.38	Sfmbt2	Scm-like with four mbt domains 2,Scm-like with four mbt domains 2,Scm-like with four mbt domains 2,Scm-like with four mbt domains 2,	0.000511117	0.39
54378	2.92	2.40	3.34	0.49	1.55	1.30	Cacng6	voltage-dependent calcium channel gamma-6	0.032546376	0.38
320817	6.84	8.62	6.50	2.76	2.92	2.69	Atad2b	ATPase family, AAA domain containing 2B	1.50E-10	0.38
230073	1.78	1.92	2.01	0.80	0.49	0.86	Ddx58	DEAD/H box polypeptide RIG-I,DEAD/H box polypeptide RIG-I,DEAD/H box polypeptide RIG-I,	0.000263836	0.37
72119	1.61	0.95	1.55	0.34	0.37	0.80	Tpx2	TPX2, microtubule-associated protein homolog,TPX2, microtubule-associated protein homolog,TPX2, microtubule-associated protein homolog,	0.001123116	0.36
17427	3.65	2.50	2.11	1.11	0.93	0.88	Mns1	meiosis-specific nuclear structural protein 1	0.001707621	0.35
69550	4.07	4.22	7.04	2.62	0.98	1.74	Bst2	DAMP-1 protein	0.022727081	0.35
225631	1.17	2.43	1.55	0.40	0.60	0.76	Onecut2	one cut domain, family member 2	9.49E-11	0.34
12544	3.04	1.42	2.22	0.97	0.44	0.75	Cdc45l	cell division cycle 45 homolog (S.,cell division cycle 45 homolog (S.,	0.015981664	0.33
75732	1.07	0.44	2.13	0.29	0.39	0.48	Iqcd	IQ motif containing D	0.021737995	0.31
53867	1.60	0.78	1.36	0.40	0.30	0.44	Col5a3	procollagen, type V, alpha 3,procollagen, type V, alpha 3,	0.000216493	0.31
15959	5.97	3.81	5.83	1.62	1.76	1.29	Ifit3	interferon-induced protein with	9.13E-10	0.29
15957	2.68	2.94	3.14	1.06	0.86	0.56	Ifit1	interferon-induced protein with	1.65E-07	0.28
21349	0.58	1.50	1.25	0.35	0.30	0.27	Tal1	T-cell acute lymphocytic leukemia 1,T-cell acute lymphocytic leukemia 1,T-cell acute lymphocytic leukemia 1,	0.000120749	0.28
22160	1.38	1.40	2.71	0.26	0.16	0.94	Twist1	twist gene homolog 1	0.000222318	0.25
16840	1.84	1.03	1.19	0.30	0.22	0.23	Lect1	leukocyte cell derived chemotaxin 1	0.000518802	0.18
23962	2.09	3.23	3.74	0.62	0.53	0.50	Oasl2	2'-5' oligoadenylate synthetase-like 2	1.19E-12	0.18
54123	1.63	2.20	2.50	0.47	0.43	0.15	Irf7	interferon regulatory factor 7,interferon regulatory factor 7,interferon regulatory factor 7,	5.83E-08	0.17
246709	0.81	2.12	1.59	0.23	0.37	0.08	Rgs13	regulator of G-protein signaling 13,regulator of G-protein signaling 13,	1.73E-05	0.15
99899	0.68	1.40	0.82	0.22	0.16	0.04	Ifi44	interferon-induced protein 44	6.30E-07	0.15
76933	2.26	3.14	2.93	0.36	0.49	0.34	Ifi27	interferon, alpha-inducible protein 27	0.00424764	0.14
18113	1.00	0.86	1.35	0.12	0.08	0.17	Nnmt	nicotinamide N-methyltransferase	0.00120998	0.11
24110	1.30	2.67	2.41	0.25	0.09	0.30	Usp18	ubiquitin specific peptidase 18	2.52E-14	0.10

18504	1.29	0.63	1.77	0.00	0.00	0.00	Pax2	paired box gene 2,paired box gene 2,	5.29E-10	0.00
620779	1.26	1.47	1.12	0.00	0.00	0.00	LOC620779	hypothetical LOC620779	1.49E-14	0.00

Table A-5: Genes selected for an HD gene signature for 12wk cortex.

Gene	TCM9452	TCM9450	TCM9453	TCW9451	TCW9457	TCW9469	gene_symbol	gene_desc
20351	5.53	7.35	6.09	17.65	14.00	10.95	Sema4a	sema domain, immunoglobulin domain (Ig),,sema domain, immunoglobulin domain (Ig),,
225870	6.06	8.49	5.19	14.90	14.73	14.17	Rin1	Ras and Rab interactor 1
50722	7.15	5.33	8.09	19.30	10.61	14.51	Dkkl1	dickkopf-like 1
22353	6.85	6.12	7.15	18.97	18.94	12.19	Vip	vasoactive intestinal polypeptide
75668	4.72	6.83	4.83	24.34	14.81	16.70	Rasl10a	RAS-related on chromosome 22
14221	7.59	9.15	6.58	19.12	17.68	19.12	Fjx1	four jointed box 1
13371	9.25	6.75	9.63	16.79	24.22	17.59	Dio2	deiodinase, iodothyronine, type II
223626	10.70	8.63	9.89	24.53	19.06	17.91	4930572J05Rik	mesenchymal stem cell protein DSCD75 homolog
16499	11.03	6.98	10.17	21.55	25.62	18.91	Kcnab3	potassium voltage-gated channel, shaker-related,potassium voltage-gated channel, shaker-related,potassium voltage-gated channel, shaker-related,
99296	6.60	8.20	5.55	23.82	17.82	26.14	Hrh3	histamine receptor H 3
51801	10.56	9.32	8.30	16.30	29.62	22.07	Ramp1	receptor-activity modifying protein 1
15370	8.95	14.00	11.54	26.38	22.02	21.26	Nr4a1	nuclear receptor subfamily 4, group A, member 1
14403	10.15	9.45	6.93	28.97	21.81	20.40	Gabrd	gamma-aminobutyric acid (GABA-A) receptor,
103551	5.88	6.54	9.01	27.91	26.49	23.19	E130012A19Rik	hypothetical protein LOC103551
399548	5.75	7.99	4.40	27.73	29.57	26.36	Scn4b	sodium channel, type IV, beta
56213	16.08	12.03	14.24	23.20	29.42	36.02	Htra1	HtrA serine peptidase 1,HtrA serine peptidase 1,
217154	10.59	7.87	12.59	32.31	33.44	24.34	Stac2	SH3 and cysteine rich domain 2
233271	10.45	15.93	13.29	23.81	38.73	29.86	Luzp2	leucine zipper protein 2,leucine zipper protein 2,
72168	15.19	8.83	13.94	29.96	34.01	29.63	Aifm3	apoptosis-inducing factor like,apoptosis-inducing factor like,
14555	14.17	9.89	12.75	28.85	29.41	36.49	Gpd1	glycerol-3-phosphate dehydrogenase 1 (soluble),glycerol-3-phosphate dehydrogenase 1 (soluble),
20893	13.11	13.65	15.25	34.72	38.63	23.00	Bhlhb2	basic helix-loop-helix domain containing, class
217166	16.18	17.43	13.53	37.59	29.80	30.36	Nr1d1	nuclear receptor subfamily 1, group D, member 1
22317	12.65	12.92	18.78	37.61	37.34	23.24	Vamp1	vesicle-associated membrane protein 1 isoform b
27528	16.97	12.24	14.68	30.24	42.18	29.38	D0H4S114	neuronal protein 3.1
16512	14.05	15.85	14.56	47.09	30.09	28.35	Kcnh3	potassium voltage-gated channel, subfamily H,potassium voltage-gated channel, subfamily H,
70435	18.66	15.55	19.39	40.88	42.28	31.76	2610204M08Rik	formin, inverted,formin, inverted,
68337	19.03	20.13	19.59	52.84	39.48	38.61	Crip2	LIM only protein HLP
17153	20.14	18.20	25.87	44.35	38.68	48.27	Mal	myelin and lymphocyte protein, T-cell
57266	21.15	18.66	20.44	40.19	39.86	52.12	Cxcl14	kidney-expressed chemokine CXC
22174	22.12	22.66	21.75	59.83	47.75	37.38	Tyro3	TYRO3 protein tyrosine kinase 3,TYRO3 protein tyrosine kinase 3,
241638	27.96	28.52	30.76	58.04	64.13	59.63	Prosapip1	ProSAPiP1 protein
228550	18.65	17.59	25.45	66.30	66.03	56.44	Itpka	inositol 1,4,5-trisphosphate 3-kinase A
11838	14.82	17.31	21.17	63.26	79.33	65.53	Arc	activity regulated cytoskeletal-associated,activity regulated cytoskeletal-associated,
226412	34.48	42.09	36.54	75.00	90.72	64.15	R3hdm1	R3H domain (binds single-stranded nucleic,R3H domain (binds single-stranded nucleic,R3H domain (binds single-stranded nucleic,
235402	30.50	37.71	39.54	98.57	70.73	60.73	Lingo1	leucine rich repeat and Ig domain containing 1,leucine rich repeat and Ig domain containing 1,
12348	29.84	33.78	32.56	77.56	80.86	72.95	Car11	carbonic anhydrase 11

268709	38.80	36.85	37.47	74.07	106.33	109.96	BC055107	downregulated in renal cell carcinoma,downregulated in renal cell carcinoma,downregulated in renal cell carcinoma,
109648	55.44	35.45	53.05	97.44	81.07	142.21	Npy	neuropeptide Y
19894	61.46	49.42	59.44	126.26	127.24	114.11	Rph3a	rabphilin 3A,rabphilin 3A,
104418	58.10	56.44	63.62	156.06	104.63	109.02	Dgkz	diacylglycerol kinase zeta,diacylglycerol kinase zeta,diacylglycerol kinase zeta,
68404	57.86	42.80	64.18	117.81	149.22	126.95	Nrn1	neuritin 1
22360	98.40	94.71	95.25	176.33	209.06	208.10	Nrsn1	neurensin 1
12424	155.82	126.29	118.56	339.01	291.88	278.18	Cck	cholecystokinin
12322	261.59	276.30	268.14	521.04	570.88	536.99	Camk2a	calcium/calmodulin-dependent protein kinase II
66259	183.73	173.66	199.07	507.78	725.54	516.65	Camk2n1	calcium/calmodulin-dependent protein kinase II
64011	324.54	300.65	409.58	696.11	906.98	662.75	Nrgn	neurogranin

Table A-6: Genes selected for an HD gene signature for 12wk striatum.

Gene	TSM492	TSM482	TSM490	TSW478	TSW479	TSW491	gene_symbol	gene_desc
77113	48.10	62.32	58.53	99.25	124.09	116.99	Klhl2	kelch-like 2, Mayven,kelch-like 2, Mayven,
83997	32.36	42.37	32.31	56.17	91.83	67.77	Slmap	sarcolemma associated protein,sarcolemma associated protein,sarcolemma associated protein,sarcolemma associated protein,
17304	32.16	24.48	30.44	69.95	48.09	60.08	Mfge8	milk fat globule-EGF factor 8 protein isoform 1
68203	33.25	21.57	25.09	65.04	50.57	49.41	Diras2	DIRAS family, GTP-binding RAS-like 2
238130	9.52	12.48	10.74	17.10	27.62	22.68	Dock4	dedicator of cytokinesis 4,dedicator of cytokinesis 4,dedicator of cytokinesis 4,
20741	10.72	7.26	10.60	22.91	18.99	18.20	Spnb1	spectrin beta 1,spectrin beta 1,
241589	12.07	8.60	9.48	21.40	22.90	19.40	D430041D05Rik	hypothetical protein LOC241589,hypothetical protein LOC241589,hypothetical protein LOC241589,
54403	13.01	11.51	11.54	23.84	29.58	22.81	Slc4a4	solute carrier family 4 (anion exchanger),,solute carrier family 4 (anion exchanger),,
70083	7.17	6.53	9.92	19.65	14.37	16.49	Metrn	meteorin
54524	18.44	16.93	11.90	31.26	36.25	34.67	Syt6	synaptotagmin 6,synaptotagmin 6,synaptotagmin 6,synaptotagmin 6,
12331	74.04	52.76	55.80	129.56	121.75	142.08	Cap1	CAP, adenylate cyclase-associated protein 1,CAP, adenylate cyclase-associated protein 1,CAP, adenylate cyclase-associated protein 1,CAP, adenylate cyclase-associated protein 1,
24105	17.32	9.57	16.78	34.57	28.35	31.23	Rbck1	RanBP-type and C3HC4-type zinc finger containing
76157	10.46	13.63	8.15	17.49	27.66	25.32	Slc35d3	solute carrier family 35, member D3
56213	15.84	10.53	14.84	34.26	24.28	31.21	Htra1	HtrA serine peptidase 1,HtrA serine peptidase 1,
53625	19.37	18.15	16.39	33.72	45.01	40.11	B3gnt2	UDP-GlcNAc:betaGal,UDP-GlcNAc:betaGal,UDP-GlcNAc:betaGal,
320292	16.67	13.09	12.51	27.48	34.13	31.14	Rasgef1b	RasGEF domain family, member 1B isoform 1
268709	44.66	45.02	46.49	107.60	100.62	92.66	BC055107	downregulated in renal cell carcinoma,downregulated in renal cell carcinoma,downregulated in renal cell carcinoma,
100986	18.07	20.72	18.72	33.17	55.48	38.31	Akap9	A kinase (PRKA) anchor protein (yotiao) 9
108699	395.23	226.32	286.26	708.58	654.68	625.69	Chn1	chimerin (chimaerin) 1 isoform 1,chimerin (chimaerin) 1 isoform 1,
72148	6.80	7.68	5.37	11.64	15.31	17.31	2610019F03Rik	hypothetical protein LOC72148
217082	19.91	25.20	16.71	40.61	50.39	47.41	Hlf	hepatic leukemia factor,hepatic leukemia factor,hepatic leukemia factor,hepatic leukemia factor,
226922	9.03	8.48	7.56	16.96	20.62	19.16	Kcnq5	potassium voltage-gated channel, subfamily Q,
243725	37.23	47.19	36.23	74.92	112.44	86.15	Ppp1r9a	protein phosphatase 1, regulatory (inhibitor),protein phosphatase 1, regulatory (inhibitor),protein phosphatase 1, regulatory (inhibitor),protein phosphatase 1, regulatory (inhibitor),
235431	23.91	15.07	19.58	52.19	29.33	50.84	Coro2b	coronin, actin binding protein, 2B
666704	8.45	5.91	8.95	19.44	12.51	20.94	Samd1	sterile alpha motif domain containing 1
211187	10.45	7.19	9.85	21.27	17.48	24.37	Lrtm2	leucine-rich repeats and transmembrane domains,leucine-rich repeats and transmembrane domains,
66355	14.21	10.04	13.89	26.01	25.77	34.93	Gmpr	guanosine monophosphate reductase
12801	22.63	25.90	19.51	47.83	62.79	46.78	Cnr1	cannabinoid receptor 1 (brain)
21802	16.59	11.78	10.62	29.01	27.27	33.83	Tgfa	transforming growth factor alpha
11941	56.20	34.43	41.52	113.50	94.42	97.94	Atp2b2	plasma membrane calcium ATPase 2 isoform 1,plasma membrane calcium ATPase 2 isoform 1,
246317	7.61	6.18	5.91	13.09	19.37	13.91	Neto1	neuropilin- and tolloid-like protein 1
360013	13.25	8.08	14.62	33.72	22.78	27.86	Myo18a	myosin XVIIIa,myosin XVIIIa,myosin XVIIIa,myosin XVIIIa,myosin XVIIIa,
23936	34.95	35.64	33.84	104.73	58.85	84.96	Lynx1	Ly6/neurotoxin 1
210135	9.97	8.02	8.87	20.83	16.57	26.57	Zfp180	zinc finger protein 180
19699	7.06	6.03	5.80	12.16	18.46	14.09	Reln	reelin precursor,reelin precursor,

58208	36.18	30.50	27.28	58.54	74.06	92.48	Bcl11b	B-cell leukemia/lymphoma 11B isoform b
330941	27.33	30.88	24.65	55.89	68.97	74.01	AI593442	hypothetical protein LOC330941 isoform 2
50781	18.31	14.72	18.30	47.02	43.16	32.78	Dkk3	dickkopf homolog 3,dickkopf homolog 3,
24064	15.90	11.73	17.36	34.57	40.42	34.87	Spry2	sprouty homolog 2
16492	10.18	8.85	7.18	14.66	26.11	23.98	Kcna4	potassium voltage-gated channel, shaker-related
211652	12.07	8.42	11.45	29.45	21.68	26.70	Wwc1	WW, C2 and coiled-coil domain containing 1,WW, C2 and coiled-coil domain containing 1,
67326	25.51	17.49	16.51	54.21	42.04	52.09	1700037H04Rik	hypothetical protein LOC67326,hypothetical protein LOC67326,
216527	21.75	11.93	18.36	47.23	35.94	46.66	Ccm2	cerebral cavernous malformation 2 homolog,cerebral cavernous malformation 2 homolog,
66259	439.45	272.94	289.39	699.17	929.87	923.40	Camk2n1	calcium/calmodulin-dependent protein kinase II
12295	18.95	11.08	18.23	50.01	33.96	38.06	Cacnb1	calcium channel, voltage-dependent, beta 1
55984	14.67	9.37	11.53	33.78	23.17	34.55	Camkk1	calcium/calmodulin-dependent protein kinase
72003	7.16	5.40	6.50	15.20	14.76	19.37	Synpr	synaptoporin,synaptoporin,
19045	137.87	78.92	114.38	301.55	213.71	335.99	Ppp1ca	protein phosphatase 1, catalytic subunit, alpha
218194	154.47	94.47	104.71	305.78	256.12	361.56	Phactr1	phosphatase and actin regulator 1 isoform 1,phosphatase and actin regulator 1 isoform 1,
64378	201.71	192.76	137.69	391.27	502.88	502.71	Gpr88	G-protein coupled receptor 88
12294	35.54	25.59	22.57	65.07	69.19	80.26	Cacna2d3	calcium channel, voltage-dependent, alpha2/delta
18751	121.17	107.26	99.07	288.32	265.87	306.74	Prkcb1	protein kinase C, beta 1,protein kinase C, beta 1,
14608	6.16	9.11	7.72	17.54	18.16	24.81	Gpr83	G protein-coupled receptor 83
21916	15.69	10.93	14.09	26.80	41.78	38.79	Tmod1	tropomodulin 1
383787	15.01	9.72	9.56	28.74	25.55	37.03	Gm1337	hypothetical protein LOC383787
68617	7.09	5.04	6.95	19.17	16.12	15.43	1110012J17Rik	hypothetical protein LOC68617
110351	39.96	23.05	34.24	100.22	63.08	92.66	Rap1gap	Rap1 GTPase-activating protein,Rap1 GTPase-activating protein,
103534	6.82	4.10	5.64	16.58	12.96	14.25	Mgat4b	mannoside acetylglucosaminyltransferase 4,
225724	8.87	5.62	6.05	17.32	14.72	22.99	Mapk4	mitogen-activated protein kinase 4
140904	30.71	21.30	23.48	69.32	63.23	69.65	Caln1	calneuron 1,calneuron 1,
19735	7.61	6.54	5.34	15.82	19.85	17.38	Rgs2	regulator of G-protein signaling 2
56613	6.39	4.06	6.28	16.33	13.51	15.66	Rps6ka4	ribosomal protein S6 kinase, polypeptide 4
218772	16.33	20.76	11.70	32.14	53.90	49.44	Rarb	retinoic acid receptor, beta,retinoic acid receptor, beta,
29863	23.73	24.04	15.53	43.14	66.46	69.25	Pde7b	phosphodiesterase 7B
171180	7.18	4.88	4.41	14.52	14.18	18.85	Syt12	synaptotagmin XII
110279	24.05	16.90	20.93	62.95	52.80	63.32	Bcr	breakpoint cluster region homolog
12326	15.74	18.88	18.74	38.50	59.37	58.60	Camk4	calcium/calmodulin-dependent protein kinase IV
13134	7.42	8.35	5.72	17.32	20.22	25.72	Dach1	dachshund 1 isoform 1
13653	37.28	21.56	30.21	91.31	101.36	70.68	Egr1	early growth response 1
108069	11.01	9.53	9.25	22.19	39.11	27.22	Grm3	glutamate receptor, metabotropic 3
16497	60.83	62.65	52.00	136.67	235.37	185.40	Kcnab1	potassium voltage-gated channel, shaker-related,potassium voltage-gated channel, shaker-related,
19736	140.10	87.61	90.19	281.08	374.15	374.16	Rgs4	regulator of G-protein signaling 4
65112	9.59	8.39	8.36	24.14	29.72	36.41	Tmepai	transmembrane prostate androgen-induced protein
240185	16.10	10.31	11.71	46.24	45.14	44.35	9430020K01Rik	hypothetical protein LOC240185
268980	11.52	10.37	11.04	33.82	43.64	40.60	Strn	striatin, calmodulin binding protein,striatin, calmodulin binding protein,
13488	31.52	26.32	19.36	66.39	108.41	110.37	Drd1a	dopamine receptor D1A
16438	42.62	25.73	32.76	136.00	148.19	140.37	Itpr1	inositol 1,4,5-triphosphate receptor 1,inositol 1,4,5-triphosphate receptor 1,
12672	6.93	4.30	6.34	29.68	22.11	29.79	Chrm4	cholinergic receptor, muscarinic 4
59046	294.35	277.06	230.45	1236.64	1872.51	1236.21	Arpp19	cAMP-regulated phosphoprotein 19,cAMP-regulated phosphoprotein 19,
18619	250.34	166.19	168.00	1241.14	900.62	1510.07	Penk1	preproenkephalin 1,preproenkephalin 1,

Table A-7: RNA-Seq quality control statistics.

	Sample	Uniquely Mapped Reads	% RiboMapping	Exon/ Intron	Exon/Intergenic
12wk Cortex	TCM9452	94650265	1.54	66	1425
	TCM9450	63331484	1.83	53	1284
	TCM9453	43802713	0.88	71	1627
	TCW9451	51901171	1.01	64	1463
	TCW9457	36584094	1.47	50	1025
	TCW9469	38851786	2.38	63	1290
12wk Striatum	TSM492	81770912	1.54	112	1820
	TSM482	30615950	0.24	113	1386
	TSM490	35265655	1.18	74	1223
	TSW478	33903978	1.67	226	2703
	TSW479	29887303	2.64	50	860
	TSW491	38189661	1.58	166	1961
8wk Cortex	ECM184	77451625	2.08	197	3218
	ECM175	49188623	1.32	49	891
	ECM181	34519532	2.22	121	1767
	ECW176	26427631	0.40	86	1316
	ECW178	23386626	0.31	76	1043
	ECW180	49446456	0.85	261	3025
8wk Striatum	ESM181	30710040	1.26	52	479
	ESM184	39029238	1.19	66	657
	ESM192	46517561	1.26	90	812
	ESW176	21130789	0.30	41	627
	ESW180	26718080	0.80	61	522
	ESW183	27546062	0.68	56	445

Table A-8: ChIP-Seq quality control statistics.

Internal Sample Name	ChIP	Strain	Tissue	Age (weeks)	Replicate	# of aligned reads	# of events identified by GPS	gps alpha	gps mrc	total reads in events
"80-3"	H3K4me3	WT	Cortex	8	1	10222679				
"80-4"	H3K4me3	WT	Cortex	8	2	9707069				
"80-1"	H3K4me3	R6/2	Cortex	8	1	9196937				
"80-2"	H3K4me3	R6/2	Cortex	8	2	10669926				
"31-5"	H3K4me3	WT	Cortex	12	1	22215459				
"31-7"	H3K4me3	WT	Cortex	12	2	23009906				
"31-1"	H3K4me3	R6/2	Cortex	12	1	21794587				
"31-3"	H3K4me3	R6/2	Cortex	12	2	26300880				
"80-7"	H3K4me3	WT	Striatum	8	1	7828697				
"80-8"	H3K4me3	WT	Striatum	8	2	9782274				
"80-5"	H3K4me3	R6/2	Striatum	8	1	9777020				
"80-6"	H3K4me3	R6/2	Striatum	8	2	9303749				
"38-1"	H3K4me3	WT	Striatum	12	1	34136203				
"41-1"	H3K4me3	WT	Striatum	12	2	24890699				
"38-7"	H3K4me3	R6/2	Striatum	12	1	28019623				
"41-3"	H3K4me3	R6/2	Striatum	12	2	25311508				
	H3K4me3	WT	Cortex	8	1+2	19929748	19429	20	1	2041414
	H3K4me3	R6/2	Cortex	8	1+2	19866863	18671	20	1	1850555
	H3K4me3	WT	Cortex	12	1+2	45225365	40879	20	1	20473822
	H3K4me3	R6/2	Cortex	12	1+2	48095467	33583	20	1	9090196
	H3K4me3	WT	Striatum	8	1+2	17610971	16267	20	1	1247873
	H3K4me3	R6/2	Striatum	8	1+2	19080769	17997	20	1	1564600
	H3K4me3	WT	Striatum	12	1+2	59026902	51941	20	1	8770881
	H3K4me3	R6/2	Striatum	12	1+2	53331131	42639	20	1	5696703

Appendix B - Supplement for Chapter 3

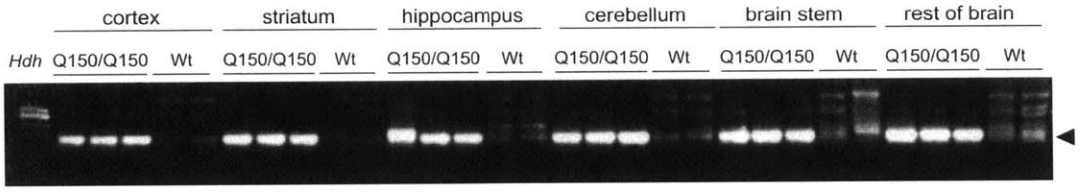

Figure B-1: 3'RACE in other brain regions.

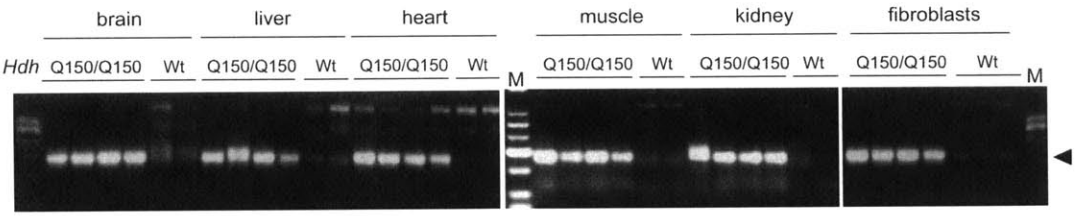

Figure B-2: 3'RACE in peripheral tissues.

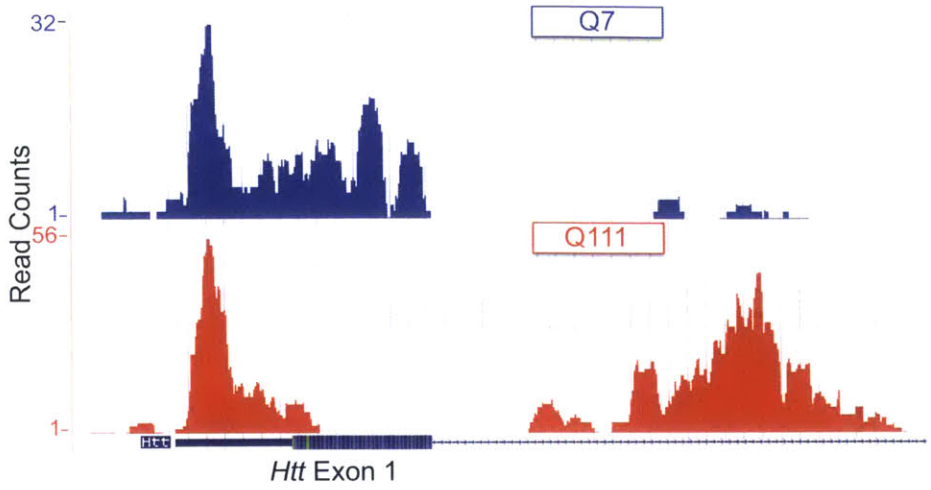

Figure B-3: Publicly available RNA-Seq data from a cell model of HD shows poor coverage of the *Htt* exon 1-intron 1 region. STHdh Q7/Q7 (are controls) and STHdh Q111/Q111 (HD) cells. Data is from (Ng et al., 2013) and visualized with the UCSC genome browser at `http://genome.ucsc.edu/cgi-bin/hgTracks?db=mm9&position=chr5%3A35103500-35106500&hgsid=431310535_rB8DiFy6yB2OfbDdipWgApaNWUNO`

> test sequence
Length of sequence - 11850
9 potential polyA sites were predicted

Pos.:	863	LDF-	3.54	sequence	GG**AATAAA**AC
Pos.:	1392	LDF-	3.09	sequence	GG**AATAAA**AT
Pos.:	1405	LDF-	2.68	sequence	GG**AATAAA**TT
Pos.:	2707	LDF-	5.30	sequence	TA**AATAAA**AT
Pos.:	4565	LDF-	1.31	sequence	GG**AATAAA**GA
Pos.:	7324	LDF-	6.73	sequence	AA**AATAAA**AT
Pos.:	8834	LDF-	1.15	sequence	GT**AATAAA**AA
Pos.:	9937	LDF-	0.76	sequence	AA**AATAAA**TA
Pos.:	11593	LDF-	1.47	sequence	AA**AATAAA**GT

Figure B-4: Prediction of cryptic polyadenylation signals in human intron 1 of *HTT* using the SoftBerry POLYAH algorithm. The algorithm predicts the potential position of a polyA signal by linear discriminant functions combining characteristics describing various contextual features of these sites. The default LDF threshold ("weight" of predicted sites) in the server is equal to 0. ♦, sites that were predicted; •, site used in YAC128 mice and in human Huntington disease tissues.

Sample no.	Total	Uniquely mapping	% uniquely mapping	Ribo mapping	% ribo mapping	Exon/intron	Exon/intergenic
6-mo.							
Hom 117	58088390	48599615	84	22723	0.05	70	1034
Hom 118	77528134	64398258	83	8146	0.01	61	935
Wt 43	90864660	75003852	83	14517	0.02	109	1354
Wt 46	44043910	36072275	82	6350	0.02	95	1294
22-mo.							
Hom 74	107693082	90260412	84	199891	0.22	181	3193
Hom 84	129917678	109578186	84	151925	0.14	92	2190
Wt 71	139655344	117257850	84	636391	0.54	76	1907
Wt 87	103948402	85726377	82	292999	0.34	217	3330

Table B-1: QC on RNA-Seq libraries.

Name	Sequence	Position from start of HTT intron 1; start/end in bp	Function
–19f	AGGAACCGCTGCACCGA	–19/–3	qRT-PCR/RT-PCR
135f	CTTGCGGGGTCTCTGGC	135/151	qRT-PCR/RT-PCR
200r	TCAGCGAGTCCCTGGCTG	183/200	qRT-PCR/RT-PCR
155p	CCTCAGAGGAGACAGAGCCGGGTCA	155/179	qRT-PCR/RT-PCR
347f	TCCTCATCAGGCCTAAGAGCTGG	347/369	qRT-PCR/RT-PCR
431r	GAGACCTCCTAAAAGCATTATGTCATC	405/431	qRT-PCR/RT-PCR
371p	AGTGCAGGACAGCGTGAGAGATGTG	371/395	qRT-PCR/RT-PCR
785r	TGAAAACTGAGCACCACCAATG	764/785	RT-PCR
1006f	GAAATCCATGCTGAGTGTTGAGC	1006/1028	qRT-PCR/RT-PCR
1072r	TGCCCAGAGTTGAGAGAAAGGA	1051/1072	qRT-PCR/RT-PCR
571f	AACCAGGTTTTAAGCATAGCCAGA	571/594	3'RACE
622f	AGTTGGATGAGTTGTATTTGTCAAGTACAT	622/651	3'RACE
Qt	CCAGTGAGCAGAGTGACGAGGACTCGAGCTCAAGC(T)18		RT
OligodT	(T)18		RT
Qo	CCAGTGAGCAGAGTGACG		3'RACE
Qi	GAGGACTCGAGCTCAAGC		3'RACE
5'UTR 1f	CTTGGTTCCGCTTCTGCC	–323/–306	qRT-PCR/RT-PCR
5'UTR 1r	TGGAGCCTACTGGCACTACG	–241/–260	qRT-PCR/RT-PCR
5'UTR 1p	CAGAGCCCCATTCATTGCCTTGCT	–298/–275	qRT-PCR/RT-PCR
ex2f	AAGAAGGAACTCTCAGCCACCA	Exon 2	qRT-PCR/RT-PCR
ex2r	CTGAGAGACTGTGCCACAATGTT	Exon 2	qRT-PCR/RT-PCR
ex2p	AGAAAGACCGTGTGAATCATTGTCTAACAATATGTGA	Exon 2	qRT-PCR/RT-PCR

f, forward; *P*, probe; qRT-PCR, qualitative RT-PCR; r, reverse.

Table B-2: Primers used for amplification of mouse *Htt* 3'RACE, RT-PCR, and QPCR products.

Tissue	Sample identification	CAG length	Postmortem delay, h	Sex	Age, y
Brain	H132	15/19	12	F	63
	H130	Normal range	13	M	32
	HC105	15/42	9	F	67
	HC76	19/42	16	M	71
	HD1	20/72	21	F	11
	HD2	17/72	3	F	20
Fibroblasts	Da.R.	15/31			
	4845*	16/20			
	5539*	18/68			
	9197*	21/181			

F, female; M, male.
*4845, 5539, and 9197 (Coriel Cell Repository).

Table B-3: Information on human postmortem brains and human fibroblasts.

Name	Sequence	Position from start of HTT intron 1: start/end in bp	Function
UAPdT18	GGCCACGCGTCGACTAGTAC(T)18		RT
UAPnest	GGCCACGCGTCGACTAGTAC		3'RACE
6568f	TCAAGACATTCTCCTGCACGG	6568/6588	3'RACE
6621f	CACCACACCCAGCTAATTTTGTAT	6621/6644	3'RACE
7128f	GAGGACTTTTGGAGATGTAAAGGC	7128/7151	3'RACE

Table B-4: Primers used for amplification of human *HTT* 3'RACE product.

Appendix C - Supplement for Chapter 4

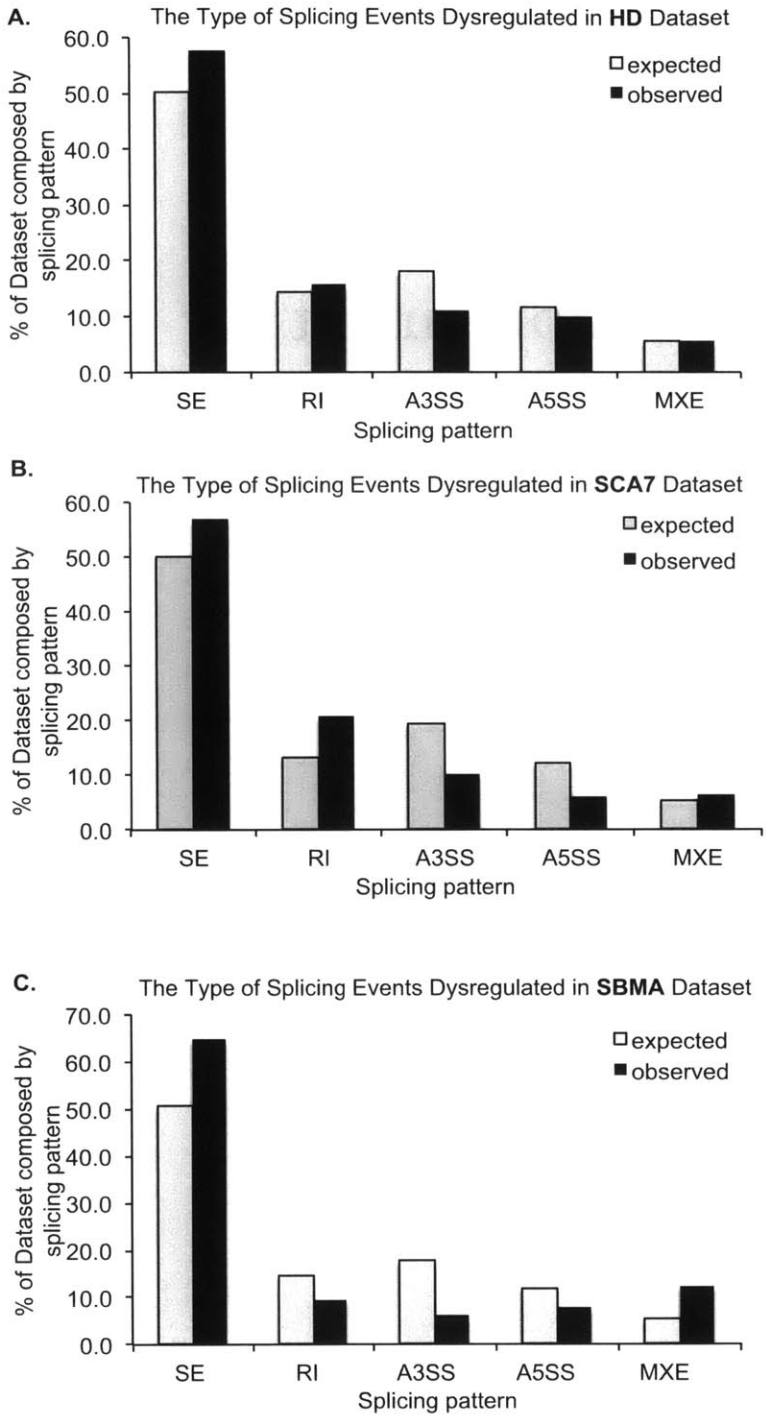

Figure C-1: Splicing pattern composition for dysregulated splicing events identified in A) HD, B) SCA7, and C) SBMA. Expected % is derived from composition of all splicing events with coverage in each dataset. PolyQ proteins do not seem to largely affect a specific type of splicing event.

Table C-1: The list of dysregulated splicing events in **HD** muscle.

gid	wt1	wt2	wt3	wt4	mut1	mut2	mut3	mut4	refseq_id	ensq_id	gsymbol	event	zscores	SigDiff	abs(Wt-Mut)
chr7:31358979:31359085:-@chr7:31355857|31355860:31355720:-	0.86	NA	0.91	NA	0.21	NA	NA	0.23	NM_029274	ENSMUSG00000006307	Wbp7	A3SS	2.06	0.63	0.66
chr5:149996136:149996382:+@chr5:149999284:149999452:+@chr5:149999921:150000049:+	0.24	0.32	NA	0.26	0.79	0.62	0.71	0.77	NM_001013378,NM_001115151,NM_001115149,NM_001115150	ENSMUSG00000041264	Uspl1	SE	4.9	0.3681	0.45
chr8:108201115:108201250:+@chr8:108203971|108203974:108204159:+	0.88	NA	0.93	0.96	0.48	0.38	0.48	0.57	NM_181322	ENSMUSG00000005698	Ctcf	A3SS	5.01	0.3647	0.45
chr11:5879676:5879724:-@chr11:5876768:5876896:-@chr11:5872816:5872891:-	0.83	0.81	0.81	0.75	0.35	0.43	0.34	0.33	NM_001174054,NM_007595,NM_001174053	ENSMUSG00000057897	Camk2b	SE	6.65	0.3917	0.44
chr16:98174258-98172635:-@chr16:98172034-98168599:-	NA	NA	0.82	0.75	0.25	0.47	0.23	0.43	NM_001081684,NM_001081685,NM_175428	ENSMUSG00000046962	Zfp295	RI	3.45	0.3014	0.44
chr14:27237599:27237733:-@chr14:27235689:27235778:-@chr14:27232661:27234474:-	0.64	0.91	0.72	0.9	0.37	0.39	0.4	0.34	NM_032008	ENSMUSG00000021870	Slmap	SE	5.63	0.3183	0.42
chr11:104163675:104163724:+@chr11:104166627:104166723:+@chr11:104167940:104168072:+	0.85	0.88	0.83	0.83	0.4	0.56	0.44	0.41	NM_001038609,NM_010838	ENSMUSG00000018411	Mapt	SE	6.31	0.3383	0.39
chr10:110387739-110387617:-@chr10:110386739-110386677:-	0.62	0.66	0.65	0.81	0.18	0.34	0.21	0.44	NM_172554	ENSMUSG00000035798	Zdhhc17	RI	5.49	0.2683	0.39
chr4:154460314:154460406:-@chr4:154457345|154457426:154457218:-	0.85	0.91	0.81	0.82	0.32	0.59	0.41	0.51	NM_026395	ENSMUSG00000029048	Rer1	A3SS	6.04	0.2867	0.39
chrX:98488764:98488960|98488969:+@chrX:98489132:98489209:+	NA	NA	0.89	0.89	0.54	0.61	0.5	0.4	NM_021521	ENSMUSG00000079487	Med12	A5SS	3.8	0.2818	0.38
chr4:116284577:116284686:-@chr4:116283008:116283982:-@chr4:116278289:116278368:-	0.45	0.79	0.57	0.71	0.18	0.41	0.14	0.3	NM_001081475,NM_016777	ENSMUSG00000028693	Nasp	SE	3.73	0.1983	0.37
chr10:126721391:126721541:-@chr10:126721268|126721271:126721099:-	NA	NA	0.9	0.9	0.65	NA	0.46	0.51	NM_033072	ENSMUSG00000025409	Mbd6	A3SS	2.52	0.265	0.36
chr5:149996136:149996382:+@chr5:149999284:149999410:+@chr5:149999921:150000049:+	0.19	0.3	NA	0.24	0.61	0.48	0.62	0.68	NM_001013378,NM_001115151,NM_001115149,NM_001115150	ENSMUSG00000041264	Uspl1	SE	4.45	0.2619	0.35
chr4:136148880:136149045:-@chr4:136137955:136138014:-@chr4:136132986:136133119:-	NA	NA	0.38	0.16	0.72	0.49	0.57	0.71	NM_133872	ENSMUSG00000036940	Kdm1a	SE	2.98	0.2025	0.35
chr2:126739268:126739324:-@chr2:126739036:126739089:-@chr2:126738379:126738481:-	0.69	0.66	0.61	0.64	0.35	0.35	0.25	0.28	NM_023220	ENSMUSG00000027366	010106G01R	SE	6.7	0.29	0.34
chr3:65760775:65760884:-@chr3:65759126:65759198:-@chr3:65755356:65755476:-	0.31	0.09	0.27	NA	0.73	0.45	0.4	0.64	NM_019937	ENSMUSG00000027829	Ccnl1	SE	2.7	0.1517	0.33
chr15:99082293:99082392:-@chr15:99080894:99081013:-@chr15:99080307:99080445:-	NA	0.36	0.43	0.33	0.74	NA	0.62	0.74	NM_001164156,NM_016766	ENSMUSG00000037570	Mcrs1	SE	3.5	0.2533	0.33
chr2:155393623-155393429:-@chr2:155392620-155392539:-	0.71	0.81	0.87	0.81	0.36	0.41	0.54	0.57	NM_008180	ENSMUSG00000027610	Gss	RI	5.37	0.2267	0.33
chr9:71717881:71717954:-@chr9:71716806:71716877:-@chr9:71715879:71716085:-	0.81	0.64	NA	NA	0.37	0.37	0.46	0.42	NM_011544	ENSMUSG00000032228	Tcf12	SE	4.66	0.25	0.32
chr11:29605535:29605591:+@chr11:29606410:29608770:+@chr11:29633633:29633840:+	0.1	0.11	0.16	0.11	0.47	0.31	0.51	0.45	NM_194053,NM_194052,NM_024226,NM_194054,NM_194051	ENSMUSG00000020458	Rtn4	SE	5.58	0.2483	0.32
chr5:111812008:111812130:+@chr5:111814540:111814624:+@chr5:111815523:111817379:+	0.8	0.87	0.68	0.52	0.32	0.52	0.33	0.45	NM_019640	ENSMUSG00000050017	Pitpnb	SE	3.11	0.155	0.31
chr6:58781883:58781926:+@chr6:58782396:58782530:+@chr6:58793598:58793852:+	NA	0.56	NA	0.49	0.7	0.92	0.9	0.82	NM_028705	ENSMUSG00000029804	Herc3	SE	3.01	0.1943	0.31
chr1:120421874:120422032:+@chr1:120428555:120428662:+@chr1:120435843:120435946:+	0.2	0.21	0.07	0.18	0.54	0.33	0.5	0.51	NM_177548,NM_029709,NM_001081276	ENSMUSG00000064302	Clasp1	SE	5	0.215	0.31
chr11:104163675:104163724:+@chr11:104166526:104166723:+@chr11:104167940:104168072:+	0.94	0.95	0.9	0.9	0.53	0.74	0.6	0.6	NM_001038609,NM_010838	ENSMUSG00000018411	Mapt	SE	5.65	0.2367	0.31
chr9:83004713-83004641:-@chr9:83004036-83003555:-	0.36	NA	NA	0.48	0.61	0.72	0.74	0.8	NM_175074,NM_026122	ENSMUSG00000066456	Hmgn3	RI	3.59	0.1961	0.3
chr18:77424586:77424964:+@chr18:77450395:77450502:+@chr18:77471532:77471624:+	0.6	0.74	0.56	0.83	0.55	NA	0.27	0.35	NM_013666,NM_153124	ENSMUSG00000025425	St8sia5	SE	2.31	0.1247	0.29
chr12:56160565:56160362|56160444:-@chr12:56158229:56158339:-	0.47	0.5	0.53	NA	0.84	0.77	0.82	0.72	NR_030764,NM_028314	ENSMUSG00000062198	700097O09R	A5SS	4.86	0.2286	0.29
chr14:70634947:70635015:-@chr14:70625735:70625761:-@chr14:70624774:70624855:-	0.74	0.58	0.63	0.59	0.4	0.42	0.35	0.24	NM_008915	ENSMUSG00000022092	Ppp3cc	SE	6.46	0.19	0.28
chr11:84671942:84672040:-@chr11:84667757:84667882:-@chr11:84667556:84667669:-	0.58	0.52	0.61	0.6	0.2	0.36	0.21	0.43	NM_153144	ENSMUSG00000020530	Ggnbp2	SE	4.56	0.1833	0.28
chr6:86906253:86906566:+@chr6:86909026:86909268:+@chr6:86913987:86914219:+	0.75	0.62	0.85	NA	NA	0.55	0.38	0.45	NM_001040106,NM_177762	ENSMUSG00000057230	Aak1	SE	2.49	0.1467	0.28

chr6:125169604-125169655:+@chr6:125170068-125172324:+	0.21	0.23	0.14	0.09	0.54	0.39	0.43	0.41	NM_009496	ENSMUSG00000030337	Vamp1	RI	6.34	0.195	0.28
chr2:148535169:148532895|148535053:-@chr2:148532682:148532759:-	0.6	0.6	0.68	0.64	0.42	0.37	0.23	0.39	NM_019632	ENSMUSG00000027438	Napb	A5SS	6.68	0.205	0.28
chr10:107689813:107689980:+@chr10:107690381:107690551:+@chr10:107696812:107696902:+	0.94	0.92	0.76	0.63	0.62	0.54	0.41	0.59	NM_027892	ENSMUSG00000019907	Ppp1r12a	SE	2.93	0.125	0.27
chr5:31846043:31846286:+@chr5:31848553:31848639:+@chr5:31850984:31851054:+	0.41	0.86	0.46	NA	0.27	0.35	0.31	0.31	NM_009206	ENSMUSG00000029141	Slc4a1ap	SE	3.28	0.14	0.27
chr2:29575113:29575370:+@chr2:29576163:29576258:+@chr2:29577744:29577829:+	0.61	0.53	0.49	0.47	0.26	0.29	0.23	0.23	NM_001039086,NM_001039087,NM_054050	ENSMUSG00000039844	Rapgef1	SE	6.57	0.2167	0.27
chr11:80068162:80068364:+@chr11:80071016:80071138:+@chr11:80079244:80081409:+	0.55	0.67	0.7	0.73	0.41	0.39	0.31	0.47	NM_001163354,NM_001163355,NM_021536	ENSMUSG00000017686	Rhot1	SE	4.95	0.1783	0.27
chr2:52042931:52043035:-@chr2:52041532:52041636:-@chr2:52040791:52040895:-@chr2:52039252:52039356:-	0.85	0.76	0.94	0.93	0.66	0.56	0.46	0.73	NM_010889	ENSMUSG00000026950	Neb	MXE	3.77	0.14	0.27
chr19:7542301:7542357:-@chr19:7531950|7532913:7530790:-	0.68	0.72	0.82	0.88	0.56	0.6	0.41	0.46	NM_001003933,NM_053076,NM_001003934	ENSMUSG00000024758	Rtn3	A3SS	4.58	0.1533	0.27
chr3:89806201:89806398:-@chr3:89805740:89805790:-@chr3:89803511:89804175:-	0.28	0.22	NA	0.29	0.58	0.51	0.47	0.52	NM_153489,NM_028475	ENSMUSG00000042520	Ubap2l	SE	5.11	0.2033	0.26
chr3:87723467:87723573:+@chr3:87723725:87723750:+@chr3:87725739:87725970:+	0.04	0.29	NA	0.39	0.53	0.52	0.55	0.38	NM_026591	ENSMUSG00000019710	Mrpl24	SE	2.65	0.1211	0.26
chr8:11628439:11628530:-@chr8:11623697:11623858:-@chr8:11619062:11619297:-	0.52	0.49	0.41	0.38	0.1	0.29	0.21	0.17	NR_030779,NM_133971,NM_001167967	ENSMUSG00000031508	Ankrd10	SE	5.12	0.165	0.26
chr15:79195715:79195909:-@chr15:79194088:79194108:-@chr15:79191114:79193315:-	0.79	0.7	NA	NA	0.49	0.55	0.54	0.34	NM_172608	ENSMUSG00000009035	Tmem184b	SE	3.32	0.155	0.26
chr15:79158640:79158801:-@chr15:79158065:79158144:-@chr15:79148191:79148440:-	0.93	0.78	0.73	0.89	0.59	0.57	0.57	0.58	NA	ENSMUSG00000042632	Pla2g6	SE	5.56	0.19	0.26
chr6:38504980:38505063:+@chr6:38518847:38518917:+@chr6:38520510:38520604:+	0.54	0.66	0.58	0.42	0.18	0.39	0.29	0.32	NM_001170849,NM_138680,NM_001170848	ENSMUSG00000029823	Luc7l2	SE	4.06	0.1367	0.26
chr6:146499161:146499296:-@chr6:146498609:146498686:-@chr6:146498154:146498507:-	0.39	0.83	NA	NA	0.34	0.29	0.41	0.35	NM_138757	ENSMUSG00000040250	9334248B01R	SE	2.29	0.1518	0.26
chr2:148535169-148535053:-@chr2:148532941-148532895:-	NA	NA	0.74	0.71	0.53	0.5	0.32	0.52	NM_019632	ENSMUSG00000027438	Napb	RI	3.21	0.1604	0.26
chr16:10595895:10596078|10596126:+@chr16:10611096:10611228:+	0.14	0.31	0.32	0.2	0.51	0.29	0.68	0.53	NM_177562,NM_001204229	ENSMUSG00000068663	Clec16a	A5SS	2.62	0.1129	0.26
chrX:99754904:99755073:-@chrX:99752435:99752611:-@chrX:99750865:99750956:-	0.76	0.8	0.71	0.78	0.43	0.59	0.51	0.52	NM_008832,NM_173021	ENSMUSG00000034055	Phka1	SE	5.96	0.185	0.25
chr4:9563048:9563116:-@chr4:9537990:9538085:-@chr4:9531663:9531776:-	0.16	0.17	0.12	0.19	0.37	0.36	0.52	0.37	NM_001177854,NM_001177852,NM_001177853,NM_001177851,NM_001177850,NM_001177849,NM_023066	ENSMUSG00000028207	Asph	SE	6.87	0.1867	0.25
chr11:102086048:102086269:-@chr11:102080459:102080595:-@chr11:102079730:102080095:-	NA	0.2	0.23	0.33	0.42	0.51	0.46	0.62	NM_010412,NM_001077696	ENSMUSG00000008855	Hdac5	SE	3.84	0.1481	0.25
chr11:80069364:80069459:+@chr11:80071016:80071138:+@chr11:80079244:80081409:+	NA	0.81	0.89	0.72	0.53	0.57	0.41	0.71	NM_001163354,NM_001163355,NM_021536	ENSMUSG00000017686	Rhot1	SE	2.36	0.1094	0.25
chr19:6335039-6335082:+@chr19:6335445-6335905:+	NA	0.15	NA	0.3	0.49	0.38	0.45	0.59	NM_001168488,NM_001168489,NM_008583,NM_001168490	ENSMUSG00000024947	Men1	RI	3.05	0.1354	0.25
chr7:13397015:13395046|13396155:-@chr7:13393261:13393322:-	0.94	0.97	0.92	0.94	0.44	0.85	0.7	0.78	NM_026046	ENSMUSG00000057894	Zfp329	A5SS	4.76	0.1283	0.25
chr19:56452545:56452661:-@chr19:56448854:56448958:-@chr19:56447297:56447404:-	0.77	0.78	0.75	0.75	0.46	0.57	0.53	0.54	NM_198059,NM_008733	ENSMUSG00000049134,ENSMUSG00000092491	ap,AC115771	SE	6.8	0.2	0.24
chr10:57226003:57226108:+@chr10:57228867:57228920:+@chr10:57231250:57231334:+	0.36	0.51	0.2	0.39	0.57	0.58	0.63	0.63	NM_008297	ENSMUSG00000019878	Hsf2	SE	4.46	0.1383	0.24
chr7:29551771:29551886:+@chr7:29552651:29552697:+@chr7:29556830:29556878:+	0.59	0.59	0.54	0.6	0.26	0.35	0.28	0.46	NM_001122765,NM_001122766	ENSMUSG00000015149	Sirt2	SE	4.8	0.1717	0.24

chr11:70422668:70422756:+@chr11:70422910:70422933:+@chr11:70423056:70423219:+	NA	NA	0.43	0.53	0.71	0.64	0.75	0.78	NM_016713,NM_001045964,NM_176893,NM_001045959	ENSMUSG00000020827	Mink1	SE	3.72	0.16	0.24
chr5:69958367-69958500:+@chr5:69959635-69959736:+	0.35	0.45	0.28	0.29	0.62	0.58	0.51	0.6	NM_172711	ENSMUSG00000029208	Guf1	RI	4.62	0.1583	0.24
chr6:140599277-140599303:+@chr6:140599837-140601347:+	0.63	0.68	0.72	0.69	0.93	0.89	0.95	0.9	NM_009637,NM_178803,NM_001005605	ENSMUSG00000030232	Aebp2	RI	6.72	0.1967	0.24
chr6:145163042-145163304:+@chr6:145163704-145163791:+	0.63	0.58	0.51	0.51	0.28	0.37	0.32	0.3	NM_001163628,NM_133688	ENSMUSG00000040370	Lyrm5	RI	6.13	0.18	0.24
chr3:88512702:88512863:+@chr3:88513752|88513780:88513864:+	0.9	0.44	0.85	NA	0.48	0.54	0.49	0.45	NM_028814	ENSMUSG00000028060	810403A07R	A3SS	2.09	0.14	0.24
chr12:99931767:99931827:-@chr12:99931082:99931166:-@chr12:99926400:99927838:-	0.93	0.81	0.9	0.88	0.59	0.74	0.6	0.66	NM_011877,NM_001146199	ENSMUSG00000021009	Ptpn21	SE	4.9	0.1583	0.23
chr9:44511886:44511975:-@chr9:44509029:44509169:-@chr9:44507639:44507779:-	NA	NA	0.74	0.54	0.4	0.35	0.45	0.45	NM_153537	ENSMUSG00000048537	Phldb1	SE	3.83	0.1489	0.23
chr4:137990587:137990794:+@chr4:137992095:137992314:+@chr4:137993543:137993630:+	0.24	0.13	0.24	0.26	0.6	0.29	0.43	0.48	NM_026689	ENSMUSG00000041241	Mul1	SE	3.64	0.1183	0.23
chr11:77275886:77276256:+@chr11:77277158:77277225:+@chr11:77277354:77277612:+	0.04	0.12	0.08	0.08	0.33	0.29	0.29	0.33	NA	NA	NA	SE	6.65	0.1967	0.23
chr17:26416906:26417073|26417109:+@chr17:26418570:26422449:+	NA	0.69	NA	0.88	0.54	NA	0.56	0.55	NM_028190	ENSMUSG00000024188	Luc7l	A5SS	2.59	0.1775	0.23
chr3:65760775:65760884:-@chr3:65759052:65759198:-@chr3:65755356:65755476:-	0.36	0.19	0.32	0.44	0.58	0.46	0.5	0.66	NM_019937	ENSMUSG00000027829	Ccnl1	SE	3.73	0.1	0.22
chr3:136539053:136539111:+@chr3:136591546:136591583:+@chr3:136597993:136598743:+	0.22	0.15	0.14	0.01	0.41	0.37	0.36	0.25	NM_008913	ENSMUSG00000028161	Ppp3ca	SE	4.23	0.1233	0.22
chr8:129933456:129933607:+@chr8:129934629:129934673:+@chr8:129939470:129939697:+	NA	0.61	NA	0.79	0.53	0.45	0.47	0.47	NM_001013581,NM_001013580,NM_033620,NM_001122850	ENSMUSG00000025812	Pard3	SE	4.13	0.16	0.22
chr12:112093210:112094082:+@chr12:112099006:112099233:+@chr12:112102174:112102266:+	0.24	0.16	NA	0.45	0.44	0.59	0.56	0.44	NM_001199785,NM_028365	ENSMUSG00000021271	Zfp839	SE	2.16	0.0997	0.22
chr2:11401825:11401998:-@chr2:11399663:11399685:-@chr2:11393058:11396170:-	0.87	0.85	0.93	NA	0.49	0.79	0.71	0.67	NM_001177758,NM_001177753,NM_001177756,NM_001177757,NM_001177754,NM_001177755,NM_133232,NM_001177752	ENSMUSG00000026773	Pfkfb3	SE	2.59	0.0961	0.22
chrX:130604384-130604446:+@chrX:130607675-130607816:+	0.7	0.79	0.75	0.64	0.45	0.45	0.54	0.57	NM_133196	ENSMUSG00000031256	Cstf2	RI	4.76	0.1383	0.22
chr15:79158801:79158065|79158640:-@chr15:79148191:79148440:-	0.76	0.74	0.75	0.92	0.52	0.58	0.54	0.64	NA	ENSMUSG00000042632	Pla2g6	A5SS	5.79	0.1433	0.22
chr19:57123952:57123999:-@chr19:57121415:57121561:-@chr19:57119371:57119462:-	0.74	0.82	0.77	0.7	0.55	0.46	0.62	0.56	NM_178688,NM_001103178,NM_001103177	ENSMUSG00000025085	Ablim1	SE	5.62	0.1367	0.21
chr10:12981572:12981730:-@chr10:12977383:12977622:-@chr10:12973148:12973685:-	0.18	0.15	0.41	0.48	0.1	0.12	0.06	0.1	NM_001033257,NM_001195066,NM_001195065,NM_001195096	ENSMUSG00000062866	Phactr2	SE	2.51	0.0933	0.21
chrX:71330849:71330975:-@chrX:71325248:71325371:-@chrX:71282321:71282671:-	NA	0.37	0.39	0.4	0.61	0.54	0.53	0.71	NM_010788,NM_001081979	ENSMUSG00000031393	Mecp2	SE	3.94	0.1364	0.21
chr9:58736208:58736300:-@chr9:58732277:58732435:-@chr9:58728399:58728662:-	0.91	0.84	0.92	0.91	0.61	0.83	0.61	0.7	NM_001042752,NM_008684	ENSMUSG00000032340	Neo1	SE	3.41	0.125	0.21
chr8:123623052-123622608:-@chr8:123621825-123621457:-	0.36	0.36	0.21	0.3	0.49	0.43	0.55	0.61	NM_172761,NM_001166482	ENSMUSG00000031816	Mthfsd	RI	4.85	0.12	0.21
chr2:32226384-32226633:+@chr2:32226769-32226928:+	0.67	0.69	0.73	0.79	0.56	0.61	0.44	0.44	NM_028412	ENSMUSG00000039205	Ciz1	RI	4.22	0.1217	0.21
chr8:11628439:11628530:-@chr8:11623697:11623858:-@chr8:11620262:11620373:-@chr8:11619062:11619297:-	0.47	0.46	0.41	0.46	0.16	0.33	0.27	0.19	NR_030779,NM_133971,NM_001167967	ENSMUSG00000031508	Ankrd10	MXE	5.09	0.1483	0.21
chr10:12981572:12981730:-@chr10:12977383:12977622:-@chr10:12975116:12975127:-@chr10:12973148:12973685:-	0.19	0.16	0.41	0.45	0.09	0.12	0.06	0.1	NM_001033257,NM_001195066,NM_001195065,NM_001195096	ENSMUSG00000062866	Phactr2	MXE	2.83	0.1033	0.21

chr1:164606822:164606948:-@chr1:164605736:164605972:-@chr1:164604234:164604282:-@chr1:164601916:164603787:-	0.69	0.77	0.65	0.61	0.33	0.6	0.53	0.41	NA	NA	NA	MXE	3.11	0.0917	0.21
chr15:79158801:79158519|79158640:-@chr15:79148191:79148440:-	0.4	0.37	0.38	0.65	0.18	0.27	0.16	0.34	NA	ENSMUSG00000042632	Pla2g6	A5SS	3.61	0.0883	0.21
chr7:134721049:134721202|134721543:+@chr7:134723181:134723246:+	0.46	0.57	0.67	NA	0.79	0.76	0.69	0.87	NM_026888	ENSMUSG00000030815	Phkg2	A5SS	3.02	0.1008	0.21
chr19:57123952:57123999:-@chr19:57121415:57121555:-@chr19:57119371:57119462:-	0.75	0.84	0.77	0.67	0.57	0.53	0.62	0.53	NM_178688,NM_001103178,NM_001103177	ENSMUSG00000025085	Ablim1	SE	4.76	0.125	0.2
chr12:70825949:70826001:+@chr12:70826442:70826541:+@chr12:70838938:70839048:+	0.47	0.55	0.84	0.62	0.43	0.38	0.44	0.42	NM_026536	ENSMUSG00000054894	Atp5s	SE	3.74	0.0883	0.2
chr12:54205502:54205717:+@chr12:54240368:54243755:+@chr12:54248798:54252002:+	0.84	0.95	0.97	0.91	0.58	0.88	0.72	0.7	NM_198111	ENSMUSG00000061603	Akap6	SE	2.71	0.09	0.2
chr16:32986062:32986113:+@chr16:32986825:32986974:+@chr16:32988517:32988567:+	NA	NA	0.81	0.67	0.9	0.96	0.98	0.9	NM_001081255	ENSMUSG00000022801	Lrch3	SE	3.98	0.1321	0.2
chr5:53658345:53658597:+@chr5:53659262:53659570:+@chr5:53668382:53668438:+	0.17	0.18	0.14	0.19	0.43	0.29	0.41	0.37	NM_001145433	ENSMUSG00000061461	3110013D10Rik	SE	5.52	0.1533	0.2
chr2:156756952:156757003:-@chr2:156755668:156755706:-@chr2:156753078:156754617:-	0.22	0.32	0.42	0.38	0.14	0.14	0.1	0.16	NA	NA	NA	SE	4.49	0.13	0.2
chr6:122283309:122283458:-@chr6:122282540:122282674:-@chr6:122275476:122275968:-	NA	0.34	NA	0.5	0.67	0.62	0.52	0.68	NM_001042623,NM_007905	ENSMUSG00000040669	Phc1	SE	2.36	0.1039	0.2
chr1:192668366:192668481:-@chr1:192657885:192657977:-@chr1:192633953:192634000:-	0.95	0.95	0.94	0.91	0.62	0.77	0.77	0.77	NM_178775	ENSMUSG00000089872	Rps6kc1	SE	6.74	0.1567	0.2
chr11:116161580:116161747:-@chr11:116158885:116158977:-@chr11:116156858:116157003:-	0.75	0.79	0.84	0.78	0.56	0.64	0.6	0.57	NM_001162872,NM_016857	ENSMUSG00000020792	Exoc7	SE	6.22	0.1517	0.2
chr11:60055320:60055395:-@chr11:60046400:60046459:-@chr11:60044603:60044639:-	0.74	0.73	0.75	0.74	0.51	0.59	0.45	0.61	NM_001039092,NM_153080	ENSMUSG00000000538	Tom1l2	SE	5.94	0.1483	0.2
chr3:95020136:95020190:-@chr3:95012762:95012858:-@chr3:95010385:95010524:-	NA	NA	0.73	0.73	NA	0.61	0.49	0.5	NM_029885,NM_172512	ENSMUSG00000038766	Gabpb2	SE	2.22	0.1367	0.2
chr4:97731972:97732137:+@chr4:97748416:97748507:+@chr4:97777909:97785567:+	0.91	0.92	0.91	0.92	NA	0.86	NA	0.58	NA	ENSMUSG00000028565	Nfia	SE	3.37	0.1493	0.2
chr17:27075731-27075672:-@chr17:27075594-27075517:-	0.46	0.49	0.44	0.44	0.73	0.45	0.77	0.67	NM_026948,NM_026307	ENSMUSG00000024194	Cuta	RI	2.43	0.1046	0.2
chr19:27291510-27291622:+@chr19:27292033-27292186:+	0.71	0.69	0.76	0.78	0.47	0.63	0.57	0.48	NA	ENSMUSG00000024924	Vldlr	RI	4.47	0.1233	0.2
chr13:99042727-99042807:+@chr13:99043333-99043873:+	0.46	0.57	0.44	0.35	0.71	0.56	0.72	0.63	NM_023472	ENSMUSG00000021661	Ankra2	RI	3.18	0.0979	0.2
chr3:106334055:106334196:-@chr3:106322927:106323011:-@chr3:106315721:106315805:-@chr3:106308639:106308770:-	0.48	0.48	0.37	0.34	0.71	0.51	0.62	0.63	NM_133869	ENSMUSG00000040774	Cept1	MXE	3.62	0.105	0.2
chr11:83795698:83795809:+@chr11:83798751:83799053:+@chr11:83800316:83800353:+@chr11:83801415:83801492:+	0.88	0.95	0.71	0.81	0.66	0.69	0.61	0.6	NM_001115009,NM_194341	ENSMUSG00000034940	Synrg	MXE	3.59	0.105	0.2
chr14:102311216:102311377:+@chr14:102312376|102312457:102312563:+	0.48	0.2	0.31	0.3	0.52	0.49	0.54	0.54	NM_201529	ENSMUSG00000033060	Lmo7	A3SS	3.32	0.115	0.2
chr7:57014476:57014515:+@chr7:57014912|57014968:57015163:+	NA	0.22	0.15	NA	0.38	0.41	0.41	0.34	NM_001146053,NM_001146049,NM_001146050,NM_016865,NM_001146052	ENSMUSG00000039745	Htatip2	A3SS	4.4	0.1557	0.2
chr11:70049526:70049713:-@chr11:70048966|70048970:70048708:-	NA	NA	0.7	0.83	0.96	0.96	0.96	0.96	NM_001177603,NM_001177606,NM_001177607,NM_026757,NM_145758	ENSMUSG00000020831	6210010K14Rik	A3SS	5.2	0.1764	0.2
chr5:53659262:53659309|53659570:+@chr5:53668382:53668438:+	0.71	0.68	0.56	0.72	0.96	0.72	0.91	0.87	NM_001145433	ENSMUSG00000061461	3110013D10Rik	A5SS	2.89	0.0917	0.2
chrX:151650144:151650227:-@chrX:151649664:151649773:-@chrX:151648576:151648677:-	0.46	0.57	0.51	0.5	0.2	0.29	0.41	0.39	NM_009121	ENSMUSG00000025283	Sat1	SE	4.39	0.0983	0.19
chr5:110807913:110808133:-@chr5:110807448:110807516:-@chr5:110807057:110807274:-	0.32	0.26	0.34	NA	0.42	0.61	0.41	0.55	NM_028596,NM_001142642	ENSMUSG00000043323	Fbrsl1	SE	2.64	0.0919	0.19
chr1:182081291:182081408:+@chr1:182085926:182086111:+@chr1:182089737:182089854:+	0.56	0.81	0.51	0.46	0.79	0.82	0.74	0.76	NM_001033285	ENSMUSG00000026490	Cdc42bpa	SE	2.21	0.0958	0.19
chr13:59883379:59883704:-@chr13:59880113:59880176:-@chr13:59873240:59874220:-	0.33	NA	0.32	0.36	0.55	0.57	0.52	0.48	NM_153538	ENSMUSG00000035248	Zcchc6	SE	4.74	0.1511	0.19
chr7:87464227-87464132:-@chr7:87463912-87463745:-	0.72	0.73	NA	NA	NA	0.57	0.46	0.58	NM_173445	ENSMUSG00000038930	Rccd1	RI	2.4	0.1258	0.19
chr11:116161580:116161747:-@chr11:116158885:116158977:-@chr11:116158044:116158112:-@chr11:116156858:116157003:-	0.97	0.92	0.93	0.98	0.74	0.83	0.7	0.75	NM_001162872,NM_016857	ENSMUSG00000020792	Exoc7	MXE	5.54	0.1433	0.19

chr7:19677557:19677603:+@chr7:19677767|19677896:19677981:+	0.29	0.29	0.29	0.26	0.5	0.44	0.49	0.44	NM_001190490,NM_032418,NM_001190491	ENSMUSG00000030409	Dmpk	A3SS	6.66	0.1583	0.19
chr17:49592120:49592167|49592182:+@chr17:49593355:49594755:+	NA	0.84	0.85	NA	0.59	0.71	0.73	0.59	NM_020042,NM_028464	ENSMUSG00000064120	Mocs1	A5SS	2.47	0.1114	0.19
chr3:94787905:94788841:+@chr3:94793225:94793269:+@chr3:94796888:94797115:+	0.29	0.2	0.24	0.27	0.03	0.06	0.12	0.05	NM_175356	ENSMUSG00000038861	Pi4kb	SE	5.62	0.1367	0.18
chr17:27693519:27693656:+@chr17:27693897:27694011:+@chr17:27696478:27696648:+	0.72	0.67	0.71	0.56	0.41	0.6	0.37	0.55	NA	NA	NA	SE	2.28	0.075	0.18
chr10:87985712:87985898:-@chr10:87984022:87984080:-@chr10:87982646:87982688:-	0.41	0.33	0.36	0.38	0.2	0.19	0.15	0.2	NM_175418	ENSMUSG00000020061	Mybpc1	SE	6.63	0.15	0.18
chr12:16817771:16818121:+@chr12:16820653:16820718:+@chr12:16823206:16823260:+	0.74	0.82	0.79	0.77	0.58	0.67	0.54	0.62	NM_033270	ENSMUSG00000057469	E2f6	SE	5.45	0.12	0.18
chr2:142565259:142565347:-@chr2:142540798:142540830:-@chr2:142540415:142540468:-	0.52	0.42	0.43	0.38	0.29	0.33	0.18	0.22	NM_001081133	ENSMUSG00000038844	Kif16b	SE	4.75	0.1033	0.18
chr2:52017588:52017692:-@chr2:52016891:52016995:-@chr2:52016176:52016268:-	0.38	0.43	0.55	0.53	0.74	0.57	0.66	0.66	NM_010889	ENSMUSG00000026950	Neb	SE	3.58	0.0917	0.18
chr2:84567320:84567425:-@chr2:84565686:84566313:-@chr2:84563279:84564374:-	0.78	0.93	0.55	0.84	0.96	0.95	0.95	0.95	NM_133840	ENSMUSG00000027079	Clp1	SE	3.27	0.075	0.18
chr6:142601047:142601152:-@chr6:142596547:142596585:-@chr6:142594792:142594893:-	0.38	0.27	0.37	0.32	0.62	0.49	0.5	0.45	NM_021042,NM_001044720,NM_021041,NM_011511	ENSMUSG00000030249	Abcc9	SE	5.65	0.105	0.18
chr1:82723803:82723911:+@chr1:82724642:82724813:+@chr1:82725791:82726011:+	0.43	0.4	0.34	0.4	0.24	0.21	0.19	0.21	NM_029409	ENSMUSG00000026150	Mff	SE	6.1	0.145	0.18
chr11:116161580:116161747:-@chr11:116158044:116158112:-@chr11:116156858:116157003:-	0.02	0.11	0.11	0.02	0.25	0.18	0.31	0.24	NM_001162872,NM_016857	ENSMUSG00000020792	Exoc7	SE	4.95	0.1167	0.18
chr11:58874346:58874609:-@chr11:58870257:58870523:-@chr11:58869463:58869726:-	0.18	0.22	0.33	0.27	0.05	0.12	0.03	0.06	NM_001171512,NM_199152	ENSMUSG00000061462	Obscn	SE	5.12	0.12	0.18
chr2:52985887:52986010:+@chr2:52989446:52989538:+@chr2:52990874:52993236:+	NA	0.29	0.27	0.21	NA	NA	0.41	0.46	NM_172409	ENSMUSG00000036053	Fmnl2	SE	2.8	0.1258	0.18
chr8:4266680-4266556:-@chr8:4265276-4265226:-	0.42	0.48	0.44	0.44	0.66	0.6	0.58	0.67	NM_011592	ENSMUSG00000002949	Timm44	RI	5.94	0.14	0.18
chr2:32226384-32226621:+@chr2:32226769-32226928:+	0.6	0.67	0.64	0.73	0.5	0.61	0.38	0.42	NM_028412	ENSMUSG00000039205	Ciz1	RI	2.89	0.0846	0.18
chr6:113327733-113327310:-@chr6:113326939-113326886:-	0.26	0.34	0.18	0.15	0.37	0.45	0.34	0.51	NM_133932	ENSMUSG00000048930	Tada3	RI	2.94	0.0817	0.18
chr8:73891116:73891268:+@chr8:73891397|73891543:73891592:+	0.51	0.48	0.54	0.51	0.31	0.39	0.32	0.32	NM_001145780,NM_025917	ENSMUSG00000002395	Use1	A3SS	5.85	0.14	0.18
chr7:19677557:19677603:+@chr7:19677767|19677892:19677981:+	0.23	0.28	0.26	0.24	0.48	0.4	0.47	0.38	NM_001190490,NM_032418,NM_001190491	ENSMUSG00000030409	Dmpk	A3SS	5.83	0.135	0.18
chr15:7134717:7134818:+@chr15:7135067|7135566:7135733:+	0.36	0.19	0.22	0.2	NA	0.41	0.47	0.38	NM_013584,NM_001113386	ENSMUSG00000054263	Lifr	A3SS	2.57	0.0986	0.18
chr15:79158801:79158065|79158519:-@chr15:79148191:79148440:-	0.8	0.85	0.86	0.95	0.64	0.72	0.68	0.71	NA	ENSMUSG00000042632	Pla2g6	A5SS	5.9	0.1167	0.18
chr6:113267542:113267670|113267688:+@chr6:113268406:113268715:+	0.14	0.11	NA	NA	0.29	0.31	0.32	NA	NM_030178	ENSMUSG00000001632	Brpf1	A5SS	3.11	0.1592	0.18
chr3:136591486:136591583:+@chr3:136594975:136595004:+@chr3:136597993:136598743:+	0.87	0.93	0.88	0.99	0.7	0.84	0.69	0.76	NM_008913	ENSMUSG00000028161	Ppp3ca	SE	3.84	0.0933	0.17
chr17:85489446:85489607:-@chr17:85487680:85487779:-@chr17:85482533:85482655:-	0.9	0.89	0.83	0.91	0.69	0.7	0.68	0.8	NM_145984,NM_001163623,NM_001163624,NM_001163622	ENSMUSG00000024127	Prepl	SE	4.29	0.1133	0.17
chr10:90621493:90621590:-@chr10:90616023:90616142:-@chr10:90615830:90615925:-	0.22	0.32	0.24	0.17	0.34	0.53	0.37	0.4	NM_001080132,NM_001080134,NM_001080131,NM_001080130,NM_001080129	ENSMUSG00000019961	Tmpo	SE	4.02	0.0833	0.17
chr2:90757586:90757666:-@chr2:90757011:90757068:-@chr2:90754141:90754332:-	0.23	0.21	0.18	0.22	0.37	0.31	0.43	0.4	NM_025576	ENSMUSG00000063235	Ptpmt1	SE	5.62	0.1217	0.17
chr1:165187892:165188073:-@chr1:165184108:165184179:-@chr1:165175250:165178527:-	0.6	0.58	0.52	0.57	0.36	0.41	0.41	0.42	NM_011127,NM_175686	ENSMUSG00000026586	Prrx1	SE	6.24	0.1317	0.17
chr9:69864626:69864998:+@chr9:69866487:69866625:+@chr9:69867196:69867322:+	0.27	0.46	0.54	0.53	0.27	0.31	0.29	0.25	NM_001039519	ENSMUSG00000033543	Gtf2a2	SE	2.32	0.0875	0.17
chr9:4309743:4309934:+@chr9:4313702:4313806:+@chr9:4316827:4317071:+	0.73	0.6	0.65	0.64	0.61	0.43	0.4	0.51	NM_026962,NM_001164574	ENSMUSG00000025893	Kbtbd3	SE	2.83	0.0763	0.17
chr4:137638808:137638903:+@chr4:137643448:137643480:+@chr4:137651824:137651844:+	0.65	0.8	NA	0.86	0.59	0.62	0.61	0.58	NM_172703	ENSMUSG00000028760	Eif4g3	SE	3.37	0.1078	0.17

chr11:116158885:116158977:-@chr11:116158044:116158194:-@chr11:116156858:116157003:-	0.04	0.07	0.07	0.02	0.23	0.17	0.26	0.22	NM_001162872,NM_016857	ENSMUSG00000020792	Exoc7	SE	6.14	0.1317	0.17
chr15:76264493-76264588:+@chr15:76265113-76265217:+	NA	0.24	0.36	0.37	0.13	0.16	0.16	0.18	NM_175457,NM_001162489	ENSMUSG00000022558	Heatr7a	RI	4.13	0.1203	0.17
chr7:109062097-109061949:-@chr7:109061726-109061503:-	0.73	0.74	NA	0.66	0.9	0.93	0.81	0.86	NM_001162974	ENSMUSG00000064307	Lrrc51	RI	3.95	0.1028	0.17
chr4:151419804-151419939:+@chr4:151420656-151420753:+	NA	0.29	0.34	0.21	0.41	0.37	0.47	0.54	NM_001159599,NM_028727	ENSMUSG00000028948	Nol9	RI	2.85	0.0753	0.17
chr11:69734665:69734888:-@chr11:69733843:69733936:-@chr11:69732951:69732980:-@chr11:69732653:69732838:-	0.34	0.41	0.44	0.48	0.23	0.22	0.27	0.27	NM_001166593,NM_001166591,NM_001166589,NM_001166595,NM_181582	ENSMUSG00000078812	Eif5a	MXE	5.15	0.1167	0.17
chr2:156571571:156571932:+@chr2:156573759|156574068:156574156:+	0.31	0.27	0.2	0.29	0.47	0.39	0.55	0.35	NM_001042488,NM_001042487,NM_146128	ENSMUSG00000061689	Dlgap4	A3SS	4.25	0.0867	0.17
chr13:55216841:55216985:+@chr13:55223643|55223691:55223876:+	0.15	0.24	NA	NA	0.35	0.35	0.43	0.33	NM_012017	ENSMUSG00000021481	Zfp346	A3SS	4.11	0.1143	0.17
chr1:171674867:171674482|171674806:-@chr1:171671608:171674051:-	0.77	0.71	0.5	NA	0.86	0.82	0.83	0.82	NM_009062	ENSMUSG00000038530	Rgs4	A5SS	3.73	0.0981	0.17
chr13:101421014:101420777|101420905:-@chr13:101419633:101419736:-	0.3	NA	0.19	NA	0.08	0.1	0.04	0.07	NM_001044371,NM_011233	ENSMUSG00000021635	Rad17	A5SS	4.65	0.1296	0.17
chr3:97514144:97514367:-@chr3:97513405:97513506:-@chr3:97510795:97510980:-	0.86	0.86	0.82	0.83	0.71	0.72	0.65	0.66	NM_001110163,NM_178080,NM_001039376	ENSMUSG00000038170	Pde4dip	SE	6.16	0.1233	0.16
chr3:89837987:89838099:-@chr3:89835218:89835292:-@chr3:89832247:89832299:-	0.4	0.42	0.24	0.42	0.53	0.5	0.51	0.59	NM_153489,NM_028475,NM_001165983,NM_001165984,NM_001165988,NM_001165986,NM_001165985,NM_001165987	ENSMUSG00000042520	Ubap2l	SE	6.56	0.0917	0.16
chr17:6035411:6035559:+@chr17:6036357:6036505:+@chr17:6037384:6038555:+	0.22	0.15	0.11	0.22	0.4	0.22	0.36	0.36	NM_001113353,NM_001113352,NM_001113351,NM_011523	ENSMUSG00000023805	Synj2	SE	2.88	0.0817	0.16
chr16:29588338:29588445:+@chr16:29588909:29588962:+@chr16:29589767:29589834:+	0.46	0.3	0.44	0.37	0.21	0.28	0.27	0.16	NM_001199177,NM_133752	ENSMUSG00000038084	Opa1	SE	3.47	0.0817	0.16
chr16:38585289:38585631:+@chr16:38585732:38585793:+@chr16:38586334:38586521:+	0.09	0.06	NA	0.06	0.21	0.19	0.23	0.31	NM_026407	ENSMUSG00000002845	Tmem39a	SE	4.43	0.1161	0.16
chr6:31170351:31170519:+@chr6:31194105:31194358:+@chr6:31235003:31235120:+	0.65	0.71	0.56	0.65	0.84	0.83	0.76	0.78	NA	ENSMUSG00000087380	210408F21R	SE	5.02	0.0983	0.16
chr7:150785887:150785995:-@chr7:150778317:150778565:-@chr7:150774397:150774488:-	0.66	0.65	0.78	0.77	0.46	0.61	0.6	0.55	NM_013742	ENSMUSG00000010755	Cars	SE	3.65	0.0767	0.16
chr13:107764575:107764642:-@chr13:107759784:107759897:-@chr13:107758718:107758868:-	0.75	0.78	0.79	0.85	0.68	0.71	0.63	0.53	NM_001145779,NM_008442	ENSMUSG00000021693	Kif2a	SE	4.87	0.08	0.16
chr4:57895896:57896074:+@chr4:57899161:57899199:+@chr4:57905741:57909856:+	NA	NA	0.48	0.24	0.24	0.16	0.24	0.18	NM_009649,NM_001035532,NM_001035533	ENSMUSG00000089945	AF064781	SE	2.02	0.0779	0.16
chr11:59585119:59585204:+@chr11:59585654:59585719:+@chr11:59589018:59594362:+	0.79	0.77	0.77	0.74	0.57	0.64	0.59	0.64	NM_201245,NM_012027	ENSMUSG00000005417	Mprip	SE	6.26	0.1233	0.16
chr11:5879676:5879724:-@chr11:5878402:5878515:-@chr11:5877815:5877943:-	0.95	0.98	0.98	0.99	0.87	0.86	NA	0.72	NM_001174054,NM_007595,NM_001174053	ENSMUSG00000057897	Camk2b	SE	5.02	0.1117	0.16
chr7:31349222-31349413:+@chr7:31349493-31349626:+	0.18	0.17	0.22	0.2	0.35	0.3	0.41	0.34	NM_170760,NM_145580	ENSMUSG00000078765	U2af1l4	RI	6.09	0.115	0.16
chr9:69864626-69864730:+@chr9:69864880-69864998:+	0.61	0.59	0.57	0.67	0.38	0.51	0.42	0.48	NM_001039519	ENSMUSG00000033543	Gtf2a2	RI	5.2	0.0983	0.16
chr4:134362606-134362432:-@chr4:134360479-134358676:-	0.47	0.47	0.52	0.43	0.26	0.24	0.21	0.53	NM_025382	ENSMUSG00000028826	Tmem57	RI	2.13	0.0871	0.16
chr4:134362606-134362432:-@chr4:134360479-134358674:-	0.47	0.46	0.52	0.43	0.26	0.24	0.21	0.53	NM_025382	ENSMUSG00000028826	Tmem57	RI	2.1	0.085	0.16
chr2:67345104:67345237:+@chr2:67345966:67355230:+@chr2:67357277:67357410:+@chr2:67362829:67364663:+	0.75	0.79	0.87	0.88	0.61	0.67	0.69	0.67	NM_001024618,NM_001083919	ENSMUSG00000027022	Xirp2	MXE	4.79	0.1033	0.16
chr17:35043640:35043822:+@chr17:35043898|35043928:35044010:+	0.16	NA	0.08	0.1	0.24	0.29	0.31	0.27	NM_145830,NM_147151	ENSMUSG00000013787	Ehmt2	A3SS	4.7	0.1208	0.16
chr1:93146896:93147014:+@chr1:93150792|93150840:93150970:+	0.12	0.03	0.07	0.1	0.31	0.22	0.22	0.21	NA	ENSMUSG00000034343	Ube2f	A3SS	6.42	0.11	0.16
chr1:136304151:136304280:+@chr1:136304394|136304981:136305064:+	0.17	0.21	0.16	0.12	0.35	0.29	0.36	0.28	NM_028057	ENSMUSG00000026456	Cyb5r1	A3SS	5.51	0.1067	0.16

chr8:12861640:12861724|12861844:+@chr8:12864920:12868728:+	0.21	0.33	0.26	0.34	0.11	0.17	0.12	0.1	NM_015804	ENSMUSG00000031441	Atp11a	A5SS	4.44	0.1033	0.16
chr17:32498406:32498909:-@chr17:32496983:32497372:-@chr17:32495888:32496439:-	0.46	0.37	0.47	0.36	0.59	0.54	0.5	0.64	NM_011717,NM_212438,NR_033525	ENSMUSG00000024050	Wiz	SE	3.74	0.0783	0.15
chr10:126913576:126913754:+@chr10:126918749:126918811:+@chr10:126921032:126921274:+	0.88	0.84	0.84	0.84	0.63	0.74	0.73	0.7	NM_001168292,NM_027900,NM_001168293	ENSMUSG00000025404	R3hdm2	SE	6.63	0.11	0.15
chr14:102328393:102328668:+@chr14:102330389:102330497:+@chr14:102331787:102331889:+	0.95	0.96	0.95	0.94	0.85	0.76	0.84	0.74	NM_201529	ENSMUSG00000033060	Lmo7	SE	5.59	0.1133	0.15
chr7:148496661:148496908:-@chr7:148487499:148487588:-@chr7:148483075:148483515:-	0.85	0.87	NA	0.83	0.67	0.65	0.76	0.71	NR_027769,NM_016874	ENSMUSG00000058886	Deaf1	SE	3.9	0.1025	0.15
chr9:96133101:96133167:+@chr9:96147469:96147507:+@chr9:96174258:96174361:+	NA	0.31	NA	0.25	0.14	0.17	0.12	0.1	NA	ENSMUSG00000032411	Tfdp2	SE	4.23	0.1061	0.15
chr9:45755919:45755971:-@chr9:45755712:45755780:-@chr9:45755067:45755138:-	NA	0.08	0.1	NA	0.18	0.26	0.26	0.26	NM_172257	ENSMUSG00000034908	Sidt2	SE	3.36	0.1129	0.15
chr4:119275014:119275097:+@chr4:119282595:119282696:+@chr4:119289113:119289241:+	0.29	0.33	0.2	0.24	0.47	0.37	0.35	0.48	NM_172699	ENSMUSG00000032998	Foxj3	SE	3.37	0.075	0.15
chr11:82625902:82626312:-@chr11:82624530:82624613:-@chr11:82623510:82623720:-	0.89	0.76	NA	NA	0.68	0.71	0.66	0.63	NM_026097,NM_001007465,NM_001164571,NM_001164570,NM_001164569	ENSMUSG00000020696	Rffl	SE	3.75	0.0993	0.15
chr11:104167940:104168072:+@chr11:104169195:104169248:+@chr11:104171583:104171848:+	0.79	0.73	0.81	0.88	0.62	0.69	0.65	0.66	NM_001038609,NM_010838	ENSMUSG00000018411	Mapt	SE	4.9	0.09	0.15
chr11:54804893:54804946:-@chr11:54800553:54800570:-@chr11:54799624:54799717:-	0.79	0.79	0.82	0.87	0.7	0.66	0.6	0.72	NM_001110211,NM_013472	ENSMUSG00000018340	Anxa6	SE	5.81	0.0917	0.15
chr6:86368872-86368926:+@chr6:86370318-86370405:+	0.74	0.74	0.81	0.78	0.62	0.61	0.59	0.65	NM_001164079,NM_011585,NM_001164078	ENSMUSG00000071337	Tia1	RI	6.24	0.1133	0.15
chr9:107166095-107165956:-@chr9:107164818-107164754:-	0.05	0.05	0.12	0.07	0.24	0.19	0.21	0.26	NM_178907	ENSMUSG00000032577	Mapkapk3	RI	5.62	0.1133	0.15
chr11:100888581-100888707:+@chr11:100890490-100890572:+	0.32	0.23	0.33	0.37	0.51	0.45	0.46	0.41	NM_016920	ENSMUSG00000019302	Atp6v0a1	RI	5.21	0.0833	0.15
chr1:44158745:44158802:-@chr1:44156693:44156846:-@chr1:44148206:44148436:-@chr1:44145321:44145372:-	0.69	0.8	NA	NA	0.58	0.59	0.62	NA	NM_029368	ENSMUSG00000026049	700029F09R	MXE	2.51	0.1008	0.15
chr11:69734665:69734888:-@chr11:69733843:69733924:-@chr11:69732951:69732980:-@chr11:69732653:69732838:-	0.29	0.35	0.41	0.41	0.2	0.19	0.24	0.22	NM_001166593,NM_001166591,NM_001166589,NM_001166595,NM_181582	ENSMUSG00000078812	Eif5a	MXE	4.65	0.1033	0.15
chr6:145159690:145159764:+@chr6:145163042|145163704:145163791:+	0.49	0.49	0.48	0.38	0.28	0.32	0.28	0.36	NM_001163628,NM_133688	ENSMUSG00000040370	Lyrm5	A3SS	3.94	0.0983	0.15
chr13:30011983:30012094:-@chr13:30010646|30010664:30010445:-	NA	0.86	0.86	NA	0.76	0.68	0.7	NA	NM_010093	ENSMUSG00000016477	E2f3	A3SS	2.48	0.1067	0.15
chr13:35085699:35085996:-@chr13:35085089|35085197:35084937:-	0.22	0.36	0.29	0.33	0.46	0.44	0.47	0.44	NM_001110332,NM_001110331,NM_011868	ENSMUSG00000021417	Eci2	A3SS	5.91	0.105	0.15
chr1:55145087:55144833|55144989:-@chr1:55143610:55143785:-	0.35	0.43	0.43	0.4	0.47	0.59	0.6	0.55	NA	ENSMUSG00000025980	Hspd1	A5SS	4.23	0.0917	0.15
chr4:137772542:137772655|137772714:+@chr4:137777441:137777638:+	0.31	0.28	0.26	0.21	0.11	0.16	0.08	0.1	NM_001122896,NM_010470	ENSMUSG00000028759	Hp1bp3	A5SS	5.17	0.105	0.15
chr4:116961673:116960968|116961631:-@chr4:116958456:116958577:-	0.59	0.65	0.68	0.67	0.79	0.74	0.83	0.82	NM_025739	ENSMUSG00000028677	Rnf220	A5SS	5.38	0.0983	0.15

Table C-2: The list of dysregulated splicing events in **SCA7** muscle.

gid	wt1	wt2	wt3	wt4	mut1	mut2	mut3	mut4	refseq_id	ensg_id	gsymbol	event	zscores	SigDiff	abs(Wt-Mut)
chr14:19109340:19109482:+@chr14:19109961:19110079:+@chr14:19110358:19110615:+@chr14:19110818:19111059:+	0.82	0.79	0.63	0.62	0.07	0.08	0.11	0.11	NM_023526	ENSMUSG00000021772	Nkiras1	MXE	6.68	0.5467	0.62
chr11:5879676:5879724:-@chr11:5876768:5876896:-@chr11:5872816:5872891:-	0.84	0.82	0.86	0.83	0.25	0.26	0.21	0.22	NM_001174054,NM_007595,NM_001174053	ENSMUSG00000057897	Camk2b	SE	6.95	0.5767	0.6
chr9:83004600:83004713:-@chr9:83004395:83004481:-@chr9:83003549:83004036:-	0.09	NA	0.09	0.14	0.69	NA	0.64	0.7	NA	NA	NA	SE	3.93	0.5333	0.57
chr2:52042931:52043035:-@chr2:52041532:52041636:-@chr2:52040791:52040895:-@chr2:52039252:52039356:-	0.91	0.9	0.89	0.92	0.39	0.41	0.29	0.29	NM_010889	ENSMUSG00000026950	Neb	MXE	6.81	0.5133	0.56
chr11:29605535:29605591:+@chr11:29606410:29608770:+@chr11:29633633:29633840:+	0.12	0.15	0.18	0.14	0.68	0.7	0.63	0.67	NM_194053,NM_194052,NM_024226,NM_194054,NM_194051	ENSMUSG00000020458	Rtn4	SE	6.9	0.4883	0.52
chr11:29721639:29721757:-@chr11:29719092|29719184:29718906:-	NA	NA	0.69	0.81	0.25	NA	0.23	NA	NM_146016	ENSMUSG00000044072	Eml6	A3SS	2.02	0.44	0.51
chr2:180116812:180116971:-@chr2:180115496:180115539:-@chr2:180106377:180106497:-	0.99	0.93	0.95	0.99	0.34	0.55	0.61	0.38	NA	ENSMUSG00000084843	B230312C02Rik	SE	6.14	0.395	0.49
chr6:140485169:140485284:+@chr6:140485527:140485544:+@chr6:140492241:140492708:+	NA	NA	0.27	0.13	0.68	0.68	0.66	0.73	NM_144920	ENSMUSG00000030231	Plekha5	SE	5.05	0.4375	0.49
chr2:20808733:20808787:-@chr2:20804827:20804856:-@chr2:20801588:20803478:-	0.26	NA	0.32	0.38	0.87	0.75	0.67	0.8	NM_001128084,NM_001081364	ENSMUSG00000036591	Arhgap21	SE	4.94	0.3536	0.45
chr6:120907717:120907811:-@chr6:120903652:120903702:-@chr6:120902393:120902503:-	0.8	0.73	0.82	0.6	0.33	0.33	0.28	0.26	NA	ENSMUSG00000051586	Mical3	SE	6.08	0.355	0.44
chr11:104163675:104163724:+@chr11:104166627:104166723:+@chr11:104167940:104168072:+	0.81	0.8	0.85	0.9	0.37	0.43	0.4	0.39	NM_001038609,NM_010838	ENSMUSG00000018411	Mapt	SE	6.89	0.3983	0.44
chr13:55578912:55579041:-@chr13:55577677|55578134:55577507:-	NA	0.03	0.08	NA	0.61	0.45	0.49	0.34	NM_019813,NM_001177372,NM_001177371	ENSMUSG00000034675	Dbn1	A3SS	3.64	0.2889	0.42
chr1:82723803:82723911:+@chr1:82724642:82724813:+@chr1:82725791:82726011:+	0.6	0.57	0.55	0.54	0.18	0.18	0.18	0.15	NM_029409	ENSMUSG00000026150	Mff	SE	6.95	0.3683	0.39
chr11:58869463:58869726:-@chr11:58868879:58869142:-@chr11:58868276:58868539:-	0.58	0.66	0.59	0.6	0.99	0.99	1	1	NM_001171512,NM_191952	ENSMUSG00000061462	Obscn	SE	6.82	0.3633	0.39
chr5:149996136:149996382:+@chr5:149999284:149999452:+@chr5:149999921:150000049:+	0.22	0.21	0.16	0.18	0.52	0.58	0.48	0.72	NM_001013378,NM_001115151,NM_001115149,NM_001115150	ENSMUSG00000041264	Uspl1	SE	6.64	0.3	0.38
chr2:156375621:156375726|156375763:+@chr2:156376385:156377185:+	NA	NA	0.76	0.82	0.33	0.4	0.37	0.55	NM_001164818,NM_026661	ENSMUSG00000027628	0610011L14Rik	A5SS	3.54	0.2704	0.38
chr2:76406166:76406299:+@chr2:76407077:76407100:+@chr2:76415069:76415176:+	0.8	0.92	0.86	0.82	0.56	0.43	0.43	0.51	NM_145525	ENSMUSG00000042359	Osbpl6	SE	6.4	0.295	0.37
chr14:19109340:19109482:+@chr14:19110358:19110615:+@chr14:19110818:19111059:+	0.48	0.47	0.34	0.36	0.04	0.04	0.06	0.06	NM_023526	ENSMUSG00000021772	Nkiras1	SE	6.5	0.3117	0.36
chr2:52012811:52012903:-@chr2:52009203:52009295:-@chr2:52008576:52008668:-	0.51	0.53	0.61	0.57	0.22	0.21	0.16	0.2	NM_010889	ENSMUSG00000026950	Neb	SE	6.86	0.3133	0.36
chr2:76393071:76393174:+@chr2:76393947:76394039:+@chr2:76398243:76398317:+	0.53	0.61	0.43	0.46	0.15	0.15	0.16	0.12	NM_145525	ENSMUSG00000042359	Osbpl6	SE	6.68	0.3017	0.36
chr7:4397049:4397259:-@chr7:4396580:4396724:-@chr7:4395805:4395923:-	0.22	0.32	0.32	0.32	0.67	0.61	0.58	0.74	NA	NA	NA	SE	6.71	0.285	0.36
chr5:136579150:136579294:+@chr5:136579417|136579707:136579876:+	0.19	0.15	0.12	0.12	0.53	0.45	0.52	0.53	NM_133914,NM_001039103	ENSMUSG00000004952	Rasa4	A3SS	6.6	0.3217	0.36
chrX:99754904:99755073:-@chrX:99752435:99752611:-@chrX:99750865:99750956:-	0.77	0.73	0.74	0.68	0.33	0.35	0.45	0.39	NM_008832,NM_173021	ENSMUSG00000034055	Phka1	SE	6.49	0.2933	0.35
chr6:42242940:42243017:+@chr6:42243443:42243521:+@chr6:42244074:42244155:+	0.31	0.41	0.27	0.28	0.63	0.69	0.71	0.64	NM_013491	ENSMUSG00000029862	Clcn1	SE	6.23	0.2883	0.35
chr1:152303467-152302605:-@chr1:152302100-152301182:-	0.64	0.23	0.42	0.66	0.72	0.92	0.86	0.86	NM_001110146,NM_021400	ENSMUSG00000006014	Prg4	RI	3.72	0.1767	0.35
chr5:43652973:43653023:+@chr5:43660108:43660131:+@chr5:43668670:43668840:+	0.25	NA	0.08	NA	0.4	0.51	NA	0.6	NM_175937,NM_001177379	ENSMUSG00000039782	Cpeb2	SE	2.33	0.1958	0.34
chr2:52017588:52017692:-@chr2:52016891:52016995:-@chr2:52016176:52016268:-	0.46	0.6	0.57	0.52	0.9	0.89	0.85	0.88	NM_010889	ENSMUSG00000026950	Neb	SE	6.7	0.29	0.34
chr1:120428555:120428662:+@chr1:120432712:120432774:+@chr1:120435843:120435946:+	0.62	NA	0.84	0.71	0.38	0.43	0.34	0.39	NM_177548,NM_029709,NM_001081276	ENSMUSG00000064302	Clasp1	SE	5.3	0.2583	0.34
chr11:104163675:104163724:+@chr11:104166526:104166723:+@chr11:104167940:104168072:+	0.92	0.91	0.94	0.95	0.57	0.63	0.59	0.59	NM_001038609,NM_010838	ENSMUSG00000018411	Mapt	SE	6.86	0.3083	0.34
chr19:7355488:7355745:-@chr19:7354476:7354502:-@chr19:7353601:7353768:-	0.92	0.93	0.95	0.88	NA	0.68	0.8	0.25	NM_001080390,NM_007928,NM_001080388,NM_001080389	ENSMUSG00000024969	Mark2	SE	3.66	0.1967	0.34
chr2:155404523-155404448:-@chr2:155404164-155404025:-	0.81	0.71	0.8	0.77	0.35	0.45	0.5	0.42	NM_008180	ENSMUSG00000027610	Gss	RI	6.42	0.275	0.34
chr1:99673903:99674096:+@chr1:99679504|99679771:99679809:+	0.74	0.91	0.72	0.87	0.49	0.53	0.45	0.4	NM_026250	ENSMUSG00000026333	Gin1	A3SS	5.9	0.2483	0.34
chr12:30684030:30684138:+@chr12:30684364:30684558:+@chr12:30684757:30684914:+	0.1	0.08	0.05	0.17	0.43	0.43	0.39	0.48	NM_181395	ENSMUSG00000020674	Pxdn	SE	6.52	0.2783	0.33
chrX:133277363:133277457:-@chrX:133274344:133274433:-@chrX:133267490:133269040:-	0.89	0.97	0.92	0.79	0.53	0.56	0.54	0.63	NM_001168228,NM_001168230	ENSMUSG00000031422	Morf4l2	SE	5.86	0.2533	0.33
chr1:40057469:40057594:+@chr1:40060602:40060832:+@chr1:40061652:40061758:+	0.23	0.33	0.57	NA	0.69	0.7	0.72	0.71	NM_008696	ENSMUSG00000026074	Map4k4	SE	4.23	0.2417	0.33
chr9:47621856:47622028:+@chr9:47626817:47626900:+@chr9:47637460:47637492:+@chr9:47656250:47656381:+	0.3	0.33	0.26	0.35	0.56	0.61	0.76	NA	NM_207676,NM_001025600,NM_018770,NM_207675	ENSMUSG00000032076	Cadm1	MXE	5.42	0.2556	0.33

chr2:52023080:52023184:-@chr2:52020687:52020797:-@chr2:52020112:52020222:-	0.39	0.5	0.46	0.43	0.82	0.76	0.75	0.74	NM_010889	ENSMUSG00000026950	Neb	SE	6.76	0.2717	0.32
chr1:120406783:120406953:+@chr1:120408752:120408799:+@chr1:120418404:120418511:+	0.65	0.88	0.83	0.83	0.51	0.48	0.39	0.52	NM_177548,NM_029709,NM_001081276	ENSMUSG00000064302	Clasp1	SE	5.06	0.23	0.32
chr13:83732039:83732242:+@chr13:83764760:83764903:+@chr13:83772658:83772844:+	0.49	0.44	0.51	0.49	0.79	0.77	0.82	0.82	NM_025282,NM_001170537	ENSMUSG00000005583	Mef2c	SE	6.86	0.285	0.32
chr19:4106712-4106962:+@chr19:4107786-4107975:+	0.63	0.91	0.69	0.71	0.49	0.37	0.38	0.43	NM_001136078,NM_008851	ENSMUSG00000024851	Pitpnm1	RI	5.94	0.2117	0.32
chr16:19884367-19884017:-@chr16:19883910-19883786:-	0.58	0.36	0.33	0.35	0.72	0.67	0.75	0.72	NA	NA	NA	RI	4.46	0.2267	0.31
chr4:107569267-107569353:+@chr4:107569476-107569723:+	0.38	0.47	0.34	0.39	0.76	0.81	0.59	0.66	NM_028754	ENSMUSG00000028608	0610037L13Rik	RI	5.31	0.2133	0.31
chr11:100888581-100888707:+@chr11:100890490-100890572:+	0.22	0.21	0.24	0.35	0.57	0.53	0.56	0.59	NM_016920	ENSMUSG00000019302	Atp6v0a1	RI	6.05	0.255	0.31
chr4:120385617:120385705:-@chr4:120383828:120383989:-@chr4:120381459:120381515:-@chr4:120376960:120377180:-	0.22	0.18	0.18	0.29	0.52	0.58	0.58	0.43	NM_001081142	ENSMUSG00000028631	Kcnq4	MXE	5.59	0.2367	0.31
chr8:124353282:124353469:-@chr8:124345773|124345897:124345682:-	0.49	0.56	0.71	0.62	0.21	0.26	0.37	0.3	NM_145605	ENSMUSG00000040263	Klhdc4	A3SS	5.52	0.2067	0.31
chr17:24322149:24323232:-@chr17:24321326:24321343:-@chr17:24320639:24320797:-	0.69	0.68	0.75	0.67	0.51	0.37	0.39	0.31	NM_001163853,NM_001163852,NM_001163849,NM_001163848,NM_001163851,NM_001163847,NM_001163850,NM_173186	ENSMUSG00000036473	Tbc1d24	SE	5.8	0.23	0.3
chr14:46221240:46221431:-@chr14:46218777:46218860:-@chr14:46212849:46215339:-	0.38	0.69	NA	NA	0.23	0.2	0.31	0.21	NM_001039106,NM_001042719,NM_176845	ENSMUSG00000037697	Ddhd1	SE	3.58	0.2032	0.3
chr5:149996136:149996382:+@chr5:149999284:149999410:+@chr5:149999921:150000049:+	0.12	0.15	0.08	0.09	0.34	0.41	0.33	0.57	NM_001013378,NM_001115151,NM_001115149,NM_001115150	ENSMUSG00000041264	Uspl1	SE	6.42	0.2167	0.3
chr1:158570570:158570743:+@chr1:158571124|158571127:158571360:+	0.88	NA	0.93	0.92	0.58	0.71	0.5	0.66	NM_001136104,NM_009595	ENSMUSG00000026596	Abl2	A3SS	4.21	0.2075	0.3
chr17:85489446:85489607:-@chr17:85487680:85487779:-@chr17:85482533:85482655:-	0.65	0.57	0.62	0.72	0.4	0.35	0.33	0.33	NM_145984,NM_001163623,NM_001163624,NM_001163622	ENSMUSG00000024127	Prepl	SE	6.35	0.2283	0.29
chr8:74092826:74092922:+@chr8:74093241:74093347:+@chr8:74094620:74094787:+	0.87	0.97	0.96	0.95	0.6	0.58	0.81	0.6	NM_011977	ENSMUSG00000031808	Slc27a1	SE	4.24	0.2067	0.29
chr8:129933456:129933607:+@chr8:129934629:129934673:+@chr8:129939470:129939697:+	0.62	0.46	0.52	0.94	0.35	0.35	0.36	0.32	NM_001013581,NM_001013580,NM_033620,NM_001122850	ENSMUSG00000025812	Pard3	SE	5.08	0.1517	0.29
chr5:93596526:93596713:+@chr5:93602499:93602563:+@chr5:93604430:93605471:+	0.36	0.36	0.28	0.3	0.61	0.65	0.61	0.59	NM_001009818	ENSMUSG00000058013	11-Sep	SE	6.76	0.25	0.29
chr2:25477525-25477454:-@chr2:25477194-25477128:-	0.88	0.81	0.89	0.88	0.63	0.53	0.6	0.55	NM_001040130	ENSMUSG00000026939	Tmem141	RI	6.33	0.2383	0.29
chr6:125169604-125169655:+@chr6:125170068-125172324:+	0.16	0.18	0.13	0.12	0.46	0.37	0.5	0.42	NM_009496	ENSMUSG00000030337	Vamp1	RI	6.47	0.2367	0.29
chrX:7299375:7299504:+@chrX:7300441|7300691:7300879:+	0.16	0.41	0.2	0.28	0.58	0.6	0.45	0.58	NM_172372	ENSMUSG00000039382	Wdr45	A3SS	4.09	0.1833	0.29
chr13:54785699:54785849:-@chr13:54785436|54785450:54785322:-	NA	NA	0.52	0.23	0.59	0.79	0.58	0.72	NM_134064,NM_001146026,NM_001146025,NM_001146027	ENSMUSG00000034928	Rnf44	A3SS	2.48	0.145	0.29
chr17:8365793:8365873:+@chr17:8368384:8368443:+@chr17:8375093:8375319:+	0.87	0.85	0.93	0.9	0.57	0.63	0.57	0.64	NM_001197046,NM_201230	ENSMUSG00000069135	Fgfr1op	SE	6.62	0.24	0.28
chr15:99569096:99569252:-@chr15:99567978:99568084:-@chr15:99566023:99566867:-	0.17	0.15	0.15	0.13	0.4	0.45	0.35	0.51	NM_028015	ENSMUSG00000023021	Lass5	SE	6.42	0.2233	0.28
chr2:142565259:142565347:-@chr2:142540798:142540830:-@chr2:142540415:142540468:-	0.5	0.48	0.54	0.42	0.21	0.17	0.21	0.21	NM_001081133	ENSMUSG00000038844	Kif16b	SE	6.61	0.2433	0.28
chr6:142601047:142601152:-@chr6:142596547:142596585:-@chr6:142594792:142594893:-	0.21	0.27	0.27	0.28	0.58	0.54	0.51	0.53	NM_021042,NM_001044720,NM_021041,NM_011511	ENSMUSG00000030249	Abcc9	SE	6.91	0.2467	0.28
chr7:73823966:73824227:-@chr7:73823043:73823131:-@chr7:73804536:73805141:-	0.66	0.75	0.75	NA	0.44	0.49	0.42	0.39	NR_003961,NM_080443	ENSMUSG00000030509	Asb7	SE	4.93	0.2294	0.28
chr17:46461863-46460642:-@chr17:46460528-46460301:-	0.17	0.22	NA	NA	0.43	0.56	0.5	0.43	NM_170680,NM_145140	ENSMUSG00000032842	Abcc10	RI	4.1	0.2121	0.28
chr1:51535243-51534669:-@chr1:51534460-51534322:-	0.27	0.34	0.23	0.34	0.4	0.56	0.65	0.69	NM_028696	ENSMUSG00000026107	Obfc2a	RI	3.87	0.1667	0.28
chr6:88855943:88856072:+@chr6:88856532:88856706:+@chr6:88857570:88857820:+@chr6:88857935:88858066:+	0.25	0.29	0.27	NA	0.68	0.49	0.42	0.59	NM_011906	ENSMUSG00000002871	Tpra1	MXE	3.47	0.1683	0.28
chr11:69734665:69734888:-@chr11:69733843:69733936:-@chr11:69732951:69732980:-@chr11:69732653:69732838:-	0.75	0.7	0.74	0.83	0.48	0.56	0.42	0.46	NM_001166593,NM_001166591,NM_001166589,NM_001166595,NM_181582	ENSMUSG00000078812	Eif5a	MXE	6.05	0.205	0.28
chr2:59821839:59822027:-@chr2:59816758|59816764:59816600:-	0.93	0.91	0.96	NA	0.7	0.66	0.66	0.59	NM_001001182	ENSMUSG00000026987	Baz2b	A3SS	5.14	0.2331	0.28
chr10:5298683:5299010:+@chr10:5301207:5301275:+@chr10:5302788:5302930:+	0.47	0.49	0.42	0.56	0.25	0.21	0.19	0.21	NM_022027,NM_153399,NM_001079686	ENSMUSG00000019769	Syne1	SE	6.5	0.2183	0.27
chr16:45742890:45743068:-@chr16:45740432:45740615:-@chr16:45737637:45737748:-	0.6	0.7	0.46	0.49	0.85	0.87	0.8	0.81	NM_172511	ENSMUSG00000033157	Abhd10	SE	4.73	0.18	0.27
chr2:26244669:26244836:-@chr2:26244012:26244080:-@chr2:26243076:26243191:-	0.45	0.63	0.51	0.58	0.26	0.25	0.32	0.25	NM_026563,NM_001085407,NM_001085408	ENSMUSG00000026927	Sdccag3	SE	5.74	0.2033	0.27
chr4:123122078:123122195:-@chr4:123118846:123118908:-@chr4:123117793:123118034:-	0.56	0.35	0.57	0.49	0.28	0.16	0.23	0.2	NM_001199137,NM_001199136	ENSMUSG00000028649	Macf1	SE	4.46	0.1817	0.27

chr11:104167940:104168072:+@chr11:104169195:104169248:+@chr11:104171583:104171848:+	0.83	0.91	0.85	0.89	0.6	0.67	0.58	0.55	NM_001038609,NM_010838	ENSMUSG00000018411	Mapt	SE	6.24	0.215	0.27
chr15:76262579-76262725:+@chr15:76263704-76263826:+	0.18	0.26	0.19	NA	0.49	0.43	0.51	0.5	NM_175457,NM_001162489	ENSMUSG00000022558	Heatr7a	RI	5.03	0.2269	0.27
chr2:148535169-148535053:-@chr2:148532941-148532895:-	0.7	0.57	0.81	0.79	0.49	0.47	0.4	0.43	NM_019632	ENSMUSG00000027438	Napb	RI	4.45	0.1767	0.27
chr11:101886468-101886391:-@chr11:101885096-101885016:-	0.04	0.12	0.18	0.07	0.42	0.44	0.3	0.33	NM_007863	ENSMUSG00000052373	Mpp3	RI	5.48	0.1883	0.27
chrX:98734407:98734526:+@chrX:98736099|98736162:98736340:+	0.67	0.64	0.6	0.67	0.4	0.43	0.45	0.22	NM_001081008	ENSMUSG00000031314	Taf1	A3SS	6.43	0.19	0.27
chr17:85489446:85489607:-@chr17:85487680:85488215:-@chr17:85482533:85482655:-	0.87	0.87	0.94	0.92	0.67	0.63	0.65	0.61	NM_145984,NM_001163623,NM_001163624,NM_001163622	ENSMUSG00000024127	Prepl	SE	6.72	0.2217	0.26
chr15:79195715:79195909:-@chr15:79194088:79194108:-@chr15:79191114:79193315:-	0.5	0.6	0.5	0.48	0.77	0.74	0.82	0.81	NM_172608	ENSMUSG00000009035	Tmem184b	SE	5.88	0.2117	0.26
chr5:29704667:29704930:-@chr5:29691461:29692355:-@chr5:29690423:29690495:-	0.52	0.44	0.65	0.4	0.27	0.18	0.2	0.33	NM_020295	ENSMUSG00000010721	Lmbr1	SE	4.71	0.145	0.26
chr2:30908505:30908687:-@chr2:30900402:30900416:-@chr2:30895925:30896034:-	0.56	NA	0.63	NA	0.81	0.91	0.84	0.86	NM_001177650,NM_001177648,NM_001177649,NM_001038700	ENSMUSG00000075415	Fnbp1	SE	4.56	0.2043	0.26
chr2:59800078:59800687:-@chr2:59797878:59798162:-@chr2:59796489:59796549:-	0.44	0.58	0.69	0.58	0.41	0.2	0.34	0.3	NM_001001182	ENSMUSG00000026987	Baz2b	SE	4.07	0.1417	0.26
chr6:4696980:4697204:-@chr6:4680006:4680113:-@chr6:4669374:4669496:-	0.22	0.16	0.23	0.1	0.47	0.4	0.38	0.49	NM_011360,NM_001130191,NM_001130189,NM_001130190,NM_001130188	ENSMUSG00000004631	Sgce	SE	6.1	0.1867	0.26
chr1:133915927:133916043:+@chr1:133920130:133920415:+@chr1:133928141:133929189:+	0.62	0.75	0.76	0.81	0.5	0.51	0.49	0.39	NM_007923	ENSMUSG00000026436	Elk4	SE	5.25	0.1833	0.26
chrX:68630779:68630805:+@chrX:68632189:68632239:+@chrX:68636375:68636450:+	NA	0.58	0.53	0.42	0.28	NA	NA	0.21	NM_016985	ENSMUSG00000015214	Mtmr1	SE	2.39	0.1675	0.26
chr15:66454323-66454379:+@chr15:66455554-66455661:+	0.38	0.29	0.55	0.51	0.75	0.6	0.73	0.7	NM_001081409	ENSMUSG00000072501	Phf20l1	RI	4.09	0.1467	0.26
chr6:140599277-140599303:+@chr6:140599837-140601347:+	0.54	0.59	0.61	0.55	0.8	0.85	0.82	0.86	NM_009637,NM_178803,NM_001005605	ENSMUSG00000030232	Aebp2	RI	6.65	0.2217	0.26
chr2:25477454:25477522:-@chr2:25477128:25477194:-@chr2:25476881:25476978:-@chr2:25476586:25476693:-	0.64	0.5	0.69	0.67	0.36	0.36	0.39	0.34	NM_001040130	ENSMUSG00000026939	Tmem141	MXE	5.13	0.2	0.26
chr13:83732039:83732242:+@chr13:83764760:83764903:+@chr13:83764965:83765102:+@chr13:83772658:83772844:+	0.27	0.25	0.28	0.24	0.5	0.49	0.53	0.54	NM_025282,NM_001170537	ENSMUSG00000005583	Mef2c	MXE	6.84	0.2283	0.26
chr2:156688335:156688681:-@chr2:156679754|156680040:156679167:-	0.24	NA	0.41	NA	0.6	0.53	0.46	0.75	NR_015591,NR_027914	ENSMUSG00000085741	5430405H02Rik	A3SS	2	0.1014	0.26
chr2:148535169:148532895|148535053:-@chr2:148532682:148532759:-	0.45	0.4	0.6	0.52	0.27	0.24	0.2	0.22	NM_019632	ENSMUSG00000027438	Napb	A5SS	5.89	0.185	0.26
chr16:84978309:84978530:-@chr16:84971653:84971706:-@chr16:84965915:84966015:-	0.53	0.56	0.55	0.5	0.77	0.77	0.8	0.79	NM_001198826,NM_001198825,NM_007471,NM_001198823,NM_001198824	ENSMUSG00000022892	App	SE	6.89	0.2217	0.25
chr16:29588338:29588445:+@chr16:29588909:29588962:+@chr16:29589767:29589834:+	0.52	0.54	0.5	0.53	0.27	0.25	0.34	0.22	NM_001199177,NM_133752	ENSMUSG00000038084	Opa1	SE	6.32	0.21	0.25
chr11:84671942:84672040:-@chr11:84667757:84667882:-@chr11:84667556:84667669:-	0.55	0.56	0.59	0.5	0.25	0.31	0.31	0.32	NM_153144	ENSMUSG00000020530	Ggnbp2	SE	6.66	0.2117	0.25
chr19:27291510-27291622:+@chr19:27292033-27292186:+	0.62	0.75	0.73	0.62	0.34	0.29	0.58	0.51	NA	ENSMUSG00000024924	Vldlr	RI	3.17	0.1217	0.25
chr5:109109130-109109225:+@chr5:109109314-109109516:+	0.15	0.23	0.18	0.44	0.54	0.55	0.38	0.53	NM_008325	ENSMUSG00000033540	Idua	RI	2.83	0.1375	0.25
chr12:103150900:103151381:-@chr12:103144023|103144026:103143965:-	0.54	0.46	0.6	NA	NA	0.71	0.74	0.9	NM_028446	ENSMUSG00000021188	Trip11	A3SS	2.9	0.14	0.25
chr18:6061845:6061970:-@chr18:6057515:6057589:-@chr18:6052860:6052921:-	0.55	0.53	0.39	0.58	0.21	0.23	0.27	0.36	NM_001039692,NM_029277	ENSMUSG00000041225	Arhgap12	SE	4.05	0.155	0.24
chr17:28453804:28453848:+@chr17:28454103:28454168:+@chr17:28454413:28454556:+	0.72	0.36	0.44	NA	0.74	0.81	0.73	0.7	NM_001163819,NR_028297,NM_001163820,NR_028296	ENSMUSG00000007570	Fance	SE	2.33	0.1239	0.24
chr12:86607102:86610424:-@chr12:86603717:86603812:-@chr12:86602611:86602702:-	0.7	0.65	0.67	0.66	0.41	0.4	0.45	0.45	NM_175337	ENSMUSG00000021245	Mlh3	SE	6.83	0.2133	0.24
chrX:46366674:46366759:-@chrX:46366310:46366357:-@chrX:46362884:46364811:-	0.83	0.76	0.71	0.83	0.58	0.53	0.51	0.57	NA	ENSMUSG00000031109	Enox2	SE	5.84	0.1783	0.24
chr5:124889939:124890024:+@chr5:124895978:124896093:+@chr5:124897223:124897379:+	0.44	0.44	0.59	0.41	0.76	0.65	0.7	0.72	NM_030241	ENSMUSG00000049327	Setd8	SE	4.52	0.1633	0.24
chr2:84453093:84453246:-@chr2:84452689:84452706:-@chr2:84452181:84452249:-	0.51	0.49	0.5	0.63	0.76	0.8	0.72	0.79	NM_001085450,NM_007615,NM_001085449,NM_001085448,NM_001085453	ENSMUSG00000034101	Ctnnd1	SE	5.15	0.1767	0.24
chr7:82821992:82822365:+@chr7:82824706:82824759:+@chr7:82830003:82830195:+	0.56	0.45	0.44	0.68	0.76	0.76	0.8	0.75	NM_029332	ENSMUSG00000066406	Akap13	SE	4.1	0.1533	0.24
chr7:82821992:82822365:+@chr7:82828280:82828345:+@chr7:82830003:82830195:+	0.41	0.48	0.39	0.55	0.72	0.73	0.65	0.69	NM_029332	ENSMUSG00000066406	Akap13	SE	5.35	0.1717	0.24
chr9:110011530:110011625:-@chr9:110010445:110010473:-@chr9:110001233:110001363:-	0.5	0.63	0.69	0.48	0.41	0.1	0.41	0.41	NM_133347	ENSMUSG00000032480	Dhx30	SE	4.14	0.1017	0.24
chr4:45360978:45361091:+@chr4:45362409:45362463:+@chr4:45372633:45372830:+	0.48	0.51	0.5	0.42	0.25	0.36	0.24	0.08	NM_153167	ENSMUSG00000035572	Dcaf10	SE	4.8	0.15	0.24

chr11:120474693:120474737:-@chr11:120474160:120474397:-@chr11:120473777:120473915:-	0.5	0.54	0.42	0.32	0.67	0.74	0.66	0.67	NM_024229	ENSMUSG00000025137	Pcyt2	SE	5.77	0.1583	0.24
chr4:75732503-75731916:-@chr4:75731462-75731365:-	0.3	0.28	NA	0.15	0.33	0.55	0.51	0.53	NM_011211,NM_001014288	ENSMUSG00000028399	Ptprd	RI	2.61	0.1278	0.24
chr2:156571571:156571932:+@chr2:156573759|156574068:156574156:+	0.16	0.17	0.19	0.19	0.46	0.44	0.39	0.39	NM_001042488,NM_001042487,NM_146128	ENSMUSG00000061689	Dlgap4	A3SS	6.76	0.2117	0.24
chr11:61307768:61307026|61307149:-@chr11:61306406:61306571:-	NA	NA	0.1	0.88	0.33	0.16	0.27	0.23	NM_011841	ENSMUSG00000001034	Mapk7	A5SS	2.19	0.2	0.24
chr12:8996711:8996896:+@chr12:9002446:9002478:+@chr12:9002875:9002935:+	0.69	0.69	0.44	0.65	0.47	0.38	0.3	0.4	NM_172470,NM_001159527	ENSMUSG00000066643	Wdr35	SE	2.87	0.1238	0.23
chr16:56647138:56647212:+@chr16:56650824:56650883:+@chr16:56652250:56652330:+	0.67	0.73	0.86	0.69	0.47	0.49	0.46	0.6	NM_001014399,NM_178790,NM_001014424,NM_001014422,NM_001014423	ENSMUSG00000035258	Abi3bp	SE	4.85	0.145	0.23
chr14:55272372:55272522:-@chr14:55272051:55272154:-@chr14:55270554:55270695:-	0.58	0.61	0.36	0.58	0.35	0.31	0.33	0.21	NM_023190,NM_001085473,NM_001085472,NM_019567	ENSMUSG00000022185	Acin1	SE	3.14	0.1333	0.23
chr2:26244436:26244585:-@chr2:26244012:26244080:-@chr2:26243076:26243191:-	0.93	0.95	0.91	0.94	0.64	0.73	0.82	0.61	NM_026563,NM_001085407,NM_001085408	ENSMUSG00000026927	Sdccag3	SE	4.86	0.1617	0.23
chr6:72368295:72368460:+@chr6:72369011:72369260:+@chr6:72372410:72372488:+	0.16	0.2	0.3	0.26	0.43	0.48	0.43	0.52	NM_019802	ENSMUSG00000053460	Ggcx	SE	5.97	0.1683	0.23
chr6:86368872:86368926:+@chr6:86369095:86369127:+@chr6:86370318:86370405:+	0.64	0.43	0.45	NA	0.73	0.76	0.76	0.7	NM_001164079,NM_011585,NM_001164078	ENSMUSG00000071337	Tia1	SE	3.73	0.1608	0.23
chr9:49365201:49365343:-@chr9:49358645:49358674:-@chr9:49354263:49354413:-	NA	0.62	0.46	0.66	0.26	0.41	0.32	0.43	NM_001081445,NM_001113204,NM_010875	ENSMUSG00000039542	Ncam1	SE	2.82	0.1139	0.23
chr11:115290594:115290719:+@chr11:115290949:115291096:+@chr11:115291200:115291515:+	0.31	0.4	NA	0.52	0.51	0.59	0.75	0.71	NM_183285	ENSMUSG00000016940	Kctd2	SE	2.08	0.0917	0.23
chr1:75547330-75547510:+@chr1:75547822-75547957:+	NA	0.55	0.47	NA	0.74	0.74	0.72	0.76	NM_009208	ENSMUSG00000006576	Slc4a3	RI	5.05	0.2014	0.23
chr2:76393071:76393174:+@chr2:76393947:76394039:+@chr2:76398243:76398317:+@chr2:76402841:76403006:+	0.3	0.38	0.27	0.24	0.06	0.07	0.09	0.05	NM_145525	ENSMUSG00000042359	Osbpl6	MXE	6.6	0.1817	0.23
chr11:70049499:70049713:-@chr11:70048966|70048970:70048706:-	0.94	0.79	0.86	NA	0.59	0.68	0.65	0.6	NA	NA	NA	A3SS	4.76	0.1644	0.23
chr2:131059799:131059863|131060091:+@chr2:131064472:131064646:+	0.53	0.61	0.5	0.6	0.38	0.35	0.29	0.32	NA	ENSMUSG00000037523	Mavs	A5SS	5.91	0.1667	0.23
chr15:79604789:79604897:-@chr15:79596217:79596283:-@chr15:79595246:79595451:-	NA	0.44	0.34	NA	0.25	0.17	0.2	0.06	NM_017470	ENSMUSG00000022420	Dnalc4	SE	3.12	0.12	0.22
chr10:29081790:29082248:-@chr10:29081091:29081151:-@chr10:29074098:29074253:-	0.58	0.45	0.68	0.7	0.48	0.34	0.39	0.33	NM_001110198,NM_001110197,NM_001110196,NM_026518	ENSMUSG00000038876	Rnf146	SE	2.85	0.1087	0.22
chr16:18289196:18289261:-@chr16:18285194:18285401:-@chr16:18283790:18284789:-	0.51	0.55	0.3	0.21	0.18	0.19	0.19	0.15	NM_033324	ENSMUSG00000022718	Dgcr8	SE	2.48	0.1017	0.22
chrX:7299375:7299504:+@chrX:7300441:7300879:+@chrX:7300979:7301046:+	0.55	0.51	0.33	0.4	0.67	0.64	0.6	0.77	NM_172372	ENSMUSG00000039382	Wdr45	SE	4.22	0.1133	0.22
chr14:70634947:70635015:-@chr14:70625735:70625761:-@chr14:70624774:70624855:-	0.75	0.71	0.71	0.74	0.42	0.52	0.53	0.54	NM_008915	ENSMUSG00000022092	Ppp3cc	SE	6.85	0.1817	0.22
chr5:118364393:118364451:+@chr5:118365556:118365657:+@chr5:118369405:118369521:+	0.79	0.69	0.73	0.73	0.46	0.5	0.51	0.59	NM_008712	ENSMUSG00000029361	Nos1	SE	5.75	0.1617	0.22
chr2:29821080:29821305:+@chr2:29824296:29824346:+@chr2:29833897:29834136:+	0.06	0.04	0.05	0.06	0.28	0.32	0.23	0.27	NM_001076554,NM_001177667,NM_001177668	ENSMUSG00000057738	Spna2	SE	6.72	0.1933	0.22
chr2:126739268:126739324:-@chr2:126739036:126739089:-@chr2:126738379:126738481:-	0.66	0.66	0.62	0.57	0.41	0.38	0.39	0.43	NM_023220	ENSMUSG00000027366	2010106G01Rik	SE	6.25	0.185	0.22
chr9:21294187:21294238:+@chr9:21295102:21295113:+@chr9:21298948:21299061:+	0.32	0.39	0.33	0.26	0.12	0.09	0.12	0.11	NM_001039520	ENSMUSG00000033335	Dnm2	SE	6.37	0.1733	0.22
chr4:9563048:9563116:-@chr4:9537990:9538085:-@chr4:9531663:9531776:-	0.94	0.85	0.92	0.92	0.61	0.69	0.78	0.68	NM_001177854,NM_001177852,NM_001177853,NM_001177851,NM_001177850,NM_001177849,NM_023066	ENSMUSG00000028207	Asph	SE	5.13	0.1517	0.22
chr11:83993375:83993428:+@chr11:84006581:84006627:+@chr11:84008940:84009189:+	0.71	0.69	0.69	0.49	0.42	NA	0.36	0.49	NM_133360	ENSMUSG00000020532	Acaca	SE	2.34	0.1194	0.22
chr8:87417820-87417641:-@chr8:87417583-87417454:-	0.5	0.46	0.51	0.45	0.23	0.25	0.26	0.28	NM_001044744	ENSMUSG00000003809	Gcdh	RI	6.71	0.1933	0.22
chr7:30697188-30697314:+@chr7:30697609-30697704:+	0.37	0.38	0.55	0.61	0.68	0.7	0.74	0.67	NA	ENSMUSG00000058402	Zfp420	RI	3.64	0.1267	0.22
chr9:71403544-71403392:-@chr9:71400171-71400046:-	0.52	0.21	0.43	0.42	0.61	0.72	0.59	0.55	NM_001033208	ENSMUSG00000092137,ENSMUSG00000041361	Gcom1	RI	4.34	0.1	0.22
chr11:51405508-51405595:+@chr11:51405671-51405787:+	0.12	0.07	0.09	0.04	0.3	0.23	0.32	0.34	NM_028398	ENSMUSG00000020359	Agxt2l2	RI	5.91	0.1667	0.22
chr2:155376091:155376205:+@chr2:155376926:155376964:+@chr2:155381590:155381727:+	0.5	0.7	0.72	0.58	0.8	0.89	0.85	0.79	NM_019811	ENSMUSG00000027605	Acss2	SE	4.39	0.1133	0.21
chr6:149137128:149137234:-@chr6:149133514:149133646:-@chr6:149131916:149132060:-	0.46	0.48	0.38	0.61	0.71	0.76	0.67	0.63	NM_001113424	ENSMUSG00000068250	Amn1	SE	3.76	0.115	0.21
chr7:151637932:151638042:-@chr7:151636883:151636993:-@chr7:151635465:151635520:-	0.6	0.52	0.76	0.52	0.37	0.34	0.43	0.4	NM_007803	ENSMUSG00000031078	Cttn	SE	5.52	0.1233	0.21
chr9:15128593:15128735:-@chr9:15128013:15128154:-@chr9:15126944:15127527:-	0.96	0.92	0.89	0.92	0.84	0.55	0.63	0.84	NM_176976	ENSMUSG00000046111	5830418K08Rik	SE	3.03	0.1	0.21

chr4:115547986:115548150:+@chr4:115549186:115549229:+@chr4:115550555:115551853:+	0.9	0.92	0.89	0.91	0.71	0.68	0.69	0.72	NM_021461	ENSMUSG00000028708	Mknk1	SE	6.86	0.185	0.21
chr4:123042516:123042590:-@chr4:123041300:123041317:-@chr4:123038153:123038270:-	0.68	0.74	0.62	0.69	0.92	0.92	0.87	0.87	NM_001199137,NM_001199136	ENSMUSG00000028649	Macf1	SE	6.26	0.165	0.21
chr4:98667724:98667893:-@chr4:98660338:98660427:-@chr4:98659060:98659149:-	0.64	0.56	0.55	NA	0.8	0.77	0.82	0.8	NM_026082	ENSMUSG00000028556	Dock7	SE	5.12	0.1775	0.21
chr3:14607293-14607177:-@chr3:14606408-14606289:-	0.32	0.33	0.3	0.32	0.54	0.5	0.54	0.54	NA	NA	NA	RI	6.76	0.195	0.21
chr8:107852222-107852384:+@chr8:107852508-107852592:+	0.31	0.25	0.25	0.32	0.46	0.51	0.53	0.46	NM_025486	ENSMUSG00000014856	Tmem208	RI	6.25	0.1633	0.21
chr8:107762323-107762366:+@chr8:107763571-107763650:+	0.32	0.4	0.34	0.53	0.66	0.65	0.62	0.5	NM_145604	ENSMUSG00000031889	D230025D16Rik	RI	3.05	0.1137	0.21
chr2:155393623-155393429:-@chr2:155392620-155392539:-	0.82	0.83	0.89	0.92	0.6	0.69	0.64	0.69	NM_008180	ENSMUSG00000027610	Gss	RI	6.17	0.1533	0.21
chr3:106334055:106334196:-@chr3:106322927:106323011:-@chr3:106315721:106315805:-@chr3:106308639:106308770:-	0.45	0.45	0.42	0.4	0.62	0.59	0.65	0.71	NM_133869	ENSMUSG00000040774	Cept1	MXE	6.52	0.165	0.21
chr7:29697259:29697340:-@chr7:29696509:29696594:-@chr7:29694922:29695007:-@chr7:29691991:29692083:-	0.08	0.05	0.06	0.04	0.26	0.34	0.23	0.24	NM_021895	ENSMUSG00000054808	Actn4	MXE	6.79	0.17	0.21
chr2:120247761:120247940|120248485:+@chr2:120249435:120249480:+	0.59	0.56	0.49	0.45	0.74	0.67	0.68	0.82	NM_172672	ENSMUSG00000062646	Ganc	A5SS	5.18	0.1217	0.21
chr9:22280175:22280499|22280634:+@chr9:22281014:22281069:+	NA	0.34	0.38	0.22	0.53	0.59	0.52	0.44	NM_181316,NM_178415	ENSMUSG00000035919	Bbs9	A5SS	3.86	0.12	0.21
chr19:46443727:46443823:+@chr19:46446426:46446597:+@chr19:46446672:46446865:+	0.69	0.66	NA	NA	0.89	0.88	0.85	0.9	NM_029186	ENSMUSG00000025227	Tmem180	SE	4.64	0.1779	0.2
chr19:40457011:40457123:-@chr19:40451474:40451506:-@chr19:40447966:40448107:-	0.28	0.24	0.2	0.17	0.5	0.32	0.37	0.52	NM_001034962,NM_009166,NM_001034963,NM_178362,NM_001034964	ENSMUSG00000025006	Sorbs1	SE	3.77	0.1133	0.2
chr15:102035002:102035314:+@chr15:102035660:102035736:+@chr15:102038202:102038351:+	0.54	0.6	0.7	NA	0.33	0.47	0.5	0.34	NM_153194	ENSMUSG00000046897	Zfp740	SE	2.66	0.0967	0.2
chr10:87985712:87985898:-@chr10:87984022:87984080:-@chr10:87982646:87982688:-	0.23	0.2	0.25	0.26	0.04	0.03	0.04	0.03	NM_175418	ENSMUSG00000020061	Mybpc1	SE	6.73	0.18	0.2
chr14:19109210:19109320:+@chr14:19110358:19110615:+@chr14:19110818:19111059:+	0.26	0.25	0.18	0.2	0.02	0.02	0.03	0.03	NM_023526	ENSMUSG00000021772	Nkiras1	SE	6.53	0.17	0.2
chr14:21113912:21114014:+@chr14:21116737:21116853:+@chr14:21119809:21119901:+	0.31	0.38	0.26	0.35	0.51	0.46	0.54	0.57	NM_026341	ENSMUSG00000021809	Nudt13	SE	5.58	0.1317	0.2
chr5:136497625:136497728:+@chr5:136502340:136502477:+@chr5:136504369:136504442:+	0.57	0.5	0.67	NA	0.39	0.4	0.33	0.38	NM_023742	ENSMUSG00000004947	Dtx2	SE	5	0.1428	0.2
chr2:76759608:76759664:-@chr2:76745365:76748010:-@chr2:76744311:76744589:-	0.54	0.4	0.42	0.46	0.66	0.65	0.59	0.71	NM_028004,NM_011652	ENSMUSG00000051747	Ttn	SE	4.72	0.1283	0.2
chr2:29575113:29575370:+@chr2:29576163:29576258:+@chr2:29577744:29577829:+	0.66	0.68	0.64	0.73	0.48	0.46	0.45	0.5	NM_001039086,NM_001039087,NM_054050	ENSMUSG00000039844	Rapgef1	SE	6.66	0.1667	0.2
chr2:35111879:35111993:+@chr2:35122340:35122423:+@chr2:35139425:35139629:+	0.03	0.02	0.03	0.02	0.29	0.2	0.22	0.18	NA	NA	NA	SE	6.79	0.165	0.2
chr2:74367688:74367858:-@chr2:74366149:74366231:-@chr2:74352894:74360354:-	0.91	0.89	0.88	0.92	0.75	0.67	0.72	0.65	NA	NA	NA	SE	6.31	0.1617	0.2
chr7:30066531:30066996:-@chr7:30048614:30048784:-@chr7:30045390:30045449:-	0.2	0.32	0.49	NA	0.17	0.15	0.05	0.17	NM_001082548,NM_011464	ENSMUSG00000074227	Spint2	SE	2.96	0.095	0.2
chr7:51747325:51747418:-@chr7:51746533:51746619:-@chr7:51745308:51746340:-	0.1	0.14	0.15	0.12	0.32	0.3	0.35	0.32	NM_197991	ENSMUSG00000008140	2310044H10Rik	SE	6.81	0.1683	0.2
chr7:135591635:135591722:-@chr7:135590245:135590621:-@chr7:135589709:135589784:-	0.1	0.12	0.09	0.11	0.34	0.31	0.21	0.34	NM_009383	ENSMUSG00000030846	Tial1	SE	5.21	0.1517	0.2
chr9:121640596:121640683:+@chr9:121647506:121649193:+@chr9:121650240:121650269:+	0.52	0.47	0.62	0.65	0.79	0.77	0.73	0.78	NM_010918	ENSMUSG00000032525	Nktr	SE	5.03	0.1333	0.2
chr13:74493904:74494265:+@chr13:74497139:74497274:+@chr13:74498053:74503231:+	0.78	0.83	0.84	0.8	0.65	0.68	0.53	0.59	NM_001168659,NM_001168658	ENSMUSG00000021578	Ccdc127	SE	5.83	0.14	0.2
chr11:54776335:54776442:-@chr11:54769523:54769680:-@chr11:54753100:54753237:-	0.26	0.29	0.4	NA	0.45	0.61	0.42	0.59	NA	NA	NA	SE	2.25	0.0908	0.2
chr11:77590767:77591816:+@chr11:77629358:77629501:+@chr11:77631121:77631208:+	0.08	0.06	0.05	0.08	0.19	0.33	0.13	0.44	NM_011586	ENSMUSG00000000631	Myo18a	SE	3.57	0.1067	0.2
chr11:29592898:29593693:+@chr11:29605535:29605591:+@chr11:29633633:29633840:+	0.03	0.02	0.05	0.01	0.21	0.22	0.26	0.2	NA	NA	NA	SE	6.82	0.1683	0.2
chr11:85627502:85627567:+@chr11:85635524:85635614:+@chr11:85638704:85639560:+	0.9	0.88	0.94	0.85	0.66	0.82	0.66	0.62	NM_138681,NM_001166643,NM_001166642	ENSMUSG00000059439	Bcas3	SE	3.81	0.1283	0.2
chr8:123626904-123626814:-@chr8:123625436-123625324:-	0.16	0.21	0.09	0.09	0.37	0.31	0.33	0.33	NM_172761,NM_001166482	ENSMUSG00000031816	Mthfsd	RI	5.58	0.1467	0.2
chr12:102320661-102322235:+@chr12:102322494-102322709:+	0.34	0.21	0.35	0.31	0.56	0.62	0.28	0.53	NA	NA	NA	RI	2.2	0.09	0.2
chr2:6468259-6468088:-@chr2:6467825-6460751:-	0.12	0.16	0.09	0.17	0.33	0.28	0.38	0.35	NM_001110229,NM_001110231,NM_001160292,NM_001110228,NM_001160293,NM_001110230,NM_001110232,NM_010160	ENSMUSG00000002107	Celf2	RI	6.09	0.15	0.2
chr2:6468259-6468088:-@chr2:6467825-6460744:-	0.12	0.16	0.09	0.17	0.33	0.29	0.37	0.35	NA	NA	NA	RI	6.29	0.155	0.2

chr7:140882849-140882769:-@chr7:140882276-140882191:-	0.47	0.45	0.36	0.34	0.64	0.56	0.67	0.57	NM_009479	ENSMUSG00000030979	Uros	RI	5.07	0.1317	0.2
chr7:28300270-28300466:+@chr7:28301059-28305233:+	0.39	0.43	0.25	0.52	0.12	0.26	0.29	0.11	NM_019412,NM_198048	ENSMUSG00000053198	Prx	RI	2.34	0.0813	0.2
chr7:28300270-28300466:+@chr7:28301059-28305060:+	0.38	0.42	0.25	0.52	0.12	0.25	0.28	0.11	NM_019412,NM_198048	ENSMUSG00000053198	Prx	RI	2.45	0.0821	0.2
chr4:107567478-107567543:+@chr4:107569476-107569723:+	0.51	0.49	0.51	0.58	0.74	0.76	0.68	0.7	NM_028754	ENSMUSG00000028608	0610037L13Rik	RI	5.84	0.1517	0.2
chr2:52018425:52018529:-@chr2:52017588:52017692:-@chr2:52016891:52016995:-@chr2:52016176:52016268:-	0.87	0.81	0.82	0.85	0.63	0.64	0.63	0.66	NM_010889	ENSMUSG00000026950	Neb	MXE	6.73	0.1717	0.2
chr4:137638808:137638903:+@chr4:137640172:137640285:+@chr4:137651824:137651844:+@chr4:137652667:137652846:+	0.13	0.27	0.1	0.2	0.4	0.33	0.3	0.46	NM_172703	ENSMUSG00000028760	Eif4g3	MXE	3.86	0.1033	0.2
chr11:69734665:69734888:-@chr11:69733843:69733924:-@chr11:69732951:69732980:-@chr11:69732653:69732838:-	0.58	0.52	0.57	0.67	0.38	0.48	0.29	0.4	NM_001166593,NM_001166591,NM_001166589,NM_001166595,NM_181582	ENSMUSG00000078812	Eif5a	MXE	4.65	0.11	0.2
chr9:119337085:119337194:+@chr9:119337319|119337343:119337686:+	0.86	0.91	0.96	0.75	0.62	0.76	0.53	0.77	NM_007397	ENSMUSG00000061393	Acvr2b	A3SS	2.42	0.0754	0.2
chr4:63219822:63219991:+@chr4:63221916|63221946:63222029:+	0.26	0.31	0.39	0.38	0.21	0.18	0.09	0.06	NM_144905	ENSMUSG00000045917	6330416G13Rik	A3SS	4.25	0.1167	0.2
chr3:31012330:31012424|31012562:+@chr3:31015738:31015961:+	0.41	0.44	0.3	NA	0.68	0.67	0.5	0.49	NM_001039090,NM_011386	ENSMUSG00000027660	Skil	A5SS	2.22	0.0883	0.2
chr17:26416906:26417073|26417109:+@chr17:26418570:26422449:+	0.24	0.27	0.36	0.25	0.54	0.44	0.42	0.52	NM_028190	ENSMUSG00000024188	Luc7l	A5SS	4.65	0.1317	0.2
chr6:42623637:42623352|42623378:-@chr6:42619465:42620322:-	0.93	0.71	NA	NA	0.65	0.66	0.67	0.51	NM_029930	ENSMUSG00000036667	Fam115a	A5SS	2.43	0.0961	0.2
chr9:61242415:61242489|61242519:+@chr9:61249660:61249864:+	0.19	NA	0.27	NA	NA	0.42	0.45	0.43	NM_001083927,NM_009389,NM_001083928	ENSMUSG00000032280	Tle3	A5SS	3.07	0.1683	0.2
chr8:107860282:107860461:-@chr8:107860137:107860160:-@chr8:107858587:107858702:-	0.46	0.65	0.48	NA	0.64	0.68	0.74	0.81	NM_177699	ENSMUSG00000014778	Fhod1	SE	2.24	0.0836	0.19
chr15:79158640:79158801:-@chr15:79158065:79158144:-@chr15:79148191:79148440:-	0.87	0.83	0.88	0.77	0.6	0.57	0.69	0.72	NA	ENSMUSG00000042632	Pla2g6	SE	4.41	0.1167	0.19
chr12:114355199:114355292:+@chr12:114358422:114358472:+@chr12:114359038:114359164:+	0.56	0.63	0.5	0.63	0.39	0.43	0.36	0.37	NM_054081	ENSMUSG00000021144	Mta1	SE	5	0.135	0.19
chr14:27237599:27237733:-@chr14:27235689:27235778:-@chr14:27232661:27234474:-	0.73	0.79	0.77	0.68	0.55	0.52	0.61	0.53	NM_032008	ENSMUSG00000021870	Slmap	SE	5.28	0.135	0.19
chr5:111170989:111171079:-@chr5:111169201:111169308:-@chr5:111168315:111168700:-	0.6	0.39	0.54	NA	0.32	0.31	0.43	0.22	NM_029337,NM_173066	ENSMUSG00000029505	Ep400	SE	2.11	0.0789	0.19
chr5:124575308:124575472:-@chr5:124574807:124574968:-@chr5:124573948:124574096:-	0.67	0.77	0.69	0.66	0.58	0.52	0.45	0.48	NM_011256	ENSMUSG00000029406	Pitpnm2	SE	5.48	0.125	0.19
chr2:30909544:30909738:-@chr2:30908505:30908600:-@chr2:30895925:30896034:-	NA	0.42	NA	0.24	0.51	0.52	0.51	0.52	NM_001177650,NM_001177648,NM_001177649,NM_001038700	ENSMUSG00000075415	Fnbp1	SE	4.56	0.1536	0.19
chr2:156756952:156757003:-@chr2:156755668:156755706:-@chr2:156753078:156754617:-	0.34	0.36	0.35	0.39	0.19	0.16	0.19	0.12	NA	NA	NA	SE	6.82	0.1617	0.19
chr2:76544497:76544650:-@chr2:76543727:76544029:-@chr2:76542041:76543386:-	0.65	0.73	0.69	0.58	0.86	0.83	0.89	0.84	NM_028004,NM_011652	ENSMUSG00000051747	Ttn	SE	6.04	0.135	0.19
chr7:135591635:135591722:-@chr7:135590245:135590312:-@chr7:135589709:135589784:-	0.08	0.05	0.06	0.03	0.26	0.29	0.17	0.25	NM_009383	ENSMUSG00000030846	Tial1	SE	5.64	0.1433	0.19
chr9:6337243:6337441:+@chr9:6359703:6359917:+@chr9:6376895:6377519:+	0.66	0.58	0.76	0.64	0.88	0.8	0.88	0.85	NM_027924	ENSMUSG00000032006	Pdgfd	SE	4.44	0.1233	0.19
chr13:107764575:107764642:-@chr13:107759784:107759897:-@chr13:107758718:107758868:-	0.78	0.72	0.88	0.88	0.68	0.58	0.67	0.57	NM_001145779,NM_008442	ENSMUSG00000021693	Kif2a	SE	3.71	0.1067	0.19
chr4:46195990:46196107:-@chr4:46193079:46193270:-@chr4:46188094:46188287:-	0.63	0.73	0.75	0.78	0.57	0.44	0.55	0.59	NM_011728	ENSMUSG00000028329	Xpa	SE	4.35	0.1067	0.19
chr4:122972445:122972564:+@chr4:122972993:122973079:+@chr4:122973173:122973300:+	0.31	0.39	0.35	0.32	0.57	0.51	0.52	0.52	NM_148917,NM_130881	ENSMUSG00000011257	Pabpc4	SE	6.37	0.15	0.19
chr11:85615287:85615454:+@chr11:85635524:85635614:+@chr11:85638704:85639560:+	0.56	0.74	0.7	0.59	0.47	0.52	0.44	0.4	NM_138681,NM_001166643,NM_001166642	ENSMUSG00000059439	Bcas3	SE	4	0.1033	0.19
chr11:59585119:59585204:+@chr11:59585654:59585719:+@chr11:59589018:59594362:+	0.62	0.67	0.65	0.63	0.48	0.49	0.43	0.42	NM_201245,NM_012027	ENSMUSG00000005417	Mprip	SE	6.47	0.1517	0.19
chr3:79399124-79399230:+@chr3:79401607-79401795:+	0.36	0.3	0.34	0.36	0.51	0.55	0.52	0.55	NM_026352	ENSMUSG00000027804	Ppid	RI	6.76	0.1633	0.19
chr17:47118391-47118303:-@chr17:47117367-47117269:-	0.31	0.38	0.42	0.34	0.51	0.45	0.62	0.63	NM_001177374,NM_146078	ENSMUSG00000023977	Ubr2	RI	3.7	0.105	0.19
chr8:90653594-90653703:+@chr8:90654240-90654300:+	0.12	0.24	0.19	0.22	0.35	0.35	0.38	0.44	NM_029074	ENSMUSG00000036810	Tmem188	RI	6.45	0.13	0.19
chr15:76162590-76162717:+@chr15:76162914-76163061:+	0.26	0.37	0.16	0.14	0.38	0.49	0.48	0.36	NM_010331	ENSMUSG00000022561	Gpaa1	RI	2.65	0.0896	0.19
chr10:18725137-18724263:-@chr10:18723563-18723382:-	0.31	0.26	0.43	0.25	0.13	0.12	0.16	0.08	NM_009397,NM_001166402	ENSMUSG00000019850	Tnfaip3	RI	6.06	0.12	0.19
chr16:20522329-20522398:+@chr16:20523483-20523604:+	0.37	0.23	0.23	0.31	0.53	0.44	0.46	0.47	NM_007889	ENSMUSG00000003233	Dvl3	RI	4.86	0.125	0.19
chr9:107481431-107481716:+@chr9:107482788-107483266:+	0.83	0.71	0.75	0.73	0.65	0.65	0.45	0.51	NM_008317,NM_019750	ENSMUSG00000079334,ENSMUSG00000001005 1	Nat6,Hyal1	RI	3.94	0.0967	0.19

chr14:121993558:121993605:-@chr14:121991034:121991104:-@chr14:121990533:121990576:-@chr14:121985449:121985564:-	0.22	0.22	0.21	0.37	0.51	0.34	0.36	0.57	NM_001081039,NM_001128308,NM_001128307,NM_134074	ENSMUSG00000025558	Dock9	MXE	2.45	0.085	0.19
chr4:149615154:149615249:+@chr4:149615876:149615934:+@chr4:149616231:149616289:+@chr4:149618114:149618183:+	0.32	0.61	0.66	0.55	0.71	0.79	0.7	0.71	NM_001025388	ENSMUSG00000063524	Eno1	MXE	4.36	0.08	0.19
chrX:7709413:7709984:-@chrX:7708717|7709003:7708511:-	0.94	0.76	0.93	0.92	0.77	0.69	0.64	0.69	NM_026137,NR_029428	ENSMUSG00000031166	Wdr13	A3SS	3.26	0.1129	0.19
chr7:19677557:19677603:+@chr7:19677767|19677896:19677981:+	0.33	0.44	0.37	0.45	0.61	0.66	0.53	0.56	NM_001190490,NM_032418,NM_001190491	ENSMUSG00000030409	Dmpk	A3SS	5.3	0.12	0.19
chr7:19677557:19677603:+@chr7:19677767|19677892:19677981:+	0.28	0.37	0.31	0.39	0.53	0.61	0.49	0.5	NM_001190490,NM_032418,NM_001190491	ENSMUSG00000030409	Dmpk	A3SS	5.94	0.13	0.19
chr4:134896762:134896950:-@chr4:134896519|134896522:134896418:-	0.93	0.92	NA	NA	0.76	0.69	0.77	0.72	NM_001130477,NM_016799	ENSMUSG00000028809	Srrm1	A3SS	4.08	0.1486	0.19
chr17:8514665:8514700|8515005:+@chr17:8516142:8516200:+	NA	0.83	0.76	NA	0.62	0.55	0.56	0.68	NM_134114	ENSMUSG00000073468	Sft2d1	A5SS	3.12	0.1182	0.19
chr8:86097821:86097608|86097770:-@chr8:86097310:86097354:-	0.31	0.24	0.22	0.26	0.45	0.46	0.46	0.43	NM_134118,NM_027179	ENSMUSG00000031708	Tecr	A5SS	6.3	0.16	0.19
chr18:14798766:14798870:-@chr18:14795901:14795993:-@chr18:14795005:14795127:-	0.62	0.73	0.58	0.49	0.77	0.77	0.77	0.84	NM_009280,NM_001161370,NM_001161369,NM_001161371	ENSMUSG00000037013	Ss18	SE	3.89	0.1017	0.18
chr17:6035411:6035559:+@chr17:6036357:6036505:+@chr17:6037384:6038555:+	0.24	0.19	0.22	0.17	0.34	0.42	0.37	0.42	NM_001113353,NM_001113352,NM_001113351,NM_011523	ENSMUSG00000023805	Synj2	SE	5.96	0.1383	0.18
chr19:40473032:40473100:-@chr19:40470169:40470258:-@chr19:40467878:40468006:-	0.61	0.61	0.63	0.64	0.81	0.79	0.83	0.77	NM_001034962,NM_009166,NM_001034963,NM_178362,NM_001034964	ENSMUSG00000025006	Sorbs1	SE	6.68	0.1517	0.18
chr19:40424389:40424503:-@chr19:40418846:40418929:-@chr19:40411476:40411525:-	0.49	0.66	0.78	0.75	0.81	0.91	0.85	0.85	NM_001034962,NM_009166,NM_001034963,NM_178362,NM_001034964	ENSMUSG00000025006	Sorbs1	SE	3.93	0.08	0.18
chr19:5406874:5407083:+@chr19:5415008:5415099:+@chr19:5415607:5415812:+	0.43	NA	0.41	NA	0.52	0.61	0.58	0.69	NR_027940,NR_015545,NR_027938	ENSMUSG00000086938	4930481A15Rik	SE	2.73	0.1	0.18
chr10:12981572:12981730:-@chr10:12977383:12977622:-@chr10:12973148:12973685:-	0.32	0.26	0.25	0.39	0.13	0.17	0.09	0.09	NM_001033257,NM_001195066,NM_001195065,NM_001195096	ENSMUSG00000062866	Phactr2	SE	5.45	0.1217	0.18
chr12:107067267:107067487:+@chr12:107072920:107072967:+@chr12:107074975:107077153:+	0.09	0.11	0.15	0.09	0.25	0.31	0.31	0.29	NA	ENSMUSG00000021111	Papola	SE	6.07	0.1467	0.18
chr16:20540406:20540488:+@chr16:20540881:20540886:+@chr16:20541048:20541183:+	0.11	0.01	0.01	0.17	0.28	0.19	0.28	0.25	NM_009679	ENSMUSG00000022841	Ap2m1	SE	3.62	0.1017	0.18
chr14:31867344:31867441:+@chr14:31869422:31869466:+@chr14:31874655:31874931:+	0.38	0.46	0.43	0.32	0.57	0.53	0.6	0.6	NM_001081251	ENSMUSG00000042323	Pbrm1	SE	5.4	0.1183	0.18
chr2:59185981:59186098:+@chr2:59188551:59188679:+@chr2:59190319:59190392:+	0.6	0.72	0.55	0.6	0.82	0.83	0.74	0.8	NM_175464,NM_026361	ENSMUSG00000026991	Pkp4	SE	3.95	0.1133	0.18
chr2:25811767:25811847:-@chr2:25810780:25810812:-@chr2:25808198:25808339:-	0.4	0.47	0.43	0.33	0.16	0.19	0.31	0.23	NM_001115076	ENSMUSG00000026933	Camsap1	SE	3.99	0.1067	0.18
chr2:79497304:79498506:+@chr2:79498827:79499003:+@chr2:79500390:79500467:+	0.65	0.51	0.56	0.48	0.66	0.79	0.64	0.82	NM_080558	ENSMUSG00000027007	Ssfa2	SE	2.6	0.0762	0.18
chr6:125101403:125101543:+@chr6:125101813:125101821:+@chr6:125102632:125102789:+	0.38	0.47	0.41	NA	0.23	0.31	0.29	0.13	NM_001039669,NM_178787	ENSMUSG00000038271	Iffo1	SE	3.43	0.0933	0.18
chr1:93194915:93195025:+@chr1:93195981:93196046:+@chr1:93197105:93197217:+	0.31	0.13	0.32	NA	0.03	0.13	0.08	0.07	NM_016717	ENSMUSG00000026307	Scly	SE	2.67	0.0992	0.18
chr1:120435843:120435946:+@chr1:120438252:120438275:+@chr1:120439679:120439923:+	0.21	0.17	0.21	0.25	0.37	0.4	0.42	0.37	NM_177548,NM_029709,NM_001081276	ENSMUSG00000064302	Clasp1	SE	6.5	0.145	0.18
chr1:157887991:157888132:+@chr1:157888205:157888264:+@chr1:157898424:157900866:+	0.67	0.63	0.69	0.64	0.49	0.41	0.54	0.48	NM_001160182,NM_001160180	ENSMUSG00000050565,ENSMUSG00000079252	Tor1aip2	SE	6.03	0.1267	0.18
chr4:131513558:131513734:-@chr4:131511443:131511493:-@chr4:131491654:131491782:-	0.46	0.45	0.4	0.37	0.23	0.29	0.19	0.24	NM_001128607,NM_001128606,NM_183428	ENSMUSG00000028906	Epb4.1	SE	5.61	0.13	0.18
chr4:148988159:148988281:+@chr4:149000196:149000225:+@chr4:149001321:149001516:+	0.57	0.64	0.68	0.54	0.85	0.78	0.72	0.8	NM_023051	ENSMUSG00000039953	Clstn1	SE	4.44	0.105	0.18
chr11:120208950:120209189:-@chr11:120208806:120208850:-@chr11:120208225:120208663:-	0.65	0.63	0.55	0.71	0.46	0.47	0.43	0.48	NM_009609	ENSMUSG00000062825	Actg1	SE	5.22	0.12	0.18
chr14:32054912:32055013:-@chr14:32054045:32054195:-@chr14:32052817:32052923:-	0.85	NA	0.78	0.78	0.6	NA	NA	0.64	NM_027949	ENSMUSG00000021902	Phf7	SE	2.86	0.1383	0.18
chr5:134986033:134986093:-@chr5:134980604:134980708:-@chr5:134978396:134979331:-	0.16	0.09	0.18	0.09	NA	NA	0.3	0.31	NM_001039162,NM_009990	ENSMUSG00000063146	Clip2	SE	3.43	0.125	0.18
chr8:90653594-90653703:+@chr8:90654251-90654300:+	0.1	0.23	0.18	0.21	0.32	0.33	0.34	0.43	NM_029074	ENSMUSG00000036810	Tmem188	RI	6.4	0.1117	0.18
chr15:85726790-85726934:+@chr15:85727265-85727347:+	0.2	0.1	0.21	0.07	0.4	0.31	0.31	0.29	NM_028063	ENSMUSG00000022386	Trmu	RI	5.07	0.1117	0.18
chr6:30458512-30458454:-@chr6:30456917-30456786:-	0.23	0.43	0.47	0.45	0.48	0.58	0.59	0.67	NM_178625	ENSMUSG00000029782	Tmem209	RI	3.51	0.075	0.18
chr7:31349222-31349413:+@chr7:31349493-31349626:+	0.4	0.26	0.32	0.22	0.48	0.56	0.39	0.47	NM_170760,NM_145580	ENSMUSG00000078765	U2af1l4	RI	3.2	0.0829	0.18
chr13:70759647-70759536:-@chr13:70757939-70757863:-	0.18	0.25	0.33	0.42	0.48	0.37	0.54	0.52	NM_144837	ENSMUSG00000034525	BC018507	RI	2.45	0.0762	0.18
chr11:120655260-120655148:-@chr11:120654424-120654342:-	0.23	0.2	0.17	0.26	0.4	0.39	0.4	0.39	NM_026824	ENSMUSG00000025155	Dus1l	RI	6.54	0.1517	0.18
chr11:120473915-120473777:-@chr11:120473397-120473315:-	0.36	0.4	0.35	0.44	0.55	0.63	0.55	0.53	NM_024229	ENSMUSG00000025137	Pcyt2	RI	5.96	0.1267	0.18

chr10:12981572:12981730:-@chr10:12977383:12977622:-@chr10:12975116:12975127:-@chr10:12973148:12973685:-	0.29	0.24	0.22	0.34	0.11	0.14	0.07	0.07	NM_001033257,NM_001195066,NM_001195065,NM_001195096	ENSMUSG00000062866	Phactr2	MXE	5.61	0.12	0.18
chr17:45732431:45732521:-@chr17:45729210|45729292:45729128:-	0.74	0.71	0.67	NA	0.92	0.88	0.92	0.82	NM_001199115,NM_001199114	ENSMUSG00000023942	Slc29a1	A3SS	4.17	0.125	0.18
chr2:127593907:127593994:-@chr2:127591854|127591857:127591760:-	0.69	0.58	0.6	0.55	0.38	0.49	0.4	0.42	NM_016902	ENSMUSG00000027378	Nphp1	A3SS	5.2	0.1167	0.18
chr7:57014476:57014515:+@chr7:57014912|57014968:57015163:+	NA	NA	0.26	0.26	0.5	0.36	0.43	0.46	NM_001146053,NM_001146049,NM_001146050,NM_016865,NM_001146052	ENSMUSG00000039745	Htatip2	A3SS	2.93	0.1132	0.18
chr17:27076396:27076423:-@chr17:27076262:27076313:-@chr17:27075829:27076037:-	0.32	0.32	0.34	0.23	0.5	0.53	0.42	0.42	NM_026948	ENSMUSG00000024194	Cuta	SE	5.47	0.1033	0.17
chr8:74452101:74452227:+@chr8:74453037:74453097:+@chr8:74455918:74458529:+	0.9	0.87	0.83	0.92	0.68	0.68	0.75	0.74	NA	NA	NA	SE	5.54	0.12	0.17
chr19:7355488:7355745:-@chr19:7354476:7354502:-@chr19:7352532:7352576:-	0.6	0.49	0.57	0.59	0.42	0.42	0.39	0.34	NM_001080390,NM_007928,NM_001080388,NM_001080389	ENSMUSG00000024969	Mark2	SE	5.13	0.1183	0.17
chr19:56452545:56452661:-@chr19:56448854:56448958:-@chr19:56447297:56447404:-	0.88	0.83	0.81	0.85	0.66	0.68	0.67	0.68	NM_198059,NM_008733	ENSMUSG00000049134,ENSMUSG00000092491	Nrap,AC115771.1	SE	6.74	0.145	0.17
chr10:107689813:107689980:+@chr10:107690381:107690551:+@chr10:107696812:107696902:+	0.74	0.78	0.84	0.73	0.65	0.62	0.55	0.59	NM_027892	ENSMUSG00000019907	Ppp1r12a	SE	5.89	0.1117	0.17
chr12:4850109:4850257:+@chr12:4855669:4855919:+@chr12:4856933:4859719:+	0.25	0.29	0.16	0.15	0.41	0.46	0.29	0.38	NM_173416	ENSMUSG00000051721	BC068281	SE	3.15	0.085	0.17
chr14:48345901:48345984:+@chr14:48346146:48346229:+@chr14:48350015:48350098:+	0.37	0.29	0.32	0.34	0.53	0.48	0.53	0.45	NM_008477	ENSMUSG00000021843	Ktn1	SE	5.71	0.1217	0.17
chr14:79751180:79751308:-@chr14:79750496:79750637:-@chr14:79744702:79744915:-	0.34	0.32	0.42	0.27	0.48	0.45	0.63	0.49	NM_025832	ENSMUSG00000022020	Naa16	SE	4.36	0.09	0.17
chr5:124864408:124864536:-@chr5:124863194:124863298:-@chr5:124860079:124860391:-	0.66	0.66	0.69	0.65	0.87	0.78	0.89	0.78	NM_001081203	ENSMUSG00000038095	Sbno1	SE	5.47	0.12	0.17
chr2:119034456:119034919:+@chr2:119035866:119035968:+@chr2:119036218:119036339:+	0.34	0.53	0.38	0.36	0.21	0.24	0.3	0.2	NM_028054,NM_001164827	ENSMUSG00000068580	Zfyve19	SE	4.75	0.0883	0.17
chr2:179807845:179807938:+@chr2:179812709:179812847:+@chr2:179813324:179813528:+	0.63	0.66	0.69	0.69	0.46	0.5	0.45	0.57	NM_181424,NM_028422,NM_001083328,NM_001083329	ENSMUSG00000039069	Gtpbp5	SE	4.99	0.1217	0.17
chr2:129627140:129627740:+@chr2:129636224:129636973:+@chr2:129653510:129658021:+	0.9	0.96	0.92	0.86	0.68	0.79	0.77	0.74	NM_001038635	ENSMUSG00000037885	Stk35	SE	5.77	0.1083	0.17
chr7:133618510:133618615:-@chr7:133616993:133617129:-@chr7:133615587:133616608:-	0.35	0.32	0.33	0.34	0.18	0.2	0.15	0.15	NM_001081459,NM_011363	ENSMUSG00000030733	Sh2b1	SE	6.6	0.1417	0.17
chr13:54666543:54666743:-@chr13:54665876:54665982:-@chr13:54665546:54665633:-	0.61	0.57	0.64	0.7	0.58	0.42	0.43	0.42	NM_133797	ENSMUSG00000025871	4833439L19Rik	SE	3.05	0.0929	0.17
chr11:70419550:70419666:+@chr11:70420133:70420219:+@chr11:70420422:70420646:+	0.37	0.3	0.4	0.4	0.52	0.57	0.48	0.59	NM_016713,NM_001045964,NM_176893,NM_001045959	ENSMUSG00000020827	Mink1	SE	5.55	0.1133	0.17
chr11:115131637:115131744:-@chr11:115131329:115131413:-@chr11:115131011:115131210:-	0.88	0.83	0.83	NA	0.64	0.67	0.67	0.74	NM_007997	ENSMUSG00000018861	Fdxr	SE	4.33	0.1222	0.17
chr11:116161580:116161747:-@chr11:116158885:116158977:-@chr11:116156858:116157003:-	0.81	0.8	0.81	0.84	0.65	0.68	0.64	0.61	NM_001162872,NM_016857	ENSMUSG00000020792	Exoc7	SE	6.68	0.1417	0.17
chr11:116155286:116155352:-@chr11:116154589:116154627:-@chr11:116153833:116153898:-	0.93	0.91	0.93	0.93	0.73	0.78	0.73	0.77	NM_001162872,NM_016857	ENSMUSG00000020792	Exoc7	SE	6.6	0.1517	0.17
chr19:4158919-4158829:-@chr19:4158717-4158610:-	0.3	0.4	0.34	0.31	0.53	0.53	0.51	0.46	NM_021485	ENSMUSG00000024830	Rps6kb2	RI	5.16	0.1233	0.17
chrX:162823323-162823413:+@chrX:162824884-162826920:+	0.77	0.84	0.93	0.8	0.6	0.74	0.62	0.69	NM_001177962,NM_023122,NM_001177961,NM_001177960,NM_001177957,NM_001177958,NM_001177955,NM_001177959,NM_001177956	ENSMUSG00000031342	Gpm6b	RI	4.04	0.0883	0.17
chrX:162823323-162823413:+@chrX:162824884-162826965:+	0.78	0.84	0.93	0.81	0.61	0.74	0.64	0.7	NA	NA	NA	RI	4.55	0.09	0.17
chr7:13567195-13567276:+@chr7:13567468-13568745:+	NA	0.33	0.83	NA	0.46	0.39	0.44	0.36	NM_175558,NM_001168561,NM_001168562	ENSMUSG00000033961	Zfp446	RI	2.11	0.1286	0.17
chr7:52152890-52152994:+@chr7:52153886-52154070:+	0.42	0.42	0.44	0.38	0.62	0.59	0.55	0.56	NM_027376	ENSMUSG00000011658	Fuz	RI	6.62	0.13	0.17
chr17:36041235:36041280:-@chr17:36041053:36041121:-@chr17:36038928:36038999:-@chr17:36038313:36038556:-	0.6	0.69	NA	NA	0.84	0.81	0.8	0.82	NM_001142744,NM_028476,NM_001142745	ENSMUSG00000024426	Atat1	MXE	4.99	0.1411	0.17
chr2:52012811:52012903:-@chr2:52011875:52011967:-@chr2:52008576:52008668:-@chr2:52006884:52006976:-	0.19	0.24	0.25	0.21	0.05	0.05	0.06	0.04	NM_010889	ENSMUSG00000026950	Neb	MXE	6.66	0.15	0.17
chr10:79013061:79013151:-@chr10:79012424|79012598:79012282:-	0.44	0.34	0.35	0.49	0.23	0.25	0.21	0.24	NM_027422	ENSMUSG00000042570	Mier2	A3SS	5.41	0.1167	0.17
chr7:51807877:51807990:-@chr7:51807606|51807615:51807325:-	0.55	0.62	0.54	0.58	0.75	0.78	0.73	0.72	NM_009473	ENSMUSG00000060601	Nr1h2	A3SS	6.16	0.1333	0.17
chr1:183853691:183853971:-@chr1:183851899|183852631:183851789:-	0.48	0.47	0.59	0.32	0.65	0.63	0.65	0.59	NM_001083120,NM_008680,NM_010135	ENSMUSG00000022995	Enah	A3SS	3.33	0.08	0.17
chr1:153201764:153201889:+@chr1:153202297|153203259:153203366:+	0.21	0.23	0.22	0.23	0.41	0.41	0.4	0.34	NM_001039511,NM_001039512,NM_054102	ENSMUSG00000023150	Ivns1abp	A3SS	6.14	0.1433	0.17

chr11:70497392:70497527:-@chr11:70496867|70496919:70496781:-	0.18	0.16	0.2	NA	0.33	0.28	0.31	0.46	NM_001190376,NM_178116,NM_001190378,NM_001190379	ENSMUSG00000040712	Camta2	A3SS	3.6	0.0939	0.17
chr15:96246378:96246160|96246208:-@chr15:96245463:96245582:-	0.52	0.6	0.6	0.58	0.72	0.74	0.75	0.75	NM_028148	ENSMUSG00000033228	Scaf11	A5SS	6.74	0.135	0.17
chr10:75379656:75379518|75379545:-@chr10:75377809:75377938:-	0.53	0.73	0.59	0.65	0.77	0.82	0.78	0.81	NM_001161853,NM_011418	ENSMUSG00000000902	Smarcb1	A5SS	4.14	0.1	0.17
chr18:77912639:77913423:-@chr18:77891868:77892035:-@chr18:77881807:77881933:-	0.21	0.27	0.2	0.28	0.44	0.32	0.43	0.41	NM_178670	ENSMUSG00000047466	8030462N17Rik	SE	4.27	0.1033	0.16
chr3:97514144:97514367:-@chr3:97513405:97513506:-@chr3:97510795:97510980:-	0.91	0.91	0.91	0.89	0.75	0.75	0.74	0.74	NM_001110163,NM_178080,NM_001039376	ENSMUSG00000038170	Pde4dip	SE	6.87	0.1517	0.16
chr3:89806201:89806398:-@chr3:89805740:89805790:-@chr3:89804210:89804913:-	0.2	0.24	0.23	0.18	0.37	0.34	0.39	0.38	NM_153489,NM_028475,NM_001165983,NM_001165984	ENSMUSG00000042520	Ubap2l	SE	6.41	0.1267	0.16
chr3:97514144:97514367:-@chr3:97513405:97513557:-@chr3:97510795:97510980:-	0.92	0.91	0.92	0.92	0.76	0.76	0.75	0.75	NM_001110163,NM_178080,NM_001039376	ENSMUSG00000038170	Pde4dip	SE	6.93	0.1567	0.16
chr17:12436366:12436462:-@chr17:12435516:12435671:-@chr17:12432836:12432936:-	0.26	0.33	0.3	0.22	0.4	0.41	0.43	0.5	NM_011948	ENSMUSG00000014426	Map3k4	SE	5.76	0.1	0.16
chr8:108632025:108633029:+@chr8:108643222:108643325:+@chr8:108651818:108654437:+	0.46	0.45	0.47	0.42	0.35	0.31	0.25	0.27	NM_010901	ENSMUSG00000031902	Nfatc3	SE	5.61	0.1133	0.16
chr15:57792398:57792538:+@chr15:57793624:57793818:+@chr15:57795359:57795479:+	0.74	NA	0.65	NA	0.5	0.56	0.58	0.49	NM_001081396	ENSMUSG00000022364	Wdr67	SE	3.52	0.1025	0.16
chr15:85642069:85642127:-@chr15:85641273:85641478:-@chr15:85639642:85639754:-	0.73	0.74	0.85	0.56	0.59	0.54	0.55	0.54	NA	ENSMUSG00000064284	2210021J22Rik	SE	2.6	0.0821	0.16
chr12:100529447:100529511:-@chr12:100457808:100457873:-@chr12:100447671:100447776:-	0.29	0.22	0.37	0.32	0.46	0.5	0.41	0.46	NM_183186	ENSMUSG00000033713	Foxn3	SE	4.88	0.095	0.16
chr14:35380043:35380079:-@chr14:35368529:35368714:-@chr14:35365363:35365508:-	0.09	0.14	0.13	0.1	0.28	0.27	0.26	0.29	NM_001039074,NM_001039071,NM_001039073,NM_001039072,NM_011918	ENSMUSG00000021798	Ldb3	SE	6.69	0.1367	0.16
chr14:26477593:26477759:+@chr14:26480753:26481007:+@chr14:26482426:26484195:+	0.75	0.66	0.69	0.71	0.58	0.41	0.57	0.6	NM_183208	ENSMUSG00000007817	Zmiz1	SE	5.93	0.09	0.16
chr2:179806499:179806591:+@chr2:179812709:179812847:+@chr2:179813324:179813528:+	0.62	0.63	0.59	0.64	0.37	0.49	0.45	0.52	NM_181424,NM_028422,NM_001083328,NM_001083329	ENSMUSG00000039069	Gtpbp5	SE	5.73	0.1083	0.16
chr2:37214663:37214852:-@chr2:37213872:37213918:-@chr2:37212724:37212900:-	0.31	0.24	0.18	0.18	0.2	0.02	0.02	0.02	NM_026176	ENSMUSG00000009030	Pdcl	SE	2.61	0.085	0.16
chr6:90617894:90618070:-@chr6:90614016:90614065:-@chr6:90609592:90612949:-	0.6	0.64	0.53	0.5	0.77	0.67	0.73	0.73	NM_001134383,NM_001134384	ENSMUSG00000034312	Iqsec1	SE	4.21	0.0917	0.16
chr7:135030464:135030609:-@chr7:135030042:135030258:-@chr7:135028958:135029795:-	0.93	0.97	0.97	0.92	0.71	0.79	0.82	0.85	NA	NA	NA	SE	5.72	0.1017	0.16
chr4:134902650:134902772:-@chr4:134901111:134901392:-@chr4:134900414:134900584:-	0.41	0.34	0.38	0.31	0.56	0.49	0.51	0.51	NM_001130477,NM_016799	ENSMUSG00000028809	Srrm1	SE	5.98	0.1117	0.16
chr4:11092237:11092594:+@chr4:11095044:11095081:+@chr4:11096857:11101524:+	0.42	0.48	0.39	NA	0.29	0.26	0.22	0.32	NM_021897,NM_001199105	ENSMUSG00000028211	Trp53inp1	SE	4.42	0.1008	0.16
chr4:137990587:137990794:+@chr4:137992095:137992314:+@chr4:137993543:137993630:+	0.35	0.3	0.33	0.42	0.51	0.53	0.56	0.45	NM_026689	ENSMUSG00000041241	Mul1	SE	4.43	0.1017	0.16
chr11:96638282:96638375:-@chr11:96636688:96636747:-@chr11:96635755:96635809:-	0.74	0.82	0.84	0.74	0.59	0.59	0.55	0.78	NM_028965,NM_001163389	ENSMUSG00000020876	Snx11	SE	2.36	0.0783	0.16
chr17:25372855-25372801:-@chr17:25372733-25372650:-	0.15	0.08	0.09	0.17	0.31	0.34	0.2	0.28	NM_172529	ENSMUSG00000035521	Gnptg	RI	4.08	0.095	0.16
chr8:72784368-72784488:+@chr8:72785130-72785216:+	0.72	0.72	0.72	0.71	0.89	0.88	0.85	0.89	NM_001168290,NM_172755	ENSMUSG00000036054	Sugp2	RI	6.71	0.1467	0.16
chr8:4266680-4266556:-@chr8:4265276-4265226:-	0.54	0.5	0.52	0.52	0.65	0.65	0.71	0.71	NM_011592	ENSMUSG00000002949	Timm44	RI	6.27	0.13	0.16
chr8:72713476-72713310:-@chr8:72712848-72712732:-	0.43	0.41	0.3	0.43	0.53	0.57	0.57	0.55	NM_001007570	ENSMUSG00000002346	Slc25a42	RI	6.57	0.1167	0.16
chrX:91497754-91498465:+@chrX:91499279-91501307:+	0.15	NA	0.09	NA	0.24	0.29	NA	0.32	NM_001039061,NM_153165,NM_001039060,NM_001039059	ENSMUSG00000043929	Klhl15	RI	2.63	0.1083	0.16
chr2:120012974-120012932:-@chr2:120012146-120012083:-	0.39	NA	0.41	0.57	0.65	0.57	0.61	0.62	NM_177845	ENSMUSG00000050211	Pla2g4e	RI	2.69	0.0881	0.16
chr2:32097173-32097319:+@chr2:32098413-32098524:+	0.11	0.28	0.15	0.07	0.27	0.31	0.36	0.33	NM_145145	ENSMUSG00000039254	Pomt1	RI	3.01	0.0863	0.16
chr11:83318144-83318212:+@chr11:83318333-83318606:+	0.59	0.53	0.57	0.68	0.37	0.4	0.5	0.47	NM_027427	ENSMUSG00000020680	Taf15	RI	4.19	0.08	0.16
chr2:30132523:30132578:+@chr2:30132668:30132730:+@chr2:30133143:30133349:+@chr2:30135475:30135603:+	0.22	0.31	0.35	0.31	0.47	0.39	0.44	0.53	NM_172267	ENSMUSG00000079484,ENSMUSG00000007476	Phyhd1,Lrrc8a	MXE	4.93	0.09	0.16
chr9:107479884:107480807:+@chr9:107481212:107481301:+@chr9:107481431:107481716:+@chr9:107485148:107486379:+	0.37	0.36	0.21	0.26	0.2	0.16	0.1	0.11	NA	NA	NA	MXE	3.18	0.08	0.16
chr4:98667724:98667893:-@chr4:98660338:98660427:-@chr4:98659060:98659149:-@chr4:98658055:98658150:-	0.67	0.77	0.81	NA	0.65	0.56	0.54	0.63	NM_026082	ENSMUSG00000028556	Dock7	MXE	2.87	0.0794	0.16
chr3:94193397:94193518:+@chr3:94194322|94194996:94195128:+	0.27	0.21	0.21	0.25	0.39	0.42	0.37	0.38	NM_011281	ENSMUSG00000028150	Rorc	A3SS	6.34	0.1233	0.16
chr7:134716862:134716970:+@chr7:134717259|134717368:134717480:+	0.24	0.21	0.2	0.13	0.36	0.24	0.37	0.46	NA	ENSMUSG00000030815	Phkg2	A3SS	3.18	0.0783	0.16
chr4:147992774:147992900:-@chr4:147991814|147991934:147991675:-	0.42	0.47	0.49	0.5	0.7	0.67	0.6	0.55	NM_001003898,NM_001003899,NM_001008545,NM_001008546,NM_145556	ENSMUSG00000041459	Tardbp	A3SS	4.54	0.095	0.16

chr4:107567478:107567543:+@chr4:107569267|107569476:107569723:+	0.17	0.19	0.15	0.16	0.36	0.37	0.28	0.32	NM_028754	ENSMUSG00000028608	0610037L13Rik	A3SS	5.94	0.1283	0.16
chr11:59609252:59609365:-@chr11:59608766|59609077:59608643:-	0.36	0.43	0.43	0.46	0.56	0.56	0.57	0.62	NM_146018	ENSMUSG00000032633	Flcn	A3SS	6.64	0.1167	0.16
chr17:31646857:31646714|31646766:-@chr17:31640455:31640611:-	0.91	0.89	0.87	0.96	0.85	0.74	0.72	0.68	NM_021322	ENSMUSG00000024037	Wdr4	A5SS	3.73	0.0917	0.16
chr2:165633429:165633019|165633175:-@chr2:165630687:165630877:-	0.74	0.7	0.79	0.57	0.84	0.83	0.89	0.89	NM_027230	ENSMUSG00000039671	Zmynd8	A5SS	4.52	0.085	0.16
chr7:72444699:72444556|72444616:-@chr7:72441051:72442553:-	0.68	0.72	0.74	0.72	0.87	0.88	0.88	0.88	NM_009386,NM_001163574	ENSMUSG00000030516	Tjp1	A5SS	6.85	0.145	0.16
chr11:114729810:114729959|114730017:+@chr11:114731635:114733931:+	0.1	0.18	0.14	0.23	0.27	0.34	0.31	0.36	NM_001110337	ENSMUSG00000051043	Gprc5c	A5SS	4.7	0.0967	0.16
chr18:3295038:3295180:-@chr18:3287902:3288090:-@chr18:3273420:3273576:-	0.21	0.17	0.24	0.3	0.09	0.11	0.05	0.06	NM_001110851,NM_001110859,NM_001110857,NM_001110858,NM_013498,NM_001110850,NM_001110856,NM_001110854,NM_001110855,NM_001110853	ENSMUSG00000063889	Crem	SE	5.47	0.1	0.15
chr3:107698561:107699131:-@chr3:107696969:107697910:-@chr3:107691768:107696425:-	0.31	0.26	0.31	0.32	0.43	0.5	0.38	0.48	NR_015459	ENSMUSG00000086968	4933431E20Rik	SE	5.09	0.0983	0.15
chr19:7355488:7355745:-@chr19:7353601:7353768:-@chr19:7352532:7352576:-	0.39	0.35	0.39	0.36	0.19	0.22	0.27	0.22	NM_001080390,NM_007928,NM_001080388,NM_001080389	ENSMUSG00000024969	Mark2	SE	5.96	0.115	0.15
chr15:72881025:72881153:-@chr15:72872607:72872633:-@chr15:72861952:72862073:-	0.92	0.86	0.92	0.91	0.76	0.75	0.71	0.78	NM_029640,NR_002864,NM_180662,NM_001164641,NM_001164642,NM_001164643	ENSMUSG00000047921	Trappc9	SE	5.98	0.1183	0.15
chr14:35384904:35385107:-@chr14:35382899:35382913:-@chr14:35380584:35380753:-	0.79	0.81	0.77	0.77	0.92	0.93	0.93	0.94	NM_001039074,NM_001039071,NM_001039073,NM_001039072,NM_011918,NM_001039075,NM_001039076	ENSMUSG00000021798	Ldb3	SE	6.67	0.1283	0.15
chr5:31846043:31846286:+@chr5:31848553:31848639:+@chr5:31850984:31851054:+	0.66	0.71	0.71	0.69	0.57	0.56	0.54	0.5	NM_009206	ENSMUSG00000029141	Slc4a1ap	SE	6.32	0.1167	0.15
chr6:146946689:146946803:+@chr6:146948184:146948216:+@chr6:146949463:146949524:+	0.21	0.14	0.23	0.23	0.05	0.06	0.03	0.06	NM_001170433,NM_026221	ENSMUSG00000016487	Ppfibp1	SE	5.5	0.12	0.15
chr7:24922065:24922191:+@chr7:24923312:24923521:+@chr7:24925319:24928260:+	0.1	0.11	0.08	0.08	0.29	0.22	0.19	0.28	NA	NA	NA	SE	5.59	0.1133	0.15
chr9:13586721:13586826:+@chr9:13588050:13588154:+@chr9:13590296:13590371:+	0.55	0.49	0.52	0.39	0.33	0.34	0.34	0.33	NM_023858	ENSMUSG00000031918	Mtmr2	SE	4.34	0.1067	0.15
chr13:94125895:94126034:+@chr13:94156300:94156335:+@chr13:94157479:94157635:+	0.29	0.28	0.33	0.32	0.13	0.15	0.17	0.16	NM_147176,NM_152134	ENSMUSG00000007617	Homer1	SE	6.64	0.1267	0.15
chr11:77500961:77501313:+@chr11:77501789:77501833:+@chr11:77505044:77506756:+	0.05	0.04	0.27	0.07	0.3	0.25	0.23	0.26	NM_001024205	ENSMUSG00000037857	Nufip2	SE	2.4	0.0838	0.15
chr11:79272273:79272408:+@chr11:79276735:79276797:+@chr11:79282219:79282377:+	0.36	0.34	0.27	NA	0.19	0.16	0.14	0.2	NM_010897	ENSMUSG00000020716	Nf1	SE	4.55	0.1075	0.15
chr11:120474693:120474737:-@chr11:120474344:120474397:-@chr11:120473777:120473915:-	0.66	0.65	0.67	0.53	0.78	0.77	0.73	0.84	NM_024229	ENSMUSG00000025137	Pcyt2	SE	5.9	0.0883	0.15
chr11:101904286:101904618:+@chr11:101907381:101907512:+@chr11:101908168:101908501:+	0.33	0.32	0.24	0.34	0.51	0.42	0.45	0.43	NM_001160712,NM_001160711,NM_001160713,NM_027987	ENSMUSG00000017309	Cd300lg	SE	6.6	0.095	0.15
chr11:58136071:58136231:-@chr11:58133369:58133456:-@chr11:58132826:58133092:-	0.76	0.76	0.83	0.89	0.68	0.67	0.67	0.64	NM_178761	ENSMUSG00000049755	Zfp672	SE	5.67	0.0967	0.15
chr11:3193283:3193346:+@chr11:3194459:3194550:+@chr11:3199037:3199208:+	0.39	0.33	0.46	NA	0.22	0.26	0.24	0.24	NM_019574	ENSMUSG00000020453	Patz1	SE	4.98	0.1111	0.15
chr8:70243799:70243943:-@chr8:70237582:70237725:-@chr8:70212981:70221086:-	0.95	0.98	0.97	0.96	0.91	NA	0.9	0.63	NM_177698,NM_027626,NM_030263	ENSMUSG00000030465	Psd3	SE	2.97	0.0783	0.15
chr19:8893784-8893511:-@chr19:8893174-8892926:-	0.49	0.51	0.39	0.47	0.65	0.64	0.57	0.61	NM_027412	ENSMUSG00000071660	Ttc9c	RI	5.55	0.0983	0.15
chr10:127562325-127562457:+@chr10:127562555-127562701:+	0.34	0.47	0.4	0.36	0.27	0.27	0.22	0.23	NM_054078	ENSMUSG00000040054	Baz2a	RI	5.69	0.0933	0.15
chr5:136502340-136502477:+@chr5:136504369-136504442:+	0.63	0.68	0.58	NA	0.77	0.8	0.83	0.7	NM_023742	ENSMUSG00000004947	Dtx2	RI	2.98	0.0761	0.15
chr2:158652041-158652153:+@chr2:158653639-158653735:+	0.51	0.48	0.44	0.54	0.63	0.59	0.62	0.73	NM_145742	ENSMUSG00000027655	Dhx35	RI	5.48	0.0867	0.15
chr7:19677288-19677385:+@chr7:19677557-19677603:+	0.22	0.26	0.25	0.19	0.39	0.39	0.42	0.31	NM_001190490,NM_032418,NM_001190491	ENSMUSG00000030409	Dmpk	RI	4.88	0.1	0.15
chr7:112900243-112900104:-@chr7:112898844-112898694:-	0.19	0.23	0.18	0.22	0.34	0.35	0.35	0.4	NM_009906	ENSMUSG00000030894	Tpp1	RI	6.67	0.125	0.15
chr7:52152890-52152994:+@chr7:52153873-52154070:+	0.21	0.18	0.15	0.16	0.34	0.34	0.29	0.32	NM_027376	ENSMUSG00000011658	Fuz	RI	6.05	0.1167	0.15
chr7:73214310-73214412:+@chr7:73215476-73215551:+	0.62	0.65	0.69	0.69	0.78	0.85	0.85	0.78	NM_021336	ENSMUSG00000030512	Snrpa1	RI	5.64	0.1083	0.15
chr13:115615419-115615569:+@chr13:115616366-115616489:+	0.25	0.2	0.24	0.27	0.39	0.39	0.38	0.39	NM_013826,NM_001113374,NM_001113375	ENSMUSG00000015536	Mocs2	RI	6.76	0.1267	0.15
chr4:43439100-43439237:+@chr4:43439320-43439960:+	0.38	0.39	0.5	0.33	0.23	0.28	0.27	0.24	NM_001037709,NM_199057	ENSMUSG00000035969	Rusc2	RI	5.32	0.0867	0.15
chr11:29053232-29053338:+@chr11:29054144-29054215:+	0.22	0.24	0.1	0.19	0.34	0.3	0.35	0.34	NM_027869	ENSMUSG00000020464	Pnpt1	RI	5.74	0.095	0.15
chr11:51407106-51407188:+@chr11:51407418-51407643:+	0.14	0.11	0.05	0.14	0.28	0.25	0.25	0.25	NM_028398	ENSMUSG00000020359	Agxt2l2	RI	6.75	0.115	0.15

chr11:98579456-98579224:-@chr11:98577839-98577728:-	0.47	0.44	0.41	0.5	0.61	0.65	0.55	0.6	NM_011869	ENSMUSG00000017210	Med24	RI	5.26	0.0967	0.15
chr11:50872759:50872904:+@chr11:50873288:50873543:+@chr11:50873574:50873656:+@chr11:50874362:50874488:+	0.62	NA	0.63	NA	0.46	0.44	0.55	0.43	NA	ENSMUSG00000020364	Zfp354a	MXE	2.67	0.0993	0.15
chr16:43973581:43974279:-@chr16:43971670|43971679:43971512:-	NA	0.94	0.95	0.91	0.84	0.8	0.72	0.79	NM_001007460	ENSMUSG00000036304	Zdhhc23	A3SS	4.12	0.0958	0.15
chr1:134915354:134915461:-@chr1:134909288|134909291:134909214:-	0.4	0.4	0.41	0.37	0.49	0.51	0.6	0.58	NM_008575	ENSMUSG00000054387	Mdm4	A3SS	5.53	0.1067	0.15
chr11:104156173:104156238:+@chr11:104159812|104159860:104160570:+	0.39	0.32	0.43	0.45	0.53	0.56	0.56	0.56	NM_001038609.NM_010838	ENSMUSG00000018411	Mapt	A3SS	6.04	0.1117	0.15
chr17:24815541:24815649|24815658:+@chr17:24815982:24816169:+	0.63	0.7	0.6	0.76	0.84	0.83	0.81	0.82	NM_183149	ENSMUSG00000041130	Zfp598	A5SS	4.45	0.0983	0.15
chr5:23033880:23033715|23033742:-@chr5:23032608:23032633:-	0.76	0.72	0.77	0.64	0.83	0.95	0.88	0.85	NM_009274	ENSMUSG00000062604	Srpk2	A5SS	5.63	0.0867	0.15
chr9:83004713:83004600|83004641:-@chr9:83003549:83004036:-	0.44	0.4	NA	NA	0.61	0.61	0.49	0.57	NA	NA	NA	A5SS	2.51	0.0871	0.15
chr17:31646857:31646714|31646766:-@chr17:31640482:31640672:-	0.92	0.85	0.92	0.92	0.88	NA	0.62	NA	NM_021322	ENSMUSG00000024037	Wdr4	A5SS	2.3	0.0929	0.15

Table C-3: The list of dysregulated splicing events in **SBMA** muscle.

gid	wt1	wt2	wt3	mut1	mut2	mut3	rescue1	rescue2	rescue3	krkr1	krkr2	krkr3	refseq_id	ensq_id	gsymbol	event	zscores	SigDiff	abs(Wt-Mut)
chr6:48543882:48544051:+@chr6:48544861:48544975:+@chr6:48546295:48549081:+	0.69	0.81	NA	0.15	0.27	NA	0.93	0.27	0.39	0.37	0.52	NA	NA	NA	NA	SE	2.2	0.42	0.54
chr3:87965113:87965303:+@chr3:87965703:87965723:+@chr3:87966880:87967009:+	0.45	0.02	0.47	0.68	0.92	0.65	0.97	0.03	0.96	0.92	0.53	0.94	NM_133665	ENSMUSG00000001419	Mef2d	SE	21.82	0.1967	0.44
chr5:65670696:65671053:-@chr5:65670059|65670062:65669950:-	NA	0.68	0.69	NA	0.35	0.48	NA	0.64	0.69	0.62	0.42	0.5	NM_011258	ENSMUSG00000029191	Rfc1	A3SS	2.02	0.2	0.27
chr5:149996136:149996382:+@chr5:149999284:149999410:+@chr5:149999921:150000049:+	NA	0.07	0.14	0.4	NA	0.32	0.24	0.1	0.09	0.5	0.35	0.62	NM_001013378,NM_001115151,NM_001115149,NM_001115150	ENSMUSG00000041264	Uspl1	SE	2.12	0.18	0.26
chrX:7174858-7174664:-@chrX:7173919-7173857:-	0.53	0.57	0.55	0.23	0.36	0.33	0.5	0.51	0.57	0.51	0.41	0.46	NM_138603	ENSMUSG00000039556,ENSMUSG00000031143	Ppp1r3f,Ccdc2	RI	20.71	0.1867	0.24
chr17:26644664-26644519:-@chr17:26644149-26643930:-	0.62	0.72	0.63	0.46	0.46	0.32	0.64	0.6	0.63	0.57	0.43	0.61	NM_013642	ENSMUSG00000024190	Dusp1	RI	65.32	0.1633	0.24
chr2:168592412:168592701:-@chr2:168579934:168582300:-@chr2:168577954:168578240:-	0.77	0.91	0.84	0.52	0.59	0.7	0.83	0.8	0.91	0.74	0.75	0.88	NM_201395,NM_201396,NM_175303	ENSMUSG00000027547	Sall4	SE	3.99	0.13	0.24
chr7:149698437:149698527:+@chr7:149699570:149699610:+@chr7:149700231:149700271:+@chr7:149701681:149701914:+	0.56	0.3	0.38	0.25	0.16	0.16	0.2	0.09	0.31	0.23	0.26	0.3	NA	NA	NA	MXE	3.54	0.1067	0.22
chr2:24712126:24712246:-@chr2:24708185:24708322:-@chr2:24703464:24703609:-@chr2:24695050:24695276:-	0.31	0.18	NA	0.43	0.51	0.46	0.34	0.14	0.35	0.39	0.23	0.34	NM_172545,NM_001012518,NM_001109686,NM_001109687	ENSMUSG00000036893	Ehmt1	MXE	4.81	0.1492	0.22
chr17:28457735:28457801:+@chr17:28459591:28459716:+@chr17:28463097:28463519:+	0.27	0.37	0.43	0.57	0.54	0.63	0.43	0.65	0.41	0.49	0.4	0.5	NA	NA	NA	SE	8.35	0.14	0.22
chr3:87729353-87728869:-@chr3:87728450-87728266:-	0.91	0.94	0.94	0.67	0.81	0.67	0.79	0.9	0.81	0.82	0.76	0.9	NM_153562	ENSMUSG00000004896	Rrnad1	RI	4.38	0.1567	0.21
chr6:34695619:34696015|34696639:+@chr6:34697886:34697969:+	0.52	0.58	NA	NA	0.33	0.35	0.55	0.65	0.75	0.4	0.21	0.54	NM_145575	ENSMUSG00000029761	Cald1	A5SS	2.2	0.17	0.21
chr8:74452101:74452227:+@chr8:74453037:74453097:+@chr8:74455918:74458529:+	0.96	0.84	0.88	0.72	0.76	0.57	0.83	0.81	0.76	0.56	0.61	0.69	NA	NA	NA	SE	7.54	0.1067	0.21
chr6:35001062:35001559:-@chr6:34974128:34974340:-@chr6:34972065:34973432:-	0.4	0.32	0.55	0.63	0.68	0.58	0.4	0.52	0.53	0.6	0.59	0.49	NA	NA	NA	SE	2.45	0.0967	0.21
chr4:61953666:61953732:+@chr4:61956921:61957110:+@chr4:61958009:61959445:+	NA	0.63	0.75	0.94	0.95	0.82	0.96	0.85	0.88	0.87	0.83	0.9	NM_025286	ENSMUSG00000066152	Slc31a2	SE	2.34	0.1183	0.21
chr11:5879676:5879724:-@chr11:5876768:5876896:-@chr11:5872816:5872891:-	0.95	0.95	0.93	0.67	0.82	0.73	0.94	0.87	0.94	0.65	0.61	0.66	NM_001174054,NM_007595,NM_001174053	ENSMUSG00000057897	Camk2b	SE	6.36	0.1467	0.2
chr7:130439924:130440080:-@chr7:130437986:130438219:-@chr7:130435550:130435719:-	0.56	0.53	0.47	0.27	0.35	0.33	0.48	0.69	0.33	0.42	0.43	0.43	NM_001122640,NM_001122642,NM_001122643,NM_001122641,NM_144529	ENSMUSG00000030766	Arhgap17	SE	9.28	0.1467	0.2
chr11:120208950:120209189:@chr11:120208806:120208850:-@chr11:120208225:120208663:-	0.73	0.76	0.68	0.49	0.59	0.48	0.52	0.58	0.69	0.41	0.38	0.29	NM_009609	ENSMUSG00000062825	Actg1	SE	5.01	0.14	0.2
chr19:10956142:10956491:-@chr19:10954670:10954792:-@chr19:10952569:10952639:-@chr19:10948732:10948976:-	0.57	0.5	0.55	0.3	0.34	0.38	0.56	0.63	0.45	0.27	0.26	0.31	NM_134142	ENSMUSG00000034659	Tmem109	MXE	9.37	0.15	0.2
chr7:149088181:149088311:-@chr7:149084600:149084688:-@chr7:149078645:149078794:-	NA	0.06	0.26	0.37	0.34	0.36	0.24	0.33	0.21	0.2	0.18	0.21	NM_023764	ENSMUSG00000025139	Tollip	SE	3.95	0.1317	0.2

chr2:91774246-91774213:-@chr2:91773999-91773900:-	0.29	0.19	0.26	0.44	0.54	0.35	0.34	0.47	0.24	0.31	0.36	0.34	NM_138306, NM_001166597	ENSMUSG00000040479	Dgkz	RI	4.22	0.1	0.2
chr1:188528308:188529871:-@chr1:188514600:188514683:-@chr1:188473614:188473777:-	0.03	0.04	0.06	0.14	0.36	0.23	0.19	0.05	0.05	0.15	0.18	0.17	NM_009367	ENSMUSG00000039239	Tgfb2	SE	5.06	0.1167	0.2
chr19:10651944:10652573:+@chr19:10653472:10653564:+@chr19:10654953:10655052:+	0.8	NA	0.84	0.66	0.62	0.6	0.68	0.49	0.7	0.86	0.82	0.71	NM_201351	ENSMUSG00000034445	Cybasc3	SE	4.63	0.1533	0.19
chr7:86887796:86887911:-@chr7:86885051:86885166:-@chr7:86882150:86882796:-	NA	0.46	0.47	0.7	0.58	0.67	0.42	0.63	0.69	0.6	0.81	0.54	NM_011068	ENSMUSG00000030545	Pex11a	SE	2.62	0.1225	0.19
chr13:83732039:83732242:+@chr13:83764760:83764903:+@chr13:83772658:83772844:+	0.6	0.64	0.6	0.85	0.73	0.82	0.76	0.75	0.74	0.88	0.85	0.82	NM_025282, NM_001170537	ENSMUSG00000005583	Mef2c	SE	5.41	0.1333	0.19
chr16:77556167:77556212:+@chr16:77594867:77595507:+@chr16:77597144:77598776:+	0.25	NA	0.13	0.41	0.38	0.34	0.17	0.33	0.46	0.25	0.35	0.2	NA	ENSMUSG00000052450	2810055G20Ri	SE	4.34	0.1217	0.19
chr7:19609726:19609855:+@chr7:19613246:19613371:+@chr7:19614213:19614336:+	0.34	0.44	0.38	0.63	0.56	0.54	0.51	0.56	0.6	0.38	0.5	0.45	NM_026605	ENSMUSG00000023118	Sympk	SE	8.01	0.1267	0.19
chr11:29605535:29605591:+@chr11:29606410:29608770:+@chr11:29633633:29633840:+	0.11	0.11	0.1	0.38	0.19	0.33	0.17	0.2	0.16	0.6	0.52	0.46	NM_194053, NM_194052, NM_024226, NM_194054, NM_194051	ENSMUSG00000020458	Rtn4	SE	3.62	0.1267	0.19
chr11:82625902:82626312:-@chr11:82624530:82624613:-@chr11:82623510:82623720:-	0.87	NA	0.8	0.68	0.71	0.56	0.48	0.54	0.76	0.78	0.53	0.72	NM_026097, NM_001007465,NM_001164571,NM_001164570,NM_001164569	ENSMUSG00000020696	Rffl	SE	2.61	0.0925	0.18
chr4:154460314:154460406:-@chr4:154457218:154457426:-@chr4:154456776:154456863:-	0.43	0.43	0.37	0.22	0.25	0.21	0.28	0.38	0.4	0.36	0.22	0.31	NM_026395	ENSMUSG00000029048	Rer1	SE	8.94	0.15	0.18
chr3:95142954-95142268:-@chr3:95141187-95141071:-	0.51	0.4	0.51	0.3	0.27	0.3	0.56	0.54	0.37	0.6	0.6	0.48	NM_001163641,NM_001163642,NM_018877	ENSMUSG00000015697	Setdb1	RI	4.97	0.1367	0.18
chr15:76543297-76543650:+@chr15:76544246-76544415:+	0.88	0.94	0.85	0.75	0.8	0.58	0.94	0.92	0.84	0.9	0.88	0.81	NM_145471	ENSMUSG00000033728	Lrrc14	RI	5.26	0.0767	0.18
chr2:61451708:61451855:+@chr2:61464960|61464963:61465071:+	NA	0.33	0.43	0.22	0.21	0.17	0.21	0.34	0.21	0.15	0.31	0.22	NM_011529, NM_001164072,NM_001164071	ENSMUSG00000064289	Tank	A3SS	5.48	0.13	0.18
chr7:133618510:133618615:-@chr7:133616993:133617129:-@chr7:133615587:133616608:-	0.26	0.31	0.23	0.12	0.09	0.05	0.22	0.13	0.23	0.12	0.13	0.16	NM_001081459,NM_011363	ENSMUSG00000030733	Sh2b1	SE	12.26	0.13	0.18
chr9:118983283:118983441:-@chr9:118983040|118983098:118982881:-	0.47	NA	0.35	0.17	0.3	0.22	0.4	0.38	0.38	0.21	0.32	0.22	NM_019676	ENSMUSG00000010660	Plcd1	A3SS	2.22	0.085	0.18
chr7:150646758:150646955:-@chr7:150646583|150646621:150645700:-	0.32	0.45	0.43	0.18	0.21	0.28	0.28	0.22	0.31	0.21	0.23	0.23	NM_009876, NM_001161624	ENSMUSG00000037664	Cdkn1c	A3SS	3.07	0.1	0.18
chr18:60992081:60992278:-@chr18:60991820:60991963:-@chr18:60991428:60991649:-	0.84	0.68	NA	0.93	0.93	0.95	0.9	0.77	0.95	0.96	0.79	0.94	NM_001198984,NM_011552	ENSMUSG00000024613	Tcof1	SE	4.79	0.1267	0.18
chr11:94154241:94154346:-@chr11:94153721:94153786:-@chr11:94152375:94152892:-	NA	0.39	0.36	0.52	0.52	0.63	0.33	0.11	0.27	0.52	0.4	0.64	NM_026313	ENSMUSG00000020863	Luc7l3	SE	3.36	0.1192	0.18
chr3:115590694:115590977:-@chr3:115589132:115589293:-@chr3:115584497:115584756:-	0.57	0.63	0.67	0.35	0.49	0.51	0.51	0.58	0.44	0.45	0.36	0.48	NA	NA	NA	SE	5.48	0.0867	0.17
chr10:5298683:5299010:+@chr10:5301207:5301275:+@chr10:5302788:5302930:+	0.58	0.41	0.46	0.31	0.33	0.29	0.28	0.5	0.47	0.4	0.34	0.27	NM_022027, NM_153399, NM_001079686	ENSMUSG00000019769	Syne1	SE	7.67	0.1033	0.17
chr4:34725473:34725586:-@chr4:34719123:34719302:-@chr4:34718507:34718663:-	0.37	0.44	0.4	0.24	0.3	0.16	0.23	0.28	0.19	0.29	0.24	0.2	NM_025471	ENSMUSG00000028295	1810030N24Ri	SE	5.96	0.1	0.17

chr6:34695619:34696015|34696639:+@chr6:34703443:34703588:+	0.4	0.43	0.33	0.15	0.27	0.24	0.37	0.41	0.54	0.19	0.16	0.33	NM_145575	ENSMUSG00000029761	Cald1	A5SS	4.9	0.0933	0.17
chr2:6481836:6481705|6481717:-@chr2:6474831:6475010:-	0.36	0.44	0.55	0.29	0.3	0.26	0.32	0.33	0.27	0.2	0.37	0.26	NM_001110229,NM_001110231,NM_001160292,NM_001110228,NM_001160293,NM_001110230,NM_001110232,NM_010160	ENSMUSG00000002107	Celf2	A5SS	4.47	0.09	0.17
chr2:29575113:29575370:+@chr2:29576163:29576258:+@chr2:29577744:29577829:+	0.61	0.67	0.6	0.39	0.54	0.45	0.75	0.66	0.65	0.47	0.44	0.45	NM_001039086,NM_001039087,NM_054050	ENSMUSG00000039844	Rapgef1	SE	4.12	0.0933	0.17
chr4:123042516:123042590:-@chr4:123041300:123041317:-@chr4:123038153:123038270:-	NA	0.89	0.82	0.69	0.69	NA	0.64	0.58	0.75	0.77	0.77	0.83	NM_001199137,NM_001199136	ENSMUSG00000028649	Macf1	SE	2.08	0.13	0.17
chr2:156002139:156002193:-@chr2:155999833:155999904:-@chr2:155998564:155998758:-	0.09	0.07	NA	0.24	0.2	0.3	0.18	0.32	0.1	0.09	0.21	0.15	NM_133242	ENSMUSG00000027620	Rbm39	SE	3.33	0.1117	0.17
chr5:93596526:93596713:+@chr5:93602499:93602563:+@chr5:93604430:93605471:+	0.28	0.16	0.3	0.41	0.36	0.48	0.21	0.25	0.31	0.46	0.49	0.42	NM_001009818	ENSMUSG00000058013	11-Sep	SE	6.19	0.0833	0.17
chr2:76393071:76393174:+@chr2:76393947:76394039:+@chr2:76398243:76398317:+@chr2:76402841:76403006:+	NA	0.34	0.17	0.05	0.11	0.11	0.42	0.33	0.18	0.1	0.11	0.02	NM_145525	ENSMUSG00000042359	Osbpl6	MXE	3.1	0.0925	0.16
chr5:130221559:130221785|130221816:+@chr5:130222602:130222741:+	0.3	0.45	0.35	0.22	0.23	0.16	0.34	0.28	0.29	0.38	0.22	0.24	NM_025450	ENSMUSG00000034211	Mrps17	A5SS	7.06	0.09	0.16
chr4:129952702:129952830:-@chr4:129952059:129952214:-@chr4:129950122:129950167:-@chr4:129942313:129942474:-	0.29	0.27	0.23	0.04	0.17	0.09	0.23	NA	0.41	0.1	0.24	0.15	NM_172702	ENSMUSG00000023232	Serinc2	MXE	4.47	0.1	0.16
chr5:143666916:143667155:-@chr5:143666767:143666829:-@chr5:143666023:143666461:-	0.51	0.53	0.57	0.39	0.39	0.35	0.34	0.47	0.44	0.48	0.36	0.32	NM_007393	ENSMUSG00000029580	Actb	SE	25.34	0.1267	0.16
chr14:27279528:27279696:-@chr14:27279390:27279440:-@chr14:27278896:27278946:-@chr14:27262061:27262120:-	0.86	0.83	NA	NA	0.68	0.69	0.74	0.66	0.73	0.78	0.67	0.81	NM_032008	ENSMUSG00000021870	Slmap	MXE	2.25	0.14	0.16
chr4:137638808:137638903:+@chr4:137643448:137643480:+@chr4:137652667:137652846:+	0.62	0.69	0.59	0.43	0.48	0.52	0.62	0.69	0.6	0.59	0.62	0.65	NM_172703	ENSMUSG00000028760	Eif4g3	SE	7.46	0.0933	0.16
chr7:127987114:127987299:+@chr7:127988210:127988303:+@chr7:128001858:128002176:+	0.23	0.33	0.21	0.1	0.1	NA	0.17	0.09	0.16	0.31	0.08	NA	NM_007908	ENSMUSG00000035064	Eef2k	SE	2.69	0.0967	0.16
chr6:34695619:34696015:+@chr6:34697886:34697969:+@chr6:34703443:34703588:+	0.3	NA	0.21	0.07	0.11	0.12	0.15	0.18	0.26	0.21	0.04	0.09	NM_145575	ENSMUSG00000029761	Cald1	SE	5.15	0.1075	0.16
chr7:130323231:130323373:+@chr7:130323763:130323909:+@chr7:130324054:130324191:+	NA	0.8	0.63	0.59	0.55	0.54	0.9	0.69	0.77	0.61	0.75	0.71	NM_144925	ENSMUSG00000052707	Tnrc6a	SE	2.79	0.0875	0.16
chr7:52249733:52249819:-@chr7:52249181:52249641:-@chr7:52248114:52248401:-	0.74	0.8	0.74	0.66	0.66	0.51	0.82	NA	0.69	0.73	0.56	0.73	NM_029410	ENSMUSG00000003190	Bcl2l12	SE	Inf	0.08	0.15
chr4:155317940:155318122|155318259:+@chr4:155320364:155320526:+	0.54	0.55	0.61	0.48	0.38	0.39	0.43	0.66	0.48	0.46	0.44	0.57	NM_001039159,NM_001039158	ENSMUSG00000023286	Ube2j2	A5SS	4.12	0.0933	0.15
chr10:128391002:128391127:+@chr10:128393667:128393779:+@chr10:128394677:128395333:+	0.65	0.58	0.6	0.48	0.48	0.43	0.62	0.39	0.52	0.36	0.47	0.46	NM_008398	ENSMUSG00000025348	Itga7	SE	21.34	0.1067	0.15
chr6:91207719:91207820:+@chr6:91209624:91209764:+@chr6:91213333:91213467:+	0.53	0.61	0.56	0.75	0.65	0.75	0.8	0.83	0.68	0.53	0.62	0.74	NM_007992,NM_001081437	ENSMUSG00000064080	Fbln2	SE	3.22	0.09	0.15

chr14:14793699:14793739:-@chr14:14790068:14790145:-@chr14:14789974:14790049:-@chr14:14787053:14787170:-	0.39	0.42	0.53	0.59	0.58	0.62	0.42	0.69	0.51	0.43	0.46	0.53	NM_025435,NM_001013578	ENSMUSG00000053453	Thoc7	MXE	3.26	0.09	0.15
chr17:35042287:35042401:+@chr17:35042555:35042656:+@chr17:35042855:35043003:+	0.86	0.79	0.78	0.97	0.98	0.93	0.94	0.91	0.9	0.86	0.95	0.92	NM_145830,NM_147151	ENSMUSG00000013787	Ehmt2	SE	5.29	0.1067	0.15
chr4:122972445:122972564:+@chr4:122972993:122973079:+@chr4:122973173:122973300:+	0.31	0.29	0.31	0.44	0.44	0.48	0.29	0.3	0.33	0.44	0.45	0.41	NM_148917,NM_130881	ENSMUSG00000011257	Pabpc4	SE	Inf	0.13	0.15
chr5:92493351:92493531:-@chr5:92492363:92492461:-@chr5:92486994:92487096:-	0.54	0.61	0.51	0.68	0.73	0.71	0.57	0.52	0.49	0.64	0.66	0.68	NM_001080797,NM_001080796,NM_001080794,NM_011816,NM_001080795	ENSMUSG00000029405,ENSMUSG00000084111	3bp2,Gm1571	SE	5.43	0.1033	0.15
chr1:133964240:133964639:-@chr1:133955737:133955935:-@chr1:133954293:133954544:-@chr1:133950636:133950801:-	0.57	0.68	0.6	0.77	0.81	0.73	0.79	0.71	0.74	0.65	0.58	0.68	NA	ENSMUSG00000059149	Mfsd4	MXE	4.02	0.09	0.15

Table C-4: Sequencing statistics for splicing datasets.

Internal Name	General Name	Total Reads	Reads Quality Filtered	Reads uniquely mapping	% uniquely mapping
SBMA					
krkr34453	krkr1	61,265,908	58,795,976	49,575,401	84
krkr34454	krkr2	54,419,782	52,271,241	44,217,027	85
krkr34455	krkr3	55,965,016	53,720,886	45,476,650	85
mut22534	mut1	49,977,618	48,434,563	39,905,098	82
mut22535	mut2	42,808,016	41,591,813	34,039,514	82
mut22536	mut3	49,266,056	47,798,845	39,056,179	82
rescue34450	rescue1	59,828,862	57,510,016	48,726,258	85
rescue34451	rescue2	62,375,708	60,124,140	50,154,497	83
rescue34452	rescue3	59,480,174	57,134,411	47,509,707	83
wt22531	wt1	51,150,550	49,640,908	39,354,701	79
wt22532	wt2	48,575,542	47,131,155	37,285,170	79
wt22533	wt3	50,115,656	48,632,837	39,238,800	81
HD					
HTC510	mut1	75,496,824	73,224,866	59,421,398	81
HTC519	mut2	68,198,228	66,002,241	53,116,259	80
VDT600	mut3	75,715,440	74,189,848	61,878,310	83
VDT610	mut4	70,831,096	68,332,445	55,237,489	81
HWC549	wt1	54,546,180	53,034,069	41,794,876	79
HWC562	wt2	66,404,168	64,572,822	51,311,282	79
VDW617	wt3	65,841,822	64,567,293	50,373,116	78
VDW619	wt4	72,756,276	70,220,065	54,229,905	77
SCA7					
1132M	mut1	121,457,234	116,909,364	99,498,783	85
1133M	mut2	119,500,322	114,836,315	96,995,400	84
1138M	mut3	115,330,306	111,146,016	96,308,561	87
1140M	mut4	126,977,706	122,148,695	104,606,805	86
1141W	wt1	129,774,742	125,324,785	102,392,127	82
1142W	wt2	140,926,144	138,849,239	111,354,154	80
1147W	wt3	154,346,480	151,585,982	123,543,238	82
1154W	wt4	117,626,202	112,606,079	89,416,249	79

Bibliography

Aid, T., Kazantseva, A., Piirsoo, M., Palm, K., & Timmusk, T. (2007). Mouse and rat BDNF gene structure and expression revisited. *Journal of neuroscience research*, *85*(3), 525–535.

Aird, D., Ross, M. G., Chen, W.-S., Danielsson, M., Fennell, T., Russ, C., Jaffe, D. B., Nusbaum, C., & Gnirke, A. (2011). Analyzing and minimizing PCR amplification bias in Illumina sequencing libraries. *Genome biology*, *12*(2), R18.

Akerman, M., David-Eden, H., Pinter, R. Y., & Mandel-Gutfreund, Y. (2009). A computational approach for genome-wide mapping of splicing factor binding sites. *Genome biology*, *10*(3), R30.

Altar, C. A., Cai, N., Bliven, T., Juhasz, M., Conner, J. M., Acheson, A. L., Lindsay, R. M., & Wiegand, S. J. (1997). Anterograde transport of brain-derived neurotrophic factor and its role in the brain. *Nature*, *389*(6653), 856–860.

Ambrose, C. M., Duyao, M. P., Barnes, G., Bates, G. P., Lin, C. S., Srinidhi, J., Baxendale, S., Hummerich, H., Lehrach, H., & Altherr, M. (1994). Structure and expression of the Huntington's disease gene: evidence against simple inactivation due to an expanded CAG repeat. *Somatic cell and molecular genetics*, *20*(1), 27–38.

Anders, S., & Huber, W. (2010). Differential expression analysis for sequence count data. *Genome biology*, *11*(10), R106.

Andrade, M. A., & Bork, P. (1995). HEAT repeats in the Huntington's disease protein. *Nature genetics*, *11*(2), 115–116.

Ansorge, O., Giunti, P., Michalik, A., Van Broeckhoven, C., Harding, B., Wood, N., & Scaravilli, F. (2004). Ataxin-7 aggregation and ubiquitination in infantile SCA7 with 180 CAG repeats. *Annals of Neurology*, *56*(3), 448–452.

Arrasate, M., Mitra, S., Schweitzer, E. S., Segal, M. R., & Finkbeiner, S. (2004). Inclusion body formation reduces levels of mutant huntingtin and the risk of neuronal death. *Nature*, *431*(7010), 805–810.

Attaix, D., & Taillandier, D. (2012). The Missing Link: Mul1 Signals Mitophagy and Muscle Wasting. *Cell Metabolism*, *16*(5), 551–552.

Atwal, R. S., Xia, J., Pinchev, D., Taylor, J., Epand, R. M., & Truant, R. (2007). Huntingtin has a membrane association signal that can modulate huntingtin aggregation, nuclear entry and toxicity. *Human molecular genetics*, *16*(21), 2600–2615.

Bae, B. I., Xu, H., Igarashi, S., Fujimuro, M., & Agrawal, N. (2005). p53 Mediates Cellular Dysfunction and Behavioral Abnormalities in Huntington's Disease. *Neuron*, *47*, 29–41.

Balasubramanian, D., Akhtar-Zaidi, B., Song, L., Bartels, C. F., Veigl, M., Beard, L., Myeroff, L., Guda, K., Lutterbaugh, J., Willis, J., Crawford, G. E., Markowitz, S. D., & Scacheri, P. C. (2012). H3K4me3 inversely correlates with DNA methylation at a large class of non-CpG-island-containing start sites. *Genome medicine*, *4*(5), 47.

Bañez-Coronel, M., Porta, S., Kagerbauer, B., Mateu-Huertas, E., Pantano, L., Ferrer, I., Guzmán, M., Estivill, X., & Martí, E. (2012). A Pathogenic Mechanism in Huntington's Disease Involves Small CAG-Repeated RNAs with Neurotoxic Activity. *PLoS Genetics*, *8*(2), e1002481.

Baquet, Z. C., Gorski, J. A., & Jones, K. R. (2004). Early striatal dendrite deficits followed by neuron loss with advanced age in the absence of anterograde cortical brain-derived neurotrophic factor. *Journal of Neuroscience*, *24*(17), 4250–4258.

Bates, G., Harper, P. S., & Jones, L. (2002). *Huntington's Disease*. Oxford: Oxford University Press, third ed.

Batsché, E., Yaniv, M., & Muchardt, C. (2005). The human SWI/SNF subunit Brm is a regulator of alternative splicing. *Nature Publishing Group*, *13*(1), 22–29.

Bäumer, D., Lee, S., Nicholson, G., Davies, J. L., Parkinson, N. J., Murray, L. M., Gillingwater, T. H., Ansorge, O., Davies, K. E., & Talbot, K. (2009). Alternative Splicing Events Are a Late Feature of Pathology in a Mouse Model of Spinal Muscular Atrophy. *PLoS Genetics*, *5*(12), e1000773.

Baxendale, S., Abdulla, S., Elgar, G., Buck, D., Berks, M., Micklem, G., Durbin, R., Bates, G., Brenner, S., & Beck, S. (1995). Comparative sequence analysis of the human and pufferfish Huntington's disease genes. *Nature genetics*, *10*(1), 67–76.

Benn, C. L. (2005). Contribution of nuclear and extranuclear polyQ to neurological phenotypes in mouse models of Huntington's disease. *Human molecular genetics*, *14*(20), 3065–3078.

Benn, C. L., Fox, H., & Bates, G. P. (2008a). Optimisation of region-specific reference gene selection and relative gene expression analysis methods for pre-clinical trials of Huntington's disease. *Molecular neurodegeneration*, *3*(17).

Benn, C. L., Sun, T., Sadri-Vakili, G., McFarland, K. N., DiRocco, D. P., Yohrling, G. J., Clark, T. W., Bouzou, B., & Cha, J.-H. J. (2008b). Huntingtin modulates

transcription, occupies gene promoters in vivo, and binds directly to DNA in a polyglutamine-dependent manner. *Journal of Neuroscience*, *28*(42), 10720–10733.

Benton, C. S., de Silva, R., Rutledge, S. L., Bohlega, S., Ashizawa, T., & Zoghbi, H. Y. (1998). Molecular and clinical studies in SCA-7 define a broad clinical spectrum and the infantile phenotype. *Neurology*, *51*(4), 1081–1086.

Berg, M. G., Singh, L. N., Younis, I., Liu, Q., Pinto, A. M., Kaida, D., Zhang, Z., Cho, S., Sherrill-Mix, S., Wan, L., & Dreyfuss, G. (2012). U1 snRNP Determines mRNA Length and Regulates Isoform Expression. *Cell*, *150*(1), 53–64.

Bernstein, B. E., Humphrey, E. L., & Erlich, R. L. (2002). Methylation of histone H3 Lys 4 in coding regions of active genes. In *Proceedings of the National Academy of Sciences of the USA*, (pp. 8695–8700).

Bernstein, B. E., Meissner, A., & Lander, E. S. (2007). The Mammalian Epigenome. *Cell*, *128*(4), 669–681.

Binder, D. K., & Scharfman, H. E. (2004). Brain-derived neurotrophic factor. *Growth Factors*, *22*(3), 123–131.

Bolton, E. C., So, A. Y., Chaivorapol, C., Haqq, C. M., Li, H., & Yamamoto, K. R. (2007). Cell- and gene-specific regulation of primary target genes by the androgen receptor. *Genes & Development*, *21*(16), 2005–2017.

Bradnam, K. R., & Korf, I. (2008). Longer first introns are a general property of eukaryotic gene structure. *PloS one*, *3*(8), e3093.

Busch, A. (2003). Mutant Huntingtin Promotes the Fibrillogenesis of Wild-type Huntingtin: A Potential Mechanism for Loss of Huntingtin Function in Huntington's Disease. *Journal of Biological Chemistry*, *278*(42), 41452–41461.

Cai, Q., & Sheng, Z.-H. (2009). Moving or Stopping Mitochondria: Miro as a Traffic Cop by Sensing Calcium. *Neuron*, *61*(4), 493–496.

Cancel, G., Duyckaerts, C., Holmberg, M., Zander, C., Yvert, G., Lebre, A. S., Ruberg, M., Faucheux, B., Agid, Y., Hirsch, E., & Brice, A. (2000). Distribution of ataxin-7 in normal human brain and retina. *Brain*, *123*, 2519–2530.

Caron, N. S., Desmond, C. R., Xia, J., & Truant, R. (2013). Polyglutamine domain flexibility mediates the proximity between flanking sequences in huntingtin. *Proceedings of the National Academy of Sciences of the USA*, *110*(36), 14610–14615.

Cartegni, L. (2003). ESEfinder: a web resource to identify exonic splicing enhancers. *Nucleic Acids Research*, *31*(13), 3568–3571.

Cartegni, L., Wang, J., Zhu, Z., Zhang, M. Q., & Krainer, A. R. (2003). ESEfinder: A web resource to identify exonic splicing enhancers. *Nucleic Acids Research*, *31*(13), 3568–3571.

Castle, J. C., Zhang, C., Shah, J. K., Kulkarni, A. V., Kalsotra, A., Cooper, T., & Johnson, J. M. (2008). Expression of 24,426 human alternative splicing events and predicted cis regulation in 48 tissues and cell lines. *Nature genetics*, *40*(12), 1416–1425.

Cattaneo, E., Zuccato, C., & Tartari, M. (2005). Normal huntingtin function: an alternative approach to Huntington's disease. *Nature Reviews Neuroscience*, *6*(12), 919–930.

Caviston, J. P., Ross, J. L., Antony, S. M., Tokito, M., & Holzbaur, E. L. F. (2007). Huntingtin facilitates dynein/dynactin-mediated vesicle transport. *Proceedings of the National Academy of Sciences of the United States of America*, *104*(24), 10045–10050.

Cha, J. (2007). Transcriptional signatures in Huntington's disease. *Progress in neurobiology*, *83*(4), 228–248.

Cha, J. H. (2000). Transcriptional dysregulation in Huntington's disease. *Trends in neurosciences*, *23*(9), 387–392.

Chaturvedi, R. K., Adhihetty, P., & Shukla, S. (2009). Impaired PGC-1α function in muscle in Huntington's disease. *Hum Molecular Genetics*, *18*(16), 3048–3065.

Choo, Y. S., Mao, Z., Johnson, G. V. W., & Lesort, M. (2005). Increased glutathione levels in cortical and striatal mitochondria of the R6/2 Huntington's disease mouse model. *Neuroscience letters*, *386*(1), 63–68.

Chort, A., Alves, S., Marinello, M., Dufresnois, B., Dornbierer, J.-G., Tesson, C., Latouche, M., Baker, D. P., Barkats, M., El Hachimi, K. H., Ruberg, M., Janer, A., Stevanin, G., Brice, A., & Sittler, A. (2013). Interferon β induces clearance of mutant ataxin 7 and improves locomotion in SCA7 knock-in mice. *Brain*, *136*, 1732–1745.

Ciammola, A., Sassone, J., Alberti, L., Meola, G., Mancinelli, E., Russo, M. A., Squitieri, F., & Silani, V. (2006). Increased apoptosis, Huntingtin inclusions and altered differentiation in muscle cell cultures from Huntington's disease subjects. *Cell death and differentiation*, *13*(12), 2068–2078.

Ciammola, A., Sassone, J., Sciacco, M., Mencacci, N. E., Ripolone, M., Bizzi, C., Colciago, C., Moggio, M., Parati, G., Silani, V., & Malfatto, G. (2011). Low anaerobic threshold and increased skeletal muscle lactate production in subjects with Huntington's disease. *Movement Disorders*, *26*(1), 130–137.

Clabough, E. B. D., & Zeitlin, S. O. (2006). Deletion of the triplet repeat encoding polyglutamine within the mouse Huntington's disease gene results in subtle behavioral/motor phenotypes in vivo and elevated levels of ATP with cellular senescence in vitro. *Human molecular genetics*, *15*(4), 607–623.

Cornett, J., Cao, F., Wang, C.-E., Ross, C. A., Bates, G. P., Li, S.-H., & Li, X.-J. (2005). Polyglutamine expansion of huntingtin impairs its nuclear export. *Nature genetics*, *37*(2), 198–204.

Crook, Z. R., & Housman, D. (2011). Huntington's Disease: Can Mice Lead the Way to Treatment? *Neuron*, *69*(3), 423–435.

Culver, B. P., Savas, J. N., Park, S. K., Choi, J. H., Zheng, S., Zeitlin, S. O., Yates, J. R., & Tanese, N. (2012). Proteomic analysis of wild-type and mutant huntingtin-associated proteins in mouse brains identifies unique interactions and involvement in protein synthesis. *Journal of Biological Chemistry*, *287*(26), 21599–21614.

Cummings, C. J., & Zoghbi, H. Y. (2000). Fourteen and counting: unraveling trinucleotide repeat diseases. *Human molecular genetics*, *9*(6), 909–916.

Daigle, J. G., Lanson, N. A., Smith, R. B., Casci, I., Maltare, A., Monaghan, J., Nichols, C. D., Kryndushkin, D., Shewmaker, F., & Pandey, U. B. (2013). RNA-binding ability of FUS regulates neurodegeneration, cytoplasmic mislocalization and incorporation into stress granules associated with FUS carrying ALS-linked mutations. *Human molecular genetics*, *22*(6), 1193–1205.

David, G., Dürr, A., Stevanin, G., Cancel, G., Abbas, N., Benomar, A., Belal, S., Lebre, A. S., Abada-Bendib, M., Grid, D., Holmberg, M., Yahyaoui, M., Hentati, F., Chkili, T., Agid, Y., & Brice, A. (1998). Molecular and clinical correlations in autosomal dominant cerebellar ataxia with progressive macular dystrophy (SCA7). *Human molecular genetics*, *7*(2), 165–170.

de Mezer, M., Wojciechowska, M., Napierala, M., Sobczak, K., & Krzyzosiak, W. J. (2011). Mutant CAG repeats of Huntingtin transcript fold into hairpins, form nuclear foci and are targets for RNA interference. *Nucleic Acids Research*, *39*(9), 3852–3863.

de Tommaso (2011). Management of Huntington' Disease: Role of Tetrabenazine. *Therapeutic and Clinical Risk Management*, *7*, 123–129.

Deaton, A. M., Webb, S., Kerr, A. R. W., Illingworth, R. S., Guy, J., Andrews, R., & Bird, A. (2011). Cell type-specific DNA methylation at intragenic CpG islands in the immune system. *Genome Research*, *21*(7), 1074–1086.

Dejager, S., Bry-Gauillard, H., Bruckert, E., Eymard, B., Salachas, F., LeGuern, E., Tardieu, S., Chadarevian, R., Giral, P., & Turpin, G. (2002). A Comprehensive Endocrine Description of Kennedy's Disease Revealing Androgen Insensitivity Linked to CAG Repeat Length. *The Journal of Clinical Endocrinology & Metabolism*, *87*(8), 3893–3901.

Difiglia, M. (1997). Aggregation of Huntingtin in Neuronal Intranuclear Inclusions and Dystrophic Neurites in Brain. *Science*, *277*(5334), 1990–1993.

Dillies, M. A., Rau, A., Aubert, J., Hennequet-Antier, C., Jeanmougin, M., Servant, N., Keime, C., Marot, G., Castel, D., Estelle, J., Guernec, G., Jagla, B., Jouneau, L., Laloe, D., Le Gall, C., Schaeffer, B., Le Crom, S., Guedj, M., Jaffrezic, F., & on behalf of The French StatOmique Consortium (2013). A comprehensive evaluation of normalization methods for Illumina high-throughput RNA sequencing data analysis. *Briefings in Bioinformatics*, *14*(6), 671–683.

Doi, H., Okamura, K., Bauer, P. O., Furukawa, Y., Shimizu, H., Kurosawa, M., Machida, Y., Miyazaki, H., Mitsui, K., Kuroiwa, Y., & Nukina, N. (2008). RNA-binding Protein TLS Is a Major Nuclear Aggregate-interacting Protein in Huntingtin Exon 1 with Expanded Polyglutamine-expressing Cells. *Journal of Biological Chemistry*, *283*(10), 6489–6500.

Duan, W., Guo, Z., Jiang, H., Ware, M., Li, X.-J., & Mattson, M. P. (2003). Dietary restriction normalizes glucose metabolism and BDNF levels, slows disease progression, and increases survival in huntingtin mutant mice. *Proceedings of the National Academy of Sciences of the United States of America*, *100*(5), 2911–2916.

Duan, W., Peng, Q., Masuda, N., Ford, E., Tryggestad, E., Ladenheim, B., Zhao, M., Cadet, J. L., Wong, J., & Ross, C. A. (2008). Sertraline slows disease progression and increases neurogenesis in N171-82Q mouse model of Huntington's disease. *Neurobiology of Disease*, *30*(3), 312–322.

Dunah, A. W. (2002). Sp1 and TAFII130 Transcriptional Activity Disrupted in Early Huntington's Disease. *Science*, *296*(5576), 2238–2243.

Duzdevich, D., Li, J., Whang, J., Takahashi, H., Takeyasu, K., Dryden, D. T. F., Morton, A. J., & Edwardson, J. M. (2011). Unusual structures are present in DNA fragments containing super-long Huntingtin CAG repeats. *PloS one*, *6*(2), e17119.

Dyer, R. B., & McMurray, C. T. (2001). Mutant protein in Huntington disease is resistant to proteolysis in affected brain. *Nature genetics*, *29*(3), 270–278.

Eden, E., Navon, R., Steinfeld, I., Lipson, D., & Yakhini, Z. (2009). GOrilla: a tool for discovery and visualization of enriched GO terms in ranked gene lists. *BMC bioinformatics*, *10*, 48.

Engelender, S., Sharp, A. H., Colomer, V., Tokito, M. K., Lanahan, A., Worley, P., Holzbaur, E. L., & Ross, C. A. (1997). Huntingtin-associated protein 1 (HAP1) interacts with the p150Glued subunit of dynactin. *Human molecular genetics*, *6*(13), 2205–2212.

Faber, P. W., Barnes, G. T., Srinidhi, J., Chen, J., Gusella, J. F., & MacDonald, M. E. (1998). Huntingtin interacts with a family of WW domain proteins. *Human molecular genetics*, *7*(9), 1463–1474.

Forsgren, L., Libelius, R., Holmberg, M., von Dobeln, U., Wibom, R., Heijbel, J., Sandgren, O., & Holmgren, G. (1996). Muscle morphology and mitochondrial

investigations of a family with autosomal dominant cerebella ataxia and retinal degeneration mapped to chromosome 3p12-p21.1. *Journal of Neurological Sciences*, *144*, 91–98.

Fujimoto, M., Takaki, E., Hayashi, T., Kitaura, Y., Tanaka, Y., Inouye, S., & Nakai, A. (2005). Active HSF1 significantly suppresses polyglutamine aggregate formation in cellular and mouse models. *The Journal of biological chemistry*, *280*(41), 34908–34916.

Gaffney, D. J., & Keightley, P. D. (2006). Genomic Selective Constraints in Murid Noncoding DNA. *PLoS Genetics*, *2*(11), e204.

Gafni, J., Hermel, E., Young, J. E., Wellington, C. L., Hayden, M. R., & Ellerby, L. M. (2004). Inhibition of Calpain Cleavage of Huntingtin Reduces Toxicity: Accumulation of Calpain/Caspase Fragments in the Nucleus. *Journal of Biological Chemistry*, *279*(19), 20211–20220.

Gauthier, L. R., Charrin, B. C., & Borrell-Pagès, M. (2004). Huntingtin Controls Neurotrophic Support and Survival of Neurons by Enhancing BDNF Vesicular Transport along Microtubules. *Cell*, *118*, 127–138.

Gazave, E., Marqués-Bonet, T., Fernando, O., Charlesworth, B., & Navarro, A. (2007). Patterns and rates of intron divergence between humans and chimpanzees. *Genome biology*, *8*(2), R21.

Gerashchenko, M. V., Lobanov, A. V., & Gladyshev, V. N. (2012). Genome-wide ribosome profiling reveals complex translational regulation in response to oxidative stress. *Proceedings of the National Academy of Sciences*, *109*(43), 17394–17399.

Giles, P., Elliston, L., Higgs, G. V., Brooks, S. P., Dunnett, S. B., & Jones, L. (2012). Longitudinal analysis of gene expression and behaviour in the HdhQ150 mouse model of Huntington's disease. *Brain research bulletin*, *88*(2-3), 199–209.

Gipson, T. A., Neueder, A., Wexler, N. S., Bates, G. P., & Housman, D. (2013). Aberrantly spliced HTT, a new player in Huntington's disease pathogenesis. *RNA biology*, *10*(11), 1647–1652.

Gizatullina, Z. Z., Lindenberg, K. S., Harjes, P., Chen, Y., Kosinski, C. M., Landwehrmeyer, B. G., Ludolph, A. C., Striggow, F., Zierz, S., & Gellerich, F. N. (2006). Low stability of huntington muscle Mitochondria against Ca2+ in R6/2 mice. *Annals of Neurology*, *59*(2), 407–411.

Gordon, D. B., Nekludova, L., McCallum, S., & Fraenkel, E. (2005). TAMO: a flexible, object-oriented framework for analyzing transcriptional regulation using DNA-sequence motifs. *Bioinformatics (Oxford, England)*, *21*(14), 3164–3165.

Gottfried, M., Lavine, L., & Roessmann, U. (1981). Neuropathological findings in Wolf-Hirschhorn (4p-) syndrome. *Acta neuropathologica*, *55*(2), 163–165.

Gu, M., Gash, M. T., Mann, V. M., Javoy-Agid, F., Cooper, J. M., & Schapira, A. H. (1996). Mitochondrial defect in Huntington's disease caudate nucleus. *Annals of Neurology*, *39*(3), 385–389.

Gu, X., Cantle, J. P., Greiner, E. R., Lee, C. Y. D., Barth, A. M., Gao, F., Park, C. S., Zhang, Z., Sandoval-Miller, S., Zhang, R. L., Diamond, M., Mody, I., Coppola, G., & Yang, X. W. (2015). N17 Modifies mutant Huntingtin nuclear pathogenesis and severity of disease in HD BAC transgenic mice. *Neuron*, *85*(4), 726–741.

Gunawardena, S., Her, L.-S., Brusch, R. G., Laymon, R. A., Niesman, I. R., Gordesky-Gold, B., Sintasath, L., Bonini, N. M., & Goldstein, L. S. B. (2003). Disruption of axonal transport by loss of huntingtin or expression of pathogenic polyQ proteins in Drosophila. *Neuron*, *40*(1), 25–40.

Guo, H., Ingolia, N. T., Weissman, J. S., & Bartel, D. P. (2010a). Mammalian microRNAs predominantly act to decrease target mRNA levels. *Nature*, *466*(7308), 835–840.

Guo, X., Disatnik, M.-H., Monbureau, M., Shamloo, M., Mochly-Rosen, D., & Qi, X. (2013). Inhibition of mitochondrial fragmentation diminishes Huntington's disease–associated neurodegeneration. *Journal of Clinical Investigation*, *123*(12), 5371–5388.

Guo, Y., Papachristoudis, G., Altshuler, R. C., Gerber, G. K., Jaakkola, T. S., Gifford, D. K., & Mahony, S. (2010b). Discovering homotypic binding events at high spatial resolution. *Bioinformatics (Oxford, England)*, *26*(24), 3028–3034.

Gupta, S., Kim, S. Y., Artis, S., Molfese, D. L., Schumacher, A., Sweatt, J. D., Paylor, R. E., & Lubin, F. D. (2010). Histone methylation regulates memory formation. *Journal of Neuroscience*, *30*(10), 3589–3599.

Han, J., Xiong, J., Wang, D., & Fu, X.-D. (2011). Pre-mRNA splicing: where and when in the nucleus. *Trends in Cell Biology*, *21*(6), 336–343.

Han, Y., Deng, B., Liu, M., Jiang, J., Wu, S., & Guan, Y. (2010). Clinical and genetic study of a Chinese family with spinocerebellar ataxia type 7. *Neurology India*, *58*(4), 622–626.

Harjes, P., & Wanker, E. E. (2003). The hunt for huntingtin function: interaction partners tell many different stories. *Trends in biochemical sciences*, *28*(8), 425–433.

Harper, S. (2009). Progress and challenges in RNA interference therapy for Huntington disease. *Archives of neurology*, *66*(8), 933–939.

Heintzman, N. D., Stuart, R. K., Hon, G., Fu, Y., Ching, C. W., Hawkins, R. D., Barrera, L. O., Van Calcar, S., Qu, C., Ching, K. A., Wang, W., Weng, Z., Green, R. D., Crawford, G. E., & Ren, B. (2007). Distinct and predictive chromatin signatures of transcriptional promoters and enhancers in the human genome. *Nature genetics*, *39*(3), 311–318.

Helmlinger, D., Hardy, S., Sasorith, S., Klein, F., Robert, F., Weber, C., Miguet, L., Potier, N., Van-Dorsselaer, A., Wurtz, J.-M., Mandel, J.-L., Tora, L., & Devys, D. (2004). Ataxin-7 is a subunit of GCN5 histone acetyltransferase-containing complexes. *Human molecular genetics*, *13*(12), 1257–1265.

Ho, S. H., So, G. M. K., & Chow, K. L. (2001). Postembryonic expression of-Caenorhabditis elegans mab-21 and its requirement in sensory ray differentiation. *Developmental Dynamics*, *221*(4), 422–430.

Hockly, E., Woodman, B., Mahal, A., & Lewis, C. M. (2003). Standardization and statistical approaches to therapeutic trials in the R6/2 mouse. *Brain research bulletin*, *61*, 469–479.

Hodges, A., Strand, A. D., Aragaki, A. K., Kuhn, A., Sengstag, T., Hughes, G., Elliston, L. A., Hartog, C., Goldstein, D. R., Thu, D., Hollingsworth, Z. R., Collin, F., Synek, B., Holmans, P. A., Young, A. B., Wexler, N. S., Delorenzi, M., Kooperberg, C., Augood, S. J., Faull, R. L. M., Olson, J. M., Jones, L., & Luthi-Carter, R. (2006). Regional and cellular gene expression changes in human Huntington's disease brain. *Human molecular genetics*, *15*(6), 965–977.

Holmberg, M. (1998). Spinocerebellar ataxia type 7 (SCA7): a neurodegenerative disorder with neuronal intranuclear inclusions. *Human molecular genetics*, *7*(5), 913–918.

Hoss, A. G., Kartha, V. K., Dong, X., Latourelle, J. C., Dumitriu, A., Hadzi, T. C., MacDonald, M. E., Gusella, J. F., Akbarian, S., Chen, J.-F., Weng, Z., & Myers, R. H. (2014). MicroRNAs located in the Hox gene clusters are implicated in huntington's disease pathogenesis. *PLoS Genetics*, *10*(2), e1004188.

Huang, E. J., & Reichardt, L. F. (2001). Neurotrophins: Roles in Neuronal Development and Function 1. *Annual Review of Neuroscience*, *24*(1), 677–736.

Huang, H.-Y., Chien, C.-H., Jen, K.-H., & Huang, H.-D. (2006). RegRNA: an integrated web server for identifying regulatory RNA motifs and elements. *Nucleic Acids Research*, *34*(Web Server issue), W429–34.

Hunter, R. G., McCarthy, K. J., Milne, T. A., Pfaff, D. W., & McEwen, B. S. (2009). Regulation of hippocampal H3 histone methylation by acute and chronic stress. *Proceedings of the National Academy of Sciences*, *106*(49), 20912–20917.

Huntington, G. (2003). On Chorea. *The Journal of Neuropsychiatry and Clinical Neurosciences*, *15*(1), 109–112.

Hutten, S., Chachami, G., Winter, U., Melchior, F., & Lamond, A. I. (2014). A role for the Cajal-body-associated SUMO isopeptidase USPL1 in snRNA transcription mediated by RNA polymerase II. *Journal of Cell Science*, *127*, 1065–1078.

Ingolia, N. T., Ghaemmaghami, S., Newman, J. R. S., & Weissman, J. S. (2009). Genome-Wide Analysis in Vivo of Translation with Nucleotide Resolution Using Ribosome Profiling. *Science*, *324*(5924), 218–223.

Ivkovic, S., Polonskaia, O., Fariñas, I., & Ehrlich, M. E. (1997). Brain-derived neurotrophic factor regulates maturation of the DARPP-32 phenotype in striatal medium spiny neurons: studies in vivo and in vitro. *Neuroscience*, *79*(2), 509–516.

Jana, N. R., Dikshit, P., Goswami, A., Kotliarova, S., Murata, S., Tanaka, K., & Nukina, N. (2005). Co-chaperone CHIP Associates with Expanded Polyglutamine Protein and Promotes Their Degradation by Proteasomes. *Journal of Biological Chemistry*, *280*(12), 11635–11640.

Jenkins, K., Khoo, J. J., Sadler, A., Piganis, R., Wang, D., Borg, N. A., Hjerrild, K., Gould, J., Thomas, B. J., Nagley, P., Hertzog, P. J., & Mansell, A. (2013). Mitochondrially localised MUL1 is a novel modulator of antiviral signaling. *Immunology and Cell Biology*, *91*(4), 321–330.

Jeon, J. S., Lee, S., Jung, K. H., Jun, S. H., Kim, C., & An, G. (2000). Tissue-preferential expression of a rice alpha-tubulin gene, OsTubA1, mediated by the first intron. *Plant physiology*, *123*(3), 1005–1014.

Jiang, Y., Langley, B., Lubin, F. D., Renthal, W., Wood, M. A., Yasui, D. H., Kumar, A., Nestler, E. J., Akbarian, S., & Beckel-Mitchener, A. C. (2008). Epigenetics in the Nervous System. *Journal of Neuroscience*, *28*(46), 11753–11759.

Jiang, Y. J., Che, M. X., Yuan, J. Q., Xie, Y. Y., Yan, X. Z., & Hu, H. Y. (2011). Interaction with Polyglutamine-expanded Huntingtin Alters Cellular Distribution and RNA Processing of Huntingtin Yeast Two-hybrid Protein A (HYPA). *Journal of Biological Chemistry*, *286*(28), 25236–25245.

Jin, Y. N., & Johnson, G. V. W. (2010). The interrelationship between mitochondrial dysfunction and transcriptional dysregulation in Huntington disease. *Journal of Bioenergetics and Biomembranes*, *42*(3), 199–205.

Johansson, J. (1998). Expanded CAG repeats in Swedish spinocerebellar ataxia type 7 (SCA7) patients: effect of CAG repeat length on the clinical manifestation. *Human molecular genetics*, *7*(2), 171–176.

Johnson, D. S., Mortazavi, A., Myers, R. M., & Wold, B. (2007). Genome-wide mapping of in vivo protein-DNA interactions. *Science*, *316*(5830), 1497–1502.

Jonasson, J., Ström, A.-L., Hart, P., Bränström, T., Forsgren, L., & Holmberg, M. (2002). Expression of ataxin-7 in CNS and non-CNS tissue of normal and SCA7 individuals. *Acta neuropathologica*, *104*(1), 29–37.

Jonsson, J. J., Foresman, M. D., Wilson, N., & McIvor, R. S. (1992). Intron requirement for expression of the human purine nucleoside phosphorylase gene. *Nucleic Acids Research*, *20*(12), 3191–3198.

KA, W. (2015). DNA Sequencing Costs: Data from the NHGRI Genome Sequencing Program (GSP). Tech. rep.

Kalari, K. R. K., Casavant, M. M., Bair, T. B. T., Keen, H. L. H., Comeron, J. M. J., Casavant, T. L. T., & Scheetz, T. E. T. (2006). First exons and introns–a survey of GC content and gene structure in the human genome. *In Silico Biology*, *6*(3), 237–242.

Kalchman, M. A., Graham, R. K., Xia, G., Koide, H. B., Hodgson, J. G., Graham, K. C., Goldberg, Y. P., Gietz, R. D., Pickart, C. M., & Hayden, M. R. (1996). Huntingtin is ubiquitinated and interacts with a specific ubiquitin-conjugating enzyme. *The Journal of biological chemistry*, *271*(32), 19385–19394.

Katsuno, M., Adachi, H., Kume, A., Li, M., Nakagomi, Y., Niwa, H., Sang, C., Kobayashi, Y., Doyu, M., & Sobue, G. (2002). Testosterone Reduction Prevents Phenotypic Expression in a Transgenic Mouse Model of Spinal and Bulbar Muscular Atrophy. *Neuron*, *35*(5), 843–854.

Katsuno, M., Adachi, H., Waza, M., Banno, H., Suzuki, K., Tanaka, F., Doyu, M., & Sobue, G. (2006). Pathogenesis, animal models and therapeutics in spinal and bulbar muscular atrophy (SBMA). *Experimental Neurology*, *200*(1), 8–18.

Katz, Y., Li, F., Lambert, N. J., Sokol, E. S., Tam, W.-L., Cheng, A. W., Airoldi, E. M., Lengner, C. J., Gupta, P. B., Yu, Z., Jaenisch, R., & Burge, C. B. (2014). Musashi proteins are post-transcriptional regulators of the epithelial-luminal cell state. *eLife*, *3*, e03915.

Katz, Y., Wang, E. T., Airoldi, E. M., & Burge, C. B. (2010). Analysis and design of RNA sequencing experiments for identifying isoform regulation. *Nature Methods*, *7*(12), 1009–1015.

Katz, Y., Wang, E. T., Silterra, J., Schwartz, S., Wong, B., Thorvaldsdóttir, H., Robinson, J. T., Mesirov, J. P., Airoldi, E. M., & Burge, C. B. (2015). Quantitative visualization of alternative exon expression from RNA-seq data. *Bioinformatics (Oxford, England)*, *31*(14), 2400–2402.

Kegel, K. B., Sapp, E., Yoder, J., Cuiffo, B., Sobin, L., Kim, Y. J., Qin, Z.-H., Hayden, M. R., Aronin, N., Scott, D. L., Isenberg, G., Goldmann, W. H., & DiFiglia, M. (2005). Huntingtin associates with acidic phospholipids at the plasma membrane. *The Journal of biological chemistry*, *280*(43), 36464–36473.

Kim, J., Moody, J. P., Edgerly, C. K., Bordiuk, O. L., Cormier, K., Smith, K., Beal, M. F., & Ferrante, R. J. (2010). Mitochondrial loss, dysfunction and altered dynamics in Huntington's disease. *Human molecular genetics*, *19*(20), 3919–3935.

Kim, T. H., Barrera, L. O., Zheng, M., Qu, C., Singer, M. A., Richmond, T. A., Wu, Y., Green, R. D., & Ren, B. (2005). A high-resolution map of active promoters in the human genome. *Nature Cell Biology*, *436*(7052), 876–880.

Kim, Y. J., Yi, Y., Sapp, E., Wang, Y., Cuiffo, B., Kegel, K. B., Qin, Z. H., Aronin, N., & Difiglia, M. (2001). Caspase 3-cleaved N-terminal fragments of wild-type and mutant huntingtin are present in normal and Huntington's disease brains, associate with membranes, and undergo calpain-dependent proteolysis. *Proceedings of the National Academy of Sciences of the United States of America*, *98*(22), 12784–12789.

Ko, J., Ou, S., & Patterson, P. H. (2001). New anti-huntingtin monoclonal antibodies: implications for huntingtin conformation and its binding proteins. *Brain research bulletin*, *56*(3-4), 319–329.

Konieczny, P., Stepniak-Konieczna, E., & Sobczak, K. (2014). MBNL proteins and their target RNAs, interaction and splicing regulation. *Nucleic Acids Research*, *42*(17), 10873–10887.

Kosinski, C. M., Schlangen, C., Gellerich, F. N., Gizatullina, Z., Deschauer, M., Schiefer, J., Young, A. B., Landwehrmeyer, G. B., Toyka, K. V., Sellhaus, B., & Lindenberg, K. S. (2007). Myopathy as a first symptom of Huntington's disease in a Marathon runner. *Movement Disorders*, *22*(11), 1637–1640.

Kriventseva, E. V., & Gelfand, M. S. (1999). Statistical Analysis of the Exon-Intron Structure of Higher and Lower Eukaryote Genes. *Journal of Biomolecular Structure and Dynamics*, *17*(2), 281–288.

Krol, J., Fiszer, A., Mykowska, A., Sobczak, K., de Mezer, M., & Krzyzosiak, W. J. (2007). Ribonuclease dicer cleaves triplet repeat hairpins into shorter repeats that silence specific targets. *Molecular Cell*, *25*(4), 575–586.

Labbadia, J., Cunliffe, H., Weiss, A., Katsyuba, E., Sathasivam, K., Seredenina, T., Woodman, B., Moussaoui, S., Frentzel, S., Luthi-Carter, R., Paganetti, P., & Bates, G. P. (2011). Altered chromatin architecture underlies progressive impairment of the heat shock response in mouse models of Huntington disease. *Journal of Clinical Investigation*, *121*(8), 3306–3319.

Labourier, E. E., Bourbon, H. M. H., Gallouzi, I. E. I., Fostier, M. M., Allemand, E. E., & Tazi, J. J. (1999). Antagonism between RSF1 and SR proteins for both splice-site recognition in vitro and Drosophila development. *Genes & Development*, *13*(6), 740–753.

Landan, G., Cohen, N. M., Mukamel, Z., Bar, A., Molchadsky, A., Brosh, R., Horn-Saban, S., Zalcenstein, D. A., Goldfinger, N., Zundelevich, A., Gal-Yam, E. N., Rotter, V., & Tanay, A. (2012). Epigenetic polymorphism and the stochastic formation of differentially methylated regions in normal and cancerous tissues. *Nature genetics*, *44*(11), 1207–1214.

Landles, C., Sathasivam, K., Weiss, A., Woodman, B., Moffitt, H., Finkbeiner, S., Sun, B., Gafni, J., Ellerby, L. M., Trottier, Y., Richards, W. G., Osmand, A., Paganetti, P., & Bates, G. P. (2010). Proteolysis of mutant huntingtin produces

an exon 1 fragment that accumulates as an aggregated protein in neuronal nuclei in Huntington disease. *The Journal of biological chemistry*, *285*(12), 8808–8823.

Langmead, B., Trapnell, C., Pop, M., & Salzberg, S. L. (2009). Ultrafast and memory-efficient alignment of short DNA sequences to the human genome. *Genome biology*, *10*(3), R25.

Lerner, T. N., & Kreitzer, A. C. (2012). RGS4 is required for dopaminergic control of striatal LTD and susceptibility to parkinsonian motor deficits. *Neuron*, *73*(2), 347–359.

Levin, J. Z., Yassour, M., Adiconis, X., Nusbaum, C., Thompson, D. A., Friedman, N., Gnirke, A., & Regev, A. (2010). Comprehensive comparative analysis of strand-specific RNA sequencing methods. *Nature Methods*, *7*(9), 709–715.

Li, H., Handsaker, B., Wysoker, A., Fennell, T., Ruan, J., Homer, N., Marth, G., Abecasis, G., Durbin, R., & 1000 Genome Project Data Processing Subgroup (2009). The Sequence Alignment/Map format and SAMtools. *Bioinformatics (Oxford, England)*, *25*(16), 2078–2079.

Li, L.-B., & Bonini, N. M. (2010). Roles of trinucleotide-repeat RNA in neurological disease and degeneration. *Trends in neurosciences*, *33*(6), 292–298.

Li, S. H., Cheng, A. L., Zhou, H., Lam, S., Rao, M., Li, H., & Li, X. J. (2002). Interaction of Huntington Disease Protein with Transcriptional Activator Sp1. *Molecular and cellular biology*, *22*(5), 1277–1287.

Li, S. H., Gutekunst, C. A., Hersch, S. M., & Li, X. J. (1998). Interaction of huntingtin-associated protein with dynactin P150Glued. *The Journal of Neuroscience*, *18*(4), 1261–1269.

Li, S. H., & Li, X. J. (2004). Huntingtin–protein interactions and the pathogenesis of Huntington's disease. *TRENDS in Genetics*, *20*(3), 146–154.

Li, S. H., Schilling, G., Young, W. S., Li, X. J., Margolis, R. L., Stine, O. C., Wagster, M. V., Abbott, M. H., Franz, M. L., & Ranen, N. G. (1993). Huntington's disease gene (IT15) is widely expressed in human and rat tissues. *Neuron*, *11*(5), 985–993.

Li, Z., Karlovich, C. A., Fish, M. P., Scott, M. P., & Myers, R. M. (1999). A putative Drosophila homolog of the Huntington's disease gene. *Human molecular genetics*, *8*(9), 1807–1815.

Lieberman, A. P., & Fischbeck, K. H. (2000). Triplet repeat expansion in neuromuscular disease. *Muscle & nerve*, (pp. 843–850).

Lieberman, A. P., Yu, Z., Murray, S., Peralta, R., Low, A., Guo, S., Yu, X. X., Cortes, C. J., Bennett, C. F., Monia, B. P., La Spada, A. R., & Hung, G. (2014). Peripheral androgen receptor gene suppression rescues disease in mouse models of spinal and bulbar muscular atrophy. *Cell reports*, *7*(3), 774–784.

Lifschytz, T., Broner, E. C., Zozulinsky, P., Slonimsky, A., Eitan, R., Greenbaum, L., & Lerer, B. (2012). Relationship between Rgs2 gene expression level and anxiety and depression-like behaviour in a mutant mouse model: serotonergic involvement. *The International Journal of Neuropsychopharmacology*, *15*(9), 1307–1318.

Lin, B., Nasir, J., MacDonald, H., Hutchinson, G., Graham, R. K., Rommens, J. M., & Hayden, M. R. (1994). Sequence of the murine Huntington disease gene: evidence for conservation, alternate splicing and polymorphism in a triplet (CCG) repeat [corrected]. *Human molecular genetics*, *3*(1), 85–92.

Lin, C. H., Tallaksen-Greene, S., Chien, W. M., Cearley, J. A., Jackson, W. S., Crouse, A. B., Ren, S., Li, X. J., Albin, R. L., & Detloff, P. J. (2001). Neurological abnormalities in a knock-in mouse model of Huntington's disease. *Human molecular genetics*, *10*(2), 137–144.

Lloret-Llinares, M., Carré, C., Vaquero, A., de Olano, N., & Azorín, F. (2008). Characterization of Drosophila melanogaster JmjC+N histone demethylases. *Nucleic Acids Research*, *36*(9), 2852–2863.

Lodi, R., Schapira, A. H. V., Manners, D., Styles, P., Wood, N. W., Taylor, D. J., & Warner, T. T. (2001). Abnormal in vivo skeletal muscle energy metabolism in Huntington's disease and dentatorubropallidoluysian atrophy. *Annals of Neurology*, *48*(1), 72–76.

Lokireddy, S., Wijesoma, I. W., Teng, S., Bonala, S., Gluckman, P. D., McFarlane, C., Sharma, M., & Kambadur, R. (2012). The Ubiquitin Ligase Mul1 Induces Mitophagy in Skeletal Muscle in Responseto Muscle-Wasting Stimuli. *Cell Metabolism*, *16*(5), 613–624.

Lu, X.-H., & Yang, X. W. (2012). "Huntingtin Holiday": Progress toward an Antisense Therapy for Huntington's Disease. *Neuron*, *74*(6), 964–966.

Luco, R. F., Pan, Q., Tominaga, K., Blencowe, B. J., Pereira-Smith, O. M., & Misteli, T. (2010). Regulation of Alternative Splicing by Histone Modifications. *Science*, *327*(5968), 996–1000.

Lunkes, A., Lindenberg, K. S., Ben-Haiem, L., Weber, C., Devys, D., Landwehrmeyer, G. B., Mandel, J.-L., & Trottier, Y. (2002). Proteases acting on mutant huntingtin generate cleaved products that differentially build up cytoplasmic and nuclear inclusions. *Molecular Cell*, *10*(2), 259–269.

Luthi-Carter, R., Hanson, S., Strand, A., Bergstrom, D., Chun, W., Peters, N., Woods, A., Chan, E., Kooperberg, C., & Krainc, D. (2002). Dysregulation of gene expression in the R6/2 model of polyglutamine disease: parallel changes in muscle and brain. *Human molecular genetics*, *11*(17), 1911.

Ma, B., Savas, J. N., Yu, M.-S., Culver, B. P., Chao, M. V., & Tanese, N. (2011). Huntingtin mediates dendritic transport of β-actin mRNA in rat neurons. *Scientific reports*, *1*, 140.

MacAskill, A. F., Rinholm, J. E., Twelvetrees, A. E., Arancibia-Carcamo, I. L., Muir, J., Fransson, A., Aspenstrom, P., Attwell, D., & Kittler, J. T. (2009). Miro1 Is a Calcium Sensor for Glutamate Receptor-Dependent Localization of Mitochondria at Synapses. *Neuron*, *61*(4), 541–555.

Macisaac, K. D., & Fraenkel, E. (2010). Sequence analysis of chromatin immunoprecipitation data for transcription factors. *Methods in molecular biology (Clifton, N.J.)*, *674*, 179–193.

Mangiarini, L., Sathasivam, K., Seller, M., Cozens, B., Harper, A., Hetherington, C., Lawton, M., Trottier, Y., Lehrach, H., Davies, S. W., & Bates, G. P. (1996). Exon 1 of the HD gene with an expanded CAG repeat is sufficient to cause a progressive neurological phenotype in transgenic mice. *Cell*, *87*(3), 493–506.

Maniatis, T., & Reed, R. (2002). An extensive network of coupling among gene expression machines. *Nature*, *416*(6880), 499–506.

Mankodi, A. (2001). Muscleblind localizes to nuclear foci of aberrant RNA in myotonic dystrophy types 1 and 2. *Human molecular genetics*, *10*(19), 2165–2170.

Marais, G. (2005). Intron Size and Exon Evolution in Drosophila. *Genetics*, *170*(1), 481–485.

Marioni, J. C., Mason, C. E., Mane, S. M., Stephens, M., & Gilad, Y. (2008). RNA-seq: An assessment of technical reproducibility and comparison with gene expression arrays. *Genome Research*, *18*(9), 1509–1517.

Marsh, J. L., Pallos, J., & Thompson, L. M. (2003). Fly models of Huntington's disease. *Human molecular genetics*, *12*(2), R187–R193.

Martin, J. J., Van Regemorter, N., Krols, L., Brucher, J. M., de Barsy, T., Szliwowski, H., Evrard, P., Ceuterick, C., Tassignon, M. J., & Smet-Dieleman, H. (1994). On an autosomal dominant form of retinal-cerebellar degeneration: an autopsy study of five patients in one family. *Acta neuropathologica*, *88*(4), 277–286.

Martinez, E., Palhan, V. B., Tjernberg, A., Lymar, E. S., Gamper, A. M., Kundu, T. K., Chait, B. T., & Roeder, R. G. (2001). Human STAGA complex is a chromatin-acetylating transcription coactivator that interacts with pre-mRNA splicing and DNA damage-binding factors in vivo. *Molecular and cellular biology*, *21*(20), 6782–6795.

Mascarenhas, D. D., Mettler, I. J. I., Pierce, D. A. D., & Lowe, H. W. H. (1990). Intron-mediated enhancement of heterologous gene expression in maize. *Plant Molecular Biology*, *15*(6), 913–920.

Matsuyama, N., Hadano, S., Onoe, K., Osuga, H., Showguchi-Miyata, J., Gondo, Y., & Ikeda, J.-E. (2000). Identification and Characterization of the Miniature Pig Huntington's Disease Gene Homolog: Evidence for Conservation and Polymorphism in the CAG Triplet Repeat. *Genomics*, *69*(1), 72–85.

McLaughlin, B. A., Spencer, C., & Eberwine, J. (1996). CAG trinucleotide RNA repeats interact with RNA-binding proteins. *The American Journal of Human Genetics*, *59*(3), 561–569.

Menalled, L. B., Sison, J. D., & Dragatsis, I. (2003). Time course of early motor and neuropathological anomalies in a knockin mouse model of Huntington's disease with 140 CAG repeats. *Journal of Comparative Neurology*, *465*(1), 11–26.

Merkin, J., Russell, C., Chen, P., & Burge, C. B. (2012). Evolutionary dynamics of gene and isoform regulation in Mammalian tissues. *Science*, *338*(6114), 1593–1599.

Miller, J. P., Holcomb, J., Al-Ramahi, I., De Haro, M., & Gafni, J. (2010). Matrix Metalloproteinases Are Modifiers of Huntingtin Proteolysis and Toxicity in Huntington's Disease. *Neuron*, *67*, 199–212.

Mizuno, K., Carnahan, J., & Nawa, H. (1994). Brain-derived neurotrophic factor promotes differentiation of striatal GABAergic neurons. *Developmental Biology*, *165*, 243–256.

Moffitt, H., McPhail, G. D., Woodman, B., Hobbs, C., & Bates, G. P. (2009). Formation of polyglutamine inclusions in a wide range of non-CNS tissues in the HdhQ150 knock-in mouse model of Huntington's disease. *PloS one*, *4*(11), e8025.

Morello, L. L., Bardini, M. M., Sala, F. F., & Breviario, D. D. (2002). A long leader intron of the Ostub16 rice beta-tubulin gene is required for high-level gene expression and can autonomously promote transcription both in vivo and in vitro. *The Plant journal : for cell and molecular biology*, *29*(1), 33–44.

Mortazavi, A., Williams, B., McCue, K., Schaeffer, L., & Wold, B. (2008). Mapping and quantifying mammalian transcriptomes by RNA-Seq. *Nature Methods*, *5*(7), 621–628.

Muchowski, P. J., Schaffar, G., Sittler, A., Wanker, E. E., Hayer-Hartl, M. K., & Hartl, F. U. (2000). Hsp70 and hsp40 chaperones can inhibit self-assembly of polyglutamine proteins into amyloid-like fibrils. *Proceedings of the National Academy of Sciences of the United States of America*, *97*(14), 7841–7846.

Myers, R. H., Leavitt, J., & Farrer, L. A. (1989). Homozygote for Huntington disease. *American journal of Human Genetics*, *45*, 615–618.

Nakao, N., Brundin, P., Funa, K., Lindvall, O., & Odin, P. (1995). Trophic and protective actions of brain-derived neurotrophic factor on striatal DARPP-32-containing neurons in vitro. *Brain research. Developmental brain research*, *90*(1-2), 92–101.

Neuwald, A. F., & Hirano, T. (2000). HEAT repeats associated with condensins, cohesins, and other complexes involved in chromosome-related functions. *Genome Research*, *10*(10), 1445–1452.

Ng, C. W., Yildirim, F., Yap, Y. S., Dalin, S., Matthews, B. J., Velez, P. J., Labadorf, A., Housman, D. E., & Fraenkel, E. (2013). Extensive changes in DNA methylation are associated with expression of mutant huntingtin. *Proceedings of the National Academy of Sciences*, *110*(6), 2354–2359.

Oliveros, J. C. (2015). Venny. An interactive tool for comparing lists with Venn's diagrams.

Orozco, D., & Edbauer, D. (2013). FUS-mediated alternative splicing in the nervous system: consequences for ALS and FTLD. *Journal of Molecular Medicine*, *91*(12), 1343–1354.

Orr, A. L., Li, S., Wang, C.-E., Li, H., Wang, J., Rong, J., Xu, X., Mastroberardino, P. G., Greenamyre, J. T., & Li, X.-J. (2008). N-terminal mutant huntingtin associates with mitochondria and impairs mitochondrial trafficking. *Journal of Neuroscience*, *28*(11), 2783–2792.

Palazzolo, I., Stack, C., Kong, L., Musaro, A., Adachi, H., Katsuno, M., Sobue, G., Taylor, J. P., Sumner, C. J., Fischbeck, K. H., & Pennuto, M. (2009). Overexpression of IGF-1 in muscle attenuates disease in a mouse model of spinal and bulbar muscular atrophy. *Neuron*, *63*(3), 316–328.

Palmiter, R. D., Sandgren, E. P., Avarbock, M. R., Allen, D. D., & Brinster, R. L. (1991). Heterologous introns can enhance expression of transgenes in mice. *Proceedings of the National Academy of Sciences of the United States of America*, *88*(2), 478–482.

Pedrotti, S., Giudice, J., Dagnino-Acosta, A., Knoblauch, M., Singh, R. K., Hanna, A., Mo, Q., Hicks, J., Hamilton, S., & Cooper, T. A. (2015). The RNA-binding protein Rbfox1 regulates splicing required for skeletal muscle structure and function. *Human molecular genetics*, *24*(8), 2360–2374.

Pekowska, A., Benoukraf, T., Ferrier, P., & Spicuglia, S. (2010). A unique H3K4me2 profile marks tissue-specific gene regulation. *Genome Research*, *20*(11), 1493–1502.

Peters, M. F., Nucifora, F. C., Jr., Kushi, J., Seaman, H. C., Cooper, J. K., Herring, W. J., Dawson, V. L., Dawson, T. M., & Ross, C. A. (1999). Nuclear Targeting of Mutant Huntingtin Increases Toxicity. *Molecular and Cellular Neuroscience*, *14*(2), 121–128.

Peters-Libeu, C., Newhouse, Y., Krishnan, P., Cheung, K., Brooks, E., Weisgraber, K., & Finkbeiner, S. (2005). Crystallization and diffraction properties of the Fab fragment of 3B5H10, an antibody specific for disease-causing polyglutamine stretches. *Acta crystallographica. Section F, Structural biology and crystallization communications*, *61*, 1065–1068.

Poirier, M. A. (2005). A structure-based analysis of huntingtin mutant polyglutamine aggregation and toxicity: evidence for a compact beta-sheet structure. *Human molecular genetics*, *14*(6), 765–774.

Qin, Z.-H., Wang, Y., Sapp, E., Cuiffo, B., Wanker, E., Hayden, M. R., Kegel, K. B., Aronin, N., & DiFiglia, M. (2004). Huntingtin bodies sequester vesicle-associated proteins by a polyproline-dependent interaction. *Journal of Neuroscience*, *24*(1), 269–281.

Quail, M. A., Otto, T. D., Gu, Y., Harris, S. R., Skelly, T. F., Mcquillan, J. A., Swerdlow, H. P., & Oyola, S. O. (2012). Optimal enzymes for amplifying sequencing libraries. *Nature Methods*, *9*(1), 10–11.

Ranum, L. P. W., & Day, J. W. (2004). Pathogenic RNA repeats: an expanding role in genetic disease. *TRENDS in Genetics*, *20*(10), 506–512.

Ratovitski, T., Gucek, M., Jiang, H., Chighladze, E., Waldron, E., D'Ambola, J., Hou, Z., Liang, Y., Poirier, M. A., Hirschhorn, R. R., Graham, R., Hayden, M. R., Cole, R. N., & Ross, C. A. (2009). Mutant huntingtin N-terminal fragments of specific size mediate aggregation and toxicity in neuronal cells. *The Journal of biological chemistry*, *284*(16), 10855–10867.

Ratovitski, T., Nakamura, M., D'Ambola, J., Chighladze, E., Liang, Y., Wang, W., Graham, R., Hayden, M. R., Borchelt, D. R., Hirschhorn, R. R., & Ross, C. A. (2007). N-terminal proteolysis of full-length mutant huntingtin in an inducible PC12 cell model of Huntington's disease. *Cell Cycle*, *6*(23), 2970–2981.

Ravache, M., Weber, C., Mérienne, K., & Trottier, Y. (2010). Transcriptional activation of REST by Sp1 in Huntington's disease models. *PloS one*, *5*(12), e14311–e14311.

Ravikumar, B., Duden, R., & Rubinsztein, D. C. (2002). Aggregate-prone proteins with polyglutamine and polyalanine expansions are degraded by autophagy. *Human molecular genetics*, *11*(9), 1107–1117.

Ravikumar, B., Vacher, C., Berger, Z., Davies, J. E., Luo, S., Oroz, L. G., Scaravilli, F., Easton, D. F., Duden, R., O'Kane, C. J., & Rubinsztein, D. C. (2004). Inhibition of mTOR induces autophagy and reduces toxicity of polyglutamine expansions in fly and mouse models of Huntington disease. *Nature genetics*, *36*(6), 585–595.

Ribchester, R. R., Thomson, D., & Wood, N. I. (2004). Progressive abnormalities in skeletal muscle and neuromuscular junctions of transgenic mice expressing the Huntington's disease mutation. *European Journal of Neuroscience*, *20*, 3092–3114.

Rinaldi, C., Bott, L. C., Chen, K.-l., Harmison, G. G., Katsuno, M., Sobue, G., Pennuto, M., & Fischbeck, K. H. (2012). Insulinlike growth factor (IGF)-1 administration ameliorates disease manifestations in a mouse model of spinal and bulbar muscular atrophy. *Molecular medicine (Cambridge, Mass)*, *18*, 1261–1268.

Rivero, G., Gabilondo, A. M., García-Sevilla, J. A., Callado, L. F., La Harpe, R., Morentin, B., & Meana, J. J. (2013). Brain RGS4 and RGS10 protein expression in schizophrenia and depression. Effect of drug treatment. *Psychopharmacology*, *226*(1), 177–188.

Rose, A. B., & Last, R. L. (1997). Introns act post-transcriptionally to increase expression of the Arabidopsis thaliana tryptophan pathway gene PAT1. *The Plant Journal*, *11*(3), 455–464.

Rose, A. B. A. (2002). Requirements for intron-mediated enhancement of gene expression in Arabidopsis. *RNA (New York, NY)*, *8*(11), 1444–1453.

Ross, C. A., & Tabrizi, S. J. (2011). Huntington's disease: from molecular pathogenesis to clinical treatment. *Lancet neurology*, *10*(1), 83–98.

Roy, M., Kim, N., Xing, Y., & Lee, C. (2008). The effect of intron length on exon creation ratios during the evolution of mammalian genomes. *RNA (New York, NY)*, *14*(11), 2261–2273.

S L Wolin, P. W. (1988). Ribosome pausing and stacking during translation of a eukaryotic mRNA. *The EMBO Journal*, *7*(11), 3559.

Sadri-Vakili, G., & Cha, J.-H. J. (2006). Histone deacetylase inhibitors: a novel therapeutic approach to Huntington's disease (complex mechanism of neuronal death). *Current Alzheimer research*, *3*(4), 403–408.

Sah, D. W. Y., & Aronin, N. (2011). Oligonucleotide therapeutic approaches for Huntington disease. *Journal of Clinical Investigation*, *121*(2), 500–507.

Santos-Rosa, H., Schneider, R., Bannister, A. J., Sherriff, J., Bernstein, B. E., Emre, N. C. T., Schreiber, S. L., Mellor, J., & Kouzarides, T. (2002). Active genes are tri-methylated at K4 of histone H3. *Nature*, *419*(6905), 407–411.

Sathasivam, K. (2001). Centrosome disorganization in fibroblast cultures derived from R6/2 Huntington's disease (HD) transgenic mice and HD patients. *Human molecular genetics*, *10*(21), 2425–2435.

Sathasivam, K., Lane, A., Legleiter, J., Warley, A., Woodman, B., Finkbeiner, S., Paganetti, P., Muchowski, P. J., Wilson, S., & Bates, G. P. (2010). Identical oligomeric and fibrillar structures captured from the brains of R6/2 and knock-in mouse models of Huntington's disease. *Human molecular genetics*, *19*(1).

Sathasivam, K., Neueder, A., Gipson, T. A., Landles, C., Benjamin, A. C., Bondulich, M. K., Smith, D. L., Faull, R. L. M., Roos, R. A. C., Howland, D., Detloff, P. J., Housman, D. E., & Bates, G. P. (2013). Aberrant splicing of HTT generates the pathogenic exon 1 protein in Huntington disease. *Proceedings of the National Academy of Sciences*, *110*(6), 2366–2370.

Savas, J. N., Ma, B., Deinhardt, K., Culver, B. P., Restituito, S., Wu, L., Belasco, J. G., Chao, M. V., & Tanese, N. (2010). A role for huntington disease protein in dendritic RNA granules. *Journal of Biological Chemistry*, *285*(17), 13142–13153.

Scappini, E., Koh, T.-W., Martin, N. P., & O'Bryan, J. P. (2007). Intersectin enhances huntingtin aggregation and neurodegeneration through activation of c-Jun-NH2-terminal kinase. *Human molecular genetics*, *16*(15), 1862–1871.

Schaefer, M. H., Wanker, E. E., & Andrade-Navarro, M. A. (2012). Evolution and function of CAG/polyglutamine repeats in protein-protein interaction networks. *Nucleic Acids Research*, *40*(10), 4273–4287.

Schilling, G. (2004). Nuclear-targeting of mutant huntingtin fragments produces Huntington's disease-like phenotypes in transgenic mice. *Human molecular genetics*, *13*(15), 1599–1610.

Schilling, G., Klevytska, A., Tebbenkamp, A. T. N., Juenemann, K., Cooper, J., Gonzales, V., Slunt, H., Poirer, M., Ross, C. A., & Borchelt, D. R. (2007). Characterization of huntingtin pathologic fragments in human Huntington disease, transgenic mice, and cell models. *Journal of neuropathology and experimental neurology*, *66*(4), 313–320.

Schmitt, I., Bächner, D., Megow, D., Henkiein, P., Hamelster, H., Epplen, J. T., & Riess, O. (1995). Expression of the Huntington disease gene in rodents: cloning the rat homologue and evidence for downregulation in non-neuronal tissues during development. *Human molecular genetics*, *4*(7), 1173–1182.

Schulz, S., Chachami, G., Kozaczkiewicz, L., Winter, U., Stankovic-Valentin, N., Haas, P., Hofmann, K., Urlaub, H., Ovaa, H., Wittbrodt, J., Meulmeester, E., & Melchior, F. (2012). scientific report. *EMBO reports*, *13*(10), 930–938.

Scotto Lavino, E., Du, G., & Frohman, M. A. (2007). 3' End cDNA amplification using classic RACE. *Nature Protocols*, *1*(6), 2742–2745.

Seong, I. S., Ivanova, E., Lee, J.-M., Choo, Y. S., Fossale, E., Anderson, M., Gusella, J. F., Laramie, J. M., Myers, R. H., Lesort, M., & MacDonald, M. E. (2005). HD CAG repeat implicates a dominant property of huntingtin in mitochondrial energy metabolism. *Human molecular genetics*, *14*(19), 2871–2880.

Seredenina, T., Gokce, O., & Luthi-Carter, R. (2011). Decreased Striatal RGS2 Expression Is Neuroprotective in Huntington's Disease (HD) and Exemplifies a Compensatory Aspect of HD-Induced Gene Regulation. *PloS one*, *6*(7), e22231.

Seredenina, T., & Luthi-Carter, R. (2012). What have we learned from gene expression profiles in Huntington's disease? *Neurobiology of Disease*, *45*(1), 83–98.

Seyednasrollah, F., Laiho, A., & Elo, L. L. (2015). Comparison of software packages for detecting differential expression in RNA-seq studies. *Briefings in Bioinformatics*, *16*(1), 59–70.

Shang, J., Zhu, F., Vongsangnak, W., Tang, Y., Zhang, W., & Shen, B. (2014). Evaluation and Comparison of Multiple Aligners for Next-Generation Sequencing Data Analysis. *BioMed Research International*, *2014*(11, supplement), 1–16.

Sharma, M., Celver, J., & Kovoor, A. (2011). Regulator of G protein signaling 9-2 (RGS9-2) mRNA is up regulated during neuronal differentiation of mouse embryonic stem cells. *Neuroscience letters*, *502*(3), 123–128.

Shu, W., Chen, H., Bo, X., & Wang, S. (2011). Genome-wide analysis of the relationships between DNaseI HS, histone modifications and gene expression reveals distinct modes of chromatin domains. *Nucleic Acids Research*, *39*(17), 7428–7443.

Shulha, H. P. (2012). Epigenetic Signatures of Autism. *Archives of General Psychiatry*, *69*(3), 314.

Sittler, A., Lurz, R., Lueder, G., Priller, J., Lehrach, H., Hayer-Hartl, M. K., Hartl, F. U., & Wanker, E. E. (2001). Geldanamycin activates a heat shock response and inhibits huntingtin aggregation in a cell culture model of Huntington's disease. *Human molecular genetics*, *10*(12), 1307–1315.

Slow, E. J., van Raamsdonk, J., Rogers, D., Coleman, S. H., Graham, R. K., Deng, Y., Oh, R., Bissada, N., Hossain, S. M., Yang, Y.-Z., Li, X.-J., Simpson, E. M., Gutekunst, C.-A., Leavitt, B. R., & Hayden, M. R. (2003). Selective striatal neuronal loss in a YAC128 mouse model of Huntington disease. *Human molecular genetics*, *12*(13), 1555–1567.

Smith, M. W. (1988). Structure of vertebrate genes: a statistical analysis implicating selection. *Journal of molecular evolution*, *27*(1), 45–55.

Smith, P. J., Zhang, C., Wang, J., Chew, S. L., Zhang, M. Q., & Krainer, A. R. (2006). An increased specificity score matrix for the prediction of SF2/ASF-specific exonic splicing enhancers. *Human molecular genetics*, *15*(16), 2490–2508.

Sobue, G., Hashizume, Y., Mukai, E., Hirayama, M., Mitsuma, T., & Takahashi, A. (1989). X-linked recessive bulbospinal neuronopathy. A clinicopathological study. *Brain*, *112*, 209–232.

Sperfeld, A. D., Karitzky, J., Brummer, D., Schreiber, H., Häussler, J., Ludolph, A. C., & Hanemann, C. O. (2002). X-linked Bulbospinal Neuronopathy: Kennedy Disease. *Archives of neurology*, *59*(12), 1921–1926.

Spriggs, K., & Bushell, M. (2010). Translational Regulation of Gene Expression during Conditions of Cell Stress. *Molecular Cell*, *40*, 228–237.

Squitieri, F. (2003). Homozygosity for CAG mutation in Huntington disease is associated with a more severe clinical course. *Brain*, *126*(4), 946–955.

Squitieri, F., Cannella, M., Sgarbi, G., Maglione, V., Falleni, A., Lenzi, P., Baracca, A., Cislaghi, G., Saft, C., Ragona, G., Russo, M. A., Thompson, L. M., Solaini, G., & Fornai, F. (2006). Severe ultrastructural mitochondrial changes in lymphoblasts homozygous for Huntington disease mutation. *Mechanisms of ageing and development*, *127*(2), 217–220.

Squitieri, F., Falleni, A., Cannella, M., Orobello, S., Fulceri, F., Lenzi, P., & Fornai, F. (2010). Abnormal morphology of peripheral cell tissues from patients with Huntington disease. *Journal of neural transmission (Vienna, Austria : 1996)*, *117*(1), 77–83.

Steffan, J. S., Agrawal, N., Pallos, J., Rockabrand, E., Trotman, L. C., Slepko, N., Illes, K., Lukacsovich, T., Zhu, Y.-Z., Cattaneo, E., Pandolfi, P. P., Thompson, L. M., & Marsh, J. L. (2004). SUMO modification of Huntingtin and Huntington's disease pathology. *Science*, *304*(5667), 100–104.

Steffan, J. S., Bodai, L., Pallos, J., Poelman, M., McCampbell, A., Apostol, B. L., Kazantsev, A., Schmidt, E., Zhu, Y. Z., Greenwald, M., Kurokawa, R., Housman, D. E., Jackson, G. R., Marsh, J. L., & Thompson, L. M. (2001). Histone deacetylase inhibitors arrest polyglutamine-dependent neurodegeneration in Drosophila. *Nature*, *413*(6857), 739–743.

Steffan, J. S., & Kazantsev, A. (2000). The Huntington's disease protein interacts with p53 and CREB-binding protein and represses transcription. In *Proceedings of the National Academy of Sciences USA*, (pp. 6763–6768).

Strahl, B. D., & Allis, C. D. (2000). The language of covalent histone modifications. *Nature*, *403*(6765), 41–45.

Strand, A., Baquet, Z., Aragaki, A., Holmans, P., Yang, L., Cleren, C., Beal, M., Jones, L., Kooperberg, C., & Olson, J. (2007). Expression Profiling of Huntington's Disease Models Suggests That Brain-Derived Neurotrophic Factor Depletion Plays a Major Role in Striatal Degeneration. *The Journal of Neuroscience*, *27*(43), 11758–11768.

Strand, A. D., Aragaki, A. K., Shaw, D., Bird, T., Holton, J., Turner, C., Tapscott, S. J., Tabrizi, S. J., Schapira, A. H., Kooperberg, C., & Olson, J. M. (2005). Gene expression in Huntington's disease skeletal muscle: a potential biomarker. *Human molecular genetics*, *14*(13), 1863–1876.

Strong, T. V., Tagle, D. A., Valdes, J. M., Elmer, L. W., Boehm, K., Swaroop, M., Kaatz, K. W., Collins, F. S., & Albin, R. L. (1993). Widespread expression of the human and rat Huntington's disease gene in brain and nonneural tissues. *Nature genetics*, *5*(3), 259–265.

Suhr, S. T., Senut, M. C., Whitelegge, J. P., Faull, K. F., Cuizon, D. B., & Gage, F. H. (2001). Identities of sequestered proteins in aggregates from cells with induced polyglutamine expression. *The Journal of cell biology*, *153*(2), 283–294.

Summerton, J. (1999). Morpholino antisense oligomers: the case for an RNase H-independent structural type. *Biochimica et biophysica acta*, *1489*(1), 141–158.

Swanson, C. M., Sherer, N. M., & Malim, M. H. (2010). SRp40 and SRp55 promote the translation of unspliced human immunodeficiency virus type 1 RNA. *Journal of virology*, *84*(13), 6748–6759.

Takeyama, K.-i., Ito, S., Yamamoto, A., Tanimoto, H., Furutani, T., Kanuka, H., Miura, M., Tabata, T., & Kato, S. (2002). Androgen-dependent neurodegeneration by polyglutamine-expanded human androgen receptor in Drosophila. *Neuron*, *35*(5), 855–864.

Tartari, M., Gissi, C., Lo Sardo, V., Zuccato, C., Picardi, E., Pesole, G., & Cattaneo, E. (2008). Phylogenetic comparison of huntingtin homologues reveals the appearance of a primitive polyQ in sea urchin. *Molecular biology and evolution*, *25*(2), 330–338.

THDCR (1993). A novel gene containing a trinucleotide repeat that is expanded and unstable on Huntington's disease chromosomes. The Huntington's Disease Collaborative Research Group. *Cell*, *72*(6), 971–983.

Tranell, A., Fenyö, E. M., & Schwartz, S. (2010). Serine- and arginine-rich proteins 55 and 75 (SRp55 and SRp75) induce production of HIV-1 vpr mRNA by inhibiting the 5'-splice site of exon 3. *The Journal of biological chemistry*, *285*(41), 31537–31547.

Trapnell, C., Roberts, A., Goff, L., Pertea, G., Kim, D., Kelley, D. R., Pimentel, H., Salzberg, S. L., Rinn, J. L., & Pachter, L. (2012). Differential gene and transcript expression analysis of RNA-seq experiments with TopHat and Cufflinks. *Nature Protocols*, *7*(3), 562–578.

Tsankova, N. M., Berton, O., Renthal, W., Kumar, A., Neve, R. L., & Nestler, E. J. (2006). Sustained hippocampal chromatin regulation in a mouse model of depression and antidepressant action. *Nature neuroscience*, *9*(4), 519–525.

Valencia, A., Sapp, E., Kimm, J. S., McClory, H., Ansong, K. A., Yohrling, G., Kwak, S., Kegel, K. B., Green, K. M., Shaffer, S. A., Aronin, N., & DiFiglia, M. (2013). Striatal synaptosomes from Hdh140Q/140Q knock-in mice have altered protein levels, novel sites of methionine oxidation, and excess glutamate release after stimulation. *Journal of Huntington's disease*, *2*(4), 459–475.

van der Burg, J. M. M., Björkqvist, M., & Brundin, P. (2009). Beyond the brain: widespread pathology in Huntington's disease. *Lancet neurology*, *8*(8), 765–774.

van Dijk, K., Ding, Y., Malkaram, S., Riethoven, J.-J. M., Liu, R., Yang, J., Laczko, P., Chen, H., Xia, Y., Ladunga, I., Avramova, Z., & Fromm, M. (2010). Dynamic changes in genome-wide histone H3 lysine 4 methylation patterns in responseto dehydration stress in Arabidopsis thaliana. *BMC Plant Biology*, *10*(1), 238.

Vashishtha, M., Ng, C. W., Yildirim, F., Gipson, T. A., Kratter, I. H., Bodai, L., Song, W., Lau, A., Labadorf, A., Vogel-Ciernia, A., Troncosco, J., Ross, C. A., Bates, G. P., Krainc, D., Sadri-Vakili, G., Finkbeiner, S., Marsh, J. L., Housman, D. E., Fraenkel, E., & Thompson, L. M. (2013). Targeting H3K4 trimethylation in Huntington disease. *Proceedings of the National Academy of Sciences of the United States of America*, *110*(32), E3027–E3036.

Vellano, C. P., Lee, S. E., Dudek, S. M., & Hepler, J. R. (2011). RGS14 at the interface of hippocampal signaling and synaptic plasticity. *Trends in pharmacological sciences*, *32*(11), 666–674.

Ventimiglia, R., Mather, P. E., Jones, B. E., & Lindsay, R. M. (1995). The neurotrophins BDNF, NT-3 and NT-4/5 promote survival and morphological and biochemical differentiation of striatal neurons in vitro. *The European journal of neuroscience*, *7*(2), 213–222.

Vonsattel, J.-P., Myers, R. H., Stevens, T. J., Ferrante, R. J., Bird, E. D., & Richardson, E. P. J. (1985). Neuropathological Classification of Huntington's Disease. *Journal of neuropathology and experimental neurology*, *44*(6), 559.

Wang, E., Sandberg, R., Luo, S., Khrebtukova, I., Zhang, L., Mayr, C., Kingsmore, S., Schroth, G., & Burge, C. (2008). Alternative isoform regulation in human tissue transcriptomes. *Nature*, *456*(7221), 470–476.

Wang, Z., Gerstein, M., & Snyder, M. (2009). RNA-Seq: a revolutionary tool for transcriptomics. *Nature reviews Genetics*, *10*(1), 57–63.

Wellington, C. L., Ellerby, L. M., Gutekunst, C.-A., Rogers, D., Warby, S., Graham, R. K., Loubser, O., van Raamsdonk, J., Singaraja, R., Yang, Y.-Z., Gafni, J., Bredesen, D., Hersch, S. M., Leavitt, B. R., Roy, S., Nicholson, D. W., & Hayden, M. R. (2002). Caspase Cleavage of Mutant Huntingtin Precedes Neurodegeneration in Huntington's Disease. *The Journal of Neuroscience*, *22*(18), 7862–7872.

Wexler, N. S., Young, A. B., Tanzi, R. E., & Travers, H. (1987). Homozygotes for Huntington's disease. *Nature*, *326*, 194–197.

Wheeler, V. C., Auerbach, W., White, J. K., Srinidhi, J., Auerbach, A., Ryan, A., Duyao, M. P., Vrbanac, V., Weaver, M., Gusella, J. F., Joyner, A. L., & MacDonald, M. E. (1999). Length-dependent gametic CAG repeat instability in the Huntington's disease knock-in mouse. *Human molecular genetics*, *8*(1), 115–122.

White, J. K., Auerbach, W., Duyao, M. P., Vonsattel, J.-P., Gusella, J. F., Joyner, A. L., & MacDonald, M. E. (1997). Huntingtin is required for neurogenesis and is not impaired by the Huntington's disease CAG expansion. *Nature genetics*, *17*(4), 404–410.

Widmer, H. R., & Hefti, F. (1994). Neurotrophin-4/5 promotes survival and differentiation of rat striatal neurons developing in culture. *The European journal of neuroscience*, *6*(11), 1669–1679.

Wingender, E., Dietze, P., Karas, H., & Knüppel, R. (1996). TRANSFAC: a database on transcription factors and their DNA binding sites. *Nucleic Acids Research*, *24*(1), 238–241.

Woodman, B., Butler, R., Landles, C., Lupton, M. K., & Tse, J. (2007). The HdhQ150/Q150 knock-in mouse model of HD and the R6/2 exon 1 model develop comparable and widespread molecular phenotypes. *Brain research*, *72*, 83–97.

Xia, J., Lee, D. H., Taylor, J., Vandelft, M., & Truant, R. (2003). Huntingtin contains a highly conserved nuclear export signal. *Human molecular genetics*, *12*(12), 1393–1403.

Xiao, X., Wang, Z., Jang, M., Nutiu, R., Wang, E. T., & Burge, C. B. (2009). Splice site strength–dependent activity and genetic buffering by poly-G runs. *Nature structural & molecular biology*, *16*(10), 1094–1100.

Yang, J., Hung, L.-H., Licht, T., Kostin, S., Looso, M., Khrameeva, E., Bindereif, A., Schneider, A., & Braun, T. (2014). RBM24 Is a Major Regulator of Muscle-Specific Alternative Splicing. *Developmental Cell*, *31*(1), 87–99.

Yeo, G., & Burge, C. B. (2004). Maximum Entropy Modeling of Short Sequence Motifs with Applications to RNA Splicing Signals. *Journal of Computational Biology*, *11*(2-3), 377–394.

Yoo, S. Y., Pennesi, M. E., Weeber, E. J., Xu, B., Atkinson, R., Chen, S., Armstrong, D. L., Wu, S. M., Sweatt, J. D., & Zoghbi, H. Y. (2003). SCA7 knockin mice model human SCA7 and reveal gradual accumulation of mutant ataxin-7 in neurons and abnormalities in short-term plasticity. *Neuron*, *37*(3), 383–401.

Young, M. D., Willson, T. A., Wakefield, M. J., Trounson, E., Hilton, D. J., Blewitt, M. E., Oshlack, A., & Majewski, I. J. (2011). ChIP-seq analysis reveals distinct H3K27me3 profiles that correlate with transcriptional activity. *Nucleic Acids Research*, *39*(17), 7415–7427.

Yu, Z., Dadgar, N., Albertelli, M., Gruis, K., Jordan, C., Robins, D. M., & Lieberman, A. P. (2006). Androgen-dependent pathology demonstrates myopathic contribution to the Kennedy disease phenotype in a mouse knock-in model. *Journal of Clinical Investigation*, *116*(10), 2663–2672.

Yu, Z., Teng, X., & Bonini, N. M. (2011). Triplet repeat-derived siRNAs enhance RNA-mediated toxicity in a Drosophila model for myotonic dystrophy. *PLoS Genetics*, *7*(3), e1001340–e1001340.

Yu, Z., Wang, A. M., Robins, D. M., & Lieberman, A. P. (2009). Altered RNA splicing contributes to skeletal muscle pathology in Kennedy disease knock-in mice. *Disease Models & Mechanisms*, *2*(9-10), 500–507.

Zeitlin, S., Liu, J. P., Chapman, D. L., Papaioannou, V. E., & Efstratiadis, A. (1995). Increased apoptosis and early embryonic lethality in mice nullizygous for the Huntington's disease gene homologue. *Nature genetics*, *11*(2), 155–163.

Zhang, M. Q. (1998). Statistical features of human exons and their flanking regions. *Human molecular genetics*, *7*(5), 919–932.

Zhang, Q., & Edwards, S. V. (2012). The Evolution of Intron Size in Amniotes: A Role for Powered Flight? *Genome Biology and Evolution*, *4*(10), 1033–1043.

Zhang, Y., Liu, T., Meyer, C. A., Eeckhoute, J., Johnson, D. S., Bernstein, B. E., Nusbaum, C., Myers, R. M., Brown, M., Li, W., & Liu, X. S. (2008a). Model-based analysis of ChIP-Seq (MACS). *Genome biology*, *9*(9), R137.

Zhang, Z., Lotti, F., Dittmar, K., Younis, I., Wan, L., Kasim, M., & Dreyfuss, G. (2008b). SMN Deficiency Causes Tissue-Specific Perturbations in the Repertoire of snRNAs and Widespread Defects in Splicing. *Cell*, *133*(4), 585–600.

Zhou, Y., Liu, S., Liu, G., Öztürk, A., & Hicks, G. G. (2013). PLOS Genetics: ALS-Associated FUS Mutations Result in Compromised FUS Alternative Splicing and Autoregulation. *PLoS Genetics*, *9*(10), e1003895.

Zielonka, D., Piotrowska, I., Marcinkowski, J. T., & Mielcarek, M. (2014). Skeletal muscle pathology in Huntington's disease. *Frontiers in physiology*, *5*, 380.

Zu, T., Gibbens, B., Doty, N. S., Gomes-Pereira, M., Huguet, A., Stone, M. D., Margolis, J., Peterson, M., Markowski, T. W., Ingram, M. A. C., Nan, Z., Forster, C., Low, W. C., Schoser, B., Somia, N. V., Clark, H. B., Schmechel, S., Bitterman, P. B., Gourdon, G., Swanson, M. S., Moseley, M., & Ranum, L. P. W. (2011). Non-ATG-initiated translation directed by microsatellite expansions. *Proceedings of the National Academy of Sciences of the United States of America*, *108*(1), 260–265.

Zuccato, C., & Cattaneo, E. (2007). Role of brain-derived neurotrophic factor in Huntington's disease. *Progress in neurobiology*, *81*(5-6), 294–330.

Zuccato, C., Ciammola, A., Rigamonti, D., Leavitt, B. R., Goffredo, D., Conti, L., MacDonald, M. E., Friedlander, R. M., Silani, V., Hayden, M. R., Timmusk, T., Sipione, S., & Cattaneo, E. (2001). Loss of huntingtin-mediated BDNF gene transcription in Huntington's disease. *Science*, *293*(5529), 493–498.

Zuccato, C., Marullo, M., & Conforti, P. (2008). Systematic Assessment of BDNF and Its Receptor Levels in Human Cortices Affected by Huntington's Disease. *Brain Pathology*, *18*, 225–238.

Zuccato, C., Tartari, M., Crotti, A., Goffredo, D., Valenza, M., Conti, L., Cataudella, T., Leavitt, B. R., Hayden, M. R., Timmusk, T., Rigamonti, D., & Cattaneo, E. (2003). Huntingtin interacts with REST/NRSF to modulate the transcription of NRSE-controlled neuronal genes. *Nature genetics*, *35*(1), 76–83.